PHYSICO - CHEMICAL TECHNIQUES FOR BRIGHTNESS IMPROVEMENT OF YELLOW - STAINED CLAYS

by

V.R.AMBIKADEVI

To my parents

DECLARATION

I hereby declare that the matter embodied in this thesis is the result of the investigations carried out by me at the Clays and Clay Minerals Unit of the Regional Research Laboratory, Thiruvananthapuram, under the guidance of Dr.(Mrs) M. Lalithambika and the same has not been submitted elsewhere for a degree.
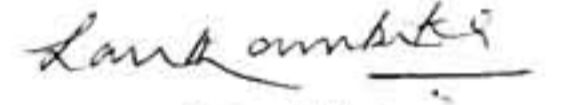
In keeping with the general practice of reporting scientific observations, due reference has been made wherever the work described is based on the findings of other investigators.

Ambikadvi. V.R

V.R. AMBIKADEVI

CERTIFICATE

Certified that the work embodied in this thesis titled **"Physico-Chemical Techniques for Brightness Improvement of Yellow-Stained Clays"** has been carried out by **Mrs. V.R. Ambikadevi** under my supervision and the same has not been submitted elsewhere for a degree.

(M. Lalithambika)

ACKNOWLEDGEMENTS

V.R. AMBIKADEVI

PREFACE

The present work deals with the beneficiation and value addition of yellow-stained kaolinitic clays. This is a very important aspect of clay research which is of great industrial significance and economic importance.

The first chapter deals, in general, with classification and genesis of kaolinitic clays followed by a detailed description on the iron containing associated impurities like hematite, goethite, lepidocrocite, etc. which are commonly found in clays imparting a hue, thereby affecting adversely the versatility of the application of kaolinite. The determinative methods employed for iron and the techniques which can be used for its dissolution from kaolinites are also described. The details on the geological setting of the clay deposits of South Kerala and Rajasthan are presented.

Chapter two begins with the profile description of the study sites viz. Akulam, Kalliyur, Mulavana, and Thonnakkal from the State of Kerala and Buchara deposits of Rajasthan. The results of detailed chemical and mineralogical characterisation are presented. The chemical assay includes macro and trace elements and associated impurities. The identification of the iron bearing mineral impurities has been facilitated by NaOH concentration treatment followed by XRD, SEM and TEM studies. The results obtained by the above methods are compared with the Munsell colour chart which is used as a practical tool for the iron-oxide mineral identification in soils. This chapter concludes with the description of the field evidences on the transformation of feldspar and mica to kaolinite. Very interesting field observations indicating the conversion of hematite to goethite in the palaeosols in clays are described. Petrological studies are also given substantiating the same.

Chapter three gives the details on the physical beneficiation of clays from the five locations. Wet high intensity magnetic separation (WHIMS), wet high gradient magnetic separation (WHGMS) and superconducting high gradient magnetic separation (SC-HGMS) are employed for separation of ferruginous impurities. The improvement in brightness after the removal of Fe impurities is monitored.

Chapter four gives an exhaustive description of the various chemical beneficiation techniques. This work is divided into three parts: (a) deferration of iron-stained clays using sodium dithionite and sucrose in acid-medium, (b) the effect of various organic acids on deferration and (c) catalytic effect of metal powders on deferration. The brightness improvement in each case is clearly indicated and the merits and demerits of these techniques are discussed. Chemical beneficiation in presence of metal powders provides a novel technique of deferration improving brightness by an order of 10-20 units.

Since goethite is the major colouring impurity in all the clay samples studied, experiments are carried out to impart colour by artificial means. Chapter five deals with the preparation of synthetic goethites and their coherent mixing on cleaned kaolinite surfaces and comparison of the yellowness developed with naturally occurring ones.

CONTENTS

CHAPTER 1

CLASSIFICATION, GENESIS AND APPLICATION OF KAOLIN WITH SPECIAL REFERENCE TO THE ASSOCIATED IRON OXIDES AND THEIR REMOVAL - AN OVERVIEW

1.1. INTRODUCTION

Clays are the most abundant substances in the sedimentary lithosphere[1]. Since centuries ago men had been familiar with their wonderful properties and innumerable uses. Now-a-days, clays have gained a unique position among the industrial minerals. In general, the term clay designates any substance which is less than 2 μm in particle size[2]. The nomenclature committees of Association Internationale Pour l'Etude des Argile (AIPEA) and The Clay Mineral Society (CMS) of the United States defined "Clay" as a naturally occurring material composed primarily of fine-grained minerals usually phyllosilicates which are generally plastic at appropriate water contents and hard when dried or fired[3]. However, in nature, they are associated with smaller amounts of finely divided quartz, feldspars, carbonates, oxides and hydroxides of Fe and Al and organic matter. The principal clay mineral groups can be summarised into the following categories[4]:

(i)	Kaolinite	-	Kaolinite, dickite, nacrite, halloysite, metahalloysite, anauxite and allophane
(ii)	Illite	-	Illite, hydro-micas, phengite, glauconite and celandite
(iii)	Smectite	-	Montmorillonite, nontronite, hectorite, saponite and sauconite
(iv)	Vermiculite		
(v)	Palygorskite	-	Palygorskite, attapulgite and sepiolite

Kaolinite probably is the most common clay mineral. The other members of the group are dickite, and nacrite (two rare polymorphs), halloysite (a hydrated form of kaolinite), metahalloysite (the dehydration product of halloysite), anauxite (a mineral with higher SiO_2 : Al_2O_3 ratio) and allophane (amorphous in nature). In commercial usage kaolin means a product composed predominantly of either kaolinite or halloysite or a mixture of these two with smaller amounts of quartz, mica, feldspar, other clay minerals and different oxides of Fe and Ti[5]. China clay is an alternative term for kaolin.

1.2. CLASSIFICATION OF KAOLIN

Kaolins are classified into two broad groups based on their origin[6-7]. They are: (a) Primary or *in situ* and (b) Secondary or *Sedimentary*.

Primary or *in situ* kaolin: is formed by the alteration of feldspathic and other aluminium silicates. According to the mode of origin, they are further classified into the following groups[7]: (a) Weathered (b) Hydrothermal and (c) Solfatara.

Secondary kaolin: is formed away from the source material. They are further classified into three[7] : (a) Sedimentary kaolin, (b) Kaolinitic sands and (c) Ball clays, fire clays and flint clays

The sedimentary kaolinite essentially yields over 60% kaolinite and it becomes white enough after mild beneficiation processes. Kaolin sands yield only less than 20% kaolinite. In ball clays, flint clays and fire clays, the important constituent is kaolin. Ball clays are mainly used in ceramics and the latter in producing refractory materials.

1.3. GENESIS OF KAOLIN

Kaolin may be formed by any one of the following mechanisms[8]:

2

(a) Neoformation by precipitation from solution.

(b) Neoformation by crystallization from amorphous colloidal material.

(c) Transformation from a non-clay precursor, through structural alteration.

(d) Layer transformation from a related phyllosilicate (eg. mica) without changing the structural order.

Weathering and hydrothermal alteration are the two ubiquitous phenomena leading to the formation of vast kaolin deposits. In the natural weathering conditions, moderate temperature and moderately high rain fall favour the decomposition of feldspars and other aluminium silicates in granites, metamorphic rocks and even other clays and shales, to a mixture of kaolinite and quartz. Granites are the commonest host rock for primary kaolin deposits[5].

The process of weathering is accomplished either by physical disintegration or by chemical decomposition. The mechanical disintegration of rocks are mainly caused by the action of weathering agents such as running water, wind, glaciers, waves etc. Chemical weathering is much more pronounced in kaolinite formation than physical weathering processes. The major chemical decomposition processes include hydrolysis, hydration, oxidation, chelation and the activities of primitive plants. Of these, the biological processes are the extremely important contributing factor to weathering process subsequent to soil formation[5]. The products of chemical weathering vary according to the severity of leaching conditions (especially the water flux). The formation of gibbsite, kaolinite and montmorillonite can be expected from the same material according to different water regimes[9].

$$H^+ + NaAlSi_3O_8 + 7H_2O \quad \rightarrow \quad Al(OH)_3 + Na^+ + 3H_4SiO_4$$

albite   gibbsite (high flow rate)

3

$$2H^+ + 2NaAlSi_3O_8 + 9H_2O \rightarrow \quad Al_2Si_2O_5(OH)_4 + 2Na^+ + 4H_4SiO_4$$
$$\text{albite} \qquad\qquad\qquad \text{kaolinite} \quad \text{(moderate flow rate)}$$

$$Mg^{2+} + 3NaAlSi_3O_8 + 4H_2O \rightarrow 2Na + AlMgSi_4O_{10}(OH)_2 + 2Na^+ + H_4SiO_4$$
$$\text{albite} \qquad\qquad\qquad\qquad \text{montmorillonite} \qquad \text{(low flow rate)}$$
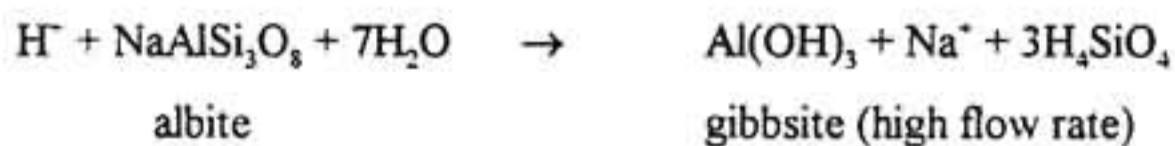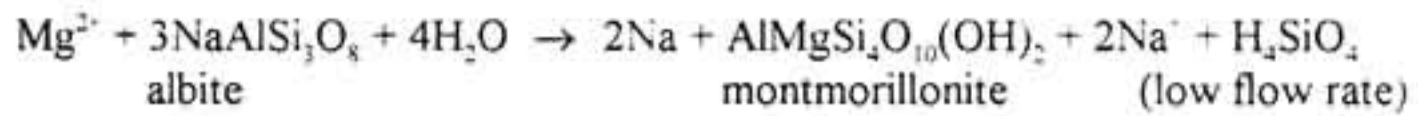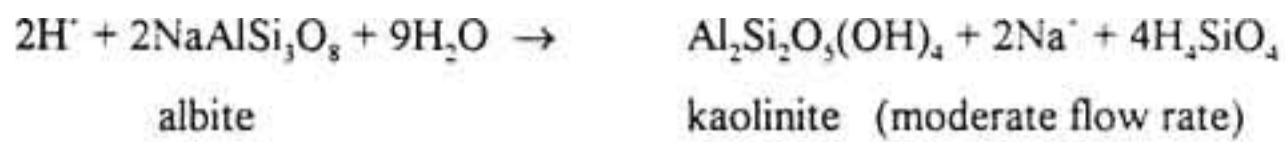
The rate of weathering is determined by the H^+ ions present in the water. The oxidation of organic matter by bacterial activity releases CO_2 which reacts with water forming carbonic acid. The reaction can be represented as[1]:

$$H_2O + CO_2 \Leftrightarrow H_2CO_3 \Leftrightarrow HCO_3 + H^+ \Leftrightarrow 2H^+ + CO_3^{2-}$$

Other sources of H^+ ions are the organic acids and exchangeable H^+ and the hydrolysis of Al^{3+}. Release of H^+ ions by the Al hydrolysis can be represented by the following equations[1]:

$$Al^{3+} + H_2O \Leftrightarrow Al(OH)^{2+} + H^+ \text{ (very high acid condition)}$$

or

$$Al^{3+} + 3H_2O \Leftrightarrow Al(OH)_3 + 3H^+ \text{ (less acid condition)}$$
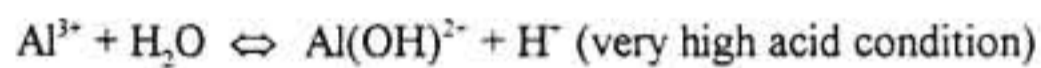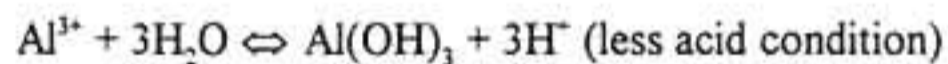
Kaolinite can be formed from a variety of minerals depending on the nature of weathering environment[10-14]. Some of the common minerals include:

Potash feldspar + water $\rightarrow$ Kaolinite + silica

Muscovite $\rightarrow$ Muscovite/Smectite (or Muscovite/Vermiculite) $\rightarrow$ Smectite $\rightarrow$

Kaolinite

Biotite $\rightarrow$ Fe dioctahedral mica $\rightarrow$ illite $\rightarrow$ kaolinite

1.3.1. Precipitation of kaolinite from a colloidal solution

The freshly fractured surfaces of the feldspars and the alumino silicate minerals have surface oxygens. Beneath the exposed oxygen, occur cations like Si, Al, Fe, Mg, Ca, K and Na. The fractured surfaces are more active than the ordered interior of the crystals[15] which when comes into contact with water, the H^+ ions will replace the alkali and alkaline earths. Thus in

4

the case of feldspars, a thin H⁺ film will be formed on the surface[16]. The reaction can be written as:

$$H^+_{aq} + K \text{ spar} \rightarrow H \text{ spar} + K^+_{aq}$$
$$\text{surface} \qquad \text{surface}$$
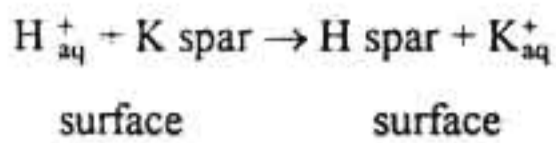
The rate of reaction is controlled by pH. At pH above 5, dissolved aluminium precipitates as $Al(OH)_3$[16]. The dissolved silica (H_4SiO_4) in the solution becomes concentrated enough and coprecipitate to form kaolinite. The electrostatic attraction between silica and alumina occurs at pH values lower than their isoelectric points. The oxides and hydroxides of Al have isoelectric points below pH 7.7 and the surface charge of SiO_2 is negative at any pH above 2. This explains the formation of Kaolinite at neutral to mild acid environments[17].

1.3.2. Structure of kaolinite

The structural unit of kaolinite[2] is built up of two individual sheets - a single tetrahedral sheet and a single octahedral sheet (Fig.1.1). These two sheets combined to from a 1:1
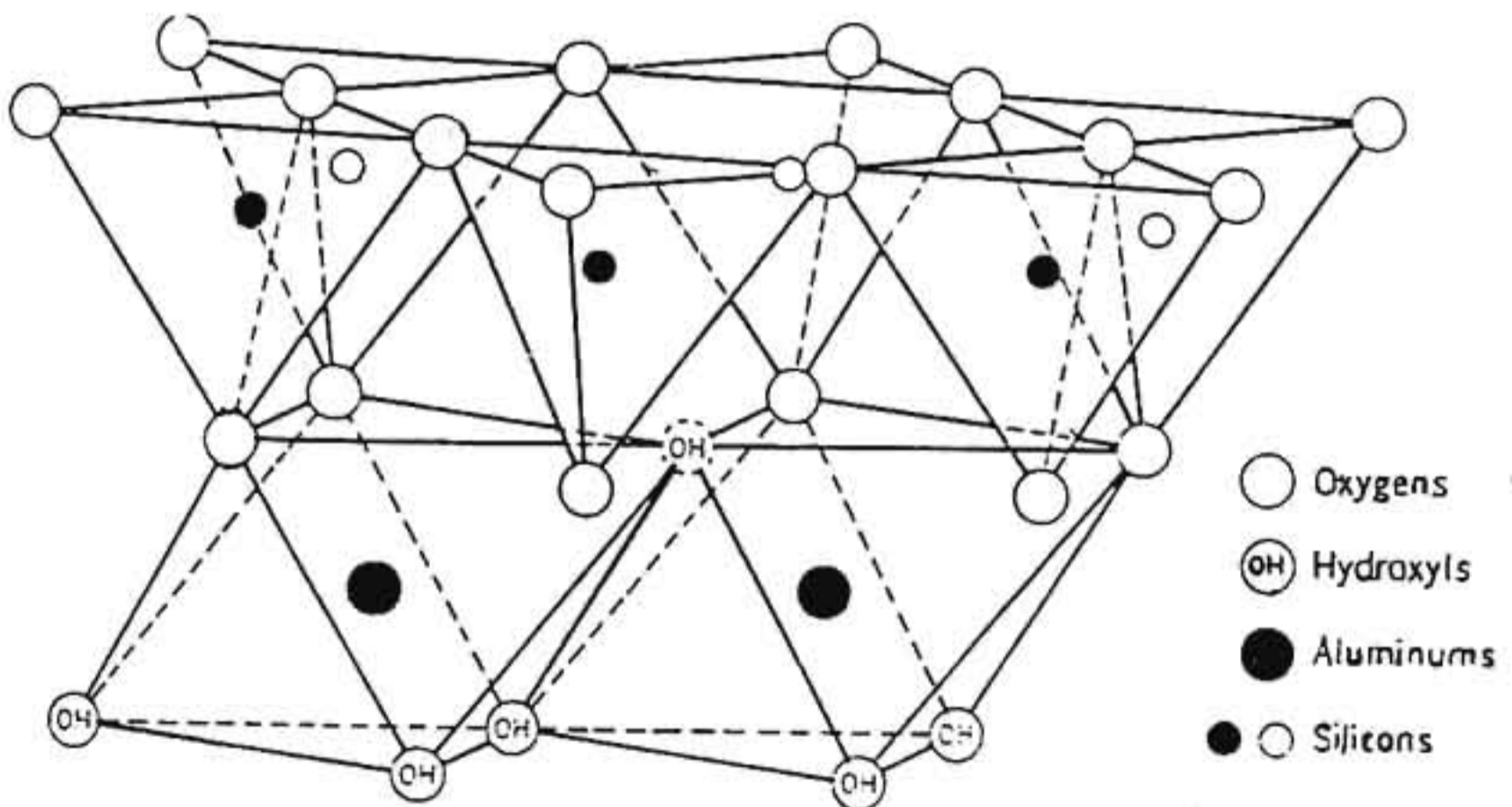
Fig.1.1. Layer structure of kaolinite[18]

5

layered structure to kaolinite. The layer thickness is 7.15 Å for a well-crystallized kaolinite and it may vary according to the interlayer water between the units[2] (Fig.1.2). The tetrahedral and the octahedral sheets have a common plane in which two-thirds of the atoms are shared by the silicon and aluminium, and then they become O instead of OH. The aluminium atoms are considered to be so placed that two aluminiums are separated by an OH above and below, which gives a hexagonal planar view in the centre of the octahedral sheet. The OH groups are placed so that each OH is directly below the perforation of the hexagonal net of oxygens in the tetrahedral sheet.

A possible mode of formation of the layered structure of kaolinite can be explained on the basis of laboratory model experiments[19]. From a dilute solution of SiO_2 and Al_2O_3, the $Si(OH)_4$ molecules polymerize to give monosilicic and disilicic acids by splitting off water: The siloxane bonds thus formed polymerize to form tetrahedral sheets.

$$2\left(\begin{array}{c} OH \\ | \\ OH-SI-OH \\ | \\ OH \end{array}\right) \longrightarrow \left(\begin{array}{c} OH \quad\quad OH \\ | \quad\quad\quad | \\ OH-SI-O-SI-OH \\ | \quad\quad\quad | \\ OH \quad\quad OH \end{array}\right) + H_2O$$

Monosilicic acid   **Disilicic acid**
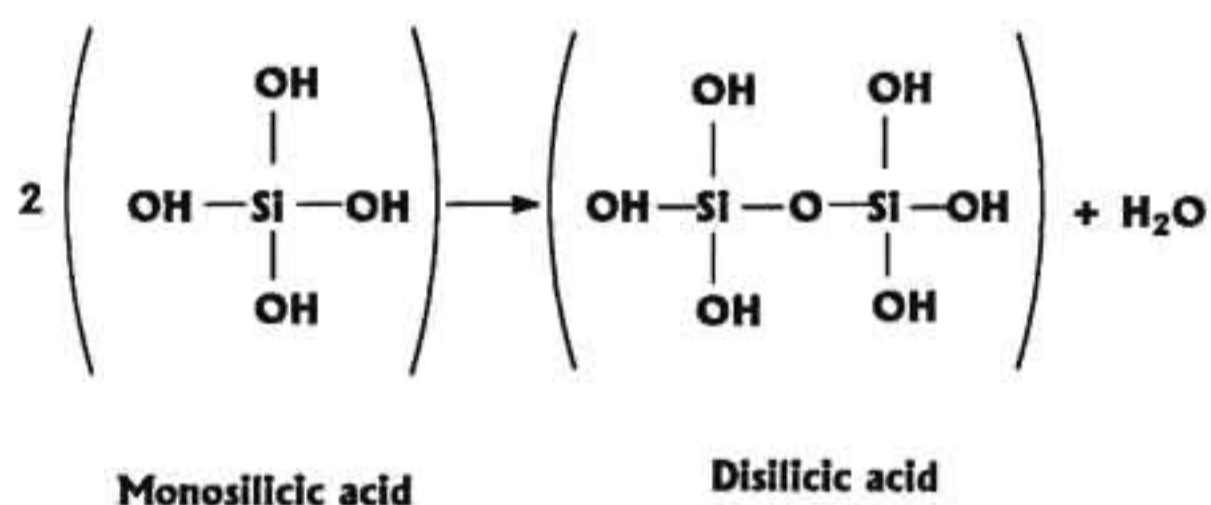
The negative end of water molecules are attracted by the Al^{3+} ions to form hydrated $[Al(H_2O)_6]^{3+}$ which progressively replaces water molecules and become $Al(H_2O)_3(OH)_3 + H_2O$. They polymerize to form octahedral sheets.

6

Fig.1.2. Lattice image of kaolinite showing layer thickness 7.1 Å
(kaolinite from Jaipur)

HO
   \
HO —— Si—O —Al—O—Si —OH   + H⁺
   / |
HO   OH

OH
   \
OH —— Si—O—Al   + H⁺
   /   \
OH   OH
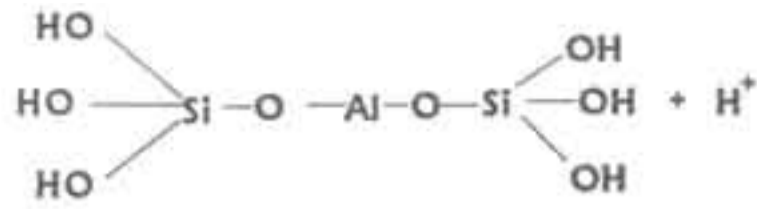
Or
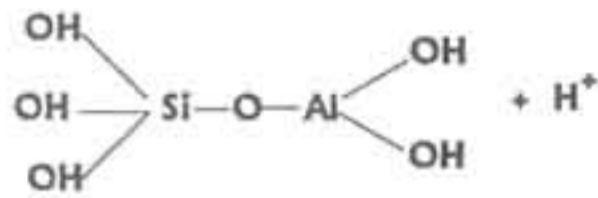
The $Si(OH)_4$ can combine with Al-hydroxy oxides to form two types of monomers. At appropriate pH and Si concentration, the 1:1 silicates are precipitated and polymerize to form sheet structures.

1.3.3. Composition of Kaolinite

Kaolinite is a hydrous aluminium silicate in which the Al/Si ratio approximates to unity[20]. The overall composition of kaolinite is $Si_4Al_4O_{10}(OH)_8$ and when expressed in individual oxides as SiO_2 - 46.5%, Al_2O_3 - 39.5% and H_2O - 14.0%. This ideal composition may vary according to their mode of origin and parent material composition. Ancillary minerals like quartz, mica, feldspars, rutile/anatase, oxides and hydroxides of iron may often encounter in smaller quantities.

In addition to inorganic chemical weathering, organic processes also play an important role in the formation of kaolinite[21,22]. The biologically produced chelating agents such as oxalic,

8

acetic, formic, fulvic and humic acids form soluble complexes by exchanging H^+ with Al, Fe, Si, Ca, Na, Mg, etc. In natural soil conditions, fulvic acid[23] promotes kaolinite crystallization from solutions of Al and Si through chelation of Al^{3+} ions while maintaining them in the octahedral coordination. Studies by Kodama et al.[24] indicates that biotite is more soluble than chlorite in fulvic acid medium.

Microbial alteration is another mode of chemical weathering in which the mineral transformation is brought about by enzymatic oxidation or reduction processes[25,26]. Fresh rocks are readily susceptible to the attack of bacteria, algae, fungi, lichen, moss etc. During their growth, the pH reduces considerably (< 3)[27] indicating the production of biogenic acids such as oxalic, citirc, glutamic etc. These acids actively take part in the dissolution of Al, Si, Fe, Ca, K etc. from the parent material.

Hydrothermal deposits are formed by the action of circulating hot water in the country rock. The circulating water gets heated up either by the presence of an intrusive body or abnormal amounts of radiogenic elements. The solutions escaping from the ore body are enriched with a large amount of acids which on reaction with the feldspathic minerals at acidic conditions below 400°C gives rise to kaolins[28]. Thus kaolin is a common alteration product of acid metasomatism.

Solfatara is the typical alteration product of volcanic rocks. When sulphur rich steam or hot water passing through the acid volcanics produces a combination of fine silica and kaolinite. These deposits are rich in silica and hence can be used as a good abrasive material. The main use of solfatara is in the manufacture of white cement.

In the case of secondary clays, the product of weathering is subjected to erosion, transportation and final deposition in sedimentary basins like lakes or oceans, where it will be

subjected to diagenesis, a process leading to the formation of secondary kaolns. In tropical climates, this compacted mass can undergo further weathering changes, resulting in more value added products. Thus, in most areas, kaolins are originated by a combination of the primary and secondary processes. The whole process in a weathering environment can be summarised in the rock cycle as shown in Fig.1.3[8].
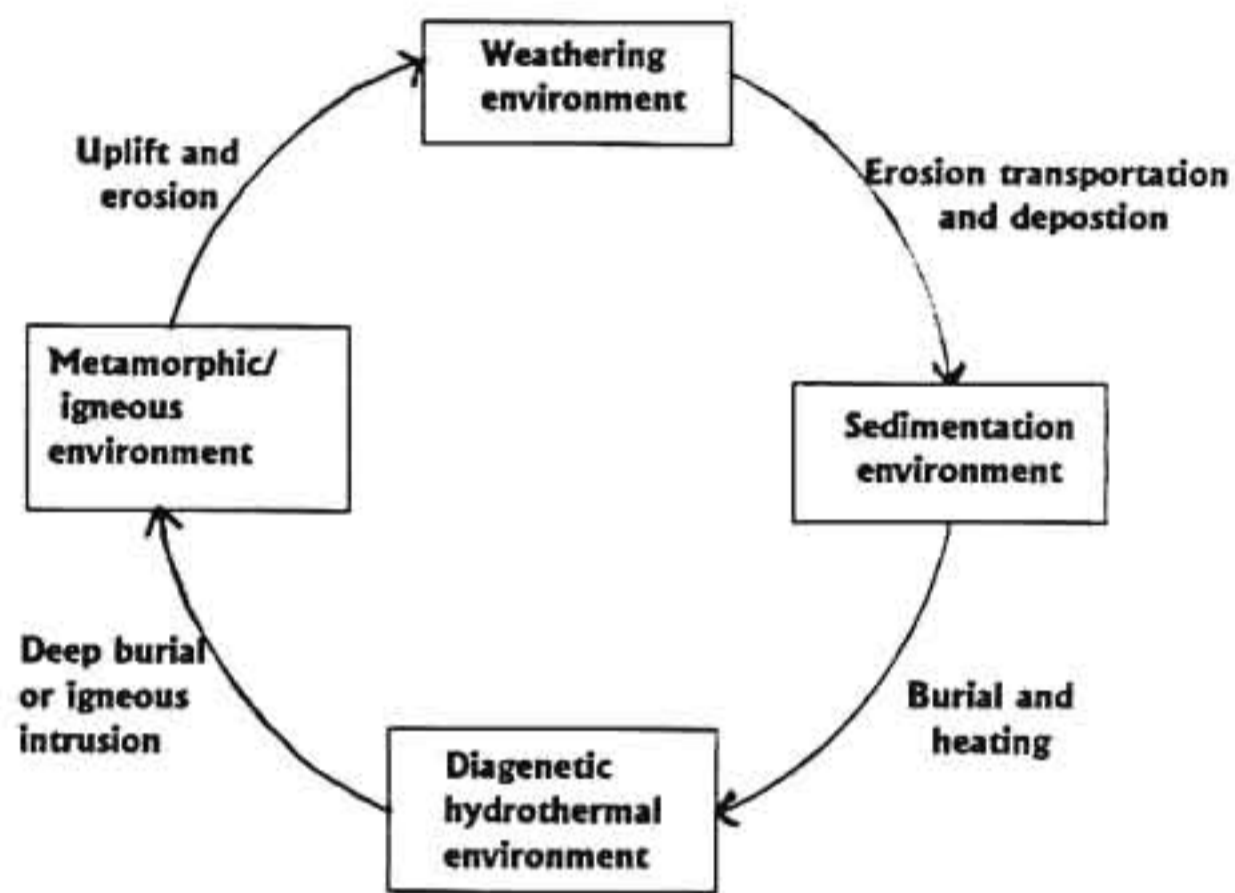
Fig.1.3. Sedimentary cycle representing the interrelationship between various environments at which clay minerals are formed

1.4. IRON OXIDES IN CLAYS

Iron is the fourth most abundant element in the earth's crust[29]. The average concentration of Fe in the earth's crust is 5.00%[30]. Because of its relative abundance, iron becomes an invariable part of many rock forming minerals including clays. It occurs in a large varieties of minerals including sulphides, oxides, hydrous oxides, and other complex hydroxides.

10

High purity kaolin deposits are rare in occurrence. However, in nature, all the economic reserves of kaolin are contaminated by small amounts (0.5 to 3%) of ferruginous minerals - mainly the oxides, hydroxides and oxyhydroxides of Fe, rutile, siderite, pyrite, mica and tourmaline. Their concentration above a certain level (generally > 0.4%) cause unacceptable colouring, which markedly reduces the whiteness of the material, thereby lowering the commercial value of the product and makes it impossible to use them in numerous traditional applications (ceramic white wares and paper filling/coating) and more advanced applications. Therefore, certain degree of whiteness is a requirement for the value addition of the product. Usually kaolinite with brightness values > 80% (ISO) are suggested for paper filling/coating applications.

Iron occurring in kaolin is grouped into two (a) the soluble or free Fe_2O_3 (b) bonded or fixed Fe_2O_3. The former represents the total content of amorphous iron oxide coating (staining) the surface of kaolinite and also the fine-grained crystalline, whereas the latter includes iron incorporated into the structure of kaolinite and mica. The discolouration of kaolin in the non-fired state is commonly attributed to the free iron oxides than the fixed ones. But at higher temperatures (350-800°C), the presence of bonded Fe reduces the whiteness due to its liberation from the kaolinite structure to a most common oxide form - hematite.

The pigmentation produced by the ferric oxide minerals varies from red to yellow depending on the minerology of associated iron oxide. In general, clays containing hematite are reddish-pink and goethite are yellowish-brown in appearance. Table 1.1 represents some of the naturally occurring iron oxides in clays and their corresponding colour designations[31].

11

Table 1.1. Commonly occurring iron oxides in clays

Mineral	Colour
Hematite	Red
Maghemite	Reddish-brown
Goethite	Brownish-yellow
Lepidocrocite	Orangish-yellow
Akaganeite	Brown
Feroxyhite	Yellowish to brown
Ferri hydrite	Yellowish brown to dark brown and reddish

A brief account of the major iron oxide minerals associated with kaolinite is given below:

Goethite (α-FeOOH): It is the commonest oxyhydroxide of iron, which is considered as the most stable iron oxide phase under normal soil conditions. The structure of goethite is depicted in Fig.1.4. The Fe(III) ions are sited in the octahedral position which forms double chains of octahedra along the c-axis as shown in the figure.
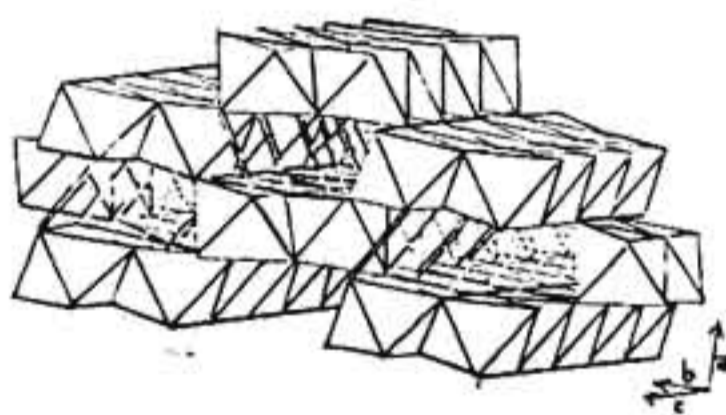
Fig.1.4. An Octahedral model of goethite structure[32]

12

Hematite (α-Fe$_2$O$_3$)

The dehydration product of poorly crystalline ferrihydrite at low temperature is hematite. The presence of small amounts of Al in the solution favours hematite formation rather than goethite[33]. The hematite structure consists of a closely packed hexagonal planes of O atoms with Fe(III) ions in the octahedral sites. Each Fe(III) is surrounded by 6 oxygen atoms and each O is shared by 4 Fe(III) ions. Hematite is readily marked by the red coloration of the soils.

Lepidocrocite (γ-FeOOH): The occurrence of lepidocrocite is limited to hydromorphic soils where microbial reduction under anaerobic conditions leads to the presence of soluble Fe(III) hydroxy species which on further oxidation under a suitable environment forms lepidocrocite[20]. It is a polymorph of FeOOH. The structure is almost similar to goethite, but the octahedral chains in lepidocrocite are jointed to form corrugated layers (Fig.1.5).
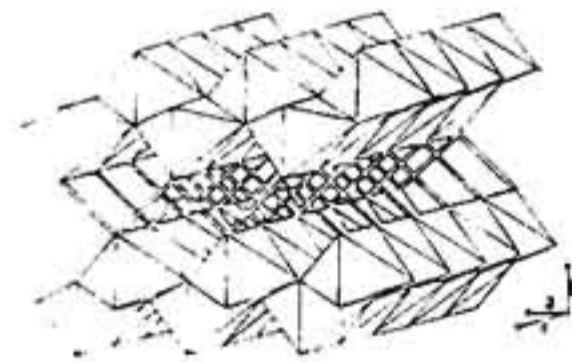
Fig.1.5. An octahedral model of lepidocrocite structure[32]

Ferrihydrite (5Fe$_2$O$_3$.6H$_2$O): It is a precursor of hematite and possible source of goethite[20]. Its colour can vary from yellow-brown to brown-red depending on the mode of formation. Rapid precipitation of ferrihydrite, at higher temperatures and higher Al concentrations

13

produces hematite and increased pH favours goethite formation. The crystallinity of ferrihydrite is very low and has only a few defined peaks in the X-ray diffraction pattern[34]. Feroxyhite (δ'-FeOOH) is another poorly crystalline material resembling ferrihydrite.

Magnetite and maghemite (Fe_3O_4 and γ-Fe_3O_4): Although they are isostructural minerals, some arbitrary definition can be used to distinguish them. According to Fasiska[35], magnetites have the Fe/O ratio in the short range, 0.74-0.75, whereas in maghemite, this value decreases from 0.72 to 0.67.

Akaganeite (β-FeOOH): It is a polymorph of FeOOH. This iron oxide is rare in normal soil conditions.

1.4.1. Separation of iron oxides from clays

The ferric oxide minerals amount only to a few percentage in the bulk clay mass. Their poor crystallinity and low concentration often require some separation and concentration techniques for their identification. Some of the commercially useful methods are froth flotation, selective flocculation and magnetic separation[36-39]. Froth flotation process is well accepted for removal of titaniferous impurities from clays. In this method, a surface active reagent is used to make the impurity particles hydrophobic which will eventually be removed through a stream of air bubbles with the help of a frothing agent. Another well practised method is selective flocculation which makes use of a polymeric flocculant to aggregate the impurities to form flocs. They settle rapidly at the bottom of the container. Another most versatile technique for iron oxide removal is magnetic separation. The process is well explained in the next chapter.

1.4.2. Dissolution techniques for iron oxides

Most of the dissolution techniques available are not mineral specific. The complexity arises when two or more minerals have the same dissolution properties. Moreover, the

14

dissolution properties are affected by the crystal size, substitution in active sites, crystallographic faces exposed, and the density of surface imperfection. Thus, the dissolution processes enable the determination of a group of Fe phases such as organic Fe, amorphous Fe etc. Generally, the dissolution processes can be classified into two major categories[40]:

i) using mineral acids, and

ii) using organic acids or organic ligands with or without reducing agents.

Some of the commonly used Fe dissolution processes are listed in Table 1.2.

Table 1.2. Some procedures for selective dissolution of Fe[40]

Reagents	Type of iron oxide phase removed
Dithionite-citrate-bicarbonate; pH-7	Total 'Free" Fe
Oxalate-dithionite	"
Dithionite-citrate; pH variable	"
Sequential 8M HCl and 0.5 M NaOH	"
NH_4-oxalate + oxalic acid, pH-3	"Amorphous" inorganic + organic Fe
Ethylenediaminetetra-acetic acid (EDTA)	"Amorphous" inorganic
Hydroxylamine hydrochloride +HCl	"
Pyrophosphate solutions	"
Acetylacetone in benzene $NaOH + Na_2B_4O_7$	"Organic" Fe
Diethylenetriaminepenta-acetic acid (DTPA)	"Availabe" Fe
$HgCl_2$ + NH_4Cl plus anion exchange	Metallic Fe

1.4.3. Determinative methods for Iron

The iron content in clays may be determined by any one of the methods like, titrimetry, colorimetry or electrical methods. In addition to this, a large number of instrumental methods are also available for the Fe analysis in clays. Table 1.3a&b give a brief account of some of the selected instrumental Fe determination methods[40].

15

Table 1.3a. Some microbeam techniques for determination of Fe

Procedure	Excitation source	Area analysed	Beam penetration	Volume analysed (μm^3)	Detection limit (mg kg^{-5})
Electron probe	W-filament	~3 μm^2	0.5 μm	1-10	>50
XPS (ESCA)	Al or Mg filament	1-50 mm^2	~20 Å	100	0.31*
AES	20-30 keV electron gun	~500 nm^2	<10 Å	<10^{-5}	-
L(AM)MA	Nd laser (UV region)	1-20 μm^2	<0.5 μm	<3	~10^{-3}
PIXE	1-4 MeV protons	Variable	Variable	Variable	10^{-3}

*percent

Table 1.3b. Some non-microbeam techniques for determination of Fe

Method	Excitation source	Recommended wavelength (nm)	Detection limit (mg dm^{-3})
AAS	Air-C_2H_2 or N_2O-C_2H_2	248.9	< 0.5
AAS-GF	Electrothermal atomizer	248.9	< 0.1
AES	N_2O-C_2H_2 flame	372	<0.5
XRFS	Au-tube	0.19	0.12
ICP-AES	Ar-plasma	259.94	<0.5
INAA	Nuclear reactor	-	<0.002*
SSMS	High-voltage "Spark"	-	<0.01

*milligrams Kg^{-1} as % of whole soil

1.5. USES OF KAOLIN

The most important use of kaolin is in the paper industry. Around 80% of this goes into paper coating and filling applications. The use of kaolin as filler improves the optical properties such as brightness and opacity. Moreover, it can replace the expensive chemically refined pulp. Kaolins are prepared for acid (rosin) papers and papers containing ground wood, whereas in

Europe, calcium carbonate is preferred for neutral and alkaline papers. Kaolins used for these purposes need to have specific rheological and optical properties.

In the ceramic industry, kaolins are used for the production of table wares, sanitary wares, flooring and facing tiles etc. Usually white china clays and ball clays are selected for these purposes.

Alumina rich clays and flint clays are used for the production of refractory bricks.

The principal function of kaolin in the paint industry is to act as a substitute for the expensive TiO_2. In alkyd undercoats and in water based paints, kaolins are used extensively. High whiteness, good opacity and extremely fine particle size give finish to the paint film.

This material imparts good reinforcing when used as filler in rubber. They also affect the primary set and colour. Calcined clays provide good electrical properties for insulation cables. In polymer industry, they have special functions. It is used as an important filler material in pharmaceuticals, cosmetics, insecticides, plastics, etc. Calcined kaolin when used as a filler in polythene films enhances the infra-red absorption character, thereby helping to retain heat in green houses. In addition to these applications kaolin finds use as raw material for the production of zeolites and acid activated clays.

Different types of surface modified kaolinites, new ceramic composite materials etc., are some of the results of modern research in this area.

1.6. WORLD KAOLIN SOURCES

The largest producers of kaolin are Georgia Kaolin Co., Engelhard & Evans, and Thiele Kaolin Co. of the United States of America and English China Clays of U.K. Brazil, UK,

17

Australia, India, Romania, Thailand, South Korea, China and Russia are the other major producers of coating grade kaolin.

1.7. NATIONAL SCENARIO

In India, the total resource including the proved, possible and probable deposits was estimated to be around 9860 lakh tonnes according to the 1990 survey[41]. Rajastan is the leading producer of china clay (29%) followed by West Bengal (17%), Kerala (12%), Delhi (10%), Gujarat (8%), Andhra Pradesh (7%), Bihar (6%) and Haryana and Orissa, (3%) each. Open cast manual mining is practised in most of these mines. Kaolin is marketed as supertextile , textile, paper, pottery and rubber grades.

In the present investigation, china clay deposits belonging to South Kerala and Jaipur (Rajasthan) are selected for different types of beneficiation studies.

1.8. A BRIEF DESCRIPTION OF GEOLOGY OF CHINA CLAY DEPOSITS OF SOUTH KERALA

The Precambrian crystalline rocks form the oldest and most prominent rock formations in Kerala[42]. They comprise the high-grade Archaean Supracrustals, khondalites, charnockites granites, pegmatites, quartz veins and basic dykes. A large part of the South Kerala is occupied by a group of meta sediments known by the name -the Khondalite group. The chief rocks of this group include granet-sillimanite-biotite-graphite schist, garnet-biotite + graphite gneiss, calc granulites, quartzites and patchy charnockites[42]. These crystalline rocks are overlained by the sedimentary formation of tertiary age. The Tertiary formations of Kerala were originally studied by King (1882)[43] and Foote (1883)[44]. Further investigations were carried out by Jacob and Sastri (1952)[45], Narayanan (1958)[46], and Desikachar and Subramanyam (1959)[47]. Based on the lithology, Paulose and Narayanaswami[48] proposed the following stratigraphic succession for these sedimentary rocks.

| Recent to sub-recent | - | Soils and alluvium
Beach sand deposits
Lime shell deposits of backwaters
Old and red Teri sands of Subrecent marine and lacustrine formations
Peat beds with semi-carbonised woods
Calcareous clays with shell etc.
Laterite |

------ *Unconformity* ----------

Warkalli Formation	Current-bedded friable variegated sandstone interbedded with plastic clay and variegated clays
	Carbonaceous and alum clays with (Mio-Pliocene) lignite seams
Quilon Formation (Middle Miocene)	Gravel and pebble beds, base marked by gibbsitic sedimentary clay
	Fossiliferous shell limestone alternating with thick beds of sandy clays, calcareous clays and sandstones.
	Base unknown

--------- *Unconformity* ---------

| Archaean | Crystalline rocks |

Three distinct formations are identified in the upper Tertiary sediments. All these formations are yielding thick deposits of sedimentary kaolin. The Warkarlli Formation is the topmost formation of this group which is underlain by the Quilon Formation. Below these, two, occur the so-called "Vaikom beds"[49].

The major china clay deposits of Kerala are located in the districts of Thiruvananthapuram, Kollam, Kannur and Kasaragod. Extensive field data indicate that all the known china clay deposits can be classified under residual and sedimentary types only[50]. The occurrence of residual kaolin is reported from places like, Karuchal (Thiruvananthapuram) Kundara (Kollam) and Palayangadi (Kannur)[51]. In Kundara, the Cenozoic sediments of the

Warkalli formation are underlain by kaolinized gneiss. Adjoining places like Mulavana, Chathannur, Nallila also yield good reserves of residual china clay deposits. The parent material for this residual clays are the underlying felsic Khondalite rocks which on chemical weathering changed to thick clay horizons.

In Kerala, sedimentary kaolin predominates over the residual variety[51]. Good deposits of sedimentary kaolin are reported from Thiruvananthapuram, Kollam, Alappuzha, Ernakulam and Kannur districts. The promising localities in the Thiruvananthapuram district include Thonnakkal, Sasthavattom, Chilambil and Pallipuram. These sedimentary clays are belonging to the Warkalli beds of Mio-Pliocene age[52,53] which attain a maximum thickness of 4.5 m at Thonnakkal and adjoining places in Thiruvananthapuram district[54]. The Warkallis Formation is well developed in nearly horizontal pattern along the entire coastal track extending from Cape Comorin in the south to Ernakulam in the north, bordering the backwaters on the east, but are obscured beneath the recent alluvium[55]. This formation can be traced in the near shore regions also. The Warkalli Formation is also well developed at places like, Vettur, Kundara, Thonnakkal and Puliyur[51]. The presence of plant fossils[52], lignite, marcasite and the angular and poorly sorted sand grains as well as the absence of non-clastic materials like limestone and detrital materials etc. suggests a shallow water shore line "littoral depositional" environment for the Warkalli Formation[55]. Based on the petrographic and mineralogic studies, Soman et al.[53] concluded a Khondalitic parent material for these kaolins. According to their view, the proximity of these deposits to the khondalite terrain and the presence of minerals such as graphite and sillimanite are the supporting evidence for the above conclusion.

The iron oxides present in the china clay beds of South Kerala are well studied by Ghosh[56,57]. He observed that distribution of Fe is not uniform within a single clay deposit and also it showed definite special variations. The explanation for higher Fe concentration in upper

profile is related to Fe-oxidising bacterial activities and presence of oxygenated waters and lower amount of Fe encounted at deeper positions are attributed to the dissolution activity of acidic water in an oxygen deficient environment.

1.9. A BRIEF DESCRIPTION OF THE GEOLOGY AND CHINA CLAY DEPOSITS OF RAJATHAN

The major rock types of this region include the Archaean and Precambrian gneisses (a pink to reddish, medium-grained, granite with chief minerals, quartz, orthoclase, microcline and a little of ferruginous minerals), pegmatites, aplites, phyllites, limestones, quartzites, composite gneisses and shales with clay concretions[58-62]. Archaean and the other Precambrian rocks have together formed the great Aravalli ranges. In many places, the Aravalli rocks are intruded by granitic masses. Vast clay deposits are encountered on the weathered crusts of these granites and pegmatites. Both primary as well as secondary clay deposits are reported from Rajasthan, of which the former predominates over the latter one. The occurrences of china clays are mainly located in the districts of Chittorgarh, Bhilwara, Jaipur and Bikaner. Minor deposits are also located in Udaipur, Sawai, Madhopur, Bundi and Pali districts[61].

The present investigation is focused on the characterization and beneficiation of five iron-stained clays from India. The whole work is divided into five chapters: (a) an overview of the classification, genesis, and application of kaolins and a general geology of South Kerala and Rajasthan, (b) characterization and identification of the major clay mineral and associated impurities in the study area, (c) physical beneficiation of the iron-stained clays by magnetic separation, (d) chemical beneficiation using sucrose, dithionite and organic acids and (e) a comparative study on the discolouration imparted by natural and synthetic goethite on kaolinite.

REFERENCES

1. Weaver, C.E., 1989., Clays, Muds and Shales - Developments in Sedimentology - 44, Elsevier, Amsterdam, 819p.

2. Grim, R.E., 1968. Clay Mineralogy, 2nd edn. McGraw-Hill, New York, 596p.

3. Guggenheim, S. and Martin, R.T., 1995. Definition of Clay and Clay Mineral: Joint Report of the AIPEA Nomenclature and CMS Nomenclature Committees. Clays Clay Miner., 43, 255-256.

4. Deer,W.A., Howie, R.A. and Zussman, J., 1962. Rock forming Minerals, Longman, London, 270p.

5. Bristow, C.M., 1987. World Kaolins: Genesis, Exploitation and Application. Ind. Miner., 45-59.

6. Kuzvart, M. 1984. Industrial Minerals and Rocks. Elsevier, Amsterdam, 307-316.

7. Bristow, C.M., 1977. A review of the evidence for the origin of the kaolin deposits in S.W.England. Proc. 8th Int. Kaolin Symposium and Meeting on Alunite, Madrid, 1977.

8. Hall, P.L., 1987. Clays: their significance, properties, origins and uses. In: Wilson, M.J. (Eds.), A Handbook of Determinative Methods in Clay Mineralogy. Blackie, 308p.

9. Berner, R.A., 1971. Principles of Chemical Sedimentology, McGraw-Hill, New York, 240p.

10. Sutner, L.J., Mack, G., James, W.C. and Young, S.W., 1976. Relative alteration of microcline and sodic plagioclase in semiarid and humid climates. Geol. Soc. Am., 8. 512p.

11. Stoch, L. and Sikora, W. 1976. Transformation of micas in the process of kaolinization of granites and gneiss. Clays Clay Miner., 24, 156-162.

12. Eswaran, H. and Wong Chaw Bin., 1978. A study of a deep weathering profile on granite in Peninsular Malaysia: III. Alteration of feldspars. Soil Sci. Soc. Am. J., 42, 154-158.

13. Heckroodt, R.O. and Bühmann, D. 1985. Genesis of South African residual kaolins from sedimentary rocks. In: Schultz, L.G., van Olphen, H. and Mumpton, F.A. (Eds.), Proc. Int. Clay Conf., Denver, 128-134.

14. Shayan, A., Lancucki, C.J. and Way, S.J., 1985. Clay mineralogy of a weathered granophyre from north Queensland, Australia. In: Schultz, L.G., van Olphen, H. and Mumpton, F.A. (Eds.), Proc. Int.Clay Conf., Denver, 111-120.

15. Keller, W.D., 1978. Kaolinization of feldspars as displayed in scanning electron micrographs. Geol., 6, 184-188.

16. Wollast, R., 1967. Kinetics of the alteration of K-feldspar in buffered solutions at low temperature. Geochim. Cosmochim. Acta, 31, 635-648.

17. Siffert, B., 1978. Genesis and Synthesis of clays and clay minerals: recent developments and future prospects. Proc. Int. Clay Conf., Oxford, 337-347.

18. Gruner, J.W., 1932. The crystal structure of kaolinite, Z. Krist., 83, 75-88. In: Grim, R.E. (Ed.), 1968. Clay Mineralogy, 2nd edn., McGraw-Hill, New York, 596p.

19. Siffert, B., 1967. Some reactions of silica in solution: Formation of clay. Israel Programs for Scientific Translations, Jerusalem, 100p.

20. Newman, A.C.D., 1987. Chemistry of clays and clay minerals. Mineralogical Society Monograph, No.6, John Wiley, New York, 480p.

21. Hughes, R.E., De Maris, P.J., White, W.A. and Cowin, D.K., 1985. Origin of clay minerals in Pennsylvanian Strata of the Illinois basin. In: Schultz, L.G., van Olphen, H. and Mumpton, F.A. (Eds.). Proc. Int. Clay Conf., Denver, 97-104.

22. Loughnan, F.C., 1981. Genesis and synthesis: Kaolins in sediments. In: van Olphen, H. and Veniale, H. (Eds.), 1982. Proc. Int. Clay Conf., 1982, Italy, 487-494.

23. Linares, J. and Huertas, F., 1971. Kaolinite synthesis at room temperature. Science, 171, 896-897.

24. Kodama, H., Schnitzer, M. and Jaakkimainen, M.J., 1983. Chlorite and biotite weathering by fulvic acid solutions in closed and open systems. Can. J. Soil Sci., 63, 619-629.

25. Parfenova, E.I. and Yarilova, E.A., 1962. Mineralogical investigations in soil science. Moscow Acad. Sci., Russia, 177p.

26. Schatz, A., 1963. Soil microorganisms and soil chelation - the pedogenic action of lichens and lichen acids. Agric. Food Chem., 11, 69-102.

27. Silverman, M.P. and Munoz, E.F., 1970. Fungal attack on rock: Solubilization and altered infrared spectra. Science, 169, 985-987.

28. Turner, F.J. and Verhoogen,J., 1987. Igneous and metamorphic petrology, 2nd edn., McGraw-Hill, New York, 694p.

29. Murad, E. and Fischer, R.F.., The Geobiochemical cycle of iron. In: Stucki, J.W., Goodman, B.A. and Schwertmann, U. (Eds.), 1988. Iron in soils and clay minerals, D. Reidel , Holland, 893p.

30. Brain Mason and Moore, C.B., 1991. Principles of goechemistry, 4th edn. (reprint), Wiley Eastern, New Delhi, 350p.

31. Schwertmann, U., 1993. Relations between iron oxides, soil colour and soil formation. In: Bigham, J.M. and Ciolkosz, E.J. (Eds.), Soil Colour, Soil Sci. Soc. Am., Special Publication, Madison, WI, 31, 51-69.

32. Ewing, F.J., 1935. The crystal structure of lepidocrocite. J. Chem. Phys., 3, 420-424. In: Stucki, J.W., Goodman, B.A. and Schwertmann, U. (Eds.), 1988. Iron in Soils and Clay Minerals, D. Reidel, Holland, 893p.

33. Schwertmann,U., Fitzpatrick, R.W., Taylor, R.M. and Lewis, D.G., 1979. The influence of aluminium on iron oxides. Part II: Preparation and properties of Al substituted hematites. Clays Clay Miner., 27,105-112.

34. Jambor, J.L. and Dutrizac, J.E., 1988. Occurrence and constitution of natural and synthetic ferrihydrite, a widespread iron oxhydroxide. Chem. Rev., 98, 2549-2585.

35. Fasiska, E.J., 1967. Structural aspects of the oxides and oxyhydrates of iron. Corrosion Sci., 7, 833-839. In: Newman, A.C.D., 1987.Chemistry of Clays and Clay Minerals. Mineralogical Society Monograph No.6, John Wiley, New York, 480p.

36. Fuerstenau, D.W., 1980. Fine particle flotation. In: Proc. Int. Sym. on Fine Particles Processing, Somasundaram, P. (Ed), Nevada, 1980, 669-605.

37. Kitchener, J.A., 1972. Principles of action of polymeric flocculants. Br. Polym. J., 4, 217-229.

38. Paterson, A.W. and Heckroodt, R.O., 1985. Effect of agitation conditions on the flocculation of kaolin with polyacrylamides. In: Schultz, L.G., van Olphen, H. and Mumpton, F.A. (Eds.). Proc. Int. Clay.Conf., Denver, 405-409.

39. Iannicelli, J., 1976. High Extraction Magnetic Filtration of kaolin clay. Clays Clay Miner., 24, 64-68.

40. Stucki, J.W., Goodman, B.A. and Schwertmann, U., 1988. Iron in Soils and Clay Minerals. D. Reidel , Holland. 893p.

41. Indian Minerals Yearbook, 1992. Indian Bureau of Mines, Nagpur, 132p.

42. Ravindrakumar, G.R., Rajendran, C.P. and Prakash,T.N., 1990. Charnockite-khondalite belt and Tertiary-Quaternary Sequences of Southern Kerala - Excrusion Guide. Geol. Soc. India, 116p.

43. King, W., 1882. General Sketch of the geology of Travancore State. Rec. Geol. Surv. India, 15, 93-102.

44. Foote, R.B., 1883. On the geology of South Travancore. Rec. Geol. Surv. India, 16, 20-35.

45. Jacob, K. and Sastri, V.V., 1952. Miocene formation fromChavara near Quilon, Travancore. Rec. Geol. Surv. India, 82, 342-353.

46. Narayanan, K., 1958. Report on the geological reconnaissance of Kerala. In: Soman, K. (Ed.), 1997. Geology of Kerala. Geol.Soc. India, 280p.

47. Desikachar, S.V. and Subramanyam, M., 1959. Progress report (Part II) on subsurface geology of parts of coastal Kerala. In: Soman, K. (Ed.), 1997. Geology of Kerala. Geol. Soc. India, 280p.

48. Paulose, K.V. and Narayanaswami, S., 1968. The Tertiaries of Kerala coast. Mem. Geol. Soc. India, 2, 330-308.

49. Raghava Rao, K.V., 1976. Groundwater exploration, development and long term aquifer management in Kerala. Proc. Symp. Mineral Resources of Kerala and their utilisation, Trivandrum, 1975, 30-36.

50. Soman, K., Terry Machado, Ancy Joseph and Sreelatha, R.K., 1993. Genetic types of china clays in South Kerala. Proc. 5th Kerala Sic. Congress, Kottayam, 37-40.

51. Soman, K., 1997. Geology of Kerala. Geol. Soc. of India, 280p.

52. Menon, K.K., 1967. Warkalli beds at Kolathur, Trivandrum district. Curr. Sci., 36, 102-103.

53. Soman, K. and Terry Machado., 1986. Origin and depositional environment of the china clay deposits of South Kerala. Proc. Indian Acad. Sci., 95, 285-292.

54. Soman, K., 1984. Geology and mineral resources of Trivandrum, Kerala (India). Unpbul. Ph.D. thesis, Peoples' Friendship Univ., Moscow, 245p.

55. Prabhakar Rao, G., 1968. Age of the Warkalli Formation and emergence of the present Kerala coast. Bull. Nat. Inst. Sci., 38, 449-456.

56. Ghosh, S.K., 1986. Geology and geochemistry of Tertiary clay deposits in South Kerala. J. Geol. Soc. India, 27, 338-351.

57. Ghosh,S.K., 1982. Geochemistry and origin of laterite and clay deposits in Southern Kerala. Technical Report-2, Centre for Earth Science Studies, 21p.

58. Krishnan, M.S. 1997. Geology of India and Burma, CBS, Delhi, 536p.

59. Srivastava, P. and Gupta, S.N., 1989. The Stratigraphy of Rajasthan. In: Mineral and Mining World, 1989. Geol. Surv. India, 9-12.

60. Mukerjee, P.K., 1990. A Textbook of Geology, World Press, Calcutta, 544p.

61. Series on Industrial minerals of Rajasthan Clays, 1992. Dept. of Mines and Geology, Govt. of Rajasthan, India, 1, 45p.

62. Sinha Roy, S., Malhotra, G. and Mohanty, M., 1998. Geology of Rajasthan. Geol. Soc. India, 278p.

Chapter 2
GEOLOGY AND CHARACTERIZATION

2.1. INTRODUCTION

The geology and geochemistry of the iron-stained clay deposits of South Kerala and Rajasthan, the techniques adopted for the identification and characterization of the major minerals and associated impurities, and the special methods used for the concentration and identification of iron oxides are dealt in this chapter.

2.2. MATERIALS AND METHODS

2.2.1. PROFILE DESCRIPTION OF CLAY DEPOSITS CHOSEN FROM KERALA AND RAJASTHAN

The geographical location of clay mines belonging to South Kerala is $8°\ 20' - 9°\ 30'$ N; $76°\ 30' - 77°\ 0'$ E and Rajasthan, $26°\ 30' - 27°\ 30'$ N; $75°\ 30' - 76°\ 30'$ E.

Both primary as well as secondary china clay deposits were selected to study the type of ferric oxide minerals which impart colour to the clay material. For this, iron-stained kaolin from five different localities namely, Akulam, Kerala (AK), Buchara, Rajathan (JK), Kalliyur, Kerala (KK), Mulavana, Kerala (MK) and Thonnakkal. Kerala (TK) were collected. Clay from Rajasthan was supplied by Sri Vishnu Kumar & Sons, Shri Modi Levigated Kaolin Pvt. Ltd., Neemkathana, Jaipur, Rajasthan.

(a) **Akulam:** The clay mine is located at a distance of 10 km north-west from Thiruvananthapuram district (South Kerala). Figure 2.1 represents the location map of the clay deposits. Basically four zones are identified in the deposit. The stratigraphic succession exposed at the mine is shown in Figure 2.2. The mottled zone in this deposit

28

is characterized by red and yellow patches of ferric oxide concentrations. Clay sample for the present investigation has been collected from the yellow mottles.
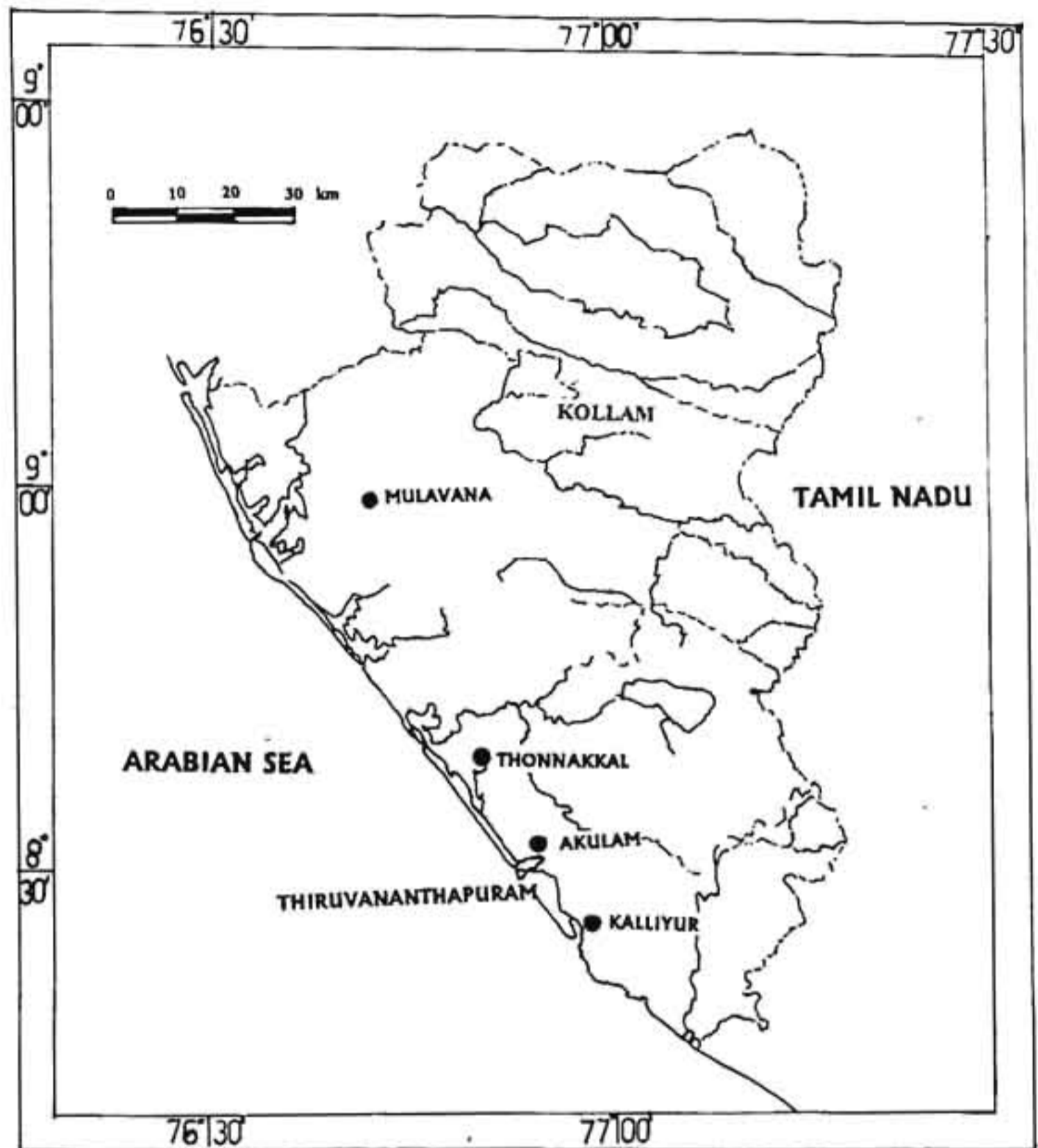
Fig.2.1. Location map of clay deposits at Akulam, Kalliyur, Mulavana and Thonnakkal
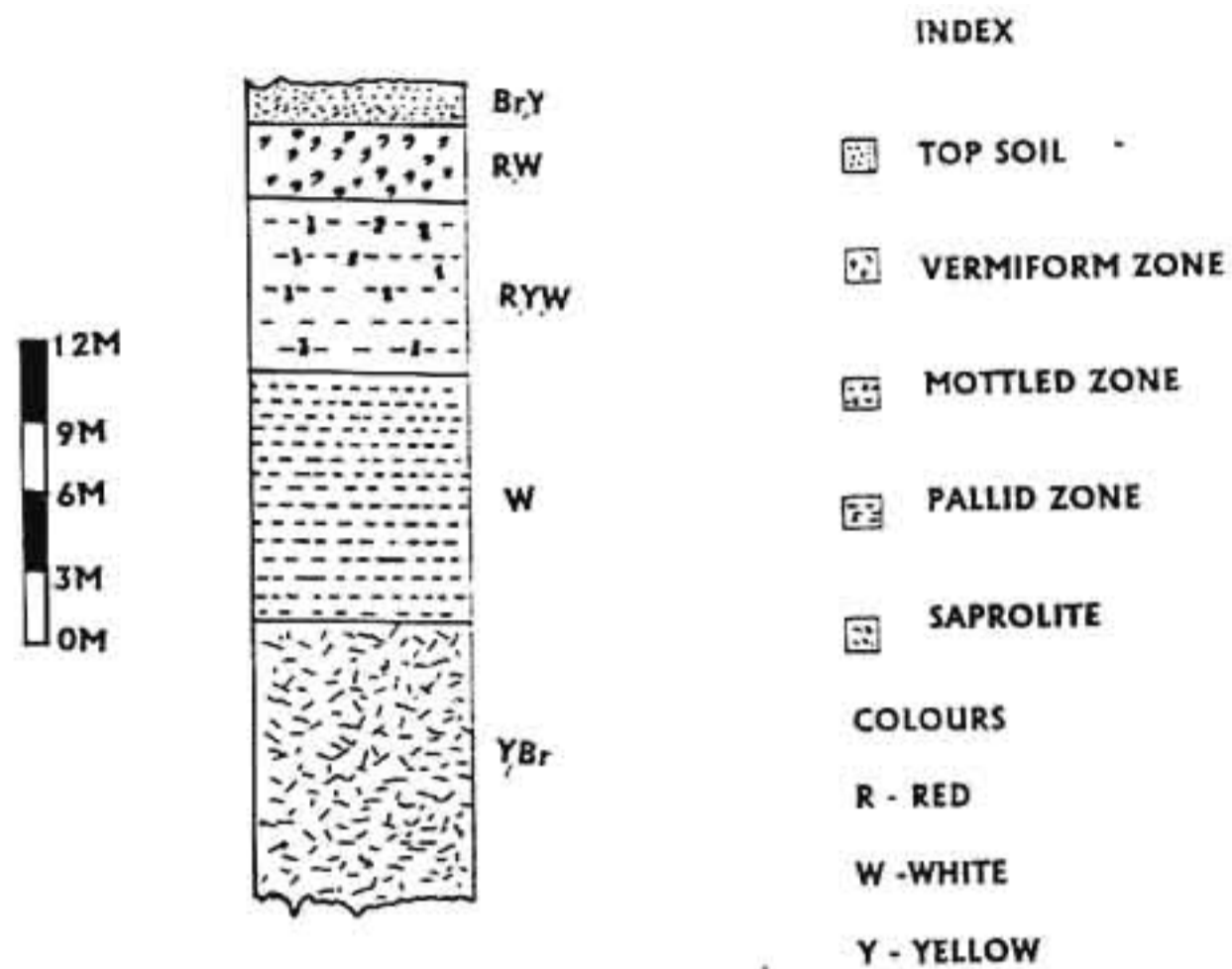
Fig.2.2. Geological succession at Akulam clay deposit

Repetition of yellow, red and white sands are numerous, within which lensoidal white clay has seen surrounded by yellowish portions. Quartzo feldspathic vein intrusions with altered feldspathic masses are common. Quartz found in the vein remnants are coarser grained and unaltered. The foliation plane of the parent rock is still preserved in the weathered zone. Occurrence of parent material (Khondalite) has been reported at 5 m depth from the mining level[1].

(b) Buchara: The deposit is located east of Buchara, Jaipur district (Rajasthan). Figure 2.3 represents the location map of the clay deposit. It is an 80 m thick clay zone, derived
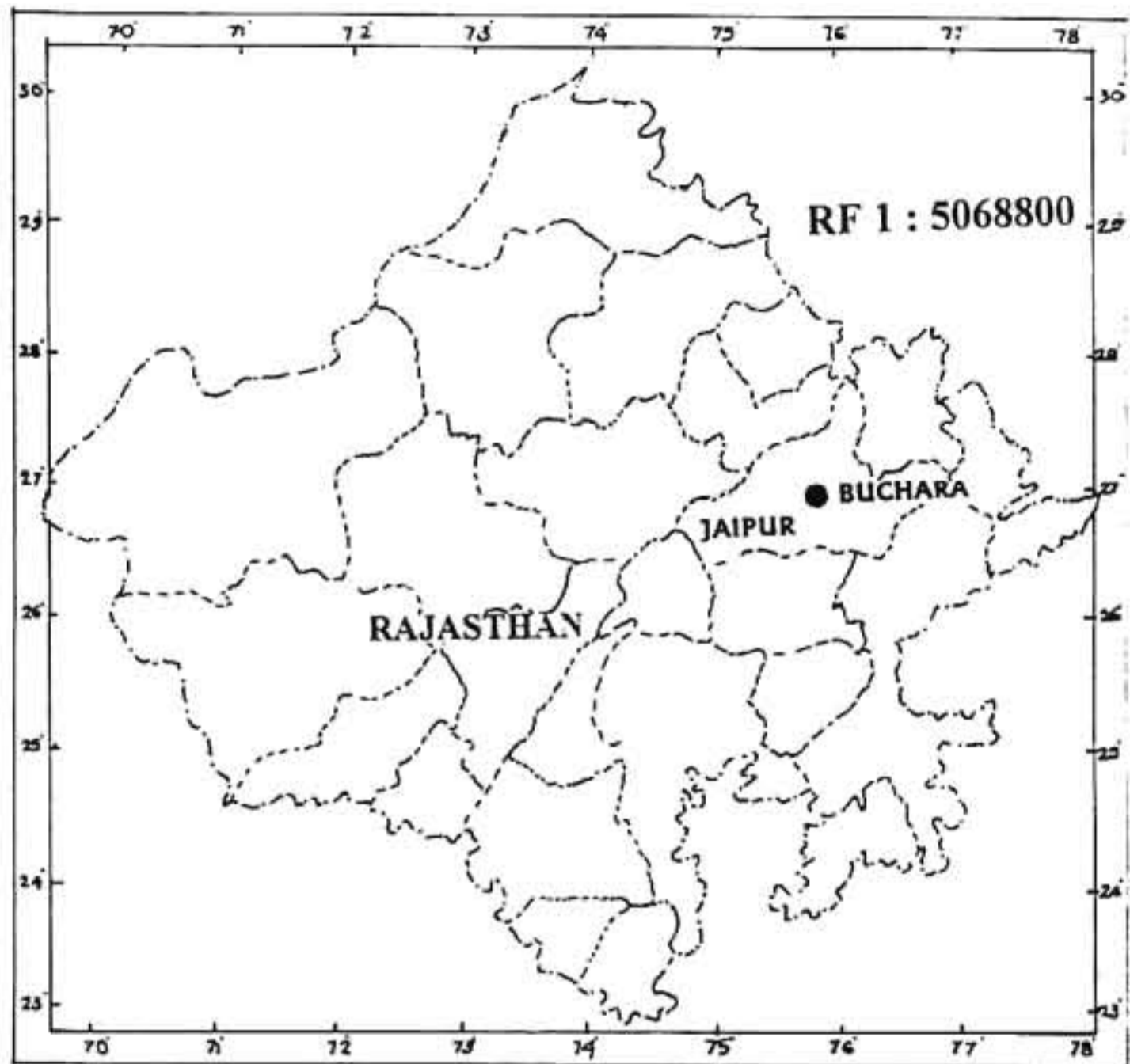
Fig.2.3. Location map of Buchara

from an altered pegmatite. The kaolin body has encountered reckonable crude production and high quality free flowing water washed kaolin as final product. The geological section of the clay deposit exposed at the mine site is shown in figure 2.4.
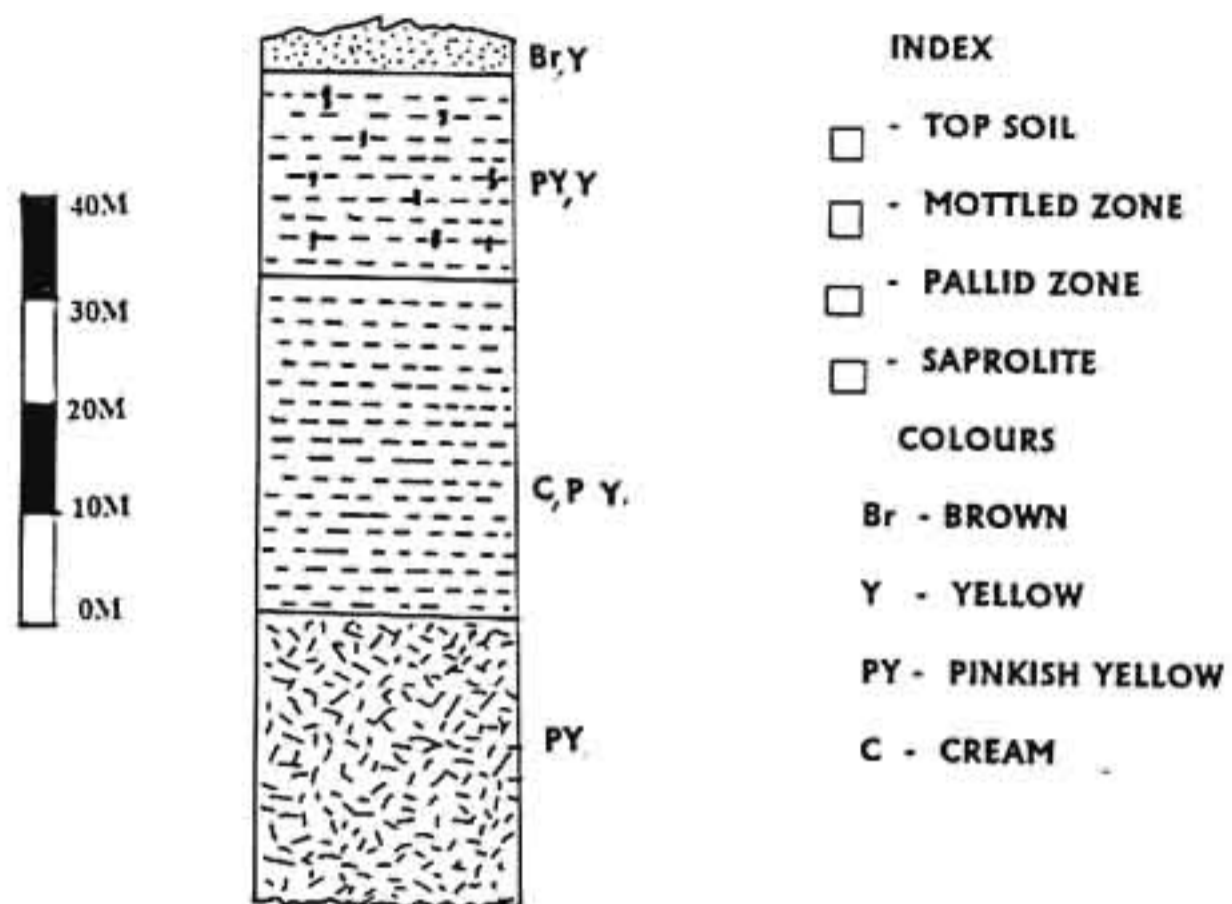
Fig.2.4. Geological succession at Buchara

(c) Kalliyur: The clay mine is located 7 km southwest of Thiruvananthapuram district, Kerala (Fig.2.1). It occurs at 14 m above the adjoining paddy fields and is flanked by the flood plain of Vellayani lagoon. The geological succession of the deposit is given in figure 2.5. The mottled zone is well-developed and characterized by red, pink and yellow coloured ferruginous concentrations with occasional greyish white clay patches. Clay samples for the present study has been selected from the reddish pink areas of the mottled zone.

32

INDEX

🔲 - TOP SOIL

🔲 - MOTTLED ZONE

🔲 - WHITE CLAY

COLOURS

Br - BROWN

Y - YELLOW

R - RED

W - WHITE

P - PINK
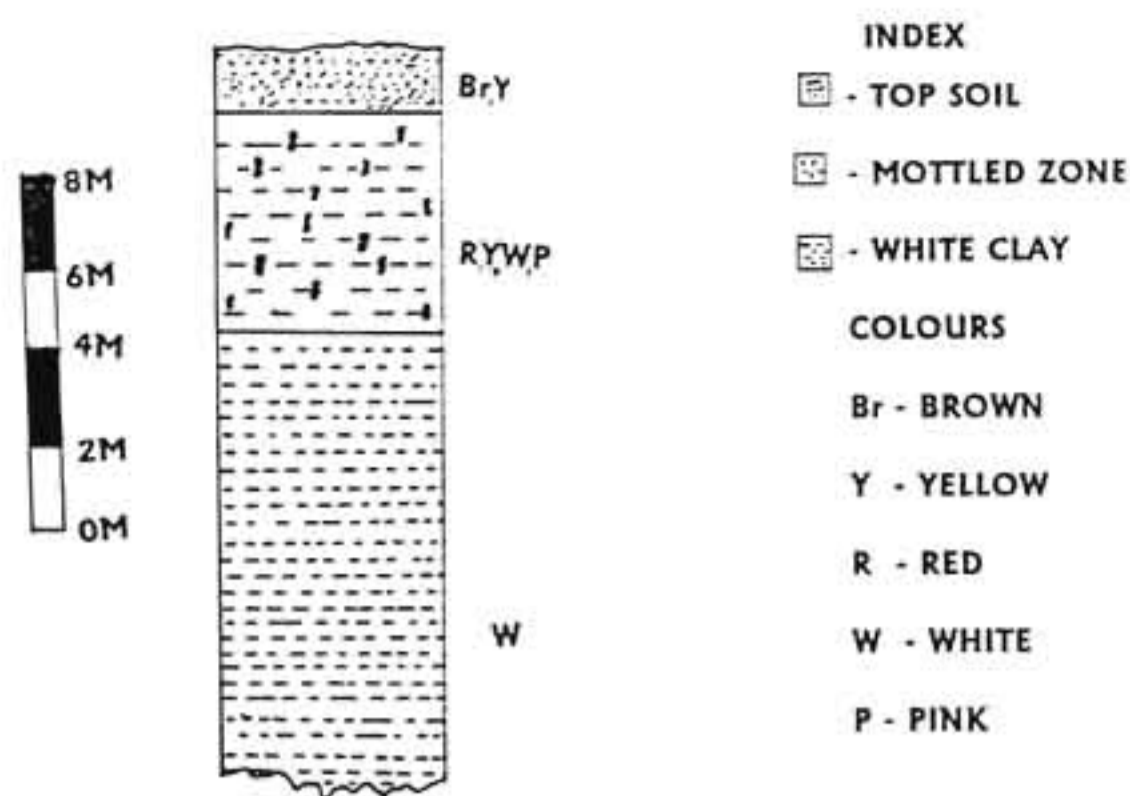
Fig.2.5. Geological succession at Kalliyur

(d) **Mulavana:** The clay mine is situated at about 2 km north east of Kundara, Kollam district, Kerala (Fig.2.1). The exposure depth of the southwest face is 8.0 m in which massive china clay occurs below the depth of 4.1 m. Between 4.1-6 m, white and light brown clay with variable sand contents are observed. At 6-8 m, the kaolin is white, pink and yellow at places. Samples were collected from the yellow coloured portions. The geological succession is shown in figure 2.6.

INDEX

🔲 - TOP SOIL

🔲 - LATERITE

🔲 - SANDY CLAY

🔲 - MOTTLED ZONE

COLOURS

Br - BROWN

R - RED

W - WHITE

Y - YELLOW

P - PINK
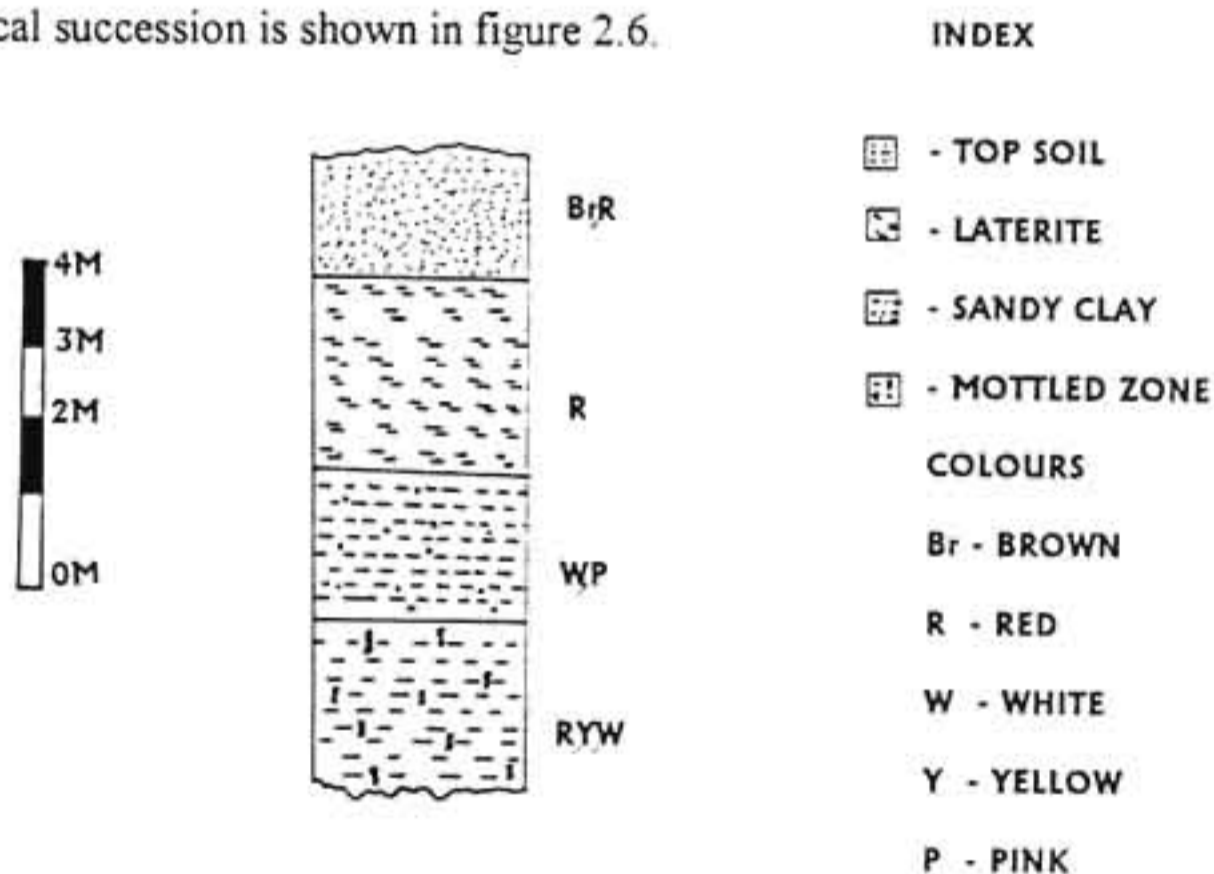
Fig.2.6. Geological succession at Mulavana

33

(e) **Thonnakkal:** The clay mine is located at a distance of 10 km northwest of Thiruvananthapuram district, Kerala (Fig.2.1). At a depth of 26.5-27.5 m below the top soil, a deep yellow coloured clay layer has been encountered. Samples for the present study were collected from this zone. The stratigraphic succession of the clay deposit is shown in figure 2.7.
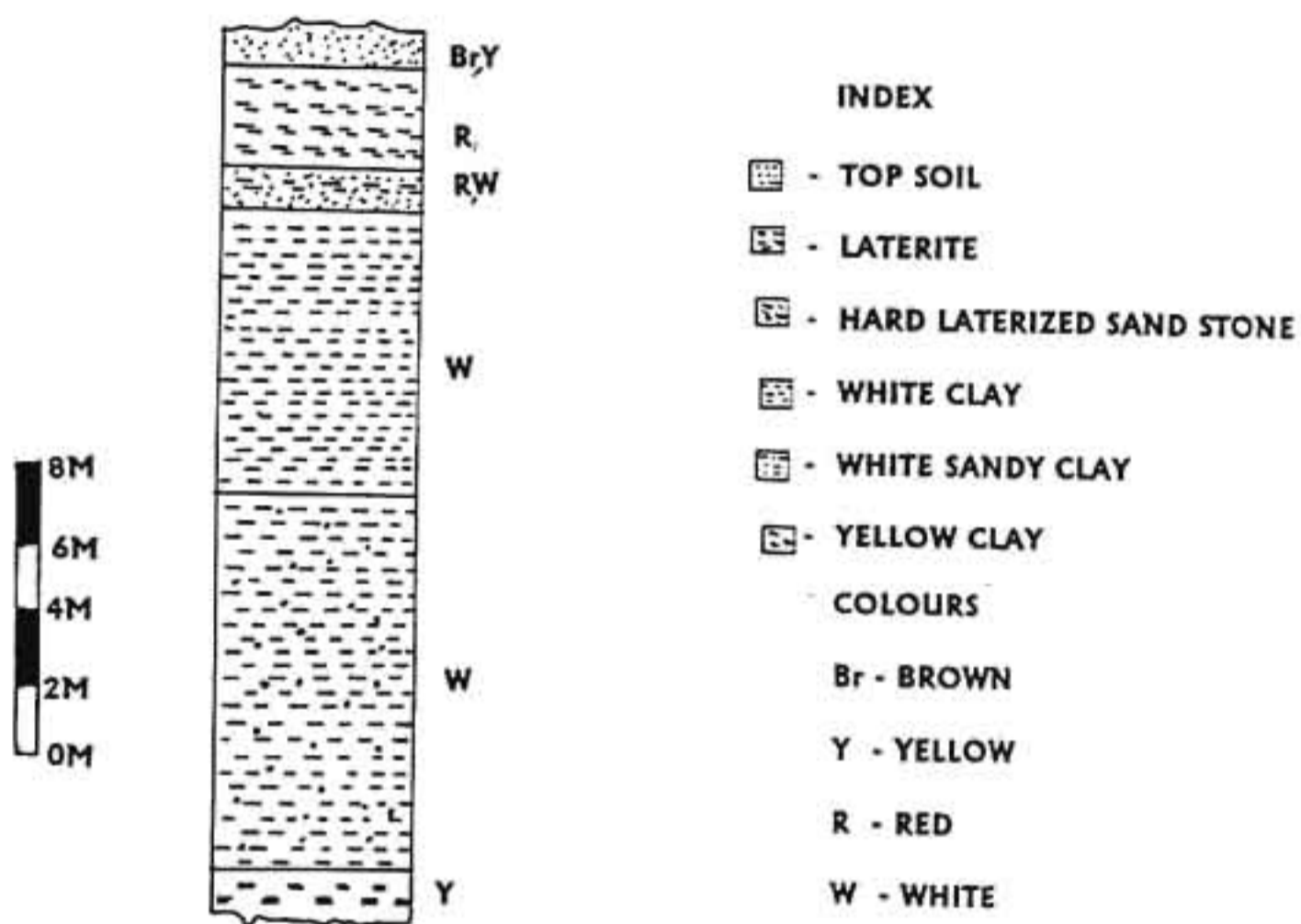
Fig.2.7.Geological succession at Thonnakkal

2.2.2. CHEMICAL AND MINERALOGICAL CHARACTERIZATION

2.2.2.1. Sampling

Samples were collected randomly from the fresh surfaces. The crude hard clay thus obtained was crushed to a maximum lump size of about one and half inch. This clay was mixed with water at about thirty percentage solids in a mechanical blunger. The blunged clay was subjected to size fractionation by wet sieving. The minus 350 mesh fraction (< 45 μm) was filtered and the oven-dried samples were powdered using a pestle and mortar and collected in air-tight polythene bags.

2.2.2.2. Preparation of samples

The less than 2 μm particle fractionation was done by sedimentation method[2] based on the Stoke's law. 5.5 g of clay was mixed with 200 ml of distilled water and 10 ml of 10% sodium hexametaphosphate was added to disperse the clay particles. The clay slurry was agitated for 17 hours. The agitated slurry was transferred to an Andreasen Pipette. Distilled water was added to bring the liquid level to the upper mark on the scale. The apparatus was kept at a constant a temperature of 30°C. The time (t seconds) required to pipette out < 2 μm fractions was determined using the Stoke's law,

$$t = \frac{9\,\eta h}{2(D_1 - D_2)\,g r^2}$$

where, η is the viscosity of the suspending medium (g cm^{-1}s^{-1}), h is the height of the liquid column (cm), D_1 and D_2 are the true specific gravities (g cm^{-3}) of the particle and the suspending medium respectively, g gravitation constant (980 cm s^{-2}) and r the radius of the particle (cm).

A chemical pretreatment for the removal of the organic and carbonate impurities often assists dispersion and separation of fine fraction and moreover facilitates identification of the clay minerals using techniques like XRD, TG/DTA, FTIR etc.[3]

2.2.2.3. Removal of organic matter

In this procedure[3], 1 g clay sample was treated with 10 ml of 30% H_2O_2. The mixture was heated on a boiling water bath for 30 min. The process was repeated twice to free off all the organic matter.

2.2.2.4. Removal of carbonate

For the removal of carbonate[3], the clay sample was heated in a boiling water bath for 30 min with acetic acid buffered to pH 5 with intermittent stirring. The suspension was centrifuged and decanted. Additional two washings were given to remove the reagent.

2.2.2.5. Methodology

(a) X-ray diffraction studies

X-ray diffraction is the finger print technique for identification of clay minerals[4-7]. This technique is based on the Bragg's equation,

$$n\lambda = 2d \sin \theta$$

where n is any whole number, λ is the wavelength of the X-rays, d is the interplanar spacing and θ is the glancing angle of incidence.

In clay mineralogy, the reflections from the basal planes 001, 002, 003 and 004 are considered as diagnostic reflections[8] because they reflect from the fundamental layer-repeat of clay minerals. Copper radiation is used almost universally for this study because

36

their loading characteristics enabled higher radiation intensities to be obtained. In order to get a low background and high quality X-ray patterns, a monochromatic radiation is desirable which can be obtained by inserting a 0.017 mm nickel foil (for Cu radiation) and 0.0166 mm iron foil (for Co radiation) in the primary beam (between the X-ray source and the sample)[9]. It will effectively filter out the shorter wavelength $K\beta$ radiation and enable the longer wavelength $K\alpha$ radiation to penerate the crystal lattices.

The X-ray diffraction patterns of the clay samples were obtained using a Ni-filtered $CuK\alpha$ radiation and Phillips PW-1710 vertical goniometer equipped with a $1°$ divergence slit. A scanning speed of $0.04°$ $2\theta/s$ at sensitivity 500 cps was used. The d-spacings thus obtained were compared with standards provided in the Powder Diffraction File published by the Joint Committee on Powder Diffraction Standards, USA. Identification of the iron oxide minerals were carried out in a similar way using a Fe-filtered $CoK\alpha$ radiation. In the study of iron-rich minerals, cobalt radiation is preferred over copper radiation[9], because the latter will be heavily adsorbed by such minerals and generates secondary flourescent radiation which leads to diffraction patterns with high background.

Specimen Preparation

Oriented Specimens: Since the clay minerals have a platy morphology, the oriented specimens are preferred over randomly oriented ones. In this method, the clay-water suspension is pipetted out onto a microscope slide. In order to avoid settling problem, the suspension was rapidly dried over a hot plate heated to 60°C.

Randomly oriented specimens: The randomly oriented mounts will give excellent diffraction patterns for iron oxides[10]. The mounts are prepared by dispersing the substance in an acetone medium and dried on a glass slide.

(b) Fourier-transform infrared spectroscopy (FTIR)

The FTIR is a versatile technique used for the study of structural analysis[11,12]. Clay minerals are sensitive to IR absorption and hence used to elucidate the chemical composition, isomorphous substituion, and crystallinity. It provides a unique method for mineral identification. The IR band consists of a series of vibrations caused by a change in dipole moment of molecular groupings. The characteristic vibrations of kaolin occurs in two major frequency regions from 3700–3500 cm^{-1} and 1150-400 cm^{-1}. The FTIR spectra of the clay samples under study was recorded at ambient temperature using NICOLET, Impact-400D spectrograph.

Sample preparation: 1 mg of clay sample and 170 mg of alkali halide (KBr) were thoroughly mixed in an agate mortar. The mixture is subjected to IR radiation in order to make the samples moisture free. The dried sample was pressed in an evacuated die to give 1 cm diameter discs. The pressed discs were allowed to cool to room temperature in a desiccator before recording the spectra.

(c)Thermal analysis (TG/DTA)

The measured parameter in thermogravimetry (TG) is the change in mass with an increase in temperature. The curves are recorded with mass of the sample on ordinate and temperature on abscissa. The differentiation of the obtained data gives the derivative thermogravimetric (DTG) curve[9]. The physical parameter measured in differential

thermal analysis (DTA) is ΔT, the difference in the temperature between the sample and the reference material (alumina) while both are subjected to a controlled temperature program. The DTA patterns are obtained by taking ΔT on the ordinate and temperature or time on the abscissa. The thermal curves thus obtained will consist of endothermic and exothermic reaction peaks corresponding to the dehydration and recrystallization changes of the specific material.

Sample preparation: The degree of aggregation of the particles is an important factor controlling the reactions when a substance undergoes heating. Therefore some standardization of the aggregate size of the clay particles are obtained by light grinding in a mortar, followed by dry sieving. In the present study, the TG/DTA/DTG patterns were obtained from a SSC 5200 thermal analysing system at temperature range 30-1020°C.

(d) Transmission electron microscopy (TEM)

The transmission electron microscope is a high-resolution instrument which provides valuable information concerning the size, shape, and composition of clay particles[13]. As a reference, the Atlas of electron microscopy of clays and their admixtures by Beutelspacher and Marel is suggested[14].

Sample preparation: 2 mg of clay is mixed in a test tube with 1.5 ml butylamine and is shaken for 5 minutes in a vibrator. Three or four drops are pipetted out and diluted. From this suspension, a drop is carefully brought to a specimen support film and the preparate is dried in air.

The TEM of the clays for this work were obtained using Phillips CM 200 FEG at a voltage of 200 kV and magnification upto 10,000. The lattice-fringe image was taken from the 001 plane, along the c-axis of the particles perpendicular to the electron beam.

(e) Scanning Electron Microscopy (SEM)

The scanning electron microscopy (SEM) is an excellent microanalysis technique used for the study of clay mineral configuration, fabric, texture and growth mechanics[15-18]. A detailed account of the preparation and examination methods of clay minerals by SEM has been published by Smart and Tovey[19].

Sample preparation: Finely ground, dried clay sample is carefully sprinkled on a carbon film provided on the top of a brass-stud. A very thin layer of gold (gold-palladium alloy) coating was given on the sample surface in order to conduct away the excess charge. The clay samples for this study was scanned using JEOL JSM-5600 LV at 10 kV.

(f) Specific surface area analysis

The specific surface area is the total surface area in square meter per gram of the material which is often important because several properties of the material including the crushing, tensile and transverse strength of the finished article and the behaviour of a material with water are all intimately related to it. One of the most universally applied procedures for specific surface area is derived from the multilayer theory of adsorption by Brunauer, Emmett and Teller (BET theory)[20].

Procedure: In this method, the finely ground clay sample is subjected to oven drying for 2 hr at 80°C. The physisorbed gases were removed by degassing at 110°C for 2 hr by passing nitrogen.

The specific surface area of the clay samples for this work were determined using Micromeritics GEMINI III 2360 surface area analyser with nitrogen as adsorbant. The instrument is provided with two identical reservoir tubes – a balance tube and a sample tube. 0.50 g of the degassed clay sample was filled in the sample tube. Nitrogen gas was introduced into both tubes while maintaining an isothermal bath provided with liquid nitrogen. The pressure imbalance in between the two tubes were recorded automatically. A free space correction can be applied using helium in order to eliminate any slight difference in volume between the two tubes.

(g) Particle size distribution

It is an important criteria in the commercial uses of kaolin because it affects the mechanical, optical and printing properties of the finished sheet of paper.

Sample preparation: The Clay containing the <45 μm fraction was dried and powdered. The organic matter and carbonates were removed by chemical treatments. The iron oxides were removed by sodium dithionite solution buffered at pH 7.3 with sodium bicarbonate and sodium acetate as a complexing agent.

The particle size distribution curves of the clay samples for this study was obtained using a Micromeritics Sedigraph 5100 window based particle size analyser. 2 g of the dried and powdered clay sample was dispersed in 40 ml distilled water using sodium hexametaphosphate as dispersant. The clay-water suspension was agitated thoroughly in a sonicater and transferred to the sample holder.

(h) Specific gravity

It is the ratio between the weight of the material and that of an equal volume of water. It is often indicative of the constituent mineral phases in the substance studied.

Procedure: About 10 g of the clay sample (a) dried at 105-110°C was accurately weighed in a previously weighed specific gravity bottle. The bottle was nearly half-filled with water, placed on an evaporating dish and evacuated the air bubbles by vacuum pump. The bottle was then filled with distilled water, the stopper was inserted and weighed (b). Then, bottle was emptied dried, filled with water and weighed again (c). Then relative weight loss was calculated using the following equation,

$$\text{Specific gravity} = \frac{a}{b-c}$$

(i) Water of plasticity

The water content of the clay at the point of maximum workability gives the value for water of plasticity. Its value varies with size and shape of the particles as well as with the constituent mineralogy[21].

Procedure: Dried clay sample was worked up with water from a burette to a soft plastic mass and thoroughly kneaded by hand. Allowed to age for 24 hr, keeping it in a wet cloth. After 24 hr aging, the plastic mass was kneaded again and pugged well with drops of water until a proper coating consistency by either extrusion or moulding into bar is obtained. Three equal portions of the clay was made into balls, and weighed. It was then allowed to age at room temperature for 24 hr, then in an air oven at 70°C for 4 hr and

finally at 110°C for 12 hr. Final weight was recorded after cooling, them in a desiccator. The water of plasticity is calculated from the equation

$$\text{Water of plasticity} = \frac{\text{Difference in weight of the plastic and dried clay mass (g)}}{\text{Weight of dried clay mass (g)}} \times 100$$

(j) pH

An account of pH of the clay samples will give valuable information regarding the depositional environments. pH of the soil may vary according to a number of parameters, of which the organic acid (mainly humic acid) content and the prevailing water flux are significant factors determining the soil type. In addition to this, the base exchange capacity and plastic properties of clays are markedly influenced by pH. In the present study, pH of the clay samples were determined by SYSTRONICS μ pH System 361.

Procedure: 100 ml of freshly boiled and cooled distilled water was added to 25 g raw clay sample and allowed to remain for ½ hr with occasional stirring. The suspensions were centrifuged and the pH of the solutions were determined.

(k) Chemical Analysis

Chemical analysis is one of the conventional and well established methods used to study clay minerals. The constituent elements are represented in the form of percentage oxides and their summation should result in a total in the range 99.75-100.5% for classical analysis. In the present work, the chemical analysis of the clays were done according to the classical scheme of Bennet and Reed[22].

Loss on ignition (LOI)

The finely ground, dried clay sample was accurately weighed in a platinum crucible and gently heated in a muffle furnace to $1025\pm25°C$. It was ignited for 1 hr and the difference in weight gave the loss of mass due to ignition.

Estimation of silica

0.5 g of finely ground, dried clay was fused with 1:1 mixture of Na_2CO_3 and K_2CO_3. The melt was allowed to cool and extracted in 1:1 HCl to which a few drops of H_2SO_4 was added. The precipitate was dehydrated and the residue was again digested in hot dilute HCl. The suspended materials were filtered through Whatmann No.40 filter paper and washed free of the chloride ions, dried incinerated in a previously weighed platinum crucible at $1050°C$ till constant weight was attained. The residue thus obtained corresponded to the silica content in the clay sample. As a cross-check, the residue was heated with conc.H_2SO_4 and HF (48%) and evaporated to dryness. After heating at $1050°C$, the weight of the crucible with residue was found out. The difference in weight gave the weight of silica in the sample.

Fusion with Na_2CO_3 and K_2CO_3 converted the clay to corresponding soluble aluminates and silicates which on addition with HCl, precipitated silicic acid which is evaporated and baked to get insoluble silica. During HF treatment, the silica gets evaporated as silicon tetrafluoride leaving behind impurities, the difference in weight representing the amount of silica.

Preparation of sample solution for the estimation of Al_2O_3, Fe_2O_3 and TiO_2

0.5 g of clay sample was weighed in a platinum dish and moistened with distilled water. 10 ml of 1:1 H_2SO_4 and 10 ml of HF (48%) were added and evaporated to dryness on a sand bath. The contents were cooled, added another 10 ml HF and evaporated to dryness. The residue was fused with potassium pyrosulphate. The melt was allowed to cool and the contents digested with 3% H_2SO_4 to obtain a clear solution, which was made up to 250 ml.

During the HF treatment, the entire silica got evaporated and the residue on fusion with potassium pyrosulphate transformed the metal ions into soluble salts.

Estimation of alumina

The estimation of alumina was done by EDTA complexometric titration. 20 ml of the sample solution was pipetted into a 250 ml conical flask, added 25 ml of EDTA (0.02M) and a drop of methyl orange indicator and then ammonia solution (1:3) dropwise until the colour of the solution changed from red to yellow. 10 ml of buffer (pH=5.3) was added and the solution heated to boiling for 5 min. The solution was allowed to cool, another 10 ml buffer added and titrated with zinc acetate (0.02 M) using xylenol orange indicator. The end point was indicated by a colour change from yellow to orange. 1 gm of sodium fluoride was added to the solution and boiled for 5 min. After cooling, 10 ml of buffer was added and titrated against 0.02 M zinc acetate (A). The percentage alumina was calculated from the following equation

$$\% \text{ alumina} = \frac{A \times X \times 100}{W} - 0.6378 \text{ T})$$

where X = equivalent Al_2O_3 in g mL^{-1} of zinc acetate solution; w = weight of the sample in 20 ml of the stock solution and T = percentage titania in the sample).

Aluminium ions form stable complex with EDTA and the excess free EDTA is titrated against zinc acetate. The addition of sodium fluoride liberates reacted EDTA from Al-EDTA complex and producing AlF_3 and free EDTA which is again estimated by titration with zinc acetate.

Estimation of iron

An aliquot of the sample solution was pipetted out into a 100 ml standard flask. 2 drops of p-nitrophenol was added, followed by 10 ml of tartaric acid (10%). A few drops of 1:3 NH_4OH was added until the colour of the solution changed to yellow. The solution was acidified with drops of HCl (1:1) and add 2 ml of hydroxyl ammonium chloride (10%) was added to reduce Fe^{+3} to Fe^{+2} followed by 10 ml of 1,10-phenanthroline (0.1%) to complex with the ferrous ions. The solution was made upto 100 ml, and the optical density measured at 510 nm using a UV-Vis spectrophotometer (HITACHI-220).

A calibration curve was prepared using standard Fe_2O_3 solution (in the range 0.2-5 ppm) and the unknown concentration of the sample solution was found out.

Estimation of TiO_2

25 ml of the sample solution was pipetted into a 100 ml standard flask. 10 ml of 6% H_2O_2 was added and the solution diluted to 100 ml. The optical density was measured at 410 nm against reference solution. A calibration curve was prepared using standard titania solution of concentration in the range 1-10 ppm. With an acidic titanium(IV)

46

solution, H_2O_2 produces an yellow colour and the compound has been stated to be $[TiO(SO_4)_2]^{2-}$ or a similar ion[23].

Estimation of Na₂O, K₂O and CaO

1.0g of the sample was digested with 5 ml HF (48%) and 1 ml of perchloric acid and evaporated to dryness on a sand bath until thick fumes of perchloric acid comes out. The basin was allowed to cool and added a few ml of distilled water, again evaporated on the sand bath to dryness. The content was digested in 1:1 HCl and the solution was made upto 100 ml. The amount of sodium, potassium and calcium were determined using flame photometer (ELICO, model CL 220) at wavelengths 589, 767 and 423 nm respectively.

Estimation of FeO

0.1g of the clay sample was weighed in a platinum crucible and added 10 ml of dilute H_2SO_4 and 10 ml of HF (48%) and covered the crucible with a tight-fitting lid. Placed the crucible on a sand bath and gently boiled the contents for 10 min. Plunged the crucible with lid in position into a beaker containing 300 ml cold, freshly boiled distilled water in which 15 g of boric acid has been dissolved. Remove the crucible and lid from the beaker and add 15 ml of H_2SO_4-H_3PO_4 mixture and 10 drops of barium diphenylamine sulphonate indicator. Titrate the solution to a purple colour with standard potassium dicromate solution (0.1 N). The amount of FeO was calculated as,

0.1 ml of 0.1 N $K_2Cr_2O_7$ = 0.00718 g FeO

(l) Trace element analysis

The trace element distribution of the clay samples for the present study was carried out by Inductively coupled plasma (ICP) technique using Jerrillash Atomscan-25 analyser.

Since the above mentioned techniques are inadequate to provide the exact mineralogy of the iron oxides present in the clay samples, certain special methods are adopted for their identification. They are described below.

(m) A comparative study using Munsell colour chart

The most important colouring impurities in clays and soils are found to be the oxides, hydroxides and oxyhydroxides of Fe(III) ion. Colour of these Fe(III) compounds vary from red to yellow in accordance with the wavelength of absorption caused by electron transitions in the d-shell[24]. Usually clays rich in hematite are reddish and those with goethite are yellowish in appearance. Hust[25] used the term "redness" to demarcate different shades of soil colours produced by various Fe-oxides. The simplest and most commonly used colour determination technique is the visual comparison of soil or clay colour with a standard colour chart (most commonly the Munsell colour chart)[26]. Fernandez and Schulze[27] used reflectance spectra for soil colour determination and showed that the CIEC (Commission Internationale de l' Clairage) tristimulus value thus calculated are well in agreement with those of Munsell colour hues and chroma.

Like other physical properties, colour may also vary with degree of crystallinity and isomorphous substitution of Fe by other trivalent and divalent elements like Al, Mn, etc. For example, studies on synthetic hematite, Barron and Torrent[28] arrived at the conclusion that, Al-substituted hematite are lighter than non-substituted ones. Similar observations on synthetic goethite showed a decrease in hue and value with increase in Al-substitution[29].

The Munsell colour notation has three variables, namely hue (H), value (V) and chroma(C). The hue notation of a colour indicate its relation to red, yellow, green and purple, the value notation indicates its lightness and chroma notation indicates its strength (or change from a neutral of the same light). In hue, R for red and YR for yellowish red and Y for yellow and are varying from 0-10 in numbers. The notation of value consists of numbers from zero for absolute black and ten for absolute white. The notation for chroma consists of numbers beginning at zero for neutral gray and varying at equal intervals to a maximum of about 20.

Procedure: The dried clay samples were usually compared in sunlight (direct sunlight is avoided) with that of colour chips provided in the Munsell colour chart and assigning numbers for hue, value and chroma, depending on which the mineral identification has been carried out.

(n) Concentration of iron oxides by 5 M NaOH treatment

The chemical concentration of Fe oxides in clays are generally accomplished by dissolving the clay fraction in boiling alkali solution. Norish and Taylor[30] used a 5 M NaOH solution for concentrating a poorly goethitic phase from kaolinite. But there was a

possibility that the strong alkali treatment might have resulted in increased crystallinity and phase transformations of these iron oxides. Kåmpf and Schwertmann[31] showed that presence of Si in the 5 M NaOH solution found to inhibit the recrystallization. According to them, a Si concentration of 0.2 M is sufficient enough to prevent any kind of such transformations. Therefore, the concentration of iron oxides from kaolin by 5 M NaOH does not affect the Fe-compounds because the solution is already saturated with Si from the kaolinite structure[32].

Procedure: 0.1g magnetic fraction of the clay sample was added to 100 ml of 5M NaOH solution in a teflon bottle. The mixture was boiled on a sand bath and centrifuged the contents. The sample was washed once with 5M NaOH, once with 0.5M HCl, kept in HCl for 20 min to dissolve the sodalite, twice with 1N $(NH_4)_2CO_3$ to remove excess ammonia and carbonate. The sample was oven dried at 80°C to volatalize the remaining $(NH_4)_2CO_3$.

Both the 5 M NaOH treated magnetic fraction and nontreated fractions were subjected to X-ray diffraction analysis using Fe-filtered CoKα radiation using Phillips PW-1710 Vertical Goniometer. The samples were scanned from 3-70° 2θ at a speed of 2°/min with a sensitivity of 500 cps.

(o) Estimation of amorphous Fe₂O₃

(i) EDTA technique

The selective extraction of amorphous iron oxides in soils and clays has been accomplished with a weak alkaline solution of EDTA[33-36]. Being a strong complexant, EDTA forms soluble Fe complexes which are easily removed through low-speed

centrifugation. A long time (90 days) EDTA extraction of X-ray amorphous Fe-oxides from a synthetic mixture of goethite and hematite was reported by Borggaard[37]. In order to simulate actual soil conditions, the extractions were carried out in presence of quartz. Extensive studies indicated that the EDTA method can be considered as a reference technique for amorphous iron oxide dissolution from clays[34].

Procedure: The EDTA extractable Fe was determined by mixing one part of clay suspension (25 mg/ml) with five parts of EDTA extractant (0.1 M in EDTA and 0.2 M in ammonium oxalate at pH 4.75), the extraction was carried out in a water bath at 90°C for periods upto 18 hr.

(ii) Oxalate technique

Similar to EDTA, oxalate also form complexes with Fe(III) ions. The oxalate method was originally proposed by Tamm[38] to extract a group of amorphous oxides (Al, Fe, Si, etc) from soils. Later, this technique has been modified by several researchers[39-42] and now it has become the most popular technique for estimating amorphous or poorly crystalline Fe in soils and clays. Though this process was wholly meant for amorphous Fe, a small amount of crystalline Fe may also get removed during the process[43].

Procedure: The oxalate soluble iron oxides from the clay samples were determined by the method of Schwertmann[41]. 40 mg samples of clay were shaken in 10 ml of acidified ammonium oxalate (pH ~ 3) at 30°C for 4 h in darkness. The Fe content of the samples were determined at pH 5 by 1,10-phenanthroline complexometry using UV-vis spectrophotometry (HITACHI-220).

(p) Estimation of total free iron by CDB technique

A more versatile technique for iron oxide dissolution is the citrate-dithionite-bicarbonate (CDB) method proposed by Mehra and Jackson[44]. Sodium dithionite, a powerful reducing agent of Fe^{3-} which is capable of dissolving even the most insoluble Fe(III) oxides such as hematite and goethite provided the redox potential is low enough. Dithionite in solution rapidly loses its reducing properties and a strong ligand (citrate) must be added to solution in order to prevent reprecipitation of dissolved Fe. At pH values below 9-10, dithionite reduces all Fe(III) oxides to Fe(II) and the optimum pH was found to be 7-8[45]. The Fe compounds dissolved by this technique include Fe-oxides of varying crystallinity and small fractions of water-soluble, exchangeable and organically bound Fe. However, the ability of this technique to dissolve Fe-oxide is affected by the size of the Fe-oxides crystals[46].

Procedure: 40 ml of 0.3 M sodium citrate and 5 ml of 1 M sodium bicarbonate are added to 2 g of clay. The temperature was maintained at 75-80°C and 1 g of sodium dithionite was added with constant stirring. A second 1 g of sodium dithionite was added after 5 min. After 15 min digestion, 10 ml of saturated NaCl solution and 10 ml acetone were added in succession. The suspension was centrifuged and the supernatant was decanted off. The clay was recovered after repeated washing till free from extracted Fe. The procedure was repeated three to five times.

(q) Microscopic examination

The polarizing or petrological microscope is one of the principal device for identification of minerals[47,48]. Since clays are too fine to view through the microscope,

other layer fragments of non-clay minerals can be identified. For this study, the heavy minerals found in the clays were separated by gravity settling and viewed through OLYMPUS, BH-2 polarizing microscope.

Specimen preparation: Heating a little canada balsam on a microscope slide, a speck of dried clay powder was sprinkled on the warm balsam and spread with a glass rod. When completely cold, the section was ground to flat and fix a glass cover on the ground surface, to prevent the scattering of light when using high magnification.

2.3. RESULTS AND DISCUSSION

2.3.1. Principal clay mineral and associated minerals

Figure 2.8 shows the X-ray diffraction patterns of the clay samples. The major indices, d-spacings and intensities of the X-ray diffraction analysis are represented in Table 2.1.

The dominant clay mineral present in the samples was kaolinite. The prominent basal reflections at around 7.05 and 3.55 Å were the characteristic d-spacings for kaolinite. These two reflections were well-defined and sharp indicating a well-crystallised kaolinitic phase. Reflections at 02*l* and 11*l* in the range 22-33° 2θ (CuKα) showed that the samples TK and KK were slightly disordered[8] and this apparently accounted for the presence of ancillary iron oxides and other mineral impurities. Similarly two triplets in the range 35-30° 2θ (CuKα) became a doublet in the case of sample MK and continuous in the case of sample TK. These structural disorders could not be entirely be assigned as stacking disorder because of the presence of non-kaolinitic minerals in the samples. Quartz was invariably present in all the five clay samples as

Table 2.1. Powder data of the clay samples with the most intense diagonstic d-spacings (d) and internsities (I)   *

Sample AK				Sample JK				Sample KK			
hkl	I	d	Mineral	hkl	I	d	Mineral	hkl	I	d	Mineral
001	100	7.05	K	001	100	7.05	K	001	100	7.09	K
020	43	4.43	K	020	27	4.47	K	020	21	4.43	K
110	54	4.32	K	110	31	4.31	K	110	22	4.33	K
100	12	4.26	Q	100	9	4.24	Q	100	22	4.24	Q
11̄1	66	4.18	K	11̄1	32	4.13	K	11̄1	23	4.13	K
002	85	3.55	K	002	82	3.35	K	002	84	3.55	K
101	32	3.35	Q	101	15	3.55	Q	101	23	3.3	Q
				13̄0	19	2.55	K	13̄0	15	2.55	K
110	32	3.22	Rt								
13̄0	38	2.55	K	200	23	2.48	K	200	18	2.48	K
200 101*	37	2.48	K+Rt	003	13	2.37	K	003	14	2.37	K

Sample MK

hkl	I	d	mineral
001	100	7.02	K
020	34	4.40	K
110	40	4.30	K
11$\bar{1}$	39	4.13	K
002	86	3.54	K
101	20	3.32	Q
1$\bar{3}$0	26	2.54	K
200	27	2.48	K
003	36	2.32	K
131	28	2.28	K
003	27	2.37	K
131	33	2.28	K
24$\bar{1}$ 211*	19	1.68	K+Rt

Sample TK

hkl	I	d	mineral
001	100	7.0	K
110	38	4.38	K
100	40	4.28	Q
11$\bar{1}$	51	4.11	K
002	85	3.52	K
101	54	3.30	Q
1$\bar{3}$0	31	2.53	K
131	33	2.46	K
200	31	2.42	K
20$\bar{3}$	28	2.35	K
131	20	2.28	K
131	16	2.28	K

*reflections correspond to rutile

K = kaolinite; Q = quartz, Rt = rutile
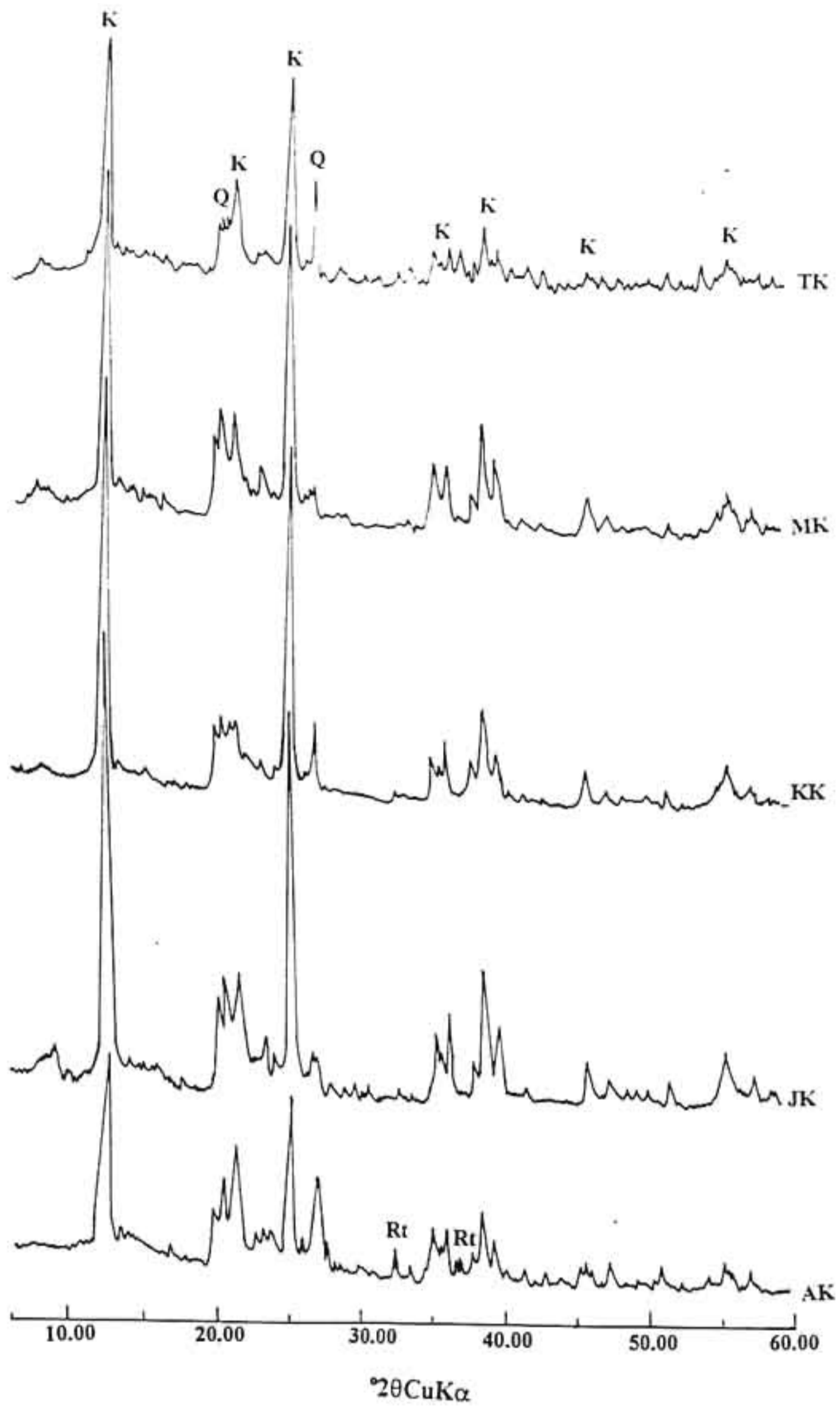
Fig.2.8. X-ray diffraction pattern of kaolinites from Akulam (AK), Jaipur (JK),
Kalliyur (KK), Mulavana (MK) andThonnakkal (TK), K – kaolinite:
Q – quartz; Rt –rutile

56

evident from its strongest reflection at 3.34 Å (101). The second strongest reflection of quartz occurred at around 4.26 Å which showed slight variations as 4.24 Å in KK and 4.28 Å in TK. This could be due to the merging of adjacent reflections caused by geothite. In sample AK, rutile was also identified. The diagonstic peaks of rutile occurs at 3.22, 2.48, and 1.68 Å. At 2.48 and 1.68 Å, the reflections from kaolinite and rutile fused together to form broad peaks.

X-ray diffraction analysis of the bulk clay samples employing CuKα radiation was unable to provide any information regarding the ferric oxide phases and other ancillary minerals except rutile present in the clays.

Figure 2.9 shows the FTIR spectrum of the clay samples in the range 400-4000 cm⁻¹. The characteristic vibrations and corresponding molecular groupings are listed in Table 2.2.

The IR spectrum of the clay samples indicated four distinct vibrations at around 3695, 3668, 3654 and 3620 cm⁻¹. These four vibration bands are characteristic of well-crystallised kaolinite[49]. The vibration at 3620 cm⁻¹ was caused by the inner hydroxy group (Al- -O - OH) located inside the octahedral sheet. The other three bands were also due to hydroxyls which were placed on the side of the sheet The 3695 and 3620 cm⁻¹ bands were intense and well-defined whereas the vibrations at 3668 and 3654 cm⁻¹ were slightly overlapped and weak but showed distinct maxima. The broad vibration band at
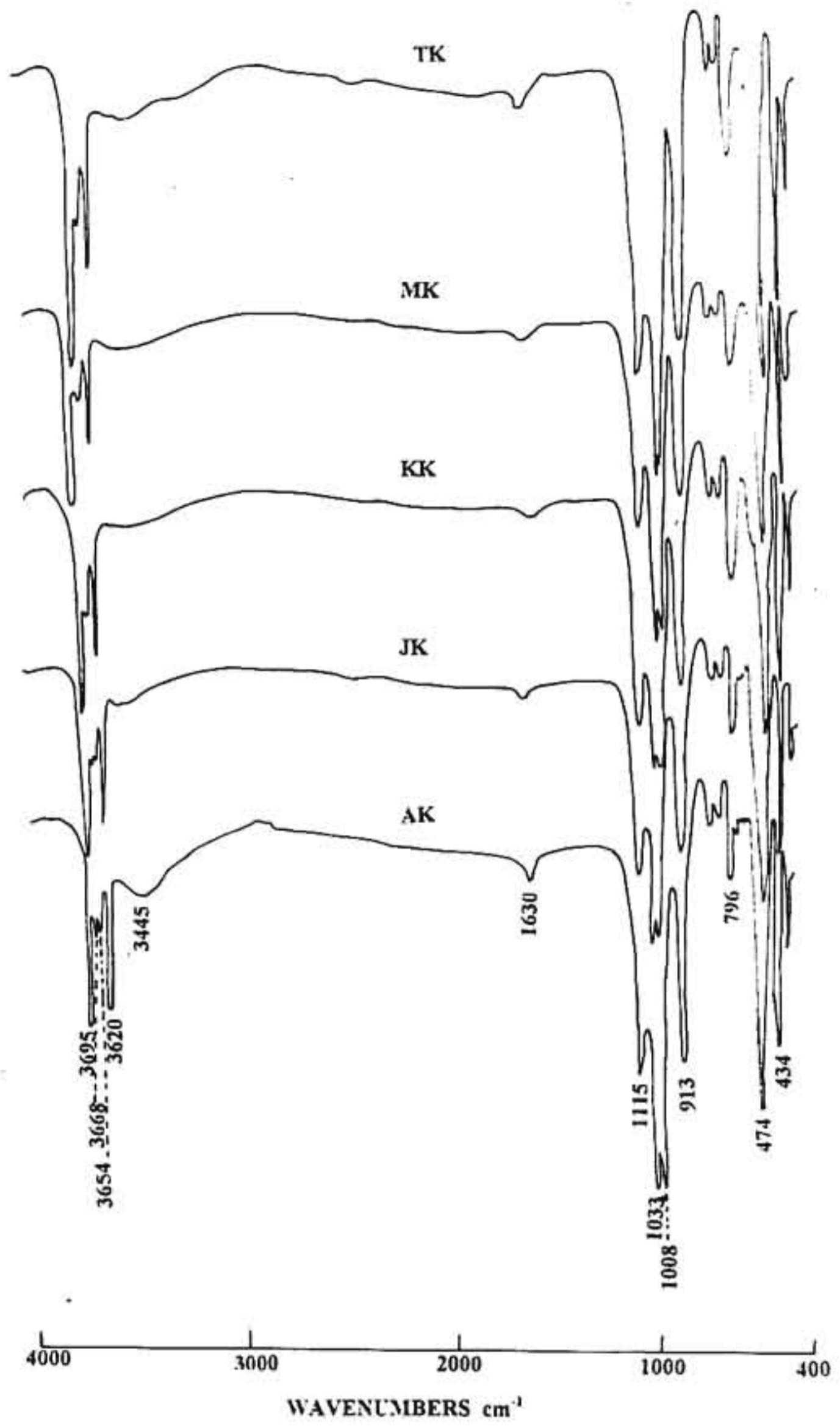
Fig.2.9. FTIR spectra of kaolinites AK, JK, KK, MK and TK in KBr discs

around 3443 cm^{-1} may be attributed to the water molecules which were adsorbed on the residual silica-alumina group[50].

Table 2.2. Results of FTIR studies

Wavelength (cm^{-1})					Band assignment
AK	JK	KK	MK	TK	
3695	3694	3693	3693	3693	Al- - O – H
3668	3667	3669	3667	3668	Al- - O – H
3654	3654	3653	-	3651	Al - - O – H
3620	3620	3620	3622	3620	Al - - O – H
3445	3433	3433	3447	3448	H_2O Str
1115	1113	1110	1116	1108	Si – O Str
1033	1032	1034	1035	1034	Si – O – Al
913	915	914	918	916	Al - - O – H
796	794	797	793	792	Si – O
755	755	756	758	756	Si –O – Al
696	695	694	693	695	Si – O – Al
509	543	543	539	543	Al – O Str
474	473	475	476	474	Si – O
434	435	437	436	434	Si – O

Figure 2.10 shows the DTA and TG curves of the clay minerals. The thermal curves were characterised by two main peaks, an endothermic peak in the temperature range 530-540°C and an exothermic peak at around 995-1007°C. These patterns are in good agreement with that of a well crystallized kaolinite[9]. For kaolinite, the dehydroxylation (loss of constitutional OH) takes place at around 530°C which is responsible for an endothermic peak in the DTA pattern. When kaolinite is heated beyond this temperature, a meta-kaolinitic stage is attained by about 650°C and the final product of the decomposition process are mullite and cristobalite with a defect spinal phase as an intermediate stage.
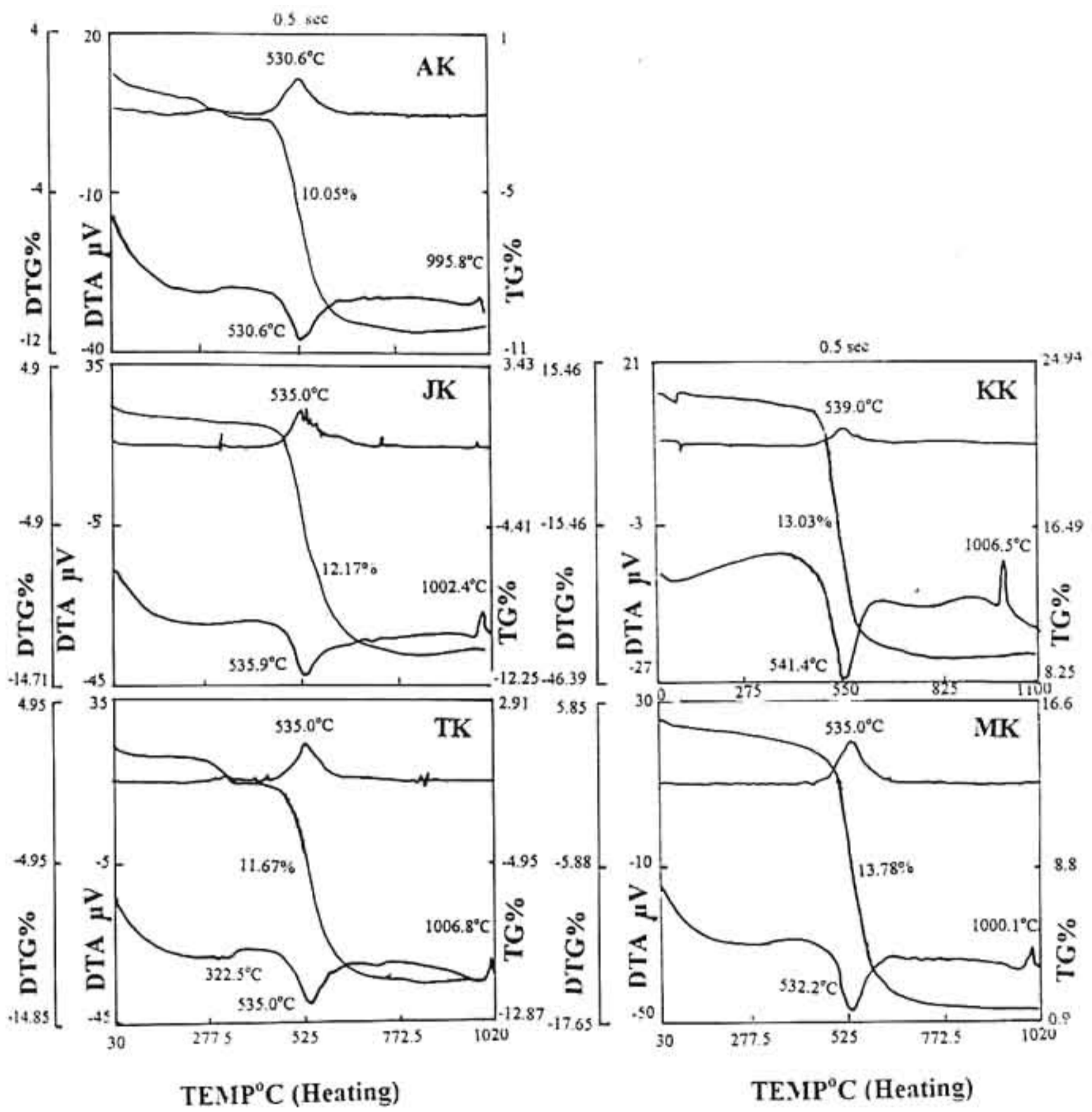
Fig.2.10. DTA/TG/DTG curves for kaolinites AK, JK, KK, MK and TK

60

$$Al_2O_3.2SiO_2.2H_2O \quad \xrightarrow{\text{500-700°C}} \quad Al_2O_3.2SiO_2 + 2H_2O$$
$$\text{Metakaolinite}$$

$$2(Al_2O_3.2SiO_2) \quad \xrightarrow{\text{900-1000°C}} \quad 2Al_2O_3.3SiO_2 + SiO_2$$
$$\text{Silicon spinel}$$

$$3(Al_2O_3.3SiO_2) \quad \xrightarrow{\text{about 1250°C}} \quad 3Al_2O_3.2SiO_2 + SiO_2$$
$$\text{Mullite} \quad \text{(cristobalite)}$$
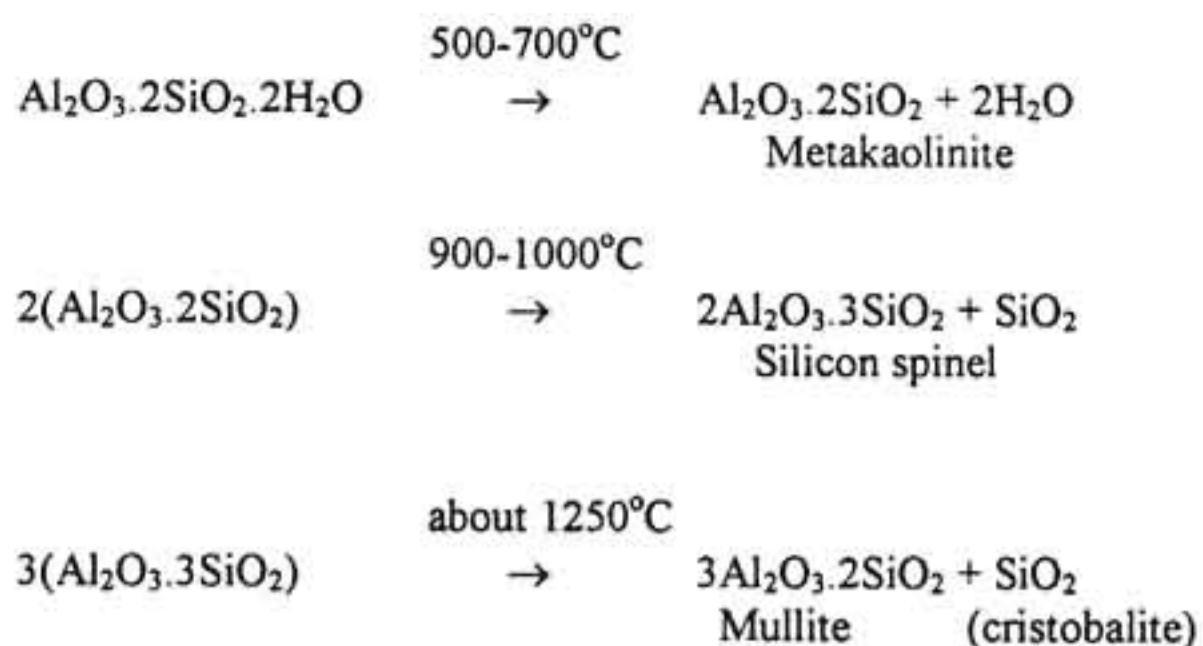
The weight loss encountered during the dehydroxylation process was marked by the DTG peak at ~ 535°C. The corresponding weight loss accounted was in the range 10-14%.

In addition to the two main peaks, the DTA pattern of sample JK was characterised by a small broad peak in between 650-700°C which indicated the presence of muscovite in the sample. In sample TK, the reaction peak at around 320°C was characteristic of the ferric oxide mineral, goethite. The exothermic reactions of all the clay samples except AK, were represented by well defined and sharp peaks, suggesting a higher crystallinity of the clays.

The TEM pictures of the clay samples are shown in Fig.2.11. Kaolinite particles showing 001 cleavage planes with pseudohexagonal borders were suggestive of a higher degree of crystallinity. Twinning of the crystals were marked by reentrant angles[14] (Fig.2.11a,b). Halloysite was invariably present in all the clay samples. Both tubular and platy morphology were observed for halloysite crystals (Figs.2.11b,c,d&g). The tubular

61
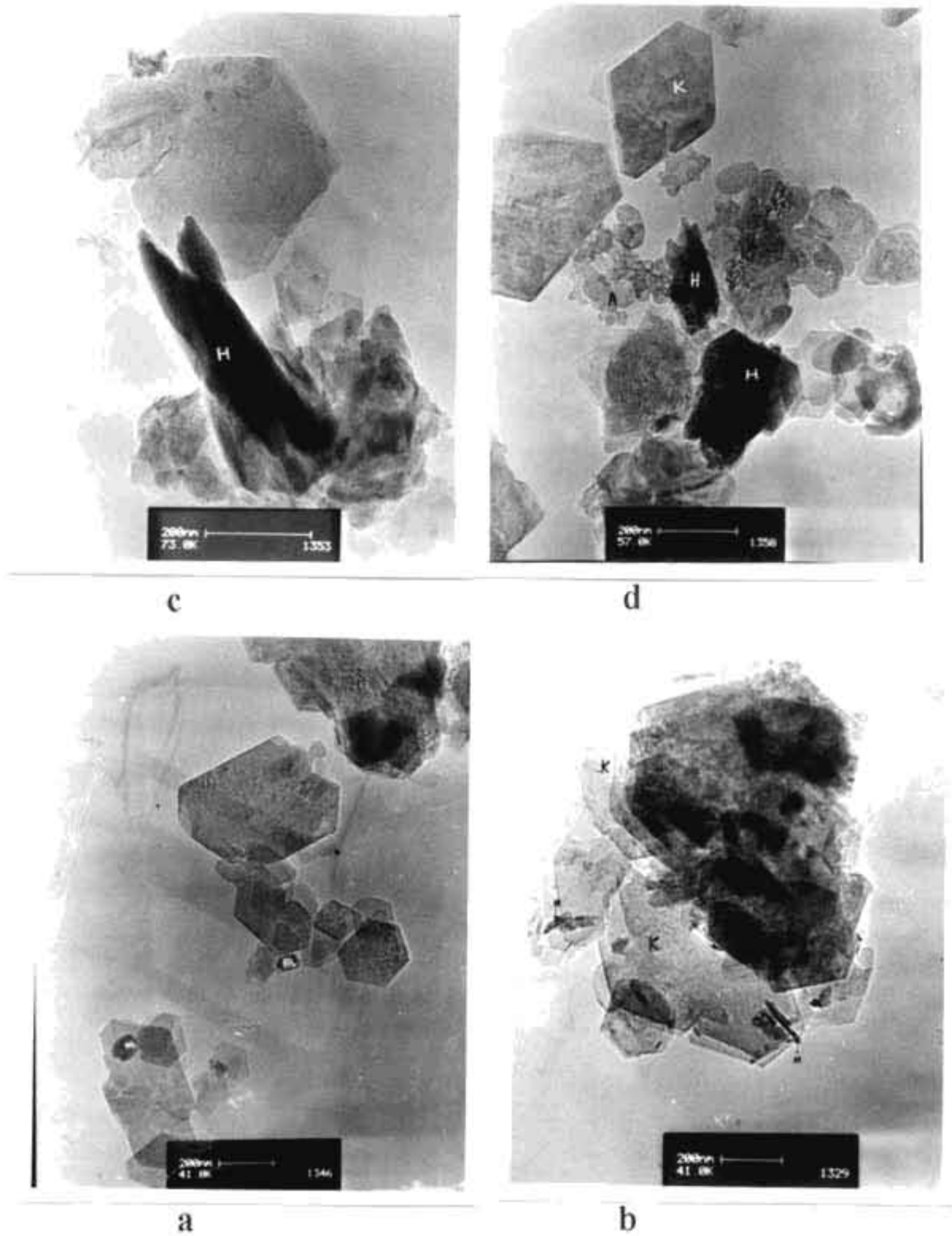
Fig.2.11. Transmission electron micrographs samples. a,b-kaolinite crystals (K) showing twinning (indicated reentrant angles); figure a also shows rounded grains of hematite (Ht) and rutile (Rt) in sampale KK; c-tubular halloysite (H) with splitted end (sample JK); d-platy halloysite (H) and allophanic material(A) in sample KK

62
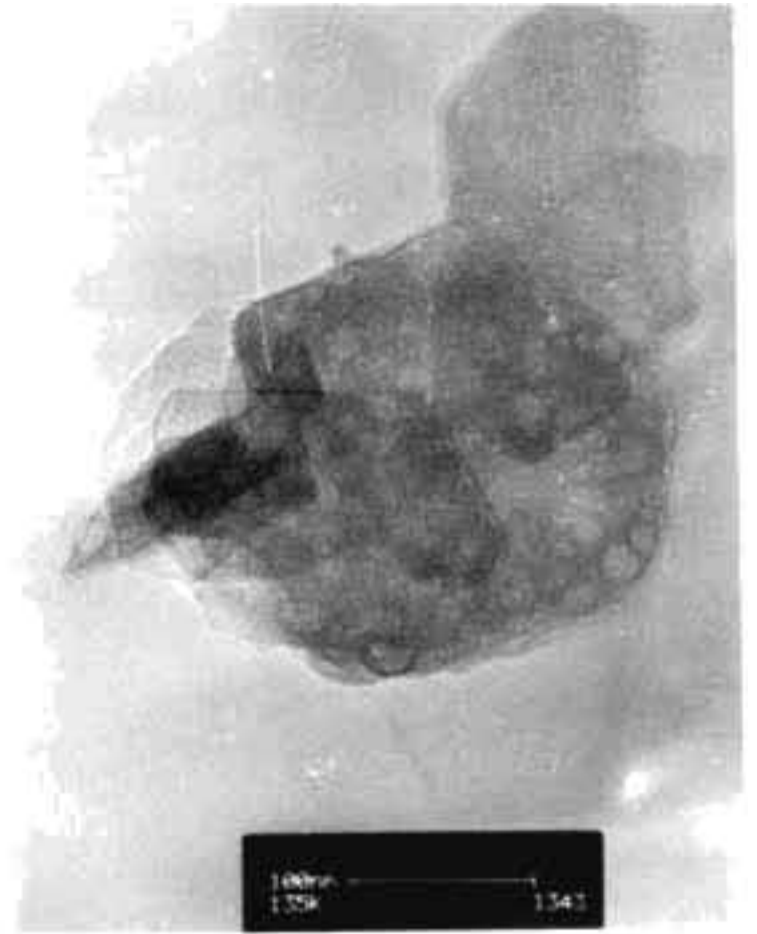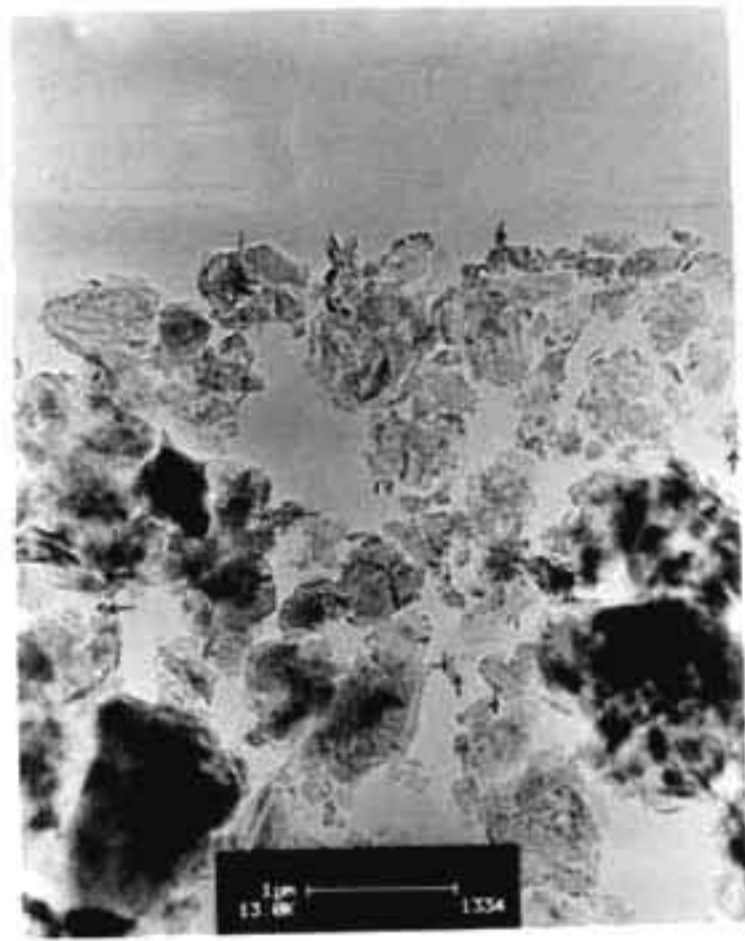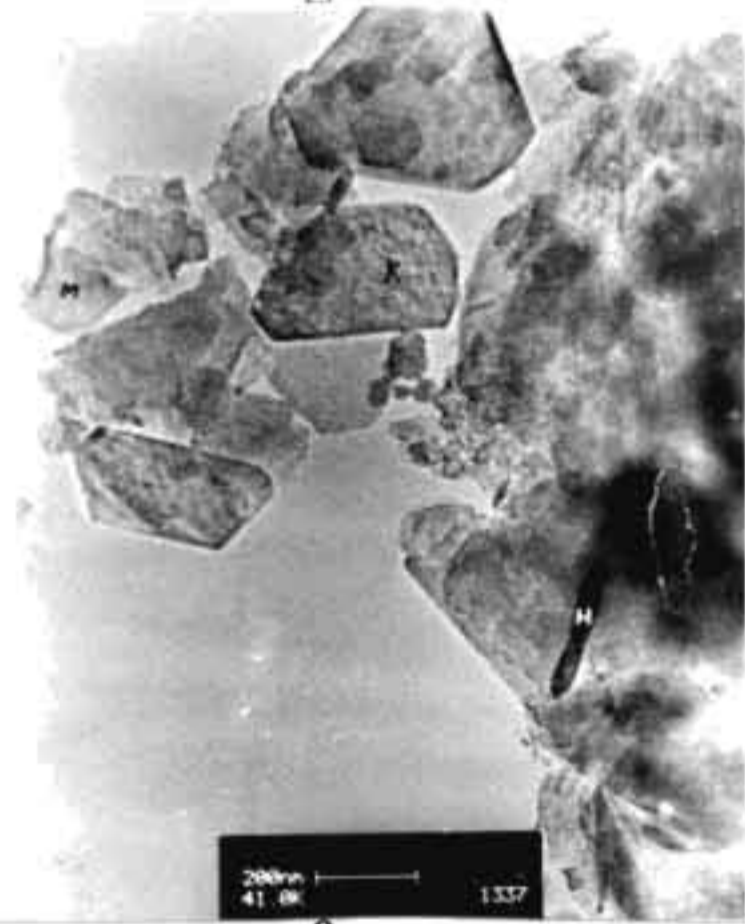
Fig.2.11. Transmission micrographs of clay sampales. e-admixtures of halloysite (H) and kaolinite (K) pseudomorphs on feldspar, and muscovite in sample MK. f,g-transformation of feldspar to halloysite (H); kaolinite (K) and allophane (A) in sample TK; h-coating of goethite on kaolinite grains (sample KK)

63

forms characterized by splitted ends and undulated surfaces with striations were common (Fig.2.11c). Halloysite showing the pseudo-crystalline outline and cleavage traces of feldspars (Fig2.11e) was a clear indication of its alteration from a feldspar precursor[51,52]. Admixtures of kaolinite and halloysite was also found on the surface of feldspar pseudomorph (Fig.2.11f), in which the kaolinite flakes were found in between halloysite tubes, indicating a transitional case for which the conditions were favourable for alteration to both types[52]. The presence of allophanic material (Fig.2.11d&g) was identified as spherules in these samples which may also be considered as an alteration product of feldspar[53].

Hematite particles with rounded morphology were observed in sample KK (Fig.2.11a). A non-uniform surface coating of geothite was clearly seen in figure 2.11h (sample KK), where the well-defined outlines of kaolinite crystals were almost completely marked by this iron oxide precipitation.

Figures 2.12a-e represent the scanning electron micrographs of the clay samples AK, JK, KK, MK and TK respectively. Well formed, pseudo hexagonal plates were distinctive of kaolinite. The kaolinite morphology varied from small crystals with less-defined outline to well ordered stacks[54] (Fig.2.12f) and were quite numerous. Most of the particles fall in the range of 0.5-10 μm. Small lath-shaped goethite crystals were seen in sample TK (Fig.2.11e). Figure 2.12g shows a partially altered fedspar grain with voids on the twinning planes which implied that the formation of kaolinite through weathering and dissolution of the original mineral (feldspar)[52].
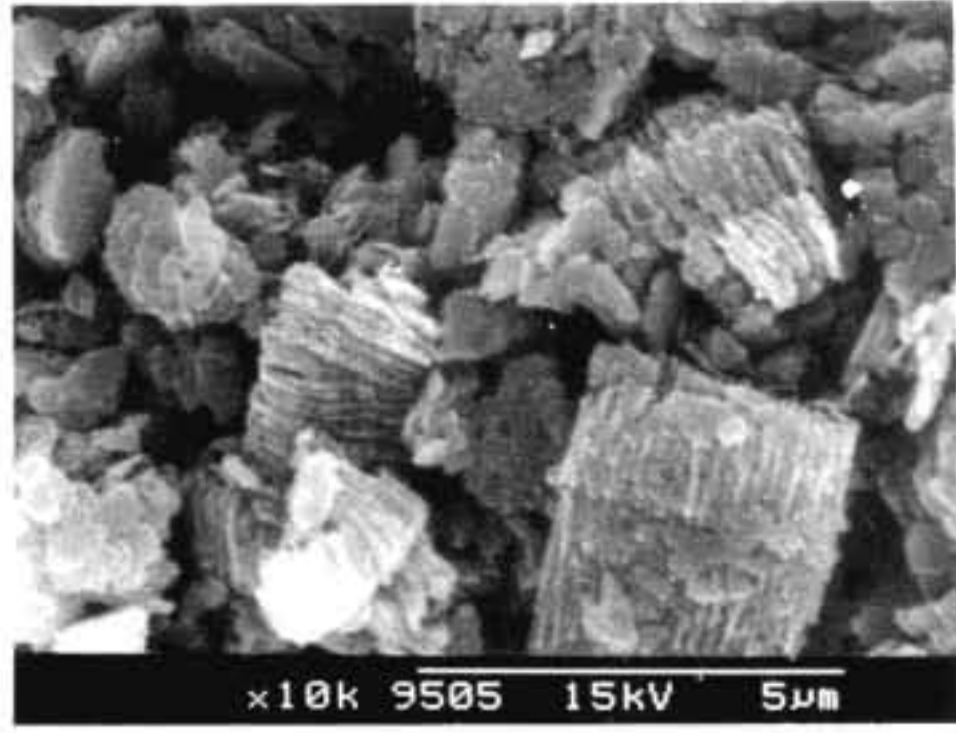
b
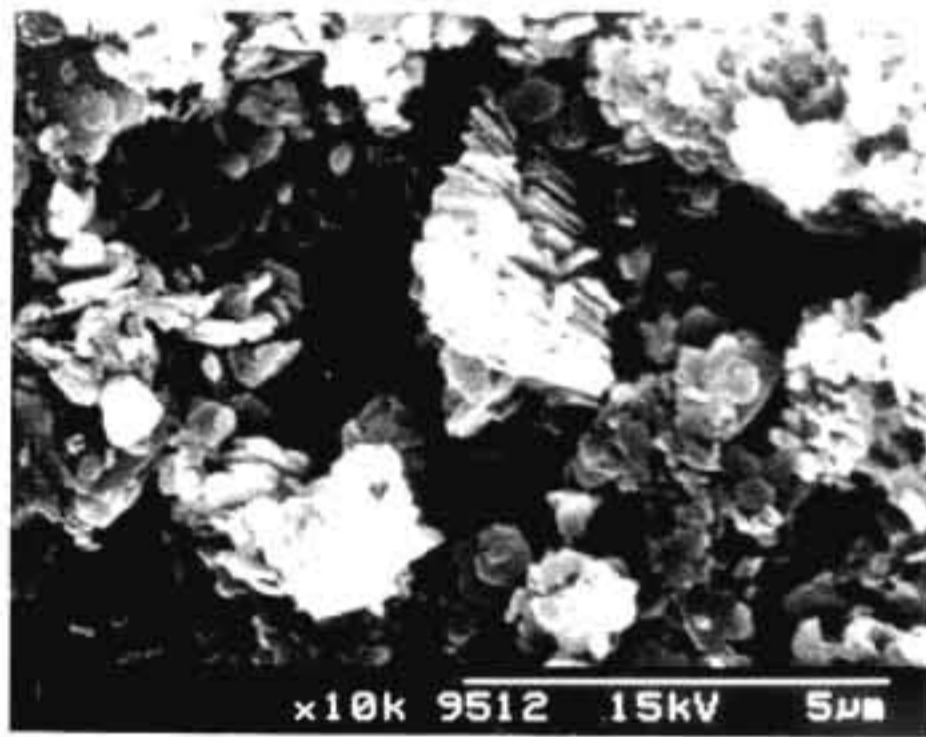
a

Fig.2.12. Scanning electron micrographs of samples AK and JK. a-hexagonal stacks of kaolinite (AK); b-vermiform stacks of kaolinite oriented in different directions (JK)

65

e

d

c
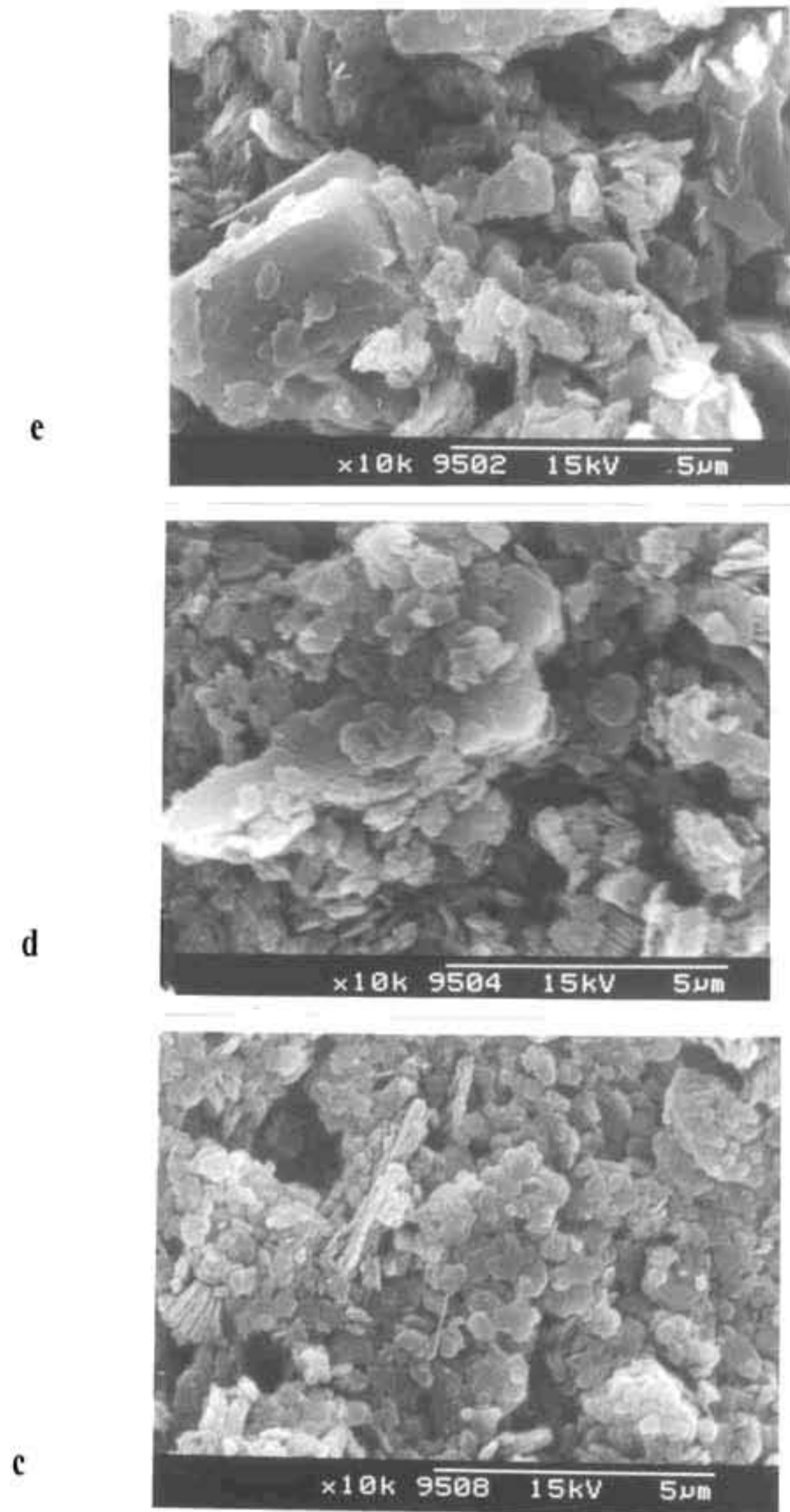
Fig.2.12. Scanning electron micrographs of clay samples KK, MK & TK. c-face to face orientation of hexagonal plates of kaolinite (KK), d-small hexagonal plates and books of kaolinite (MK); e-bigger grains of kaolinites and lath-shaped goethite (Gt) in sample TK
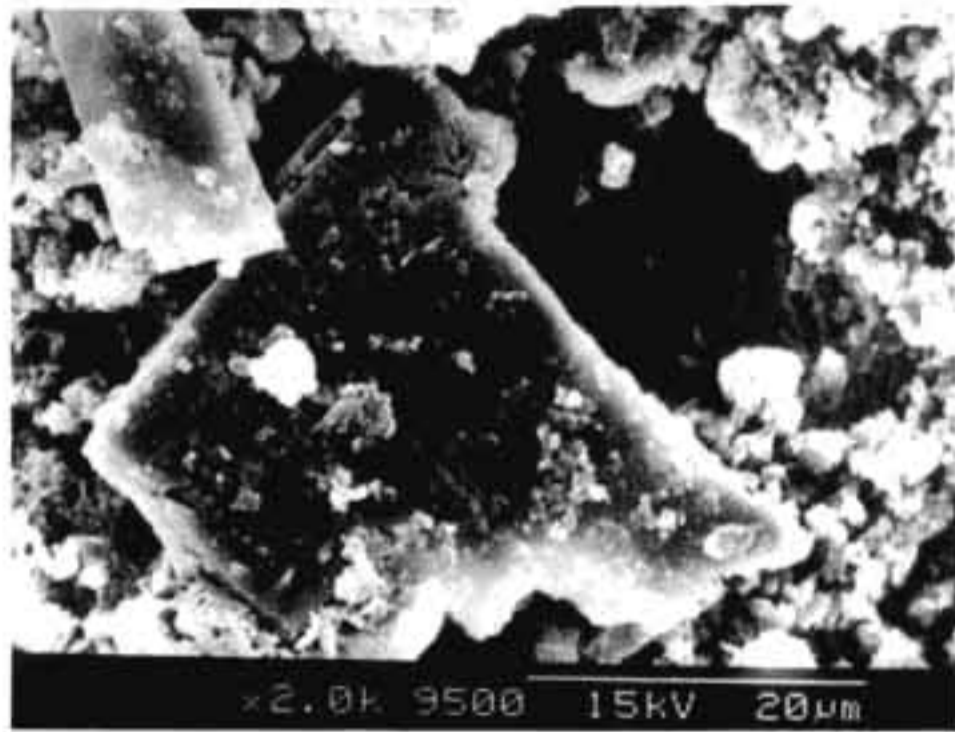
g
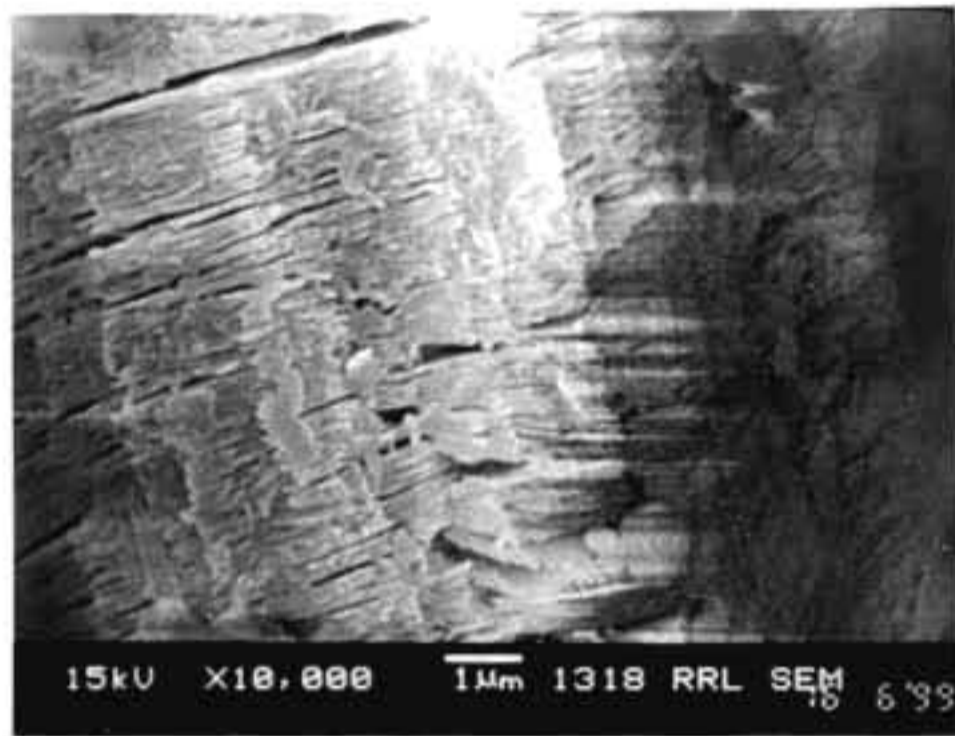
f

Fig.2.12. Scanning electron micrographs of clay sampales. f-a composite pseudohexagonal stack of kaolinite (sample TK); g-large feldspar grains with voids along the cleavage planes indicating the dissolution and alteration to kaolinite (AK)

67

The physical properties measured for the clay samples are given in Table 2.3. The surface area, specific gravity, and water of plasticity are well in agreement with that of kaolinitic clays[21]. From the particle size distribution curve (Fig.2.13), it was observed that samples JK and KK have > 63% fraction below 2 µm particle size. Kaolinite is considered to be formed under mild acid conditions[55] From the pH data, it is evident that the transformation of all these clays samples except sample JK took place under mild acid environment. The slight alkaline pH of sample JK may be attributed to the comparatively higher concentration of Ca (Table 2.4).

Table 2.3. Physical properties of clay samples

No.	Property	AK	JK	KK	MK	TK
1	Surface area (m^2g^{-1})	14.79	10.79	13.55	13.77	9.93
2	Specific gravity (gcm^{-3})	2.55	2.57	2.58	2.56	2.78
3	Water of plasticity (%)	42.36	35.54	41.90	41.52	42.56
4	Particle size (<2 µm) (%)	48.00	63.00	90.00	45.00	57.00
5	pH	5.64	7.29	5.60	5.75	6.30

The chemical analysis data (Table 2.4) showed that the Al_2O_3/SiO_2 proportion of these clay samples were similar to that of kaolinite[56]. Fe_2O_3 and TiO_2 are found to be the two major colouring impurities and their amount varied from 0.93-6.54 and 0.03-0.89% respectively in these samples. The loss on ignition values are not high suggesting a less amount of organic matter. The trace element distribution of the clays are shown in Table 2.5. Several trace elements have been quantitatively retained by Kaolin[57]. But the

68

Mass Distribution Overlays

X-axis scale unit....... micrometers
y-axis scale unit...... delta percent
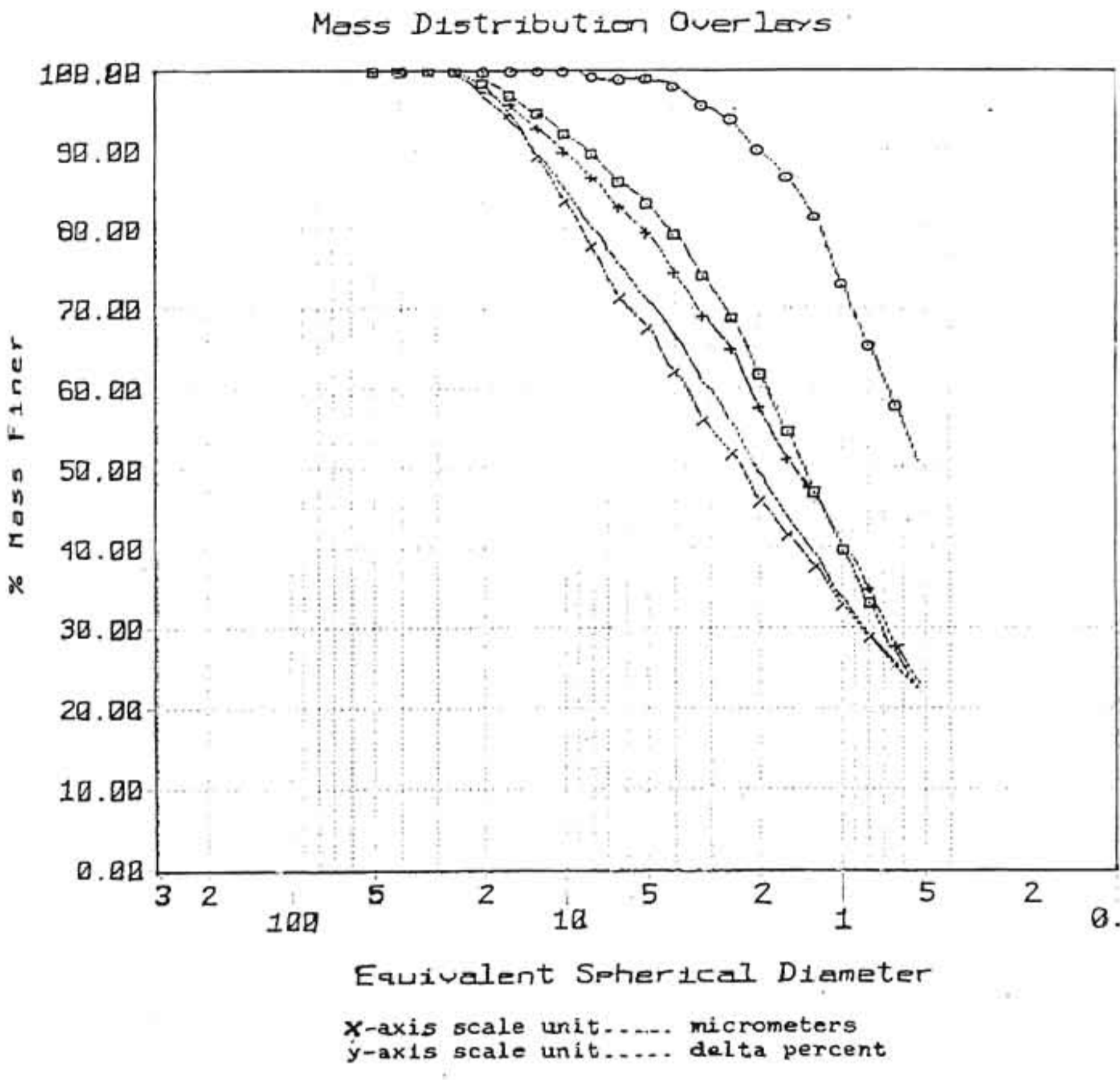
Fig.2.13. Particle size distribution of clay samples. .... – AK; ▫ – JK; ⊙ - KK; ↗ – MK; x - TK

69

depletion of Rb in the clay samples may be ascribed to the alteration of plagioclase during kaolinization because in granites and similar rocks, these trace elements are dominatly located in feldspar[57]. The extent of their retention in the host mineral is controlled by adsorptive fixation. The enrichment of Cu and Zn in the clay samples indicates a preferential dissolution of their main carrier mineral (biotite) during alteration[57].

Table 2.4. Chemical composition of clay samples

Major oxides in % w/w

Oxides	AK	JK	KK	MK	TK
SiO_2	47.87	46.48	44.47	44.35	42.26
Al_2O_3	31.92	37.65	36.08	37.38	32.89
Fe_2O_3	3.98	1.02	0.93	2.64	6.54
FeO	0.29	0.21	0.04	0.23	0.31
TiO_2	0.20	0.03	0.89	0.56	0.31
K_2O	2.7	0.36	0.36	0.30	0.16
Na_2O	0.88	0.16	0.16	0.40	0.51
CaO	0.15	0.69	0.22	0.16	0.16
LOI	11.67	14.31	14.29	14.02	13.46

Table 2.5. Trace elements (ppm)

Cr	12.90	14.70	27.40	35.80	60.60
Co	18.90	20.90	12.20	5.00	26.90
Ni	35.80	9.10	17.80	18.30	66.90
Cu	17.90	14.40	62.80	23.30	132.70
Zn	100.00	160.00	40.00	130.00	220.00
Rb.	20.80	3.60	2.40	1.60	1.30
Sr	41.60	18.10	86.30	20.40	114.60
Y	27.60	19.20	38.70	8.60	20.70
Zr	34.20	19.00	22.60	14.10	12.90
Ba	45.50	35.70	59.30	19.10	141.40

From Table 2.6. the hue for clay samples AK, MK and TK was 10 YR, indicating the presence of pure goethite[58]. The 'redness' value calculated (according to Hust[25]) for

samples JK and KK showed the presence of hematite, but sample JK was found to be devoid of hematite as evident from its X-ray diffraction analysis. A slight 'redness' shown by sample JK may be attributed to lepidocrocite which is orangish yellow in colour. In sample KK, both hematite as well as goethite were identified, but it is pinkish red in appearance. Even minute quantities of hematite is sufficient enough to mask other colours.

Table 2.6. Identification of iron oxides by Munsell colour notation

Sample	Colour Notation	Mineral	Appropriate conditions of formation
AK	10 YR 8/5	Goethite	Common mineral of all weathering environment
JK	5 YR 8/2	Lepidocrocite	Anaerobic/aerobic systems of temperate zones
KK	5 YR 3/1.5	Hematite	High soil temperature low water activity, rapid biomass turn over. Characteristics of tropics and subtropics
MK	10YR 8/2.5	Geothite	Common mineral of all weathering environments
TK	10 YR 8/6	Goethite	-do-

Iron oxide minerals are valuable indicators of the environmental conditions at which the particular deposit is formed. Hematite and lepidocrocites are characteristic of certain pedogenic conditions. Hematite is the typical weathering product of tropical and subtropical climatic zones with lower water activity[59]. Similarly lepidocrocite also represents a set of conditions. Soluble Fe^{2+} ions are the necessary precursor for Fe^{2+} lepidocrocite formation. From this redoxomorphic soils, lepidocrocite forms by slow

oxidation[60,61] of Fe^{2+}. In general, the occurrence of lepidocrocite is restricted to the redoxomorphic soils in humid temperate climates and temperate areas within subtropical regions.

Figure 2.14 show the effect of magnetic separation and 5 M NaOH treatment on the five clay samples. The absence of kaolinite peaks in the 5M NaOH treated fractions suggest a complete dissolution of the mineral by the alkali treatments. Peaks of iron oxides and other non-clay minerals become prominent after the alkali treatment.

The major iron oxide mineral identified in sample AK was goethite. The diagnostic reflections of goethite were 4.18, 2.69 and 2.45 Å. The titania mineral present in the sample is rutile which is characterised by the d-spacings at 3.25, 2.46 and 2.17 Å.

In sample JK, the dominant mineral separated was a dioctahedral mica, muscovite. Prominent reflections from the basal planes are well-defined and sharp. The diagnostic reflections occur at 10.01 (002), 5.03 (004) and 3.36 (006) Å. The medium and low intensity reflections are also observed in the X-ray pattern. The iron oxide mineral present in the sample are lepidocrocite and goethite. Strong well-defined reflections at 6.27 Å is indicative of lepidocrocite. The medium intensity peaks at 2.29 and 2.47 Å are small and broad. Goethite is identified from its characteristic d-spacings at 4.19, 2.67 and 2.45 Å.

Hematite and goethite are the two major ferric oxides in sample KK. Hematite was identified from the strong reflections at 2.69 and 2.51 Å, and the medium intensity reflections at 3.67, 2.2, 1.8 and 1.67 Å. The diagnostic d-values of goethite were 4.18.
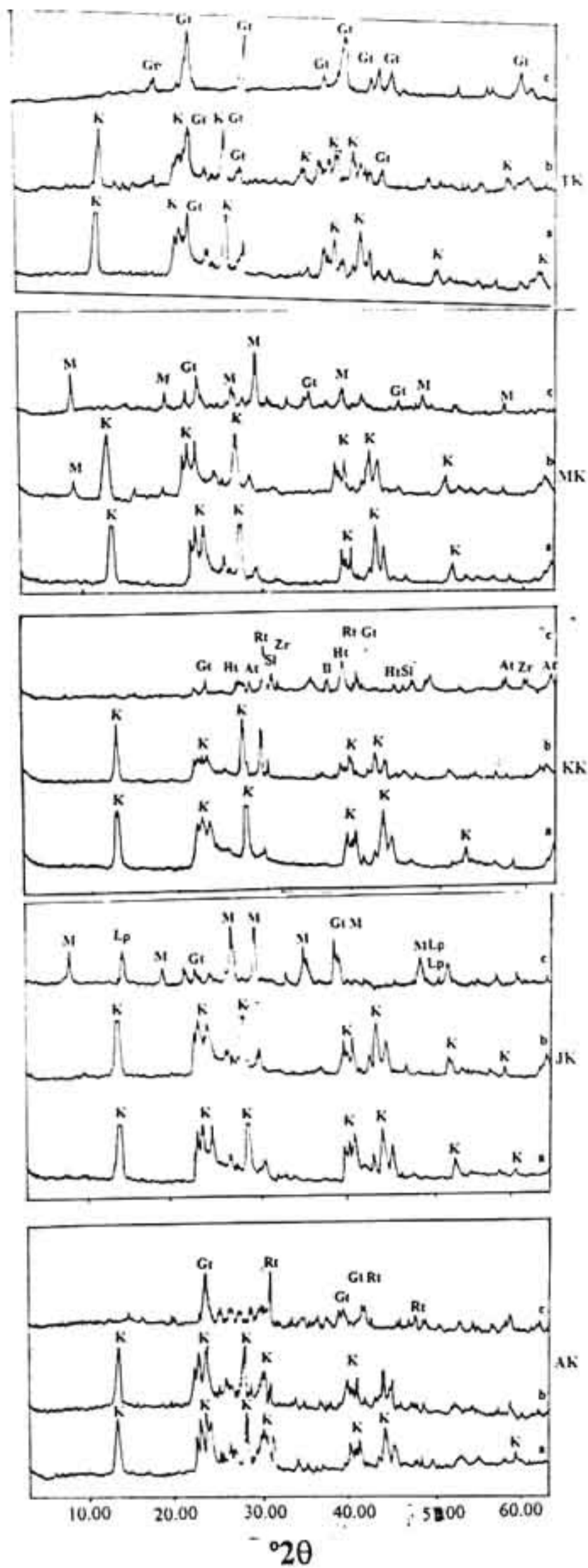
Fig.2.14. X-ray diffraction pattern of clay samples AK, JK, MK and TK. a-original sample; b-magnetic fraction: c-magnetic fraction after dissolving kaolinite in 5M NaOH solution. K – kaolinite, Ht – hematite, Gt – goethite, Rt – rutile, At – anatase, Lp – lepidocrocite, St – sillimanite, Zr – zircon, M – muscovite, Il – ilmenite

73

2.65 and 4.45 Å. The major titania minerals present in the sample were rutile, anatase and ilmenite. Ilmenite is strongly magnetic but rutile and anatase are not attracted by magnet unless they are coated with iron oxides. The possible source material for this rutile and anatase must be ilmenite present in the parent rock (Khondalite). The reflections of rutile and anatase were strong and well-defined. The characteristic peaks at 3.25 and 2.49 Å were suggestive of rutile and peaks at 3.52, 1.82 and 1.67 Å were suggestive of anatase. The ilmenite peaks (2.75 Å) was broad and short suggesting a weathering stage. In addition to the above mentioned titaniferrous minerals, two other ancillary minerals were also identified in the sample. The diagnostic reflections of zircon occurs at 3.29, 2.52 and 1.71 Å and for sillimanite at 3.38 and 2.21 Å.

The magnetic fractions of sample MK contains both micaceous as well as ferruginous minerals. The sharp peak at 10.01 Å became prominent after 5 M NaOH concentrated portion. The d-spacings at 10.01, 5.04, and 3.35 Å were characteristic of muscovite mica. The iron oxide mineral present in the sample is goethite as evident from the reflections at 4.18, 2.69 and 2.46 Å.

The X-ray diffraction pattern of the 5 M NaOH treated fraction of sample TK exhibited characteristic reflections of goethite only. The peaks at 4.19, 2.69 and 2.47Å were well-defined. The medium and low intensity reflections are also clearly observed in the pattern. Figures 2.15a-e show the scanning electron micrographs of the magnetic fractions after removing the adhered clay particles by 5 M NaOH solution. The initial stages of muscovite alteration to kaolinite were marked by the fraying out of the edges[54] (Figs.2.15a&b). Figure 2.15c&d show the spongy appearance of muscovite, indicating

the initial stages of alteration[54]. Figure 2.15e shows goethite crystals concentrated in sample TK after 5 M NaOH treatment.

The results of chemical dissolution of iron oxides by EDTA, oxalate and CDB techniques are given in Table 2.7.

Table 2.7. Percentage of Fe$_2$O$_3$ removal by EDTA, oxalate and CDB techniques

Technique used	% Fe$_2$O$_3$ extracted				
	AK	JK	KK	MK	TK
EDTA	1.32	0.88	5.33	3.09	0.66
Ammonium oxalate	0.97	1.57	4.50	3.18	0.73
CDB [f$_d$]	57.41	68.25	44.08	51.98	57.89
f$_d$/f$_t$	0.57	0.68	0.44	0.52	0.58

f$_t$ = total iron oxide content in % w/w

EDTA and oxalate techniques are the two recommended procedures for the removal of "amorphous" iron from soils and clays[34,39]. But prolonged leaching with the oxalate solutions dissolve out poorly ordered ferrihydrite and some other crystalline species like lepidocrocite and magnetite[43]. According to Schwertmann et al.[62], the crystalline Fe-oxides like goethite, hematite and lepidocrocite remain unaltered by a 2 hr treatment in oxalate solution. The oxalate solubility of these crystalline oxides are very low and is in the order of goethite $\simeq$ hematite < lepidocrocite. Therefore, it can be expected that mainly the ferrihydrite is dissolved by oxalate in 2-4 hr. The strong complexing capacity of oxalate often dissolves Fe present in organic complexes[24]. Similar to oxalate, EDTA also form complexes with Fe in soils. However, the EDTA extractable Fe includes, water soluble and exchangeable Fe as well as Fe in the organic complexes[36]. From the Table 7, the EDTA and oxalate soluble, "amorphous" Fe accounted for only a small portion (upto 5%) of the total iron oxide content in the clay samples. Therefore, it could be inferred
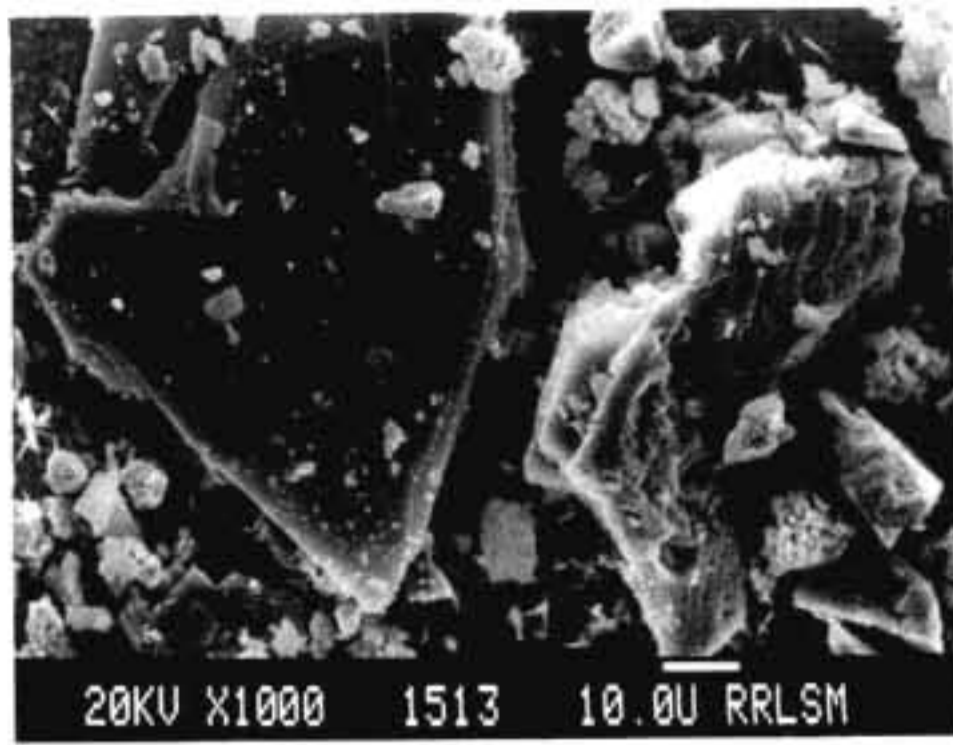
b
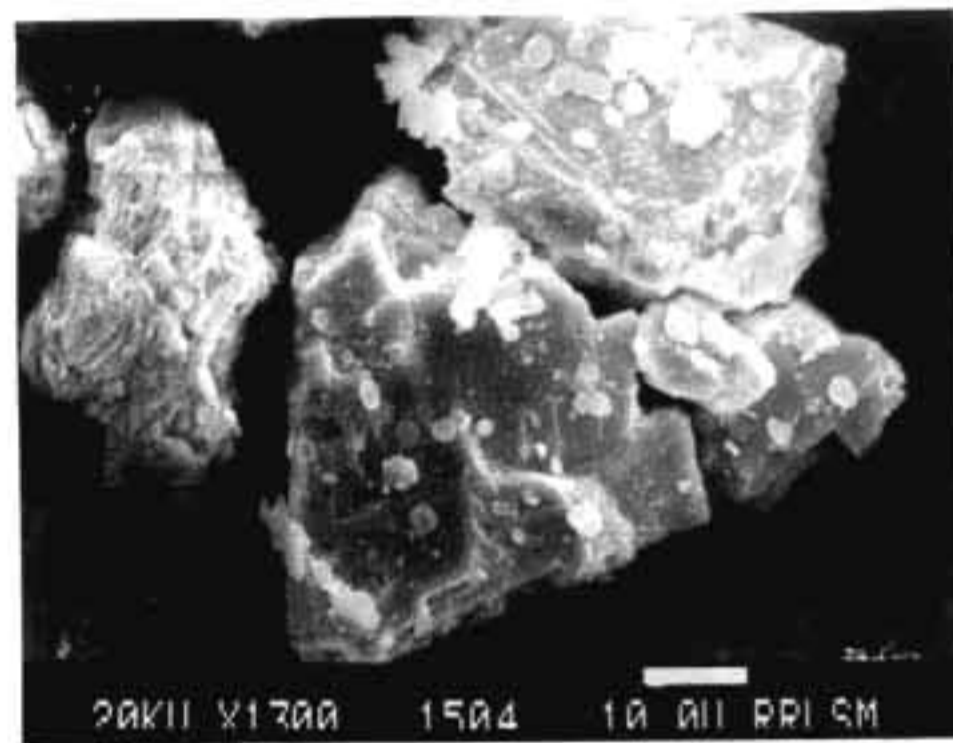
a

Fig.2.15. Scanning electron micrographs of magnetic fractions after removing the adhered clay fraction in 5M NaOH solution. a&b-muscovite alteration to kaolinite, indicated by the fraying out of the flakes (sample JK).

76
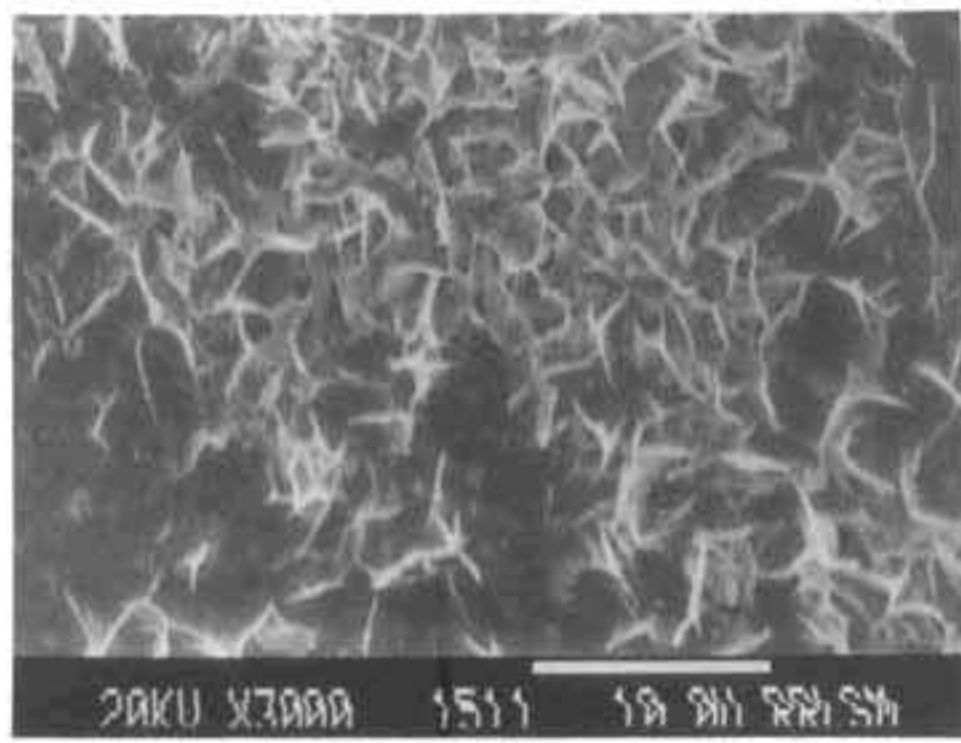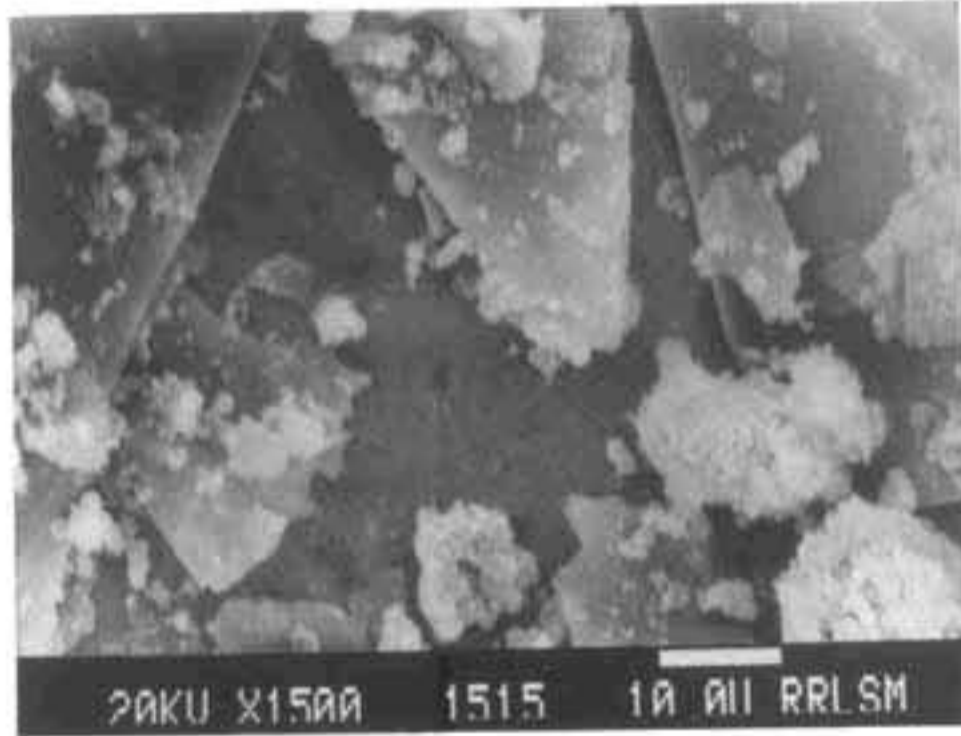
Fig.2.15. Scanning electron micrographs of magnetic fraction after removing the adhered clay fraction in 5M NaOH solution. c&d-spongy appearance of muscovite indicating initial stages of alteration (sample KK); e-clustures of goethite in sample KK

that the amount of Fe as water soluble and exchangeable as well as Fe in organic complexes was very low in the clay samples.

The CDB extractable iron oxides "Free iron oxide" content was found to be 44-68% of the total Fe_2O_3. The f_d/f_t ratio indicates a moderate rate of weathering of these deposits Usually, in situ altered clay deposits would have given rise to high f_d/f_t ratios[63]. From Table 2.7, it is obvious that the iron is not completely extracted by this technique, which indicates that some iron may be incorporated in those minerals which are unaffected by this treatment. Therefore, it can be assumed that a relatively high amount of iron is incorporated in the structure of kaolinite, mica, tourmaline, zircon rutile/anatase and ilmenite[49].

Some additional information on the ancillary minerals has been obtained from the petrological microscopic investigations. Presence of tourmaline with inclusions of iron oxide (Fig.2.16a), prismatic rutile with inclusions of opaques (iron oxide) (Fig.2.16b), and partially altered epidote with iron oxide precipitation (reddish brown) (Fig.2.16c) were identified in sample JK. Figure 2.17a shows zircon with inclusions of opaque minerals (iron oxide) in KK. The alteration of some Fe- containing minerals have seen in the microslides (Fig.2.17b). The rounded opaque grains are suspected to be hematite (Fig.2.17c).

2.3.2. Petrography

A major portion of South Kerala (Kollam and Trivandrum districts) is occupied by the rocks of Khondalite group[64]. Pegmatites, quartz-sillimanite gneisses, granite-biotite gneisses, pyroxene granulites are often found in association with Khondalite.

78

Fig.2.16. Petrological microscopic photos showing the heavy minerals in the clay samples (under open nicols). a-tourmaline with inclusions of opaque minerals (magn. 40X); b-prisomatic rutile with inclusions (magn. 40X); c-alteration epidote along the cleavage planes (magn. 40X)scale : 1 cm = 0.25 mm
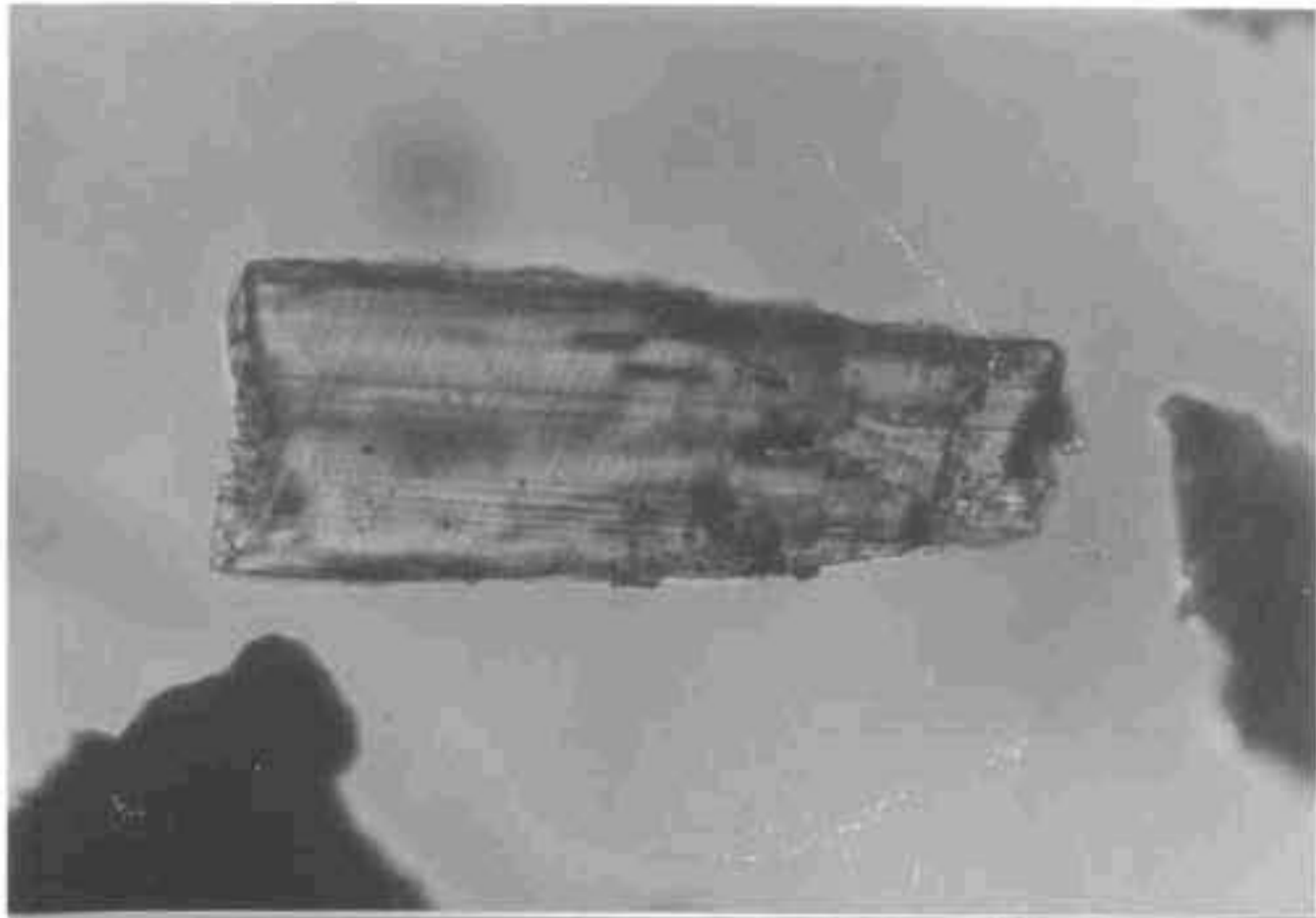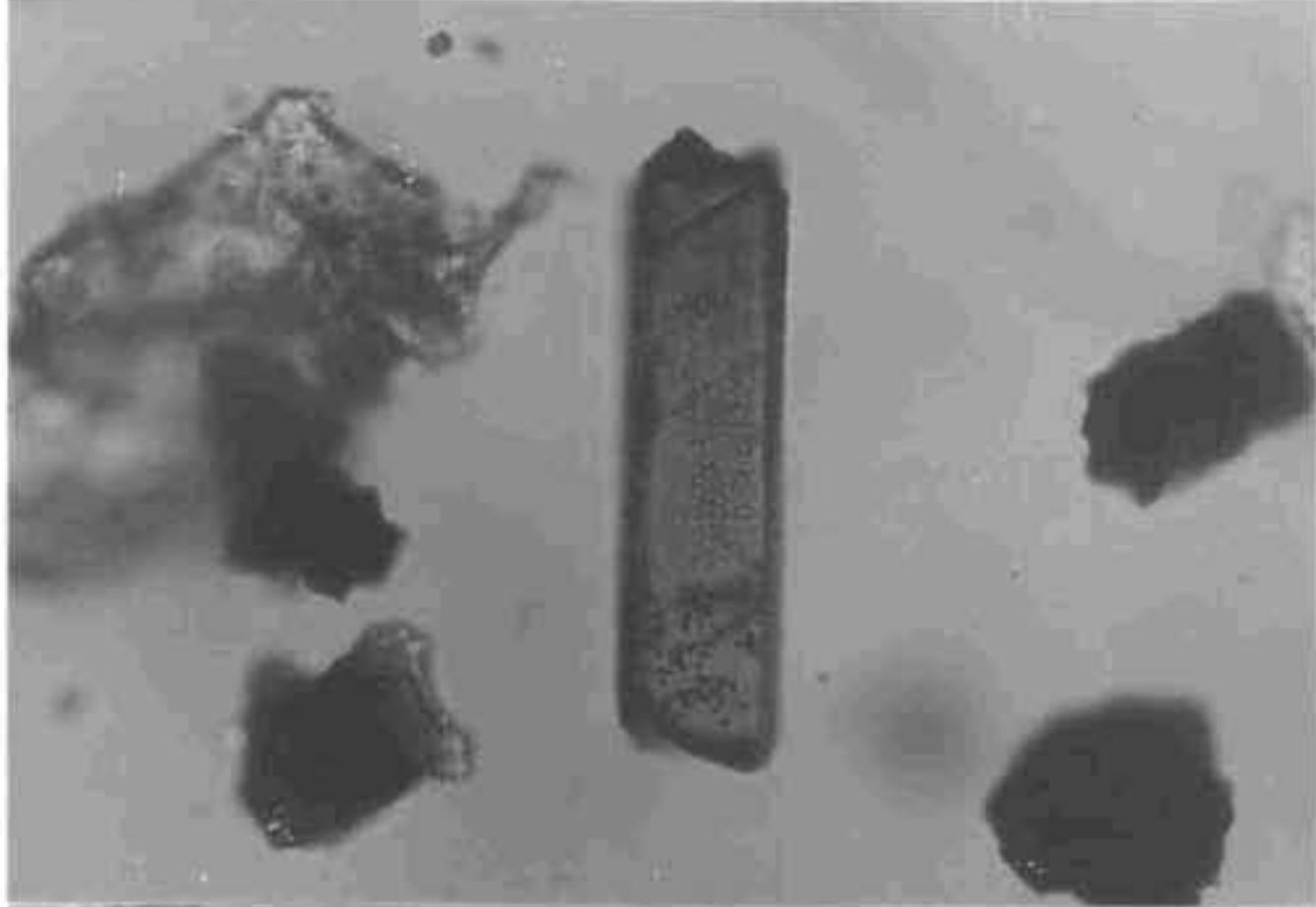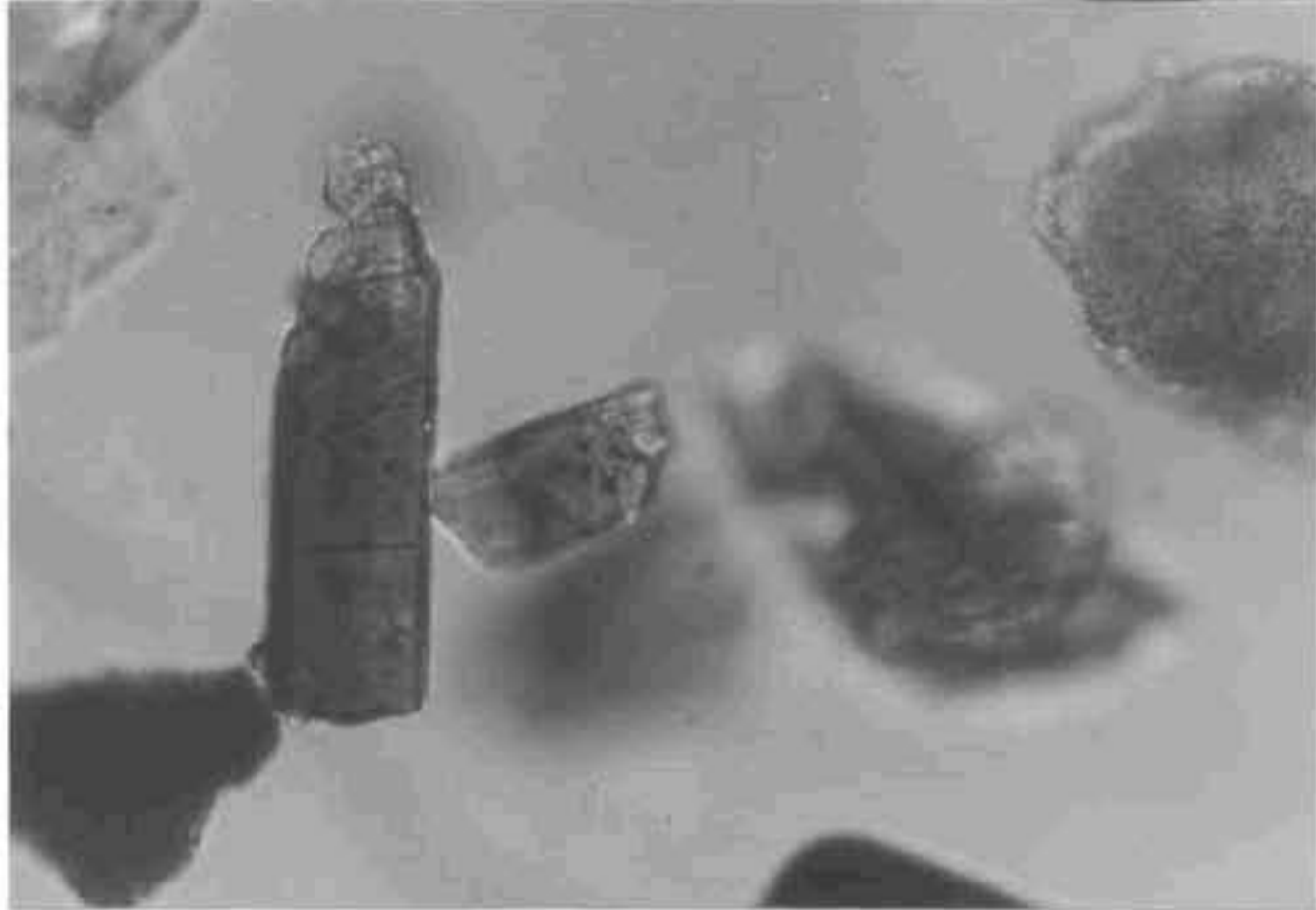
Fig.2.17.Petrological microscopic photos showing the heavy minerals in the clay samples (under open nicols). a-zircon with inclusions of opaque minerals (magn.40X); b-alteration of iron containing minerals (magn. 40X); c-rounded opaque grains (hematite?) (magn. 40X) scale : 1 cm = 0.25 mm
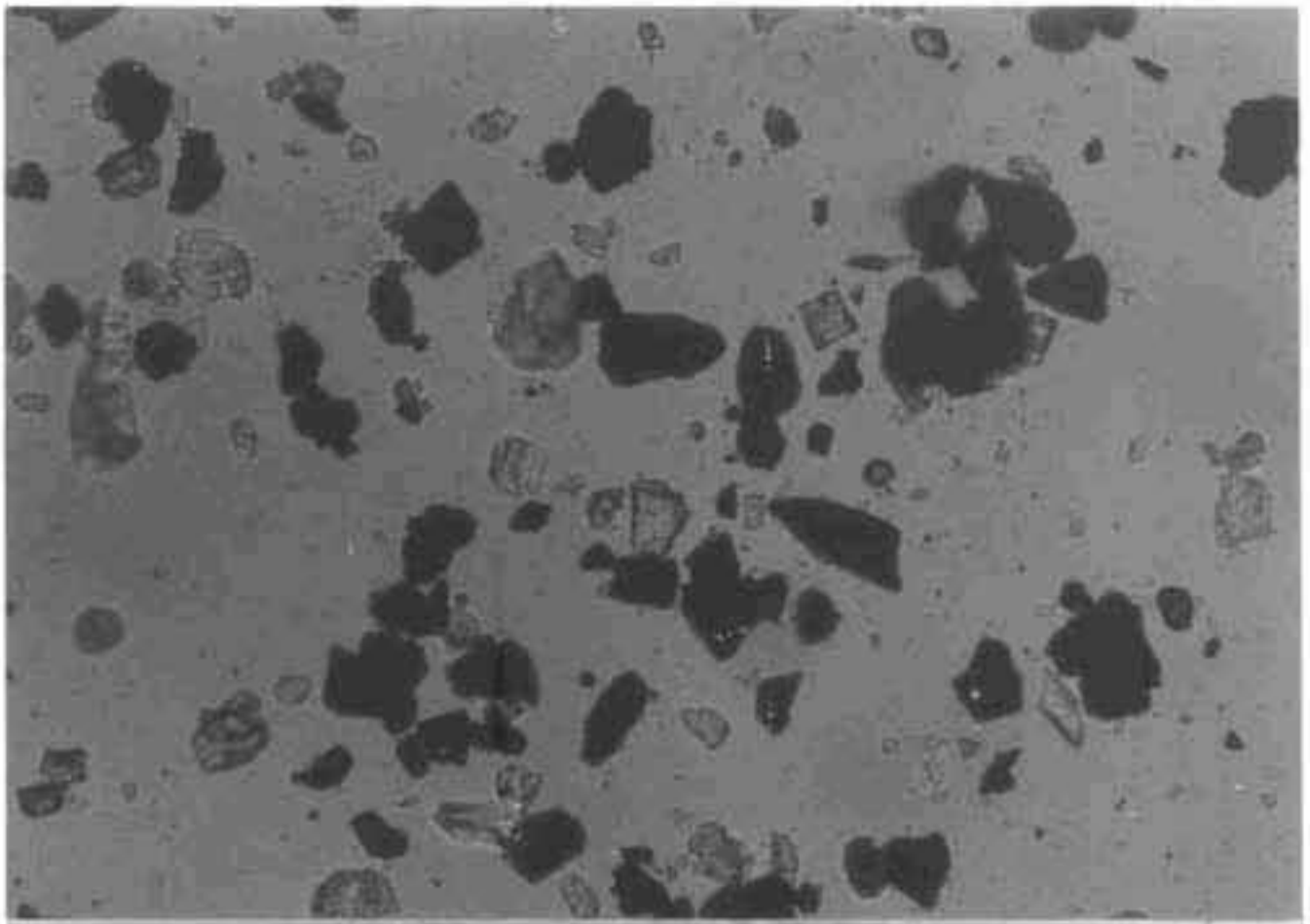
c
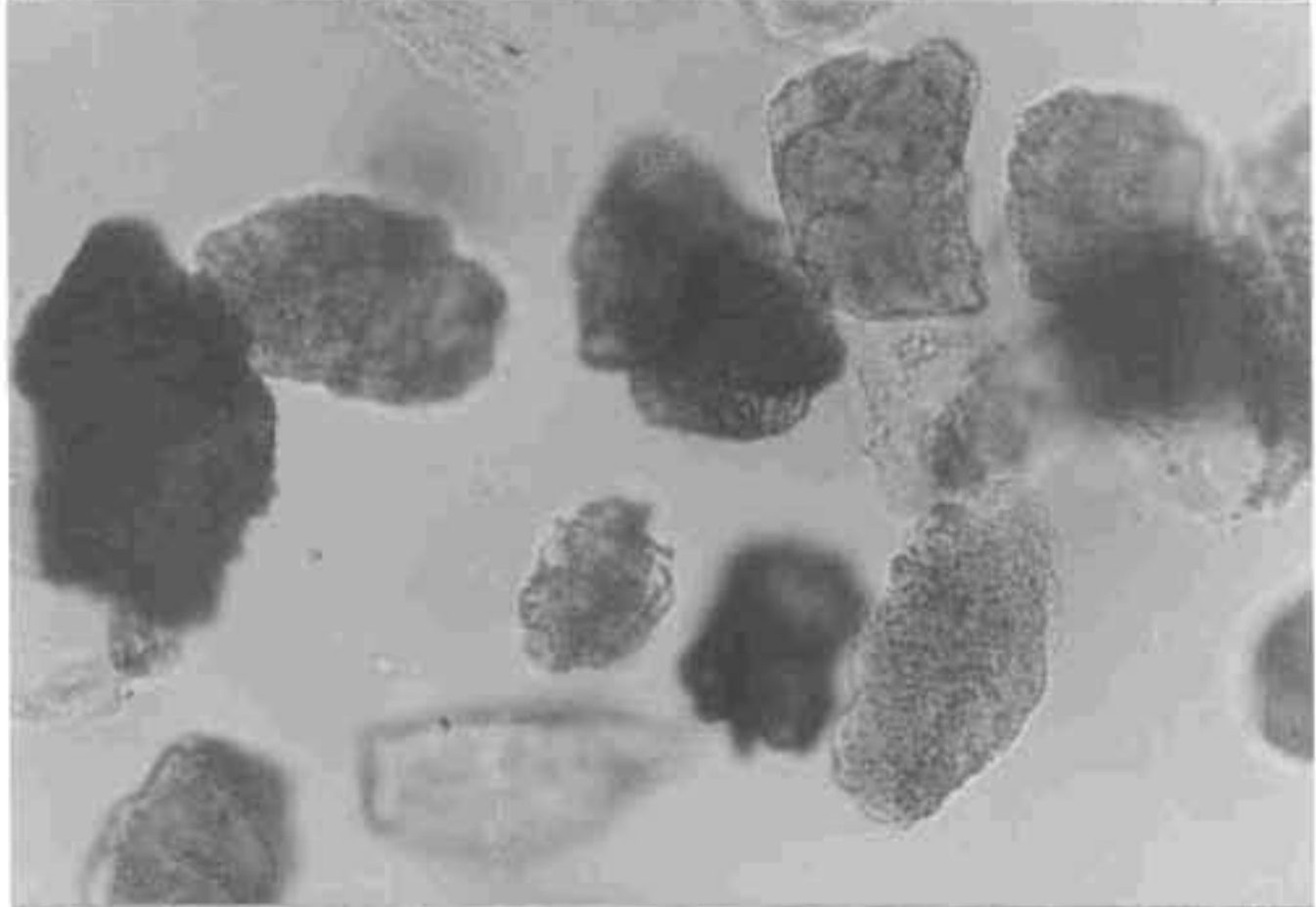
b
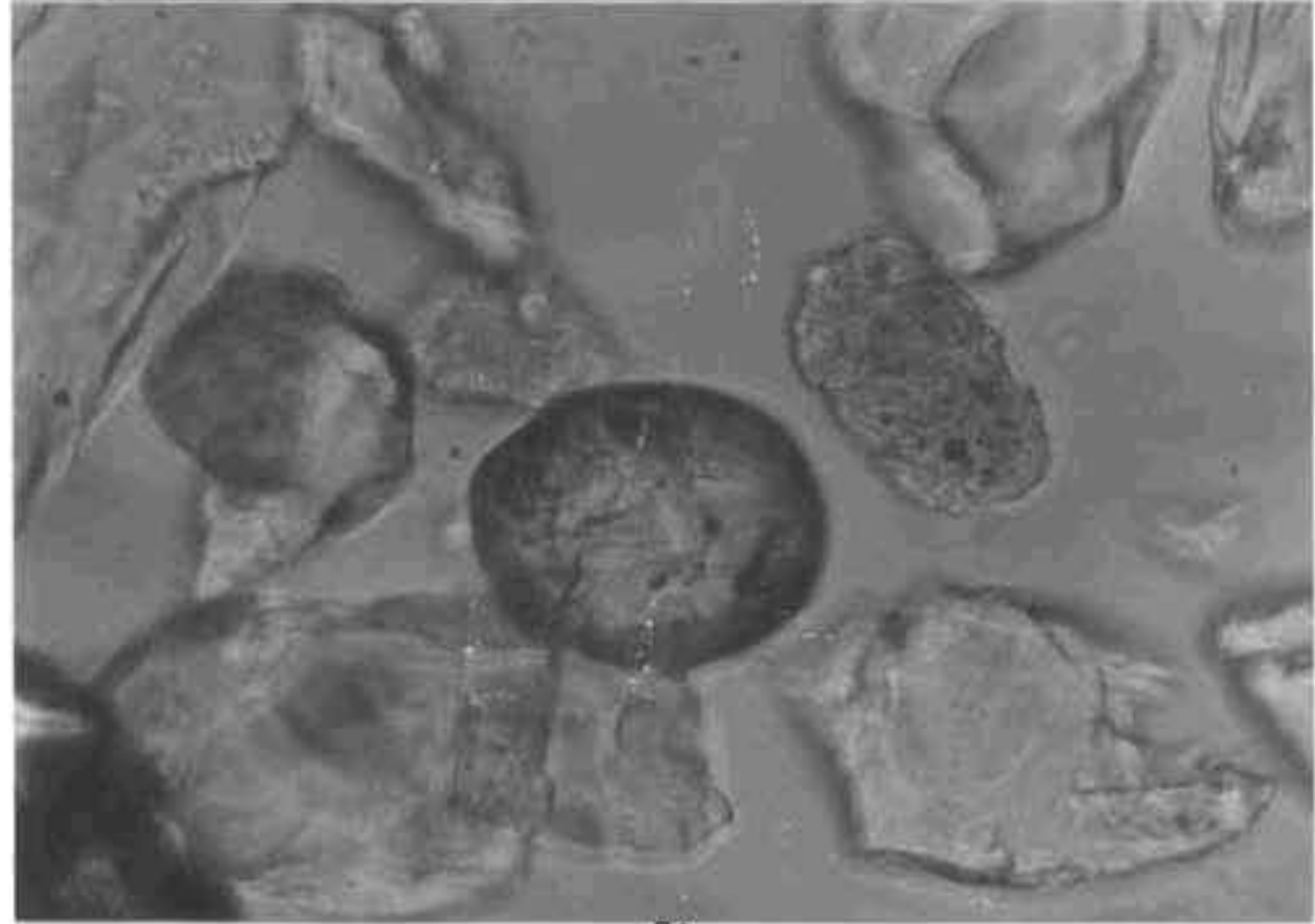
a

Occasional patches of charnockite are also seen in close association with Khondalite. Intense lateritisation of these rocks under humid tropical climate with occasional heavy rain fall and organic activity led to the formation of both kaolinite and bauxite and the processes are still active[65].

2.3.3. Modes of kaolinite formation in Akulam, Buchara, Kalliyur, Mulavana and Thonnakkal

The Akulam deposit is formed from the in situ weathering of a medium-grained garnetiferous biotite-sillimanite graphite gneiss. The depth of weathering was generally meters. The kaolinite content decreases downwards with subsequent enrichment of quartz and feldspar. The foliation of the parent rock has been preserved in the weathered saprolite (Fig.2.18). Quartzo-feldspathic vein remnants are numerous in the mottled and pallid zones. Quartz found in these veins are coarse-grained, subrounded and unaltered, and the feldspar has changed to kaolinite (Fig.2.19).

The kaolinite pseudomorphs with the cleavage traces and crystal faces of feldspar (Fig.2.11b) is indicating a direct transformation to kaolinite. Large feldspar grains with voids along the cleavage direction (Fig.2.12g) also suggests a direct alteration of feldspar to kaolinite. Sunter et al. reported a direct transformation of microcline and plagioclase to kaolinite in humid climates[51].

In Buchara, the kaolinite is formed from the alteration of a pegmatite. The invariable presence of a dioctahedral mica, muscovite was confirmed using X-ray diffraction analysis (Fig.2.14). The scanning electron micrographs of the muscovite flakes are shown in figure 2.20. The occurrence of fan-shaped composite stacks and frayed-edged mica are implications of growth of kaolinite stacks initiating from the edges of micaceous layer[54] (Fig.2.20a). Absence of intermediate phases like illite or hydromica

81
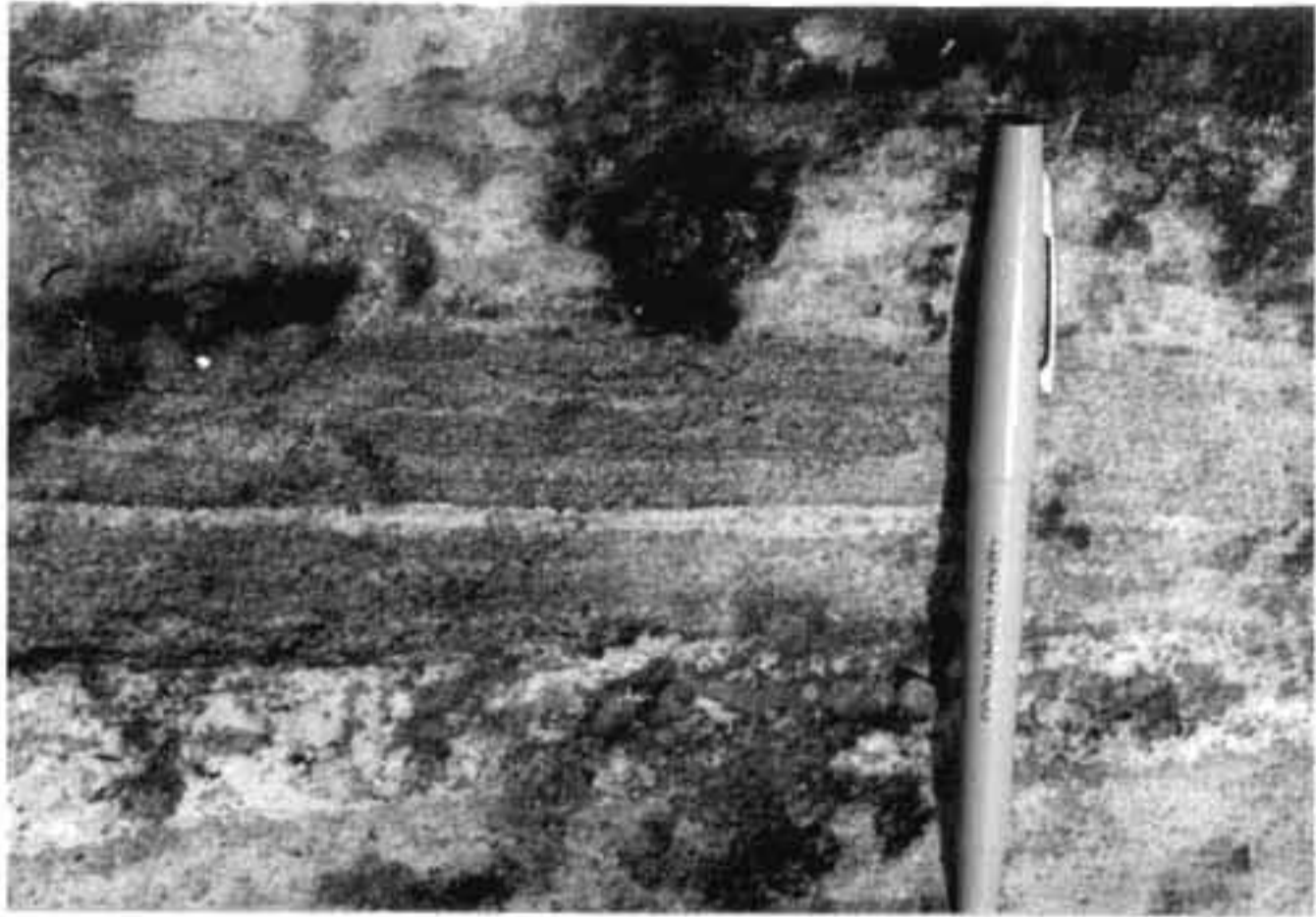
Fig.2.18. Foliation of the parent material preserved in the weathered saprolite (Akulam)

Fig.2.19. Coarse-grained subrounded quartz in the quartzo feldspathic vein remnant (Akulam)

82
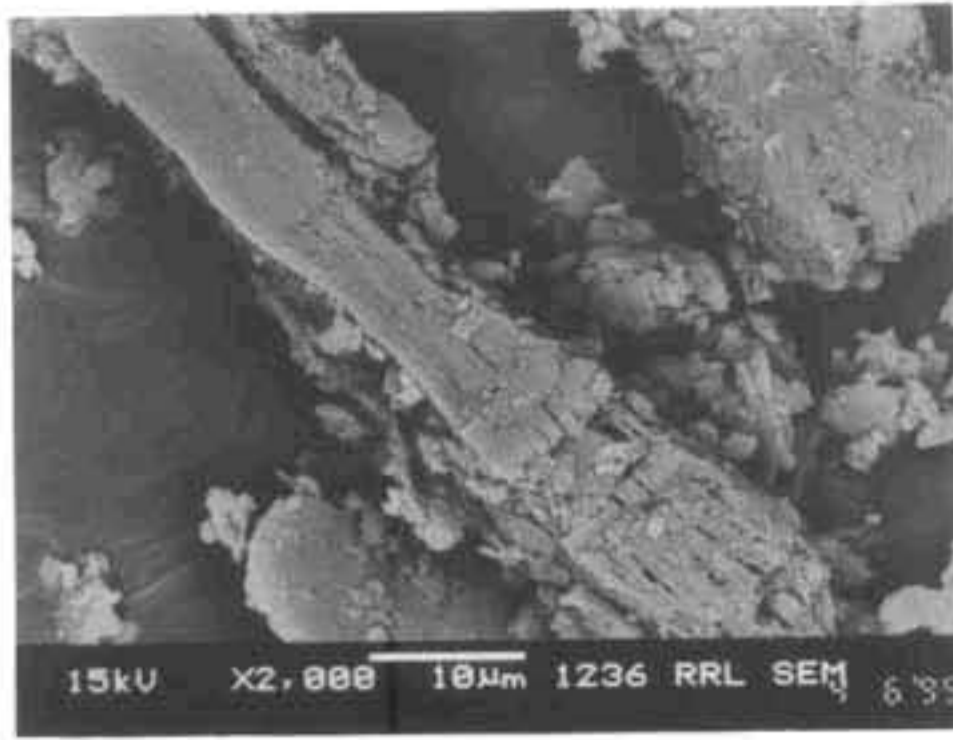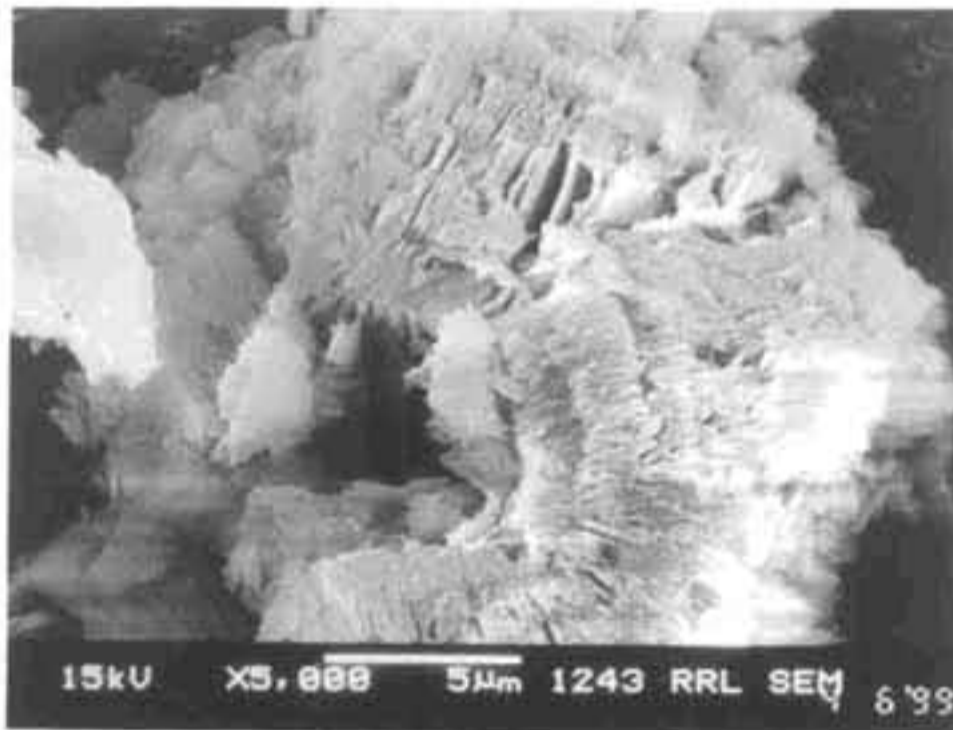
Fig.2.20. Alteration of muscovite to kaolinite (Sample JK). a-vermiform stack of kaolinite; b&c-the frayed out structure of muscovite indicating the initial stage of alteration to kaolinite

83

and montmorillonite indicate that during the process of kaolinitization of the pegmatitic rock, the structure of muscovite undergoes a direct transformation into kaolinite[66].

The occurrence of the Kalliyur clay deposit, bounded by river channels and the presence of sedimentary structures like lamination, cross-bedding are suggestive of a sedimentary origin for the clay. The dominant mineral is kaolinite with small amounts of rutile/anatase, zircon, sillimanite, hematite and goethite. Graphite is an invariable constituent and can be seen in the hand specimens. The presence of graphite and sillimanite as key minerals and the proximity of the kaolin deposits to the khondalite terrain of South Kerala would indicate a khondalitic source rock for the clay[67]. The higher crystallinity and lower surface area indicate that the materials have undergone an in situ weathering after deposition.

In Mulavana, the kaolinite is derived from a garnetiferrous biotite gneiss rich in feldspar and quartz. The presence of the dioctahedral mica may be secondary or primary. The transformation of biotite to kaolinite may occur directly or through mica (muscovite), vermiculite[66,68] etc. It has been reported that the transformation of trioctahedral to dioctahedral may take place approximately at higher concentration of Al^{3+} and K^-/H^- in the weathering medium. At low K^+/H^- values, the biotite passes directly into kaolinite[66].

The Thonnakkal clay deposit is a weathering product of khondalitic rock[67]. The direct transformation of feldspar to kaolinite is evident from the transmission electron micrographs (Fig.2.11f&g).

2.3.4. Iron oxides in clay deposits

The Fe-bearing minerals in these rocks, like biotite, garnet, pyroxenes, (hypersthene), magnetite and ilmenite are highly unstable under surface weathering conditions and decompose readily to iron oxides and alumino silicates. This is the primary reaction through which, Fe(III) was introduced into the pedogenic cycle[24].

Topography, climate, water regime, pH and Eh are major controlling factors determining the soil formation and type of iron oxide enrichment. The tropical humid climate with occasional rainfall and dense vegetation are readily conducive to intense leaching of the khondalite-charnockite rocks in South Kerala[65]. Under these conditions, feldspars are directly converted to kaolin and the iron-bearing minerals to goethite and hematite. Goethite is a common Fe-oxide devoid of any climatic zones, whereas hematite is typical of certain pedogenic environments. Higher temperature and lower water activity are the most important factors favouring the formation of hematite over goethite[59]. Near neutral pH, a high Fe-content in the parent material and rapid turnover of biomass also favour hematite over goethite. These conditions favour the formation of ferrihydrite (considered to be a necessary precursor of hematite) and its dehydration leads to hematite[59]. A direct solid state transformation of goethite to hematite by simple dehydration is not reported so far[69]. In the study area, the side by side occurrence of hematite and goethite have observed in the mottled zone (Figs.2.21&22). The transformation of red to yellow soils may be attributed to a preferential dissolution of hematite to form ferrihydrite followed by its conversion to goethite under reducing conditions and is not through a solid-phase transformation of hematite of goethite[59] (Fig.2.22).

Fig.2.21. Side by side occurrence of hematite (red) and goethite (yellow) at Akulam
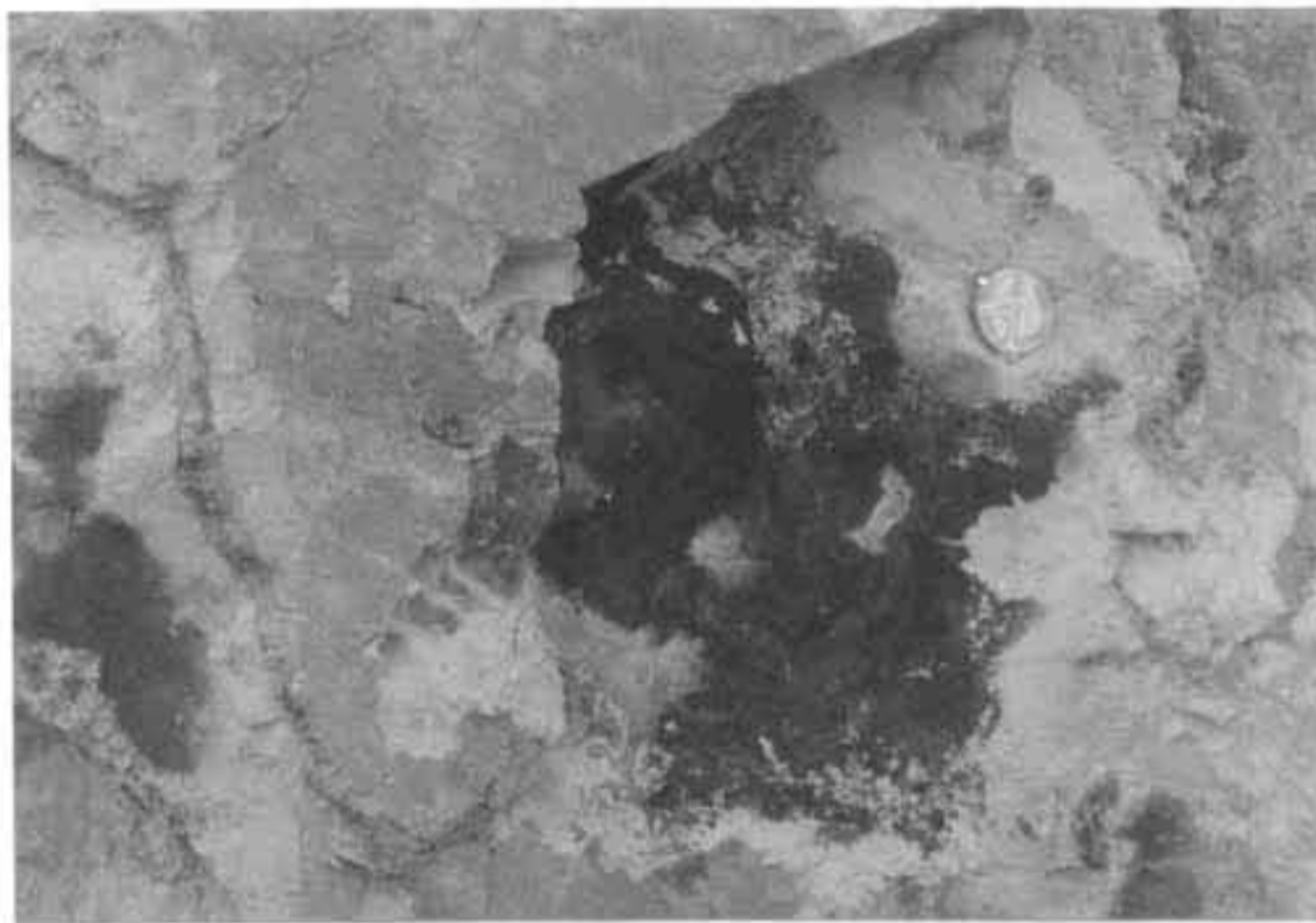
Fig.2.22. Transformation of hematite (red) to goethite (yellow) at Kalliyur clay deposit

86

Fig.2.23. An anastomizing interwoven channel system produced by the organic activity. The grey kaolin is an indication of leaching out of iron oxides from the matrix material (Kalliyur)

87
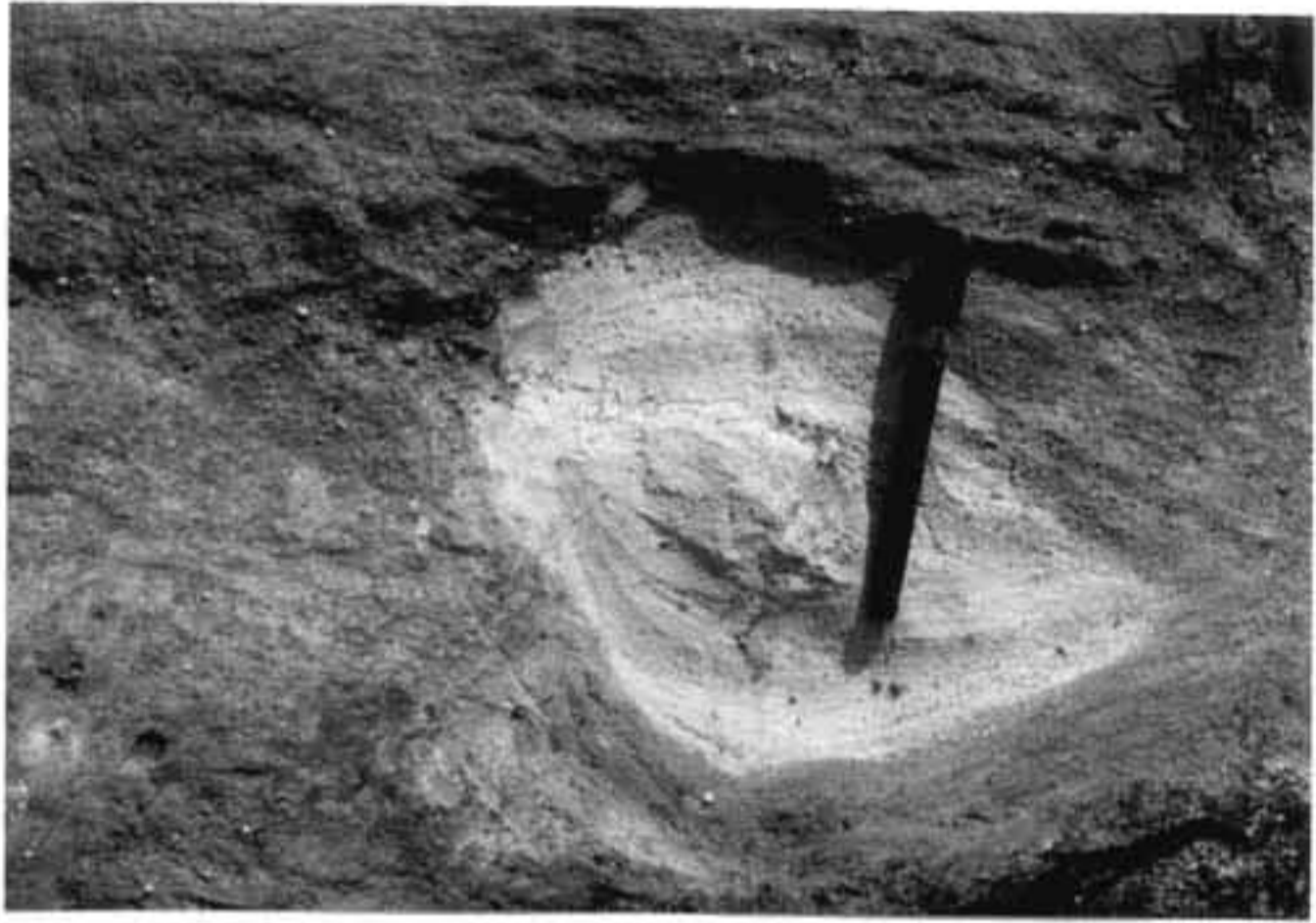
Fig.2.24. Palaeosoles in clay deposits at Kalliyur (a) and Akulam (b).

In the study area, the organic activity plays an important role in the formation of iron oxides (Fig.2.23). The presence of grey kaolinite is suggestive of the removal of iron oxides by microbial reduction[69]. Another evidence is the transformation of hematite to goethite as seen in the palaeosols (Fig.2.24a&b)) showing a radial zonation of Fe distribution. A bleached zone (white) immediately around the root (grey) is followed by goethitic (yellow) zone, beyond which is the unaffected reddish bulk soil. Similar features have been reported by Schwertmann in some tropical soils[70]. Here the redissolution of Fe(III) is also noticed, which may be through microbial reduction of Fe(III) or complexation by organic ligands[69]. The reactions can be represented as follows:

$$4FeOOH + CH_2O + H_2O \rightarrow 4Fe^{2+} + CO_2 + 8OH^-$$

$$FeOOH + 3HL \rightarrow Fe(III)L_3 + 2H_2O$$
$$(L = organic\ ligand)$$
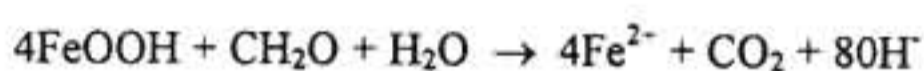
2.4. CONCLUSION

The chemical and mineralogical composition of the five clay samples with the major, minor and trace minerals are tabulated below:

Clay sample	Chemical composition		Mineralogy
	SiO_2(%)	Al_2O_3(%)	
AK	47.9	31.9	Kaolinite[M], halloysite[t], quartz[M], goethite[m], Rutile[t]
JK	46.5	37.7	Kaolinite[M], halloysite[t], muscovite[m], quartz[m], goethite[m], lepidocrocite[m], rutile[t], tourmaline[t], epidote[t]
KK	44.5	36.1	Kaolinite[m], halloysite[t], quartz[m], hematite[m], goethite[m], rutile[m], anatase[m], sillimanite[t], zircon[t], ilmenite[t], graphite[m]
MK	44.4	37.4	Kaolinite[M], halloysite[t], quartz[m], muscovite[m], goethite[m], rutile[m], zircon[t]
TK	42.3	32.9	Kaolinite[M], quartz[m], goethite[m], rutile[t], zircon[t], graphite[m]

M – major mineral; m – minor amounts; t – traces

REFERENCES

1. Ghosh, S.K., 1982. Geochemistry and origin of laterite and clay deposits in Southern Kerala. Technical Report-2, Centre for Earth Science Studies, 21p.

2. Bureau of Indian Standards (BIS): 4589-1968.

3. Al-Khalissi, F. and Worrall, W.E., 1982. The effect of crystallinity on the quantative determination of kaolinite. Trans. British Cer. Soc., 81, 43-46.

4. Powder Diffraction File – Inorganic Phases. 1988. Int. Centre for Diffraction Data, USA, 781p.

5. Brindley, G.W. and Brown, G., 1980. Crystal structures of clay minerals and their X-ray identification. Mineralogical Society, London, 495p.

6. Moore, D.M. and Reynolds, R.C., 1998., X-ray diffraction and the identification and analysis of clay minerals. Oxford Univ. Press, New York, 332p.

7. Azároff, L.V. and Buerger, M.J., 1958. The powder method in X-ray crystallography. McGraw-Hill, New York, 342p.

8. Grim, R.E., 1968. Clay Mineralogy, 2nd edn., McGraw-Hill, New York, 596p.

9. Wilson, M.J., 1987. A Handbook of Determinative Methods in Clay Mineralogy. Blackie, New York, 308p.

10. Paterson, E., Bunch, J.L. and Duthie, D.M.L., 1986. Preparation of randomly oriented sampales for X-ray diffractometry. Clay Miner., 21, 101-106.

11. van der Marel, H.W. and Beutelspacher, H., 1976. Atlas of Infrared spectroscopy of clay minerals and their admixtures. Elsevier, Amsterdam. 396p.

12. van Olphen., H. and Fripiat, J.J., 1979. Data handbook for clay minerals and other non-metallic minerals. Pergamon, New York, 346p.

13. Sudo, Shimoda, S., Yotsumoto, H. and Aita, S., 1981. Electron micrographs of clay minerals – developments in sedimentology - 31. Elsevier, Amsterdam, 203p.

14. Beutelspacher, H. and van der Marel, H.W., 1968. Atlas of electron microscopy of clay minerals and their admixtures. Elsevier, Amsterdam, 333p.

15. Keller, W.D., 1976. Scan electron micrographs of kaolins collected from diverse environment of origin-I. Clays Clay Miner., 24, 107-113.

16. Zalba, P.E., 1981. Scan electron micrographs of clay deposits of Buenos Aires Province, Argentina. In: van Olphen, H. and Veniale, F. (Eds.), 1982. Developments in Sedimentolgy-35, Elsevier, Amsterdam, 513-528.

17. Keller, W.D., 1978. Classification of kaolins exemplified by their textures in scan electron micrographs. Clays Clay Miner., 26, 1-20.

18. Keller, W.D., Hsia Cheng., Johns, W.D. and Chi-Sheng Meng., 1980. Kaolin from the original Kauling (Gaoling) mine locality, Kiangsi Provice, China. Clays Clay Miner., 28, 97-104.

19. Smart, P. and Tovey, N.K., 1981. Electron microscopy of soils and sediments: Examples. Clarendon, Oxford, 178p.

20. Gregg, S.J. and Sing, K.S.W., 1982. Adsorption, surface area and porosity. Academic Press, London.

21. Grimshaw, R.W., 1958. Chemistry and Physics of Clays, 3rd edn., Western Print. Ser., Great Britain, 942p.

22. Bennet, H. and Reed, R.A., 1971. Chemical Methods of Silicate Analysis – a Handbook, Academic Press, New York, 272p.

23. Jeffery, G.H., Bassett, J., Mendham, J. and Denney, R.C., 1989. Vogel's Textbook of Quantitative Chemical Analysis, 5th edn., ELBS, London 877p.

24. Stucki, J.W., Goodman, B.A. and Schwertmann, U., 1988. Iron in Soils and Clay Minerals. D. Reidel, Holland, 893p.

25. Hurst, V.J., 1977. Visual estimate of iron in saprolite. Geol. Soc. Am. Bull., 88, 174-176.

26. Munsell® Soil Colour Charts, 1975 (edn.). Macbeth Div. of Kollmorgen Corpn., 2441 N, Calvert Street.

27. Fernandez, R.N. and Schulze, D.G., 1987. Calculation of soil colour from reflectance spectra. Soil Sci. Soc. Am. J., 51, 1277-1282.

28. Barron, V. and Torrent, J., 1984. Influence of aluminium substitution on the colour of synthetic hematites. Clays Clay Miner., 32, 157-158.

29. Kosmas, C.S., Franzmeier. and Schulze, D.G., 1986. Relationship among derivative spectroscopy, colour, crystalline dimensions and Al substitution of synthetic goethites and hematites. Clays Clay Miner., 34, 625-634.

30. Norrish, K. and Taylor, R.M., 1961. The isomorphous replacement of iron by aluminium in soil goethites. J. Soil Sci., 12, 294-306.

31. Kämpf, N.and Schwertmann, U., 1982. The 5M NaOH concentration treatment for iron oxides in soils. Clays Clay Miner., 30, 401-408.

32. Schwertmann, U. and Thalmann, H., 1976. The influence of Fe(II), Si and pH on the formation of lepidocrocite and ferrihydrite during oxidation of aqueous $FeCl_2$ solution. Clay Miner., 14, 189-200.

33. Borggarrd, O.K., 1979. Selective extraction of amorphous iron oxides by EDTA from a Danish sandy loam. J. Soc. Sci., 30, 727-734.

34. Borggarrd, O.K., 1981. Selective extraction of amorphous iron oxides by EDTA from soils from Denmark and Tanzania. J. Soil.Sci., 32, 427-432.

35. Borggarrd, O.K., 1982. Selective extraction of amorphous iron oxides by EDTA from selected silicates and mixtures of amorphous and crystalline iron oxides. Clay Miner., 17, 365-368.

36. McBride, M.B., Goodman, B.A., Russell, J.D., Fraser, A.R., Farmer, V.C. and Dickson, D.P.E., 1983. Characterization of iron in alkaline EDTA and NH_4OH extracts of podzols. J. Soil Sci., 34, 825-840.

37. Borggarrd, O.K., 1976. Selective extraction of amorphous iron oxide by EDTA from a mixture of amorphous iron oxide, goethite and hematite. J. Soil Sci., 27, 478-486.

38. Tamm, O., 1922. Eine Methode zur Bestimunung der anorganischen Komponente des Gelkomplexes in Boden. Medd. Stat. Skogsforsoks. Stockholm, 19, 387-404. In: Stucki, J.W., Goodman, B.A. and Schwertmann, U. (Eds.), 1988. Iron in soils clay minerals. D. Reidel, Holland, 893p.

39. Schwertmann, U., 1973. Use of oxalate for Fe extraction from soils. Can. J. Soil Sci., 53, 244-246.

40. De Endredy, A.S., 1963. Estimation of free iron oxides in soils and clays by a photolytic method. Clay Miner. Bull., 5, 209-217.

41. Schwertmann, U., 1964. The differentiation of iron oxide in soils by a photochemical extraction with acid ammonium oxalate. Zeischrift für Pflanzenernährung Düngung und Bodenkunde, 105, 194-202. In: Hughes, J.C., 1982. High gradient magnetic separation of some soil clays from Nigeria, Brazil and Columbia. I. The interrelationship of iron and aluminium extracted by acid ammonium oxalate and carbon. J. Soil Sci., 33, 509-519.

42. McKeague, J.A. and Day, J.H., 1966. Dithionite and Oxalate extractable Fe and Al as aids in differentiating various classes of soils. Can. J. Soil Sci., 46, 13-22.

43. Angel, B.R. and Vincent, W.E.J., 1978. Electron spin resonance studies of iron oxides associated with the surface of kaolins. Clays Clay Miner., 26, 263-272.

44. Mehra, O.P. and Jackson, M.L., 1960. Iron oxide removal from soils and clays by a dithionite-citrate system buffered with sodium bicarbonate. In: Ada Swineford (Ed.), Clays and Clay Minerals, Proc. 7th Natl. Conf. Washington, 1958. Pergamon, New York, 317-327.

45. Sadiq, M. and Lindsay, W.L., 1979. Selection of standard free energies of formation for use in soil chemistry. Technical Bull., 134, Colorado State Univ., In: Stucki, J.W., Goodman, B.A. and Schwertmann, U. (Eds.), 1988. Iron in soils and clay minerals. D. Reidel, Holland. 893p.

46. Walker, A.L., 1983. The effects of magnetite on oxalate and dithionite extractable iron. Soil Sci. Soc. Am. J., 47, 1022-1026.

47. Ford, W.E., 1989. Dana's Textbook of Mineralogy, 4th edn., reprint. Wiley Eastern, New Delhi. 851p.

48. Kerr, P.F., 1977. Optical Mineralogy, 4th edn., McGraw-Hill, New York. 492p.

49. Mendelovici, E., SH. Yariv. and Villalba, R., 1979. Iron-bearing kaolinite in Venezuelan laterites: I. Infrared Spectroscopy and Chemical dissolution evidence. Clay Miner., 14, 323-331.

50. Rouxhet, P.G., Ngo Samudacheata., Jacobs, H. and Anton, O., 1977. Attribution of the OH stretching bands of kaolinite. Clay Miner., 12, 171-179.

51. Sutner, L.J., Mack, G., James, W.C. and Young, S.W., 1976. Relative alteration of microcline and sodic plagioclase in semiarid and humid climates. Geol. Soc. Amer., 8, 512p.

52. Eswaran, H. and Wong Chaw Bin., 1978. A study of a deep weathering profile on granite in Peninsular Malaysia: III. Alteration of feldspars. Soil Sci. Soc. Am. J., 42, 154-158.

53. Eswaran, H., 1972. Morphology of allophane, imogolite and halloysite. Clay Miner., 9, 281-285.

54. Die-Yuan Chin, Meh-Ling Lin and Zhi Zheng., 1997. On the origin of the name kaolin and the kaolin deposits of the Kauling and Dazhou areas, Kiangsi. Applied Clay Sci., 12, 1-25.

55. Siffert, B., 1978. Genesis and synthesis of clays and clay minerals: recent developments and future prospects. Proc. Int. Clay conf., Oxford, 337-347.

56. Newman, A.C.D., 1987. Chemistry of clays and clay minerals. Mineralogical Society. Monograph No.480p.

57. Wilke, B.M., Schwertmann, U. and Murad, E., 1978. An occurrence of polymorphic halloysite in granite saprolite of the Bayerischer Wald, Germany, Clay Miner., 13, 67-77.

58. Schwertmann, U., 1993. Relations between iron oxides, soil colour, and soil formation. In: Bigham, J.M. and Ciolkosz, E.J. (Eds.), Soil Colour, Soil Sci. Soc. Am., Special Publ. 31, Madison, WI, 51-69.

59. Folk, R.L., 1976. Reddening of desert sands: Simpson Desert, Northern Territory, Australia. J. Sed. Petrol, 46, 604-615.

60. Schwertmann, U. and Fitzpatrick, 1977. Occurrence of lepidocrocite and its association with goethite in Natal Soils. Soil Sci. Soc. Am. J., 41, 1013-1018.

61. Fitzpatrick, R.W., Taylor, R.M., Schwertmann, U. and childs, C.W., 1985. Occurrence and properties of lepidocrocite in some soils of New Zealand, South Africa and Australia. Austr. J. Soil. Res., 23, 543-567.

62. Schwertmann, U., Schulze, D.G. and Murad, E., 1982. Identification of ferrihydrite in soils by dissolution kinetics, Differential X-ray diffraction and Mössbauer Spectroscopy. Soil Sci. Am. J., 46, 869-875.

63. Torrent, J., Schwertmann, U. and Schulze, D.G., 1980. Iron oxide mineralogy of some soils of two river terrace sequences in Spain. Geoderma, 23, 191-208.

64. Soman, K. 1997. Geology of Kerala. Geol. Soc. India, 280p.

65. Ghosh, S.K. 1986. Geology and geochemistry of Tertiary clay deposits in South Kerala. Geol. Soc. India, 27, 338-351.

66. Stoch, L. and Sikora, W., 1976. Transformations of micas in the process of kaolinitization of granites and gneisses. Clays Clay Miner., 24, 156-162.

67. Soman, K. and Terry Machado, 1986. Origin and depositional environment of the china clay deposits of South Kerala. Proc. Indian Acad. Sic., 95, 285-292.

96

68. Mortland, M.M., Lawton, K. and Uehara, G., 1956. Alteration of biotite to vermiculite by plant growth. Soil Sci., 82, 477-481.

69. Schwertmann, U., Occurrence of iron oxides in various pedoenvironments. In: Stucki, J.W., Goodman, B.A. and Schwertmann, U. (Eds.), 1988. Iron in Soil and Clay Minerals, D. Reidel, Holland, 893p.

70. Schwertmann, U., 1971. Transformation of hematite to goethite in soils. Nature, 232, 624-625.

CHAPTER 3

PHYSICAL BENEFICIATION BY MAGNETIC SEPARATION

3.1. INTRODUCTION

Beneficiation by magnetic separation is a widely accepted technique for the separation of iron-containing minerals like, hematite, iron-stained rutile/anatase, siderite, pyrite, and mica from clays[1,2]. This process has also been suited for the beneficiation of a number of other minerals like ferruginous bauxite[3], talc, uranium[4] etc. This technique is well suited for the removal of Fe-containing minerals because of the magnetic behaviour of Fe induced on the mineral when they are brought to an external magnetic field.

Magnetic separation can be achieved either by high intensity[5] or high gradient separators[6]. The earliest model of a wet high intensity magnetic separator was introduced by Jones in 1955[7]. These separators were capable of generating only very low intensity fields intensity (upto 20 guass). Later, advances in this field led to the development of wet high gradient magnetic separators[8-10] (field strength upto 2T) and superconducting high gradient magnetic separators[11] (field strength > 5T).

The introduction of wet high gradient magnetic separation (WHGMS) is an excellent technological innovation in the field of kaolin beneficiation[12]. Important contributions in this field are given by Iannicelli[13] and Kolm[9]. In 1976, Iannicelli[13]

reported a new magnetic separation technique - the high extraction magnetic filteration (HEMF). The HEMF process was found to be well suited for separating feebly magnetic minerals like pyrite, hematite, iron stained rutile/anatase and mica from a low grade kaolin, thereby increasing its brightness from 75 to 80% (TAPPI Standards). This technique became popular as a rapid, efficient and non-destructive method for separating and concentrating a wide range of iron-containing minerals including oxides oxyhydroxides, hydroxyoxides from layer silicates and amphiboles[14-17]. Although the HGMS process was quite attractive, their high energy consumption and moderate field strengths (upto 2 tesla) demanded further innovations in this area.

Recently the superconducting high gradient magnetic separation (SC-HGMS)[18] has replaced the conventional HGMS technique by their lower power consumption and capacity to generate high field strengths (>2 tesla). High temperature superconducting permanently magnetised discs and rings are also in use for mineral purification[19].

All the three methods viz. WHIMS, WHGMS and SC-HGMS have the common working principle, but have wide differences in their instrumental details. The pictorial representation of a typical high gradient magnetic separator is shown in Fig.3.1.

The magnetic filter consists of a solenoid electromagnetic coil enclosed in a steel housing. The coil generates a uniform background magnetic field. The matrix consisting of expanded metal discs amplify the background magnetic field and produce local regions of extremely high gradient and provides collection sites for magnetic particle capture. The processor is equipped with an automated backflush system for periodic cleaning of the matrix.

99
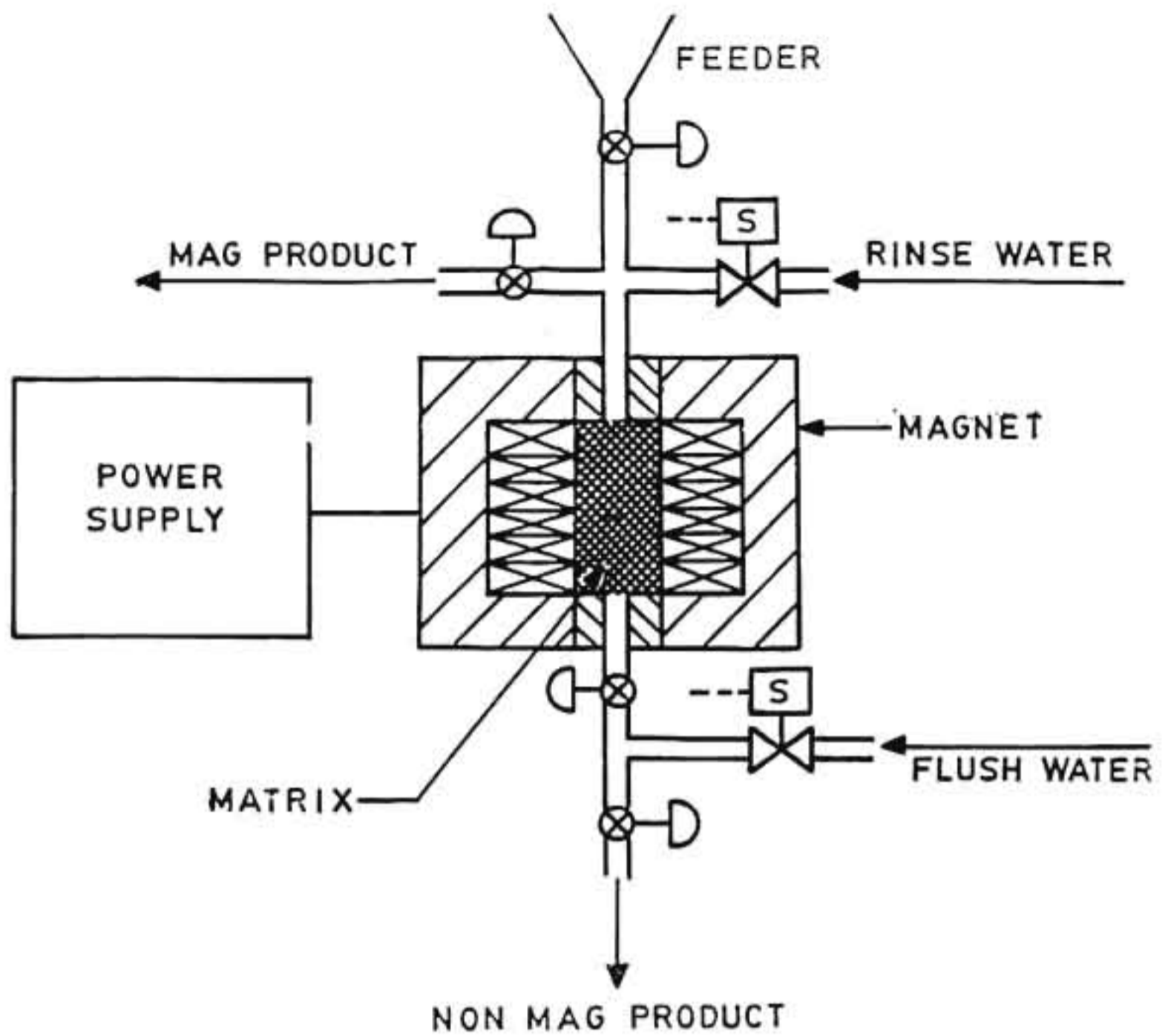
Fig.3.1. A typical High Gradient Magnetic Separation Assembly

The objective of the chapter is to compare the effect of three different types of magnetic separation processes viz. WHIMS, WHGMS and SC-HGMS on removing the titaniferrous impurities from iron-stained clays obtained from Akulam (AK), Buchara (JK), Kalliyur (KK), Mulavana (MK) and Thonnakkal (TK).

100

Working principle

The process is based on the magnetic properties of the mineral. Depending on the magnetic behaviour, materials are classified into three major groups – ferromagnetic, paramagnetic and diamagnetic.

Materials that have a very high magnetic susceptibility and are strongly influenced by a magnetic field are termed ferromagnetic. Materials that have a low magnetic susceptibility and a weak response to a magnetic field are termed paramagnetic and those with a negative magnetic susceptibility are termed as diamagnetic.

The magnetic susceptibility (χ) of a material can be expressed as,

$$\chi = \frac{M}{mH}$$

where M is the induced magnetization of the particle, m is the mass of the particle and H is the magnetic field intensity. Magnetic properties of some common soil minerals are given in Table 3.1[14].

Magnetic separation is achieved by a combined effect of magnetic forces and gravitational, frictional and inertial forces. The magnetic particles will be retained only when the magnetic force exceeds the viscous drag in the flow stream[8]. A number of other parameters such as pH, slurry concentration, field strength, flow rate and dispersant type will influence the separation process[20-22]. Particle size is also an important factor in the selective removal of paramagnetic components. A generalised theory for capturing the ultra-fines was described by Gerber[23].

101

Table 3.1. Magnetic properties of some common soil minerals

Mineral	Susceptibility $(10^8 \; x/m^3 kg^{-1})$	Magnetic behaviour
Quartz	-0.58	Diamagnetic
Orthoclase	-0.48	"
Kaolinite	-1.90*	"
Muscovite	1-15	Paramagnetic
Biotite	15-65	"
Ilmenite	170	Antiferromagnetic
Hematite	27-63	"
Goethite	35-126	"
Lepidocrocite	50-75	"
Magnetite	39,000-100,000	Ferrimagnetic
Maghemite	41,000-44,000	"

*kaolinite susceptibility can range from slightly positive depending on Fe content

3.2. MATERIALS AND METHODS

The five clay samples, viz. AK, JK, KK, MK and TK were collected according to the procedures given in Section 2.2.2.

Experimental

Boxmag-Rapid, model 51930 magnetic separator was used for WHIMS studies. The electromagnet was set at a field of 1.2 T. A 10% clay slurry in deionized water adjusted to pH 9.5 was thoroughly agitated for 30 min and slowly fed into the stainless steel wool filled canister. During the process, even the feebly paramagnetic substances also got magnetised and adhered to the matrix. The rest of the clay slurry was collected as the nonmagnetic fraction. The physically entrained material was washed out of the canister and collected with the nonmagnetic fraction. The trapped particles (magnetic fraction) were released by turning off the background power and flushing out the matrix rapidly.

WHGMS was carried out using SALA-magnetic separator, model 10-15-20. The slurry was prepared as described for WHIMS process. The system was working at a field of 1.4 T. The clay suspension was fed into the canister through an automatically controlled system of pipe lines at the rate of 0.1 m/s.

The SC-HGMS process was conducted at Bhabha Atomic Research Centre (BARC), India, using a system designed and developed by the Ore Dressing Section (ODS) and the Solid State Physics Division (SSPD). A cyclic type laboratory model SC-HGMS with Nb-Ti coil was used. The background field was set at 3.25 T.

In all the three cases, the nonmagnetic and magnetic fractions were separately collected, flocculated by acidifying to pH 4.0, washed thoroughly with deionized water, filtered, air-dried and weighed. The iron and titania contents (expressed as % Fe_2O_3 and TiO_2) of both the magnetic and nonmagnetic fractions were determined (Ref.2.2.2.5). Brightness measurements were carried out using TechniBrite microscan TB-1. The dried clay samples were powdered in a laboratory-sized mill (Anglo Pulverizer, A-1037). The powder was then poured inside a disc placed on the surface of a glass plate. It was then pressed in a standard manner (1.2 kg/cm^2; 20s). The lower surface of the disc provided the surface for brightness determination. The diffuse reflectance from the disc under diffuse illumination at wavelength, 457 nm, was recorded using a photoelectric reflection photometer. The values were measured relative to those of a standard material (barium sulphate with ISO standardisation).

3.3. RESULTS

A comparative study on the efficiency of the three methods on iron removal and the resulting brightness have been carried out. The recovery percentage of clay samples after

the magnetic separation processes are given in Table 3.2. Negligible amount (<2% w/w) of clay loss was encountered during the magnetic separation processes. The weight of magnetic fraction increased with the increase in the magnetic field strength (from 1.2 to 3.25 T), indicating a higher proportion of iron oxide concentration. Table 3.3 shows the iron retained (expressed as % Fe_2O_3) in the magnetic and nonmagnetic fractions of WHIMS, WHGMS and SC-HGMS.

Table 3.2. Recovery percentage of clay after WHIMS, WHGMS and SC-HGMS

Sample	WHIMS		WHGMS		SC-HGMS	
	Mag.	Nonmag.	Mag.	Nonmag.	Mag.	Nonmag.
AK	3.0	96.00	8.0	91.87	19.40	80.20
JK	4.0	95.00	14.0	84.99	19.00	80.20
KK	2.3	97.30	13.5	86.00	8.00	90.20
MK	1.1	96.00	5.0	94.30	20.60	79.10
TK	5.5	94.40	9.5	90.08	25.90	74.00

Table 3.3. Fe_2O_3 (%) retained after HIMS, WHGMS and SC-HGMS processes

Sample	% Fe_2O_3						
	Raw	WHIMS		WHGMS		SC-HGMS	
		Mag.	Nonmag.	Mag.	Nonmag.	Mag.	Nonmag.
AK	3.98	4.02	3.93 (1.51)	4.04	3.911 (1.76)	4.08	3.87 (2.83)
JK	1.02	1.05	0.99 (2.94)	1.08	0.960 (5.90)	1.09	0.95 (6.70)
KK	0.93	1.07	0.910 (24.0)	1.17	0.904 (2.80)	1.20	0.88 (5.00)
MK	2.64	2.75	2.53 (3.90)	2.77	2.52 (4.52)	2.79	2.500 (5.30)
TK	6.54	6.55	6.52 (0.30)	6.61	6.49 (0.76)	6.62	6.47 (1.07)

*Values in brackets indicate the corresponding Fe_2O_3 removed (%)

3.3.1. Percentage removal of Fe_2O_3 and TiO_2

In the case of WHIMS, the maximum iron oxide removed was 3.9% which was obtained for sample MK. Except sample TK, all the others showed more than 1.5% Fe_2O_3

removal. Although sample TK encountered a higher proportion of Fe_2O_3 (6.54%), only 0.3% of the total iron oxide was liberated by the WHIMS process.

In the WHGMS process, maximum value of iron removal, 5.9% was noticed from sample JK. The percentage Fe_2O_3 separated from all samples were comparatively higher than those obtained by the WHIMS process.

Similarly, in the SC-HGMS process, the percentage removal of Fe_2O_3 was increased to 6.7% from sample JK.

Together with iron oxides, a considerable amount of titania minerals were also separated during magnetic separation process. Table 3.4 shows the results of TiO_2 content of the samples after magnetic separation processes.

Table 3.4. Percentage of TiO_2 retained in the samples after WHIMS, WHGMS and SC-HGMS processes

Sample	% TiO_2						
	Raw	WHIMS		WHGMS		SC-HGMS	
		Mag.	Nonmag.	Mag.	Nonmag.	Mag.	Nonmag
AK	0.2038	0.2465	0.1535 (24.68)	0.2622	0.1525 (25.19)	0.2625	0.1520 (25.42)
JK	0.0300	0.0349	0.025 (16.67)	0.0358	0.0240 (18.67)	0.0359)	0.0243 (18.96)
KK	0.8900	0.9901	0.7981 (10.32)	1.0244	0.7542 (15.26)	1.1780	0.6021 (32.35)
MK	0.5672	0.6231	0.5102 (10.10)	0.6421	0.4908 (13.50)	0.6994	0.4300
TK	0.3076	0.3149	0.3001 (2.44)	0.3189	0.2972 (3.38)	0.3399	0.2674 (13.07)

*Values in brackets indicate the corresponding TiO_2 removal (%)

In WHIMS process, the maximum TiO_2 separated was 24.6% from the sample AK. At the same time, the lowest separation was noticed for the sample TK. In the WHGMS process, the $TiO_2\%$ extracted from the clay samples was slightly higher than

that obtained in the WHIMS process. The maximum value of 25.17% was extracted from the sample AK. Similarly experiments using the SC-HGMS showed the maximum of % TiO_2 separation from all clay samples. The maximum value of 32.35% was obtained from the sample KK (it has the highest content of TiO_2) in the washed state.

3.3.2. Brightness studies

It is noteworthy that the removal of TiO_2 and Fe_2O_3 contaminants increases the brightness of the clay. Table 3.5 shows the brightness values of nonmagnetic fractions.

Table 3.5. Brightness of clays after magnetic separation process

Sample	Brightness (%)			
	Raw	WHIMS	WHGMS	SC-HGMS
AK	36.08	36.4	36.86	37.01
JK	65.38	66.98	67.46	70.12
KK	66.30	66.79	67.23	67.85
MK	45.86	45.95	46.42	46.99
TK	26.49	27.00	27.01	27.78

3.4. DISCUSSION

Among the three magnetic separation processes viz. WHIMS, WHGMS and SC-HGMS, the higher values of % Fe_2O_3 and % TiO_2 separation were obtained by SC-HGMS process which may be due to the higher magnetic field encountered in the superconducting magnetic separator. As the field strength increases, more ferruginous fine particles get attracted by the matrix, hence higher the percentage separation.

A linear dependency was observed between the applied field strength and the % extraction or the resulting brightness of iron oxides, i.e. as the field strength increased

from 1.2 T to 3.25 T, the percentage iron removal increased from 2.9 to 6.7 (sample JK). The corresponding brightness increase was from 65 to 70% ISO.

The maximum amount of iron oxide removed was only 6.7% of the total Fe_2O_3 content, from sample JK by the SC-HGMS process. For all other clay samples, the % Fe_2O_3 extraction was still at lower values. Sample TK has higher Fe_2O_3 content than other samples, even though the liberated Fe_2O_3 content accounts for only 1%. The CoKα XRD analysis (Fig.2.14) confirmed that sample TK contains crystalline goethite as well (Ref.2.3). Therefore, it can be inferred that lower extraction percentage may either be due to the strong aggregation and cementation of the clay-iron oxide particles or due to the extreme fineness of the iron oxide minerals (Fig.5.5) existing as coating in clay particles. From the above observations, it can be inferred that only a small portion of the total Fe_2O_3 is in liberated crystalline forms and the rest may occur either as extremely fine particles or as amorphous coating on the clay surface. But the amorphous Fe_2O_3 content encountered only a smaller fraction (<6%) of the total Fe_2O_3 (Ref.2.3) of the clay samples. Hence it would be confirmed that the iron oxide occurs as ultra-fine crystalline coatings on the clay surface.

Quite a good amount of titania minerals also got separated during the magnetic separation processes. Upto 32% TiO_2 was liberated from sample KK during SC-HGMS process. The TiO_2 minerals separated were ilmenite or Fe-stained rutile/anatase. This mineralogy was confirmed by the CoKα XRD (Fig.2.14) analysis of the magnetic fractions (Ref.2.3). Presence of rutile was also confirmed by petrological microscopy (Fig.2.16b).

The magnetic separation process also results in improving brightness of the clay samples. Maximum improvement of ~5 units ISO was obtained after SC-HGMS of sample JK. The initial brightness value 65.0 was increased to 70.12%. Since brightness is directly related to removal of Fe_2O_3 content, the linear relationship seen between the % Fe_2O_3 extraction and field strength can also be observed for the brightness increase and the applied field strength values as well. The brightness improvement of clay samples except JK was very low by the magnetic separation. From these results, it can be inferred that the brightness is attracted more by surface coated iron oxides than the discrete crystalline forms in the case of these clay samples.

The CoKα X-ray diffraction patterns (Fig.2.14) of the magnetic fractions showed that a good amount of kaolinite also came out with the iron oxides. It may be attributed to the cementing or aggregating tendency of the iron oxides with the clay particles. Dissolving the clay fraction in a boiling 5 M NaOH solution increased the concentration of the Fe-containing minerals in the magnetic fraction. On the basis of CoKα XRD, SEM and petrological microscopy, it was found that the Fe-containing minerals separated during the magnetic separation include goethite, hematite, lepidocrocite, iron-stained rutile/anatase, muscovite, ilmenite, sillimanite, zircon, epidote and tourmaline. The removal of the non-magnetic minerals, rutile, zircon, sillimanite and tourmaline may be ascribed to surface coated iron oxide particles. Microscopic investigations revealed the presence of iron oxide inclusions in these minerals.

3.5. CONCLUSION

A large number of iron-containing minerals, like goethite, hematite, lepidocrocite, muscovite, ilmenite, rutile, anatase, sillimanite, zircon, epidote, tourmaline etc. could be

separated out by the magnetic separation processes. Upto 6-7% of the total Fe_2O_3 was removed by the SC-HGMS process. This technique seems excellent for removing titania minerals also. Upto 32% of the total TiO_2 could be removed by this process (SC-HGMS). Removal of these titania and iron impurities improved the brightness of the clay samples by 5 units (from 65 to 70% ISO). It was also observed that the iron oxides occur as ultra-fine particles coating the surface of clay particles.

Since the magnetic separation processes are found to be effective for the removal of liberated iron oxides, a chemical leaching/bleaching technique preceeded by the magnetic separation process shall obviously result in enhanced brightness. A detailed account of the various chemical leaching/bleaching processes studied are explained in the following chapter.

REFERENCES

1. Mills, C., 1977. High gradient magnets and the kaolin industry. Ind. Miner., Aug., 41-45.

2. Norrgran, D.A., 1990. Advances in magnetic separation of fine high-purity products. Cer. Bull., 69, 1966-1970.

3. Bolsaitis, P., Chang, V.,Schorin, H. and Aranguren,R., 1981. Beneficiation of ferruginous bauxites by high-gradient magnetic separation. Int. J. Miner. Process., 8, 249-263.

4. Jha,R.S., Natarajan, R., Sreenivas, T., Sridhar, U., Sunilkumar, T.S. and Rao, N.K., 1990. Laboratory investigations on magnetic separation of uranium values from copper plant tailings, BARC Internal Report, B.A.R.C./ I-1990.

5. High Intensity Magnetic Filters, 1991. Interceram-Technology forum, 40, 35, Eriez Magnetics, U.K.

6. Dauson, A.M., 1977. Magnetic separation of kaolin. Ind. Miner., 121, 16.

7. Jones, G.H., 1955. British Patent, 768 451 and 767 124. In: Iannicelli, J. 1976. High extraction magnetic filtration of kaolin clay. Clays Clay Miner., 24, 64-68.

8. Luborsky, F.E. and Drummond, B.J., 1975. High gradient magnetic separation: Theory versus experiment. IEEE Trans. Mag., 11, 1696-1700.

9. Kolm, H.H., Oberteuffer, L. and Kelland, D., 1975. High gradient magnetic separation. Sci. Am., 233, 47-54.

10. Oberteuffer, J.A., 1974. Magnetic Separation: A review of principles, devices and applications. IEEE Trans. Mag., 10, 223-238.

11. Stekly, Z.J.J., 1975. A superconducting high intensity magnetic separator. IEEE Trans. Mag., 11, 1594-1597.

12. Baburek, J., 1972. The preparation of kaolin by means of high gradient magnetic separation. Interceram, 1, 54-57.

13. Iannicelli, J., 1976. High extraction magnetic filtration of kaolin clay. Clays Clay Miner., 24, 64-68.

14. Jepson, W.B., 1988. Structural iron in kaolinites and in associated ancillary minerals. In: Stucki, J.W., Goodman, B.A. and Schwertmann, U. (Eds.), 1988. Iron in soils and clay minerals. D. Reidel Publ. Co., Holland, 893p.

15. Russel, J.D., Birnie, A. and Fraser, A.R., 1984. High-gradient magnetic separation (HGMS)in soil clay mineral studies. Clay Miner., 19, 771-778.

16. Hughes, J.C., 1982. High-gradient magnetic separation of some soil clays from Nigeria, Brazil and Colombia. I. The interrelationships of iron and aluminium extracted by acid ammonium oxalate and carbon. J. Soil. Sci., 35, 509-519.

17. Shoumkov, S.,Dimitrov, Z. and Brakalov, L., 1987. High-gradient magnetic treatment of kaolin. Interceram., 6, 26-28.

18. Patel, K.L., Bagool, A.P., Srinivasan, T., Dande, Y.D., Dasannacharya, B.A., Padmanabhan, N.P.H., Sridhar, U., Singh, A.K., Mohan Rao, M. and Krishna Rao, N., 1992. Design, development and testing of a superconducting high gradient magnetic separator. Technical Report BARC, 1992/1/001, 60p.

19. Watson, J.H.P., 1999. High temperature superconducting permanently magnetised discs and rings: prospects for use in magnetic separation. Miner.Engg., 12, 281-290.

20. Maurya, C.B. and Dixit, S.G., 1990. Effect of pH on the high-gradient magnetic separation of kaolin clays. Int. J. Miner. Process, 28, 199-207.

21. Dixit, S.G., 1995. Role of surface chemistry in high gradient magnetic separation. In: Pradip and Rakesh Kumar (Eds.), Selected topics in mineral processing, New Age Int., New Delhi, 300p.

22. Maurya, C.B. and Dixit, S.G., 1988. High Gradient Magnetic Separation of china clays. Bull. Mater. Sci. 10, 471-475.

23. Gerber, R., Takayasu, M. and Friedlaender, F.J., 1983. Generalization of GHMS theory: The capture of ultra-fine particles. IEEE Trans. Mag., 19, 2115-2120.

CHAPTER 4

CHEMICAL BENEFICIATION TECHNIQUES

One of the most commonly employed chemical beneficiation techniques in kaolin industry is bleaching using sodium hydrosulphite (sodium dithionite) in acid medium[1]. Dissolution of iron oxides by oxidative agents like ozone[2] and Cl_2 solution[3] are also practised in industry.

A lot of research works have been reported on the removal of naturally occurring iron oxides from clays. Apart from this, numerous research work have also been conducted on synthetic iron oxide dissolution. Chiarizia and Horwitz[4] performed investigations on the dissolution rate of synthetic goethite in several organic and inorganic acids (oxalic, malonic, succinic, maleic, glycolic, α-hydroxyisobutyric, citric, tartaric, ascorbic and tetrahydrofuran tetra carboxylic acid, HCl, HNO_3, H_2SO_4) alone or in combination with other reducing agents like hydroxylamine hydrochloride, $SnCl_2$, hydroquinone, metallic zinc, Na_2SO_3, sodium dithionite and sodium formaldehydo-sulfoxylate (SFS). The thermodynamic and the kinetic aspects of dissolution of metal oxides were discussed by Blesa and Maroto[5]. The mechanism of magnetite dissolution in oxalate solutions has been extensively studied by Blesa et al.[6]. A review on the mechanism of iron oxide dissolution in organic acids have been reported by Panias and coworkers[7]. The reaction steps involved in the photochemical dissolution of goethite in acid/oxalate solutions were reported by Cornell and Schindler[8]. Panias et al.[9] gave valuable explanations regarding the mechanism of hematite dissolution in acidic oxalate solutions – the autocatalytic effect of Fe^{2+} was explained in detail.

The weak alkaline solutions of EDTA is another effective leachant for iron oxide from soils and clays[10-16]. The interactions between EDTA and goethite at wide ranges of pH, temperature and ligand concentrations were studied by several researchers[17,18]. The effect of exogenous and autogenerated ferrous ions in the dissolution of magnetite was reported by Blesa et al.[11]. Dos Santos et al.[19] described the process involving the dissolution of iron oxides by ascorbic acid in H_2SO_4 medium.

Several other interesting studies are reported on iron oxide dissolution, like the use of mercapto acetic acid[20], picolinic acid[21], thioglycolic acid[5] and amino carboxylic acid[22]. Gill et al.[23] introduced new leaching agents for iron oxide dissolution – the studies were performed in nonaqueous systems as well, with dimethyl sulphoxide-sulphur dioxide, dimethyl formamide-sulphur dioxide and acetonitrile-sulphur dioxide.

The metabolic products of microorganisms like *Aspergillus niger*, *Agrobactor* species, *Bacillus* species etc., are found to be good reagents for iron oxide removal[24-26]. Carbohydrates[27,28] are also found to be effective for the dissolution of iron oxides from clays.

This chapter is divided into three sections as given below:

A. A comparative study on the deferration of iron-stained clays using sodium dithionite and sucrose in acid medium.

B. The effect of various organic acids on the deferration of iron-stained kaolinitic clays with special reference to oxalic acid.

C. The catalytic effect of metal powders (Al, Fe, and Zn) in oxalic acid solutions – a novel method for iron oxide dissolution from china clays.

114

PART – A

EFFECT OF SODIUM DITHIONITE AND SUCROSE ON THE BRIGHTNESS IMPROVEMENT OF IRON-STAINED CHINA CLAY

4A.1. INTRODUCTION

Sodium dithionite is widely used as a powerful bleaching agent in the purification of kaolin. In commercial production, sodium dithionite is added in small amounts to the aqueous slurry of kaolin at pH 3. The amount may vary according to the iron content of the clay sample.

A number of parameters may influence the reductive dissolution of iron oxides by dithionite and the brightness improvement of kaolin. The significant factors are the pH of the clay slurry, the leaching temperature and the time of contact. The optimum conditions were found to be - temperature 60°C, pH 3 and time 10 minutes[29]. Detailed studies conducted on the efficiency of dithionite to dissolve crystalline and amorphous Fe hydroxides indicated that only the latter was removed during these processes[30]. Smith and Mitchel used dithionite for the estimation of amorphous variety of iron, silica and alumina from kaolin samples[31].

Torrent et al.[32] compared the dissolution of synthetic and natural, hematite and goethite in dithionite and concluded that the apparent preferential dissolution of hematite may be due to either its smaller particle size or its lower level of Al substitution, or both.

Recently, carbohydrates (eg. Sucrose) in acid have proven to be powerful reducing agents for iron removal from clays. It is a least studied area and the major contributions have been given by Veglio and Toro[28]. A detailed description of the dissolution of sucrose on ferric iron reduction was reported by Toro et al.[33]. Veglio et al.[27] developed a new process for kaolin bleaching in which the dissolution of iron oxides

was carried out in a carbohydrate-H_2SO_4 medium. Later, this process was modified by the same researchers and the newly formulated system was based on pressure leaching[28]. Their experimental results demonstrate the possibility of using carbohydrates in the bleaching process of minerals of industrial interest.

In this section, a comparative study has been made on the effect of sucrose and dithionite on iron removal from kaolinite. In the case of sucrose bleaching, the experiments were carried out using a two level full factorial design in order to optimise the parameters like, sulphuric acid, sucrose concentration, temperature and time of treatment. The combined effect of physical beneficiation using magnetic separation processes (WHIMS, WHGMS and SC-HGMS) and chemical beneficiation using sodium dithionite and sucrose were also studied. The physical and structural properties of the clay before and after the above processes have also been compared.

Reactions involved in sodium dithionite bleaching

When sodium dithionite is added to a kaolin suspension, two reactions take place. The first is the disproportionation reaction

$$2S_2O_4^{2-} + H_2O \rightarrow S_2O_3^{2-} + 2HSO_3^- \tag{1}$$
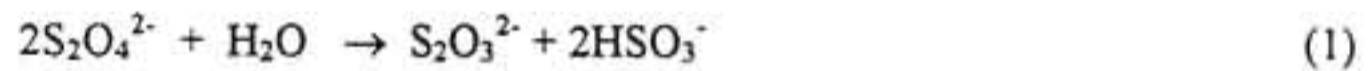
Second is the reduction reaction. The following reactions illustrate the reduction of hematite and goethite by dithionite

$$S_2O_4^{2-} + Fe_2O_3 + 4H^- \rightarrow 2HSO_4^- + 2Fe^{2+} + H_2O \tag{2}$$
$$\text{(hematite)}$$

$$S_2O_4^{2-} + 2FeOOH + 4H^- \rightarrow 2HSO_3^- + 2Fe^{2+} + 2H_2O \tag{3}$$
$$\text{(goethite)}$$

116
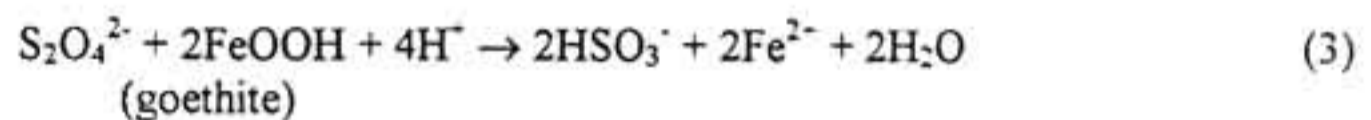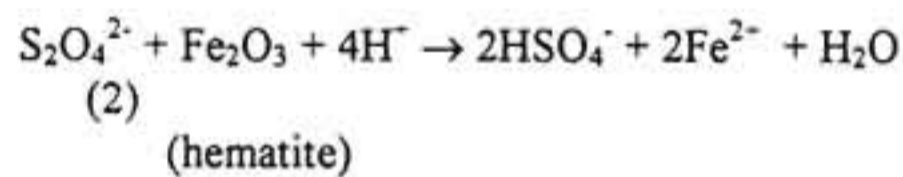
Reactions 1-3 are pH dependent and the optimum pH was 3. At this pH both the reactions, disproportionation and dissolution processes get accelerated simultaneously.

Reaction involved in sucrose bleaching

The reductive dissolution of hematite in sucrose-H_2SO_4 system is given below:

$Fe_2O_3 + 6H^- \rightarrow 2Fe^{3+} + 3H_2O$

$48Fe^{3+} + C_{12}H_{22}O_{11} + 13H_2O \rightarrow 48Fe^{2+} + 12CO_2 + 48H^-$
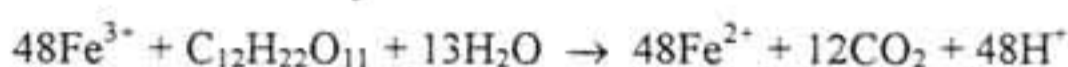
It is reported that dilute acids at room temperature have no complex reactions with sucrose, but hot conditions result in the formation of complex compounds which enhance the reduction of Fe^{3+}.

4A.2. MATERIALS AND METHODS

Two kaolinitic samples obtained from Buchara (JK) and kalliyur (JK) were selected for the chemical beneficiation studies. The iron content of these two samples were comparatively low (<1.1%) and the other clay samples viz. Akulam (AK, Mulavana (MK), and Thonnakkal (TK) have quite a high proportion of iron content (2.6-6.5%) and hence not subjected to Fe removal by this techniques.

The < 45 μm fraction of the two clay samples JK and KK were obtained according to the procedures given in section 2.2.2. The chemical analysis of the samples were given in section 2.3. The total iron content (expressed as Fe_2O_3) of the samples JK and KK were 1.02 and 0.93 respectively.

Experimental

The experiments were conducted in a two-necked round bottomed flask fitted with a stirrer and a thermometer. Heating was done in a heating mantle.

In the dithionite bleaching process 25% clay slurry having a pH 3 (adjusted using 0.5 M H_2SO_4) was treated with 2.5 g/L sodium dithionite at 60°C for 10 min. In the case of sucrose bleaching, the experiments were planned according to a two level full factorial design (FFD). The factors and levels used in the experiments are shown in Table 4.1. The leaching tests were performed at two temperatures (80°C and 100°C) in a 25% clay slurry with two acid concentration levels (0.1 M and 0.5 M) and two sucrose concentration levels (0 and 4 g/L) for two timings (30 min and 120 min). Some intermediate levels of treatment were also conducted at 85°C and 95°C for 60 and 20 min with 0.25 and 0.375 M H_2SO_4, and 0.15 and 0.25 g/L sucrose.

Table 4.1. Experimental conditions considered in sucrose bleaching

Factors	Level	
	Low	High
Sucrose concentration (A)	0.0 g/L	4.0 g/L
Time (B)	30 min	120 min
Temperature (C)	80°C	100°C
H_2SO_4 concentration (D)	0.1 M	0.5 M

The samples beneficiated by magnetic separation processes viz. WHIMS, WHGMS and SC-HGMS (Ref.3.3) were also subjected to sodium dithionite and sucrose bleaching. Dithionite treatment was carried out as described above. In sucrose bleaching, 25% of the clay slurries were treated with 0.5 M H_2SO_4 at 100°C for 60 min.

After the chemical leaching processes, the clay suspensions were filtered, washed and dried at 80°C for 2 hours and these were subjected to brightness measurements (Ref.3.2) and the leached liquors were subjected to iron content analysis (Ref.2.2.2.5)

The viscosity measurements of the raw as well as the bleached samples were made at 65% slurry concentration at pH 9.5 (adjusted using dil. NaOH) and sodium silicate as dispersant. Brookfield viscometer model RVT was used for the study. Water of plasticity of the samples was determined as per the standard procedures[34]. The crystallinity indices were compared using Ni-filtered CuKα radiation X-ray diffraction (Miniflex, ME 200 CY$_2$).

4A.3. RESULTS AND DISCUSSION

4A.3.1. Sucrose bleaching

In sucrose bleaching, the experiments were organized using a full factorial design (FFD). The factors were tested on a 2^4 level FFD. In order to obtain the combinations among the levels and the factors, 16 experiments were carried out for each sample. Table 4.2 shows the experiments investigated in FFD in a codified form using Yate's notation. For example, the experiment "ab" denotes the factors A and B are at highest levels (A = 4.0 g/L; B = 120 min and the factors C and D at lowest levels (C = 80°C; D=0.1 M).

The FFD procedure was very helpful to evaluate the main effects and the interactions among the factors investigated, independently. The results of the factorial experiments (as % iron removal and % brightness) were shown in Table 4.3.

Table 4.2. Experiments carried out (in coded form)

Experiment	A	B	C	D
1	-	-	-	-
a	+	-	-	-
b	-	+	-	-
ab	+	+	-	-
c	-	-	+	-
ac	+	-	+	-
bc	-	+	+	-
abc	+	+	+	-
d	-	-	-	+
ad	+	-	-	+
bd	-	+	-	+
abd	+	+	-	+
cd	-	-	+	+
acd	+	-	+	+
bcd	-	+	+	+
abcd	+	+	+	+

+ve - highest level; -ve – lowest level

Table 4.3. Results of FFD tests

Experiment	Sample JK		Sample KK	
	% Fe_2O_3 removal	% brightness	% Fe_2O_3 removal	% Brightness
1	4.05	66.09	1.40	66.54
a	4.40	66.20	1.50	66.63
b	6.15	66.62	4.00	67.08
ab	7.15	66.95	5.08	67.25
c	10.65	67.95	3.98	67.02
ac	10.90	67.10	4.15	67.10
bc	12.25	68.32	10.23	68.14
abc	33.45	74.31	26.07	72.50
d	8.35	67.26	4.83	67.16
ad	10.45	67.89	6.00	68.38
bd	27.00	71.00	12.15	68.49
abd	28.35	73.66	24.30	71.67
cd	24.45	72.04	14.54	68.82
acd	37.45	75.62	24.54	72.92
bcd	73.73	82.90	67.38	78.30
abcd	79.12	86.90	75.40	80.20

For both the clay samples, JK and KK, the highest percentage of iron removal was obtained in the experiment abcd. Here all the factors were considered at highest levels (A = 4.0 g/L, B =100°C, C = 120 min and D = 0.5 M H_2SO_4). The iron removal percentages are 79.12 and 75.40 for JK and KK respectively and the corresponding increase in the brightness values are 86.9 and 80.20% (ISO).

The experiment bcd also gave better results of brightness and iron removal. The brightness values were 82.9 and 78.3 for samples JK and KK. These values were corresponding to iron removal of 73.73 and 67.38%. Experiment bcd was conducted in the absence of sucrose.

Using FFD, it was possible to evaluate the effect of various factors considered and their interactions in the experiments independently. For example, in the experiment cd, the effect of acid concentration increases with increase in the time of treatment. This result is independent of the factors C and D which have a positive effect on the iron removal and therefore a combined effect exists between the two factors.

The effects of the factors alone and their interactions have been classified into three groups according to the % Fe_2O_3 removed during each test.

- main factors (> 20%)

- intermediate factors (between 10 and 20%)

- minimal factors (< 10%)

Table 4.4 represents the three group of factors, the corresponding effects (expressed in % Fe_2O_3 removed). The results are presented below:

Table 4.4. Factors and the corresponding effects (in % Fe_2O_3 removed)

Sample JK		Sample KK	
Factor	Effect	Factor	Effect
Main factors (> 20%)			
BD	27.00		
CD	24.45		
Intermediate factors (between 10 and 20%)			
C	10.65		
BC	12.25	BC	10.23
AD	10.45	BD	12.15
AC	10.90	CD	14.54
Minimal factors (< 10%)			
A	4.40	A	1.50
B	6.15	B	4.00
D	8.35	C	3.98
AB	7.15	D	4.83
		AB	5.08
		AC	4.15
		AD	6.00

1. For sample JK

(a) The main factors are: temperature-acid concentration cross interaction, time–acid concentration cross interaction

(b) The intermediate factors are: temperature, temperature-time cross interaction, sucrose-acid concentration cross interaction, sucrose-temperature cross interaction.

(c) The minimal factors are: sucrose, time-acid concentration.

2. For sample KK

(b) The intermediate factors are: temperature-acid concentration cross interaction, time-acid concentration cross interaction, temperature-time cross interaction

(d) The minimal factors are: sucrose, time, temperature, acid concentration, sucrose-time cross interaction, sucrose-temperature cross interaction, sucrose-acid concentration cross interaction

From the above values it can be inferred that the temperature-acid concentration and the time-acid concentration interactions have the highest effect in both the clays (Figs.4.1&2). It is noticed that in both cases, the effect of sucrose and its interaction effects are minimum (Fig.4.3). It is evident that the effect of sucrose at lowest levels of time, temperature and acid concentration was not significant, whereas at high temperature and higher concentrations produces significant improvement in iron removal and brightness.
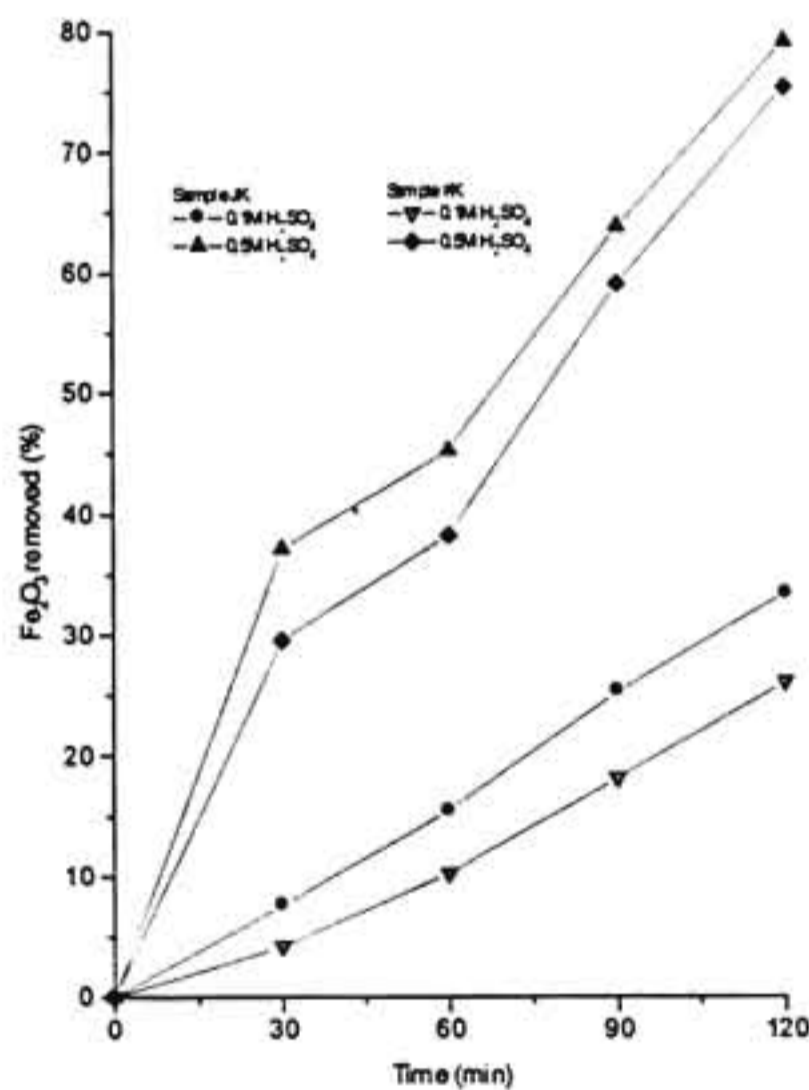
Fig.4.1. Effect of H_2SO_4 concentration

Sucrose = 4 gL^{-1}; Temp. = 100°C
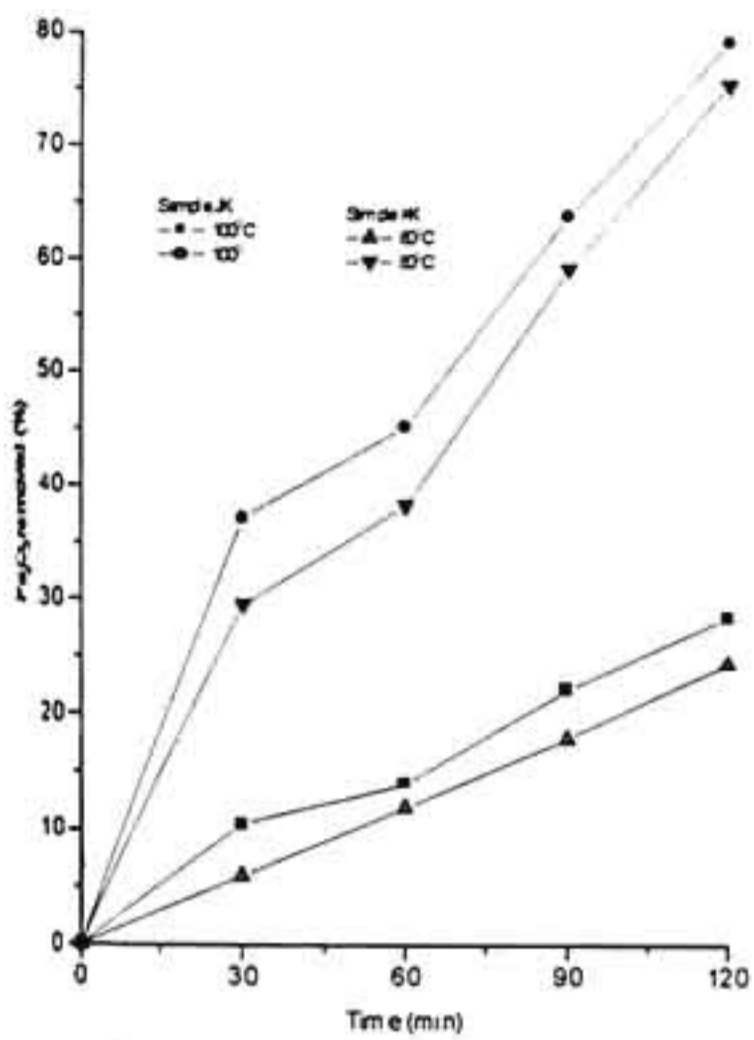
Fig. 4.2. Effect of temperature
Sucrose = 4 gL^{-1}, H$_2$SO$_4$ = 0.5M
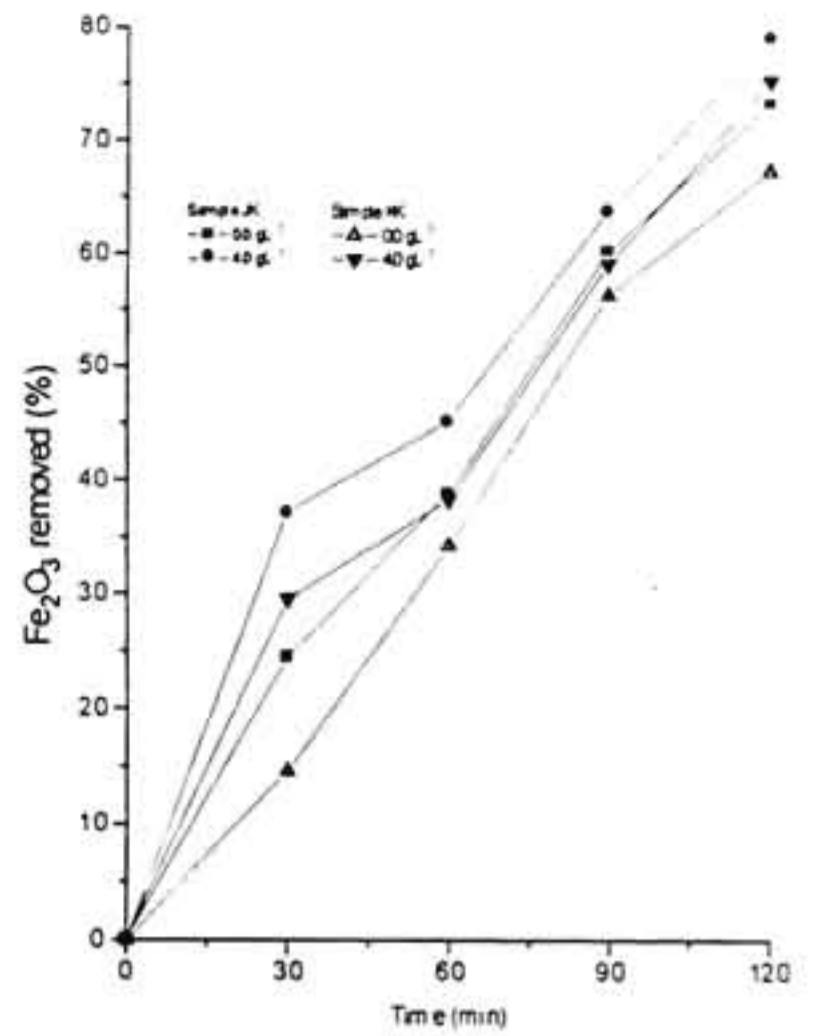
Fig. 4.3. Effect of sucrose
Temp. - 100°C; H$_2$SO$_4$ - 0.5M

However, the best results with an increase in brightness values from 65.00 to 86.90% and 66.30 to 80.07% have been obtained under the following conditions: at 100°C, with 0.5 M H$_2$SO$_4$, 4.0 g/L sucrose in 120 minutes.

4A.3.2. Dithionite bleaching

The results of brightness and iron oxide removal by dithionite dissolution are given in Table 4.5. The sodium dithionite leaching increases the brightness of the clay samples from 65.00 to 70.6% and 66.30 to 69.7%. The corresponding iron oxide removal were 19.8% for JK and 18.72% for KK respectively.

124

Table 4.5. Results of sodium dithionite bleaching

Sample JK		Sample KK	
% Fe_2O_3 removed	% Brightness	% Fe_2O_3 removed	% Brightness
19.8	70.6	18.72	69.7

4A.3.3. Comparison of sucrose bleaching and dithionite bleaching

Significant improvement in brightness as well as percentage iron removal were obtained in the sucrose sulphuric acid treatment. When compared to sodium dithionite leaching, in sucrose leaching, the reagent consumption, energy, time of reaction etc. were very high. Lower temperatures were not favoured Fe^{3+} dissolution in sucrose-H_2SO_4 medium. On the other hand, this process seemed to be environment friendly and the reagent cost can be minimised by the use of carbohydrates from industrial waste such as sugar industry, paper mill and agro-industry.

4A.3.4. Effect of chemical bleaching on the physico-chemical properties of clays

The viscous and plastic properties are of great importance in paper filling/coating applications. In paper coating, an aqueous kaolin suspension (~ 70%) is uniformily spread on the paper web at high speed. Excessive dilatency may cause sheat blockages and give unwanted marks on the paper. The viscous and plastic behaviour are often controlled by the size, and shape of the clay particles as well as their concentration in the slurry[34]. Apart from this, aggregation of the solid particles and presence of other materials like quartz, mica, iron oxides etc may have an influence on these properties.

The variation in the water of plasticity of the clay samples before and after magnetic separation (SC-HGMS) followed by chemical leaching are represented in Table 4.6.

Table 4.6. Results of physical property variation after beneficiation

Property measured	Before bleaching		SC-HGMS followed by dithionite bleaching		SC-HGMS followed by bleaching	
	JK	KK	JK	KK	JK	KK
Water of plasticity (%)	33.5	41.9	34.9	41.8	35.5	41.9
Viscosity (cP)	1440	1560	1260	1670	1060	1850

The water of plasticity of the sample JK has slightly increased after the beneficiation processes. It has been reported that micaceous minerals with a highly pronounced platy cleavage often reduce the plasticity of clays when present in sufficient quantity[35]. In the case of sample JK, a considerable portion of the dioctahedral mica, muscovite (confirmed by XRD and Scanning Electron Microscopy) has separated out during the SC-HGMS process. The mineralogical analysis indicated that only 1.5% w/w of the total clay is encountered by mica. Moreover, the clay has a higher proportion of fines (< 2 μm fraction, ~63%). The slight change in the plasticity may be attributed to the removal of mica which apparently increase the fine particle concentration in the clay slurry[36]. In the case of sample KK, there was no change in the plasticity values even after the beneficiation processes (Table 4.6).

Viscosity of sample JK was slightly increased but decreased in the case of sample KK (Table 4.6). Since viscous properties are highly sensitive, a slight change in the morphology or composition might highly reflect in the resulting values. However, the chemical beneficiation processes may have slightly modified the viscous properties[34]. The influence of grain size on the viscosity of clay suspensions is most pronounced, i.e. the finer the particle size the greater will be the viscosity for a given slurry concentration[34]. Apart from this, particle aggregation and delamination of the material

126

have an influence on the viscosity. In the case of sample JK, quite a good amount of micaceous particles were removed during the magnetic separation process which may affect the viscous flow of the clay slurry. It is known that loosely bonded grains are easily distorted and flow more easily than those of a more rigid one[34]. In the case of sample KK, aggregation, of the particles becomes destroyed by the removal of the cementing material like extremely fine crystalline and amorphous iron oxides during the chemical dissolution. In addition to this, the decrease in viscosity may also be attributed to the delamination of the clay stacks during the chemical leaching processes. However, a slight decrease in viscosity might have positively contributed to the rheology of the clay slurry during paper coating.

4A.3.5. *Effect of chemical bleaching on the structural properties of kaolin*

The crystallinity of the clay samples before and after the chemical dissolution processes were compared by calculating the Hinkley crystallinity index[37] values (Fig. 4.4a&b).

The crystallinity index values were slightly increased after the mild chemical bleaching treatments (Table 4.7). This slight improvement in crystallinity can be attributed to the removal of the extremely fine crystalline and amorphous iron oxides from the clay matrix[38].

Table 4.7. Hinkley crystallinity indices of samples JK and KK after chemical dissolution processes

Sample	Before bleaching	After dithionite bleaching	After sucrose bleaching
JK	0.91	0.96	0.98
KK	0.70	0.85	0.90

127
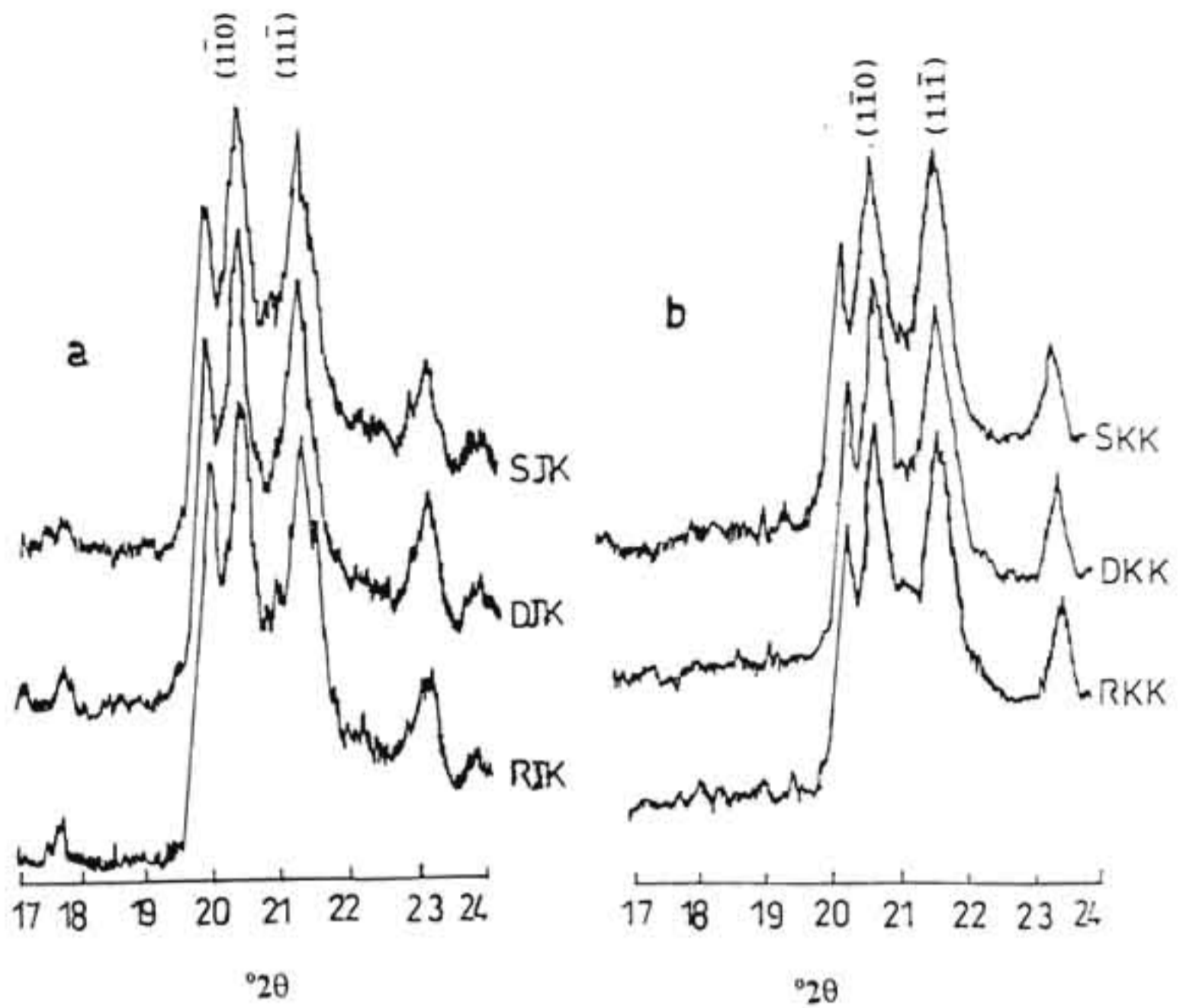
Fig.4.4.Hinkley Crystallinity Indices of samples JK and KK. RJK, RKK –
Non-treated samples of JK and KK; DJK, DKK – after dithionite
treatment; SJK, SKK – after sucrose treatment

A4.3.6. The combined effect of physical and chemical beneficiation

The effect of physical beneficiation using magnetic separation processes like
WHIMS, WHGMS and SC-HGMS and chemical beneficiation using sodium dithionite
and sucrose were already reported. The magnetic separation process prior to the
chemical leaching were found to be effective as it results in less reagent consumption and

128

minimising the time of treatment. Table 4.8 shows the combined results of physical and chemical beneficiation on samples JK and KK.

Table 4.8. Iron oxide removal and resulting brightness values after magnetic separation followed by chemical leaching

	WHIMS		WHGMS		SC-HGMS	
Sample JK						
	Sucrose	Dithionite	Sucrose	Dithionite	Sucrose	Dithionite
% Brightness	76.84	73.14	77.70	74.36	80.03	76.43
% Fe_2O_3 removed	55.49	26.65	60.48	35.42	64.51	50.35
Sample KK						
% Brightness	74.06	70.08	78.40	71.40	79.80	72.04
% Fe_2O_3 removed	45.30	23.56	67.56	24.21	72.42	25.67

In the case of sample JK, dissolution of iron oxide by dithionite increased to 26.65, 35.42 and 50.4% after WHIMS, WHGMS and SC-HGMS respectively. The brightness of the clay increased by 4 to 6 units (%) by this process.

In sample KK, the combined effect of magnetic separation (WHIMS, WHGMS & SC-HGMS) and dithionite bleaching increased the percent iron removal to 23.56%, 24.21 and 25.67% respectively. The resulting brightness was increased by the order of 3.78 to 5.74 units.

Magnetic separation processes prior to sucrose bleaching resulted in enhanced brightness and iron oxide removal for both the clay samples. For sample JK, sucrose treatment after SC-HGMS showed the maximum % of iron removal, i.e. 64.5% which corresponded to a brightness value of 80%. Similarly for sample KK, the combined effect

of SC-HGMS process followed by sucrose treatment increased the brightness from 66.3 to 79.8%. (~14 units improvement). This corresponded to an iron oxide removal of 72%. It was observed that the magnetic separation process prior to chemical leaching resulted in a fairly good enhancement in the brightness values of the two clays. The maximum values were obtained for the SC-HGMS-chemical beneficiation processes. The SC-HGMS-sucrose technique increased the brightness from 65 to 80% and 66 to 80% for samples JK and KK respectively.

4A.4. CONCLUSIONS

The FFD test is helpful in evaluating the effect of individual parameters investigated in the experiment. Effect of acid concentration and temperature are found to be significant on iron removal by sucrose in acid media.

The chemical beneficiation by sucrose and sodium dithionite in acid medium are found to be effective in removing the iron oxides from kaolin clays. The brightness of the clay samples increased from 65 to 86.9 and 66 to 80% for samples JK and KK respectively. Beneficiation by magnetic separation prior to chemical dissolution processes have reduced the time of treatment and the reagent consumption. The plastic property of the clay samples remained almost the same even after the beneficiation processes. The viscosity values slightly reduced for sample KK which has a positive effect towards the paper coating application.

130

PART-B

ORGANIC ACIDS FOR IRON REMOVAL

4B.1. INTRODUCTION

Several chemical leaching techniques have been used independently or in different combinations to remove iron oxides from kaolins. The use of organic acids seems promising for real applications especially when the conventional acid bleaching process using sodium dithionite fails to result in high-quality products.

The reductive dissolution of iron oxides using organic acids has been studied. Citric, lactic, glycolic, malonic, succinic, maleic, α-hydroxyisobutyric acids, furantetracarboxylic acid (FTCA) and 1-hydroxy ethane-1,1-diphosphonic acid (HEDPA) have been screened for their efficiency towards Fe^{3+} leaching.

Among the various organic acids, oxalic acid shows remarkable efficiency towards iron oxide dissolution. Studies conducted on the leaching of iron from Greek nickeliferrous ores by organic acids (lactic, formic, acetic, salicylic, citric and oxalic acids) showed that better results were noted for oxalic acid dissolution[39]. The purification of a ferruginous quartz sand using oxalic acid improved the quality of the product to be suitable for the ceramic industry[40]. The effect of oxalic and ascorbic acids in sulphuric acid medium were also reported[41,42]. A mixture of oxalic and citric acids in the ratio, 2:1 showed remarkable efficiency for iron removal from kaolin and quartz sands[43]. Decolouration of kaolin having greater than 4% Fe_2O_3 content was possible by an oxalic acid pressure bleaching process at 120°C[44]. The physico-chemical properties of the clay

131

remained unaltered after the leaching process. The possibility of recycling of the oxalic acid was also reported.

In previous studies on the deferration of Indian clays, a Full Factorial Design using sucrose – H_2SO_4 and dithionite-H_2SO_4 was tested[45]. Magnetic separation prior to the sucrose and dithionite bleaching enhanced the brightness of Rajastan (India) pink clays by 18 units (ISO)[46]. In the present work, a more eco-friendly and effective method of ferric iron removal using organic acids is evaluated in comparison with magnetic separation processes followed by chemical leaching. The reaction parameters such as time, temperature and reagent concentration have been optimised. Physical properties such as brightness, viscosity, plasticity, and surface area before and after the deferration treatments have been compared.

MECHANISM OF DISSOLUTION OF IRON OXIDES IN ORGANIC ACIDS

The mechanism of iron oxides dissolution in organic acids[7] has been summarised in three steps:

(a) Adsorption of organic ligands from the medium

(b) Non-reductive dissolution and

(c) Reductive dissolution

(a) Adsorption of organic ligands on the system interface

The first step of the dissolution reaction is the adsorption of carboxylic acids on the surface of iron oxides. In acidic solutions, an electrical double layer is established on the iron-oxide organic-acid medium interface. The reaction is as follows:

$$H_nL \leftrightarrow nH^+ + L^{n-} \text{ Acid ionisation} \qquad (1)$$

$$> Fe^{III} - O + H+ \leftrightarrow > Fe^{III} - O \text{ .... } H^+ \text{ Protonation of oxygens} \qquad (2)$$
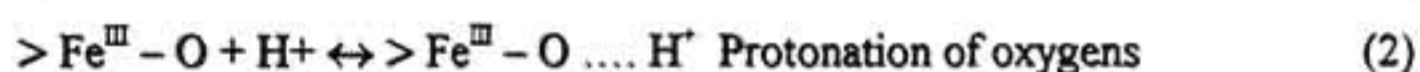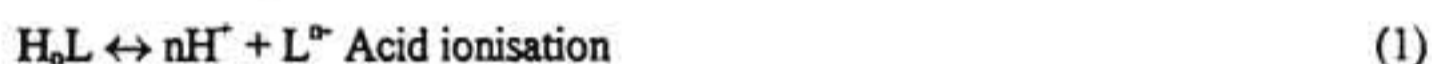
As the above reaction proceeds, the metal-oxygen bond become loosened and the surface hydroxyl groups (-OH) act as sites for the subsequent adsorption of organic ligands

132

$> Fe^{III} - OH^- + L^{n-} + H^+ \leftrightarrow [Fe^{III} - L]^{-(n-2)} + H_2O$ Surface complexation $\qquad$ (3)
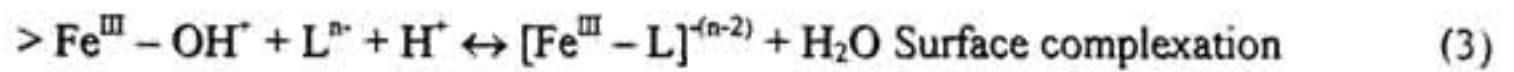
Greater the stability of the $[Fe^{III} - L]^{-(n-2)}$ complexes, more will be the surface complexation. In other words, as the chelating capacity of a ligand increases, the stability of $[Fe^{III} - L]^{-(n-2)}$ complexes also increases which favour the forward reaction (eqn.3).

In the case of oxalic acid, the surface complexation is achieved by the following reaction:

(b) Non-reductive dissolution

The nonreductive dissolution is a simple process involving the desorption of adsorbed surface ferric complex ions and their transfer to the acid solution

$$[> Fe^{III} - L]^{-(n-2)} + H^+ \rightarrow [Fe^{3+} - L]_{aq}^{-(n-3)} + > H \qquad (5)$$
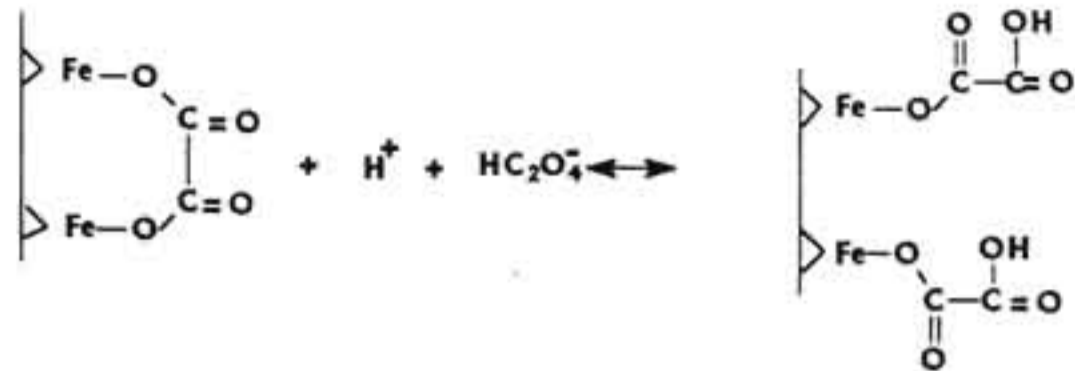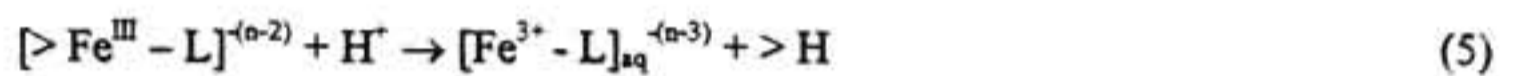
This process removes only the more reactive sites of the oxide surface. The reaction is accelerated by decrease in pH and increase in temperature. Since the desorption process is characterised by high activation energy, the non-reductive dissolution at low temperature is not an operative pathway whereas at elevated temperature, this mechanism may become increasingly important and may gradually override the reductive dissolution process as the most important pathway.

(c) Reductive dissolution

The reductive dissolution is accomplished in two steps:

(1) Induction period and

(2) Autocatalytic dissolution period

133

Induction period

During the induction period, ferrous ions are generated in the solution. The presence of lattice Fe^{II} (as in magnetite), ferrous ions dissolved and their concentration in the solution increased as shown in the following equation.
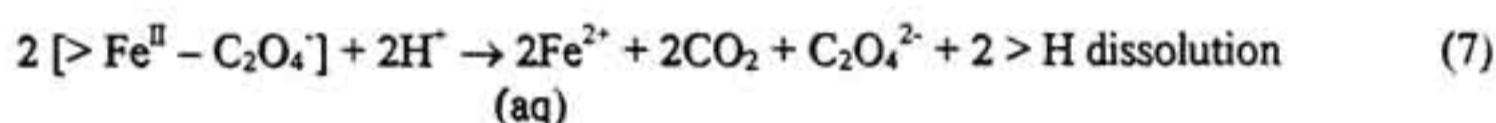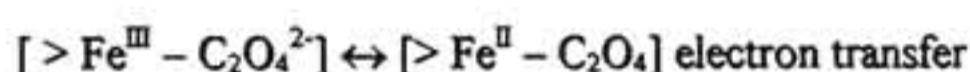
$$[> Fe^{II} - L]^{-(n-2)} \rightarrow [Fe^{2+} - L]^{-(n-2)} \tag{6}$$

Generally, Fe^{II} ions may be more readily transferred to the solution than Fe^{III} ions owing to the greater kinetic-instability of the Fe^{II}-O bond than the Fe^{III}-O bond.

In the absence of Fe^{2+} ions as in hematite, the Fe^{2+} generation is a slow process. In other words, the induction period will be longer. In a oxalic acid-iron oxide system, the electron transfer and the subsequent dissolution takes place as shown in the following eqn.

$$[> Fe^{III} - C_2O_4^{2-}] \leftrightarrow [> Fe^{II} - C_2O_4] \text{ electron transfer}$$

$$2 [> Fe^{II} - C_2O_4^{\cdot}] + 2H^{\cdot} \rightarrow 2Fe^{2+} + 2CO_2 + C_2O_4^{2-} + 2 > H \text{ dissolution} \tag{7}$$
$$\text{(aq)}$$

The rate of dissolution at this stage was affected by temperature and presence of light. At high temperatures (150°C), the dissolution of Fe^{2+} complexes by the reduction of Fe^{III} ions with oxalate through a partially or totally heterogeneous process.

Exposure to visible light or ultraviolet radiation provides an additional pathway to start dissolution. It is accomplished by the photochemical charge transfer in surface Fe^{III} – oxalate complex as represented in the equation below

$$2[Fe^{3+}(C_2O_4)_3]_{aq}^{3-} \rightarrow 2[Fe^{2+}(C_2O_4)]_{aq} + 3C_2O_4^{2-} + 2CO_2 \tag{8}$$
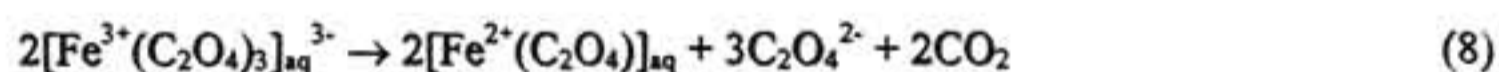
Autocatalytic dissolution period

Once a sufficient amount of ferrous oxalate ions are generated, the secondary reductive dissolution step becomes accelerated. The dissolution process can be summarised in three steps.

134

(a) adsorption of aqueous ferrous complexes on the surface ferric complexes.

(b) a fast outer sphere or inner-sphere electron transfer and formation of Fe^{II} on the system interface, and

(c) desorption of ferric complexes and transfer of trivalent iron in the solution.
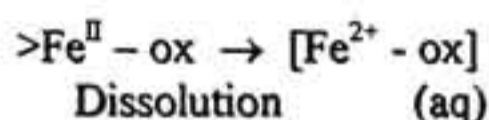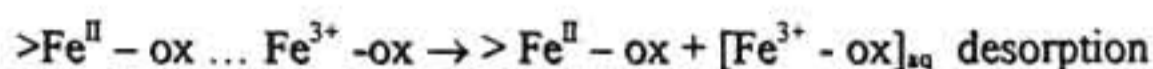
The autocatalytic dissolution period in iron-oxalate system can be illustrated by the following equations.

$$[>Fe^{III} - ox] + [Fe^{2+} - ox]_{aq} \rightarrow > Fe^{III} - ox \dots. Fe^{2+} - ox \text{ adsorption of complex}$$
$$\text{to surface}$$

$$>Fe^{III} - ox \dots. Fe^{2+} - ox \rightarrow > Fe^{II} - ox \dots Fe^{3+} - ox \text{ electron transfer}$$

$$>Fe^{II} - ox \dots Fe^{3+} -ox \rightarrow > Fe^{II} - ox + [Fe^{3+} - ox]_{aq} \text{ desorption}$$

$$>Fe^{II} - ox \rightarrow [Fe^{2+} - ox]$$
$$\text{Dissolution} \qquad \text{(aq)}$$
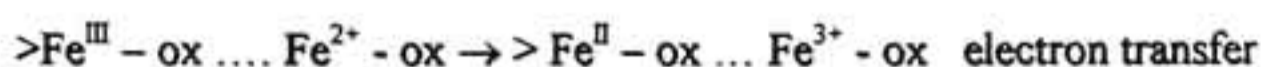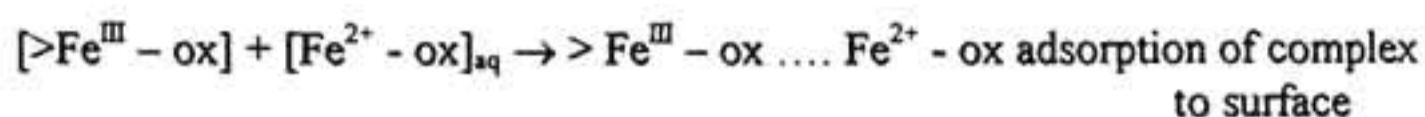
where ox denotes any species derived from oxalic acid.

The reductive dissolution can be accelerated by the external supply of ferrous ions in the initial solution. At high ferrous ion concentrations the process of ferrous ion generation (induction period) is drastically reduced, thereby eliminating the time consuming step from the dissolution mechanism.

4B.2. MATERIALS AND METHODS

Iron-stained kaolinitic clay KK has been selected for the leaching studies. The sample was prepared as per the procedures given in 2.2.2. The chemical analysis data was represented in Table 2.4.

Experimental

The amorphous Fe_2O_3, Al_2O_3 and SiO_2 content of the sample were determined using the procedure followed by Smith and Mitchell[31].

The leaching tests were carried out in a round bottomed flask which was kept stirred in a heating mantle. For a typical experiment, 20% clay slurry was treated with organic acid at 100°C for 90 minutes. Equimolar (0.15 M) solutions of formic, acetic, succinic, tartaric, citric, L-ascorbic and oxalic acids (AR grade) were used. In the case of the treatment with oxalic acid alone, experiments were carried out using three different concentrations (0.05, 0.10 and 0.15 M).

Out of the above conditions, leaching studies at the highest concentration (0.15 M) was carried out: (a) at room temperature (27°C) for 5-30 days; (b) in presence of Fe^{2+} ions introduced as $FeSO_4.7H_2O$ at 100°C for 15-90 minutes; (c) in presence of 0.1-0.5 M H_2SO_4 at 100°C for 15-90 minutes; and (d) for samples previously beneficiated by magnetic separation processes such as WHIMS, WHGMS and SC-HGMS at 100°C for 15-90 min. In all the cases, the leached liquors were analysed for Fe_2O_3 (Ref.2.2.2.k) and the dried cakes were subjected to brightness measurement (Ref.3.3). The physicochemical properties of the raw as well as the samples treated with oxalic acid (0.15M) alone and oxalic acid (0.15M) in 0.5M sulphuric acid were compared. The plasticity index was determined as per the standard procedures[47] and viscosity as given in 4A – 2. Surface area and pore volume were determined by BET multi point method (Ref.2.2.2.f). The crystallinity indices of the raw as well as the processed samples were compared (Ref. 4A-2). The representation of the entire processes is given in Fig.4.5.

4B.3. RESULTS AND DISCUSSION

The X-ray diffraction analysis indicated that the major colouring impurities associated with kaolinite were hematite, goethite and rutile [Ref.2.3). The total Fe_2O_3 content in the clay sample was found to be 0.93%.
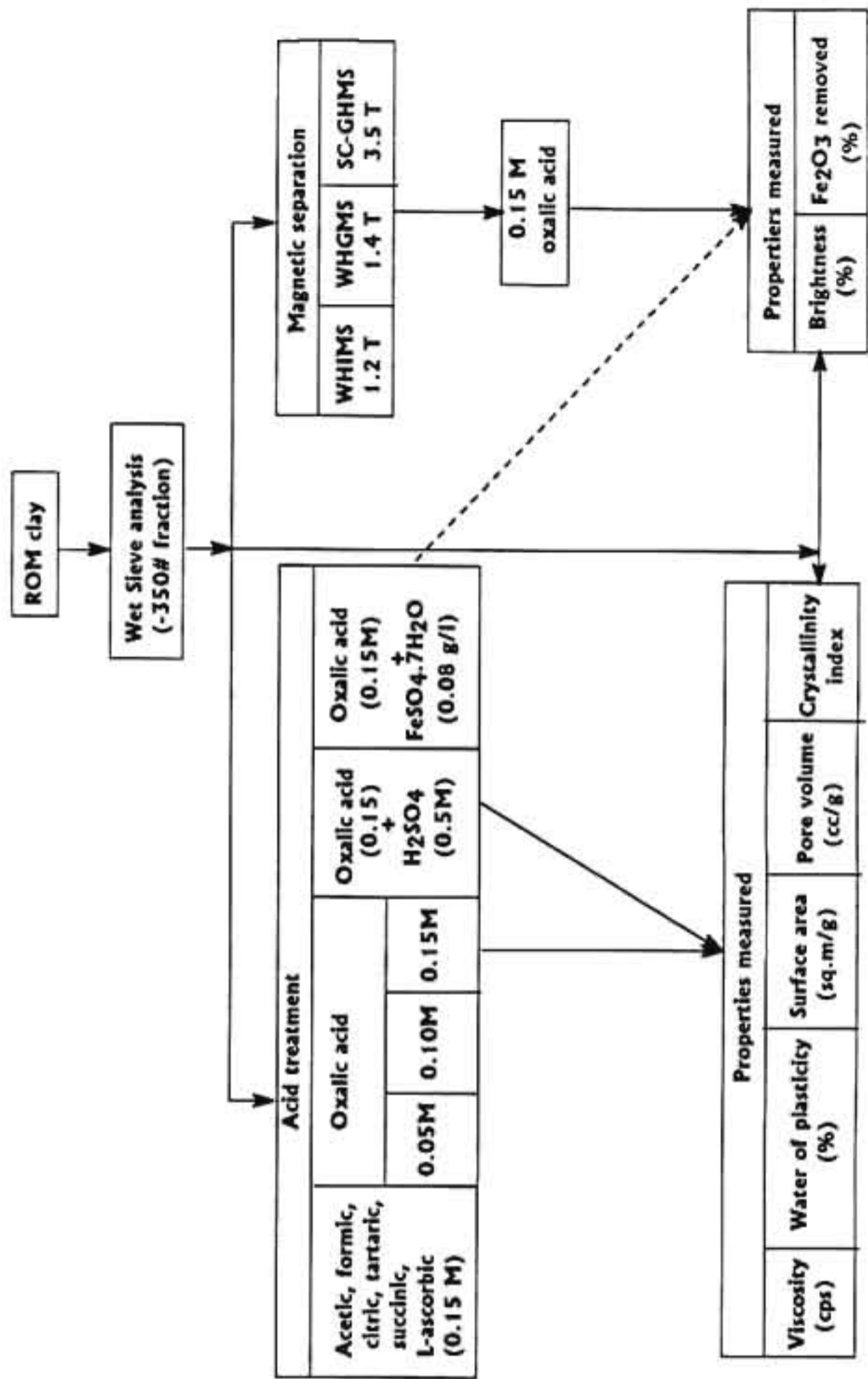
Fig.4.5. Schematic diagram of the entire process

4B.3.1. Comparison of the effect of various organic acids

The results of the organic acid treatments are shown in Table 4.9. The deferration effect of formic, acetic, succinic, citric and tartaric acids was lower than that of equimolar (0.15 M) solutions of L-ascorbic and oxalic acids under the same experimental conditions. The brightness of the clay was increased from 66.33 (raw clay) to 76.85 and 81.85% for L-ascorbic and oxalic acid treated clays respectively, the corresponding Fe_2O_3 removal being 43.60 and 66.86%. Since the iron oxide leaching mechanism is a combined effect of acidity, complexing power and reducing capacity, oxalic and ascorbic acids show better performance compared to other organic acids. Although L-ascorbic acid and oxalic acids are good complexants for Fe^{3+}, the higher acid strength of oxalic acid (pK_{a1} = 1.25) when compared to that of L-ascorbic acid (pK_{a1} = 4.17) enabled better dissolution of ferric iron. It may be mentioned here that experiments on synthetic goethite by Chiarizia and Horwitz[4] gave similar results confirming the above observations. Because of the good complexing power, oxalic acid was selected for further studies.

Table 4.9. Effect of organic acids on iron removal

Acid used	Fe_2O_3 (%)	Brightness (%)
Acetic	0.001	66.51
Succinic	0.002	66.71
Formic	0.003	66.65
Tartaric	0.010	66.89
Citric	0.020	66.95
L-ascorbic	43.600	76.85
Oxalic	66.870	81.85

4B.3.2. Effect of oxalic acid on iron removal and brightness

Initially, reactions were carried out to establish the iron dissolution with time at temperature (27°C). Figure 4.6 shows the results of deferration over a period of 30 days.

The maximum Fe_2O_3 removed was 80.93% which resulted in the improvement in brightness by 17.5 units. From these studies it can be inferred that iron dissolution at low temperature was a time consuming process. In order to optimize the time and temperature, experiments were carried out varying these parameters (Table 4.10). Higher temperature conditions considerably reduced the time of leaching to a few hours instead of days.
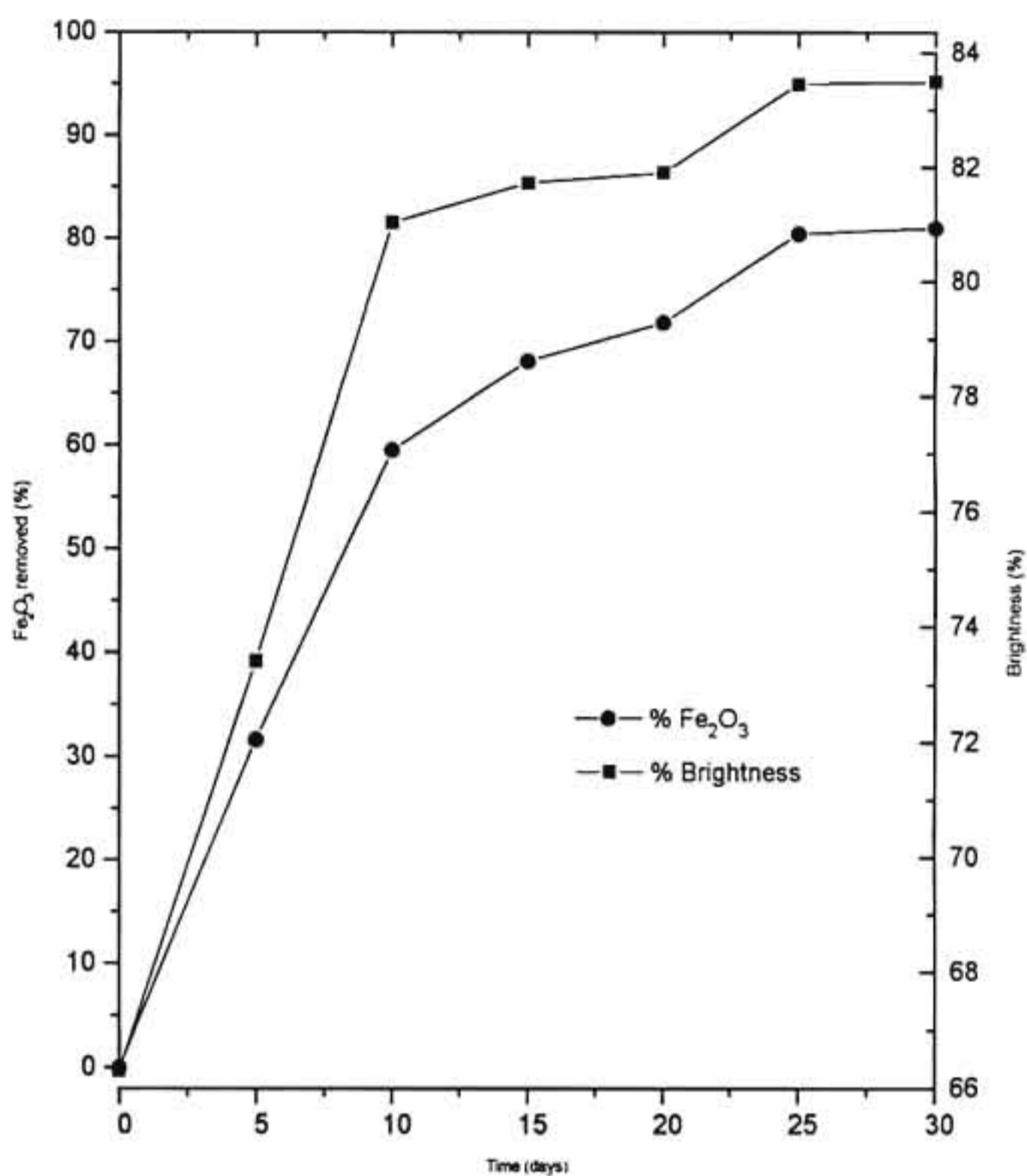

Fig.4.6. Results of room temperature (27°C) treatment with
0.15 M oxalic acid

In order to have an optimisation of the acid concentration, experiments were also carried out at 100°C for different molar concentrations (0.05, 0.10 and 0.15 M oxalic acid)
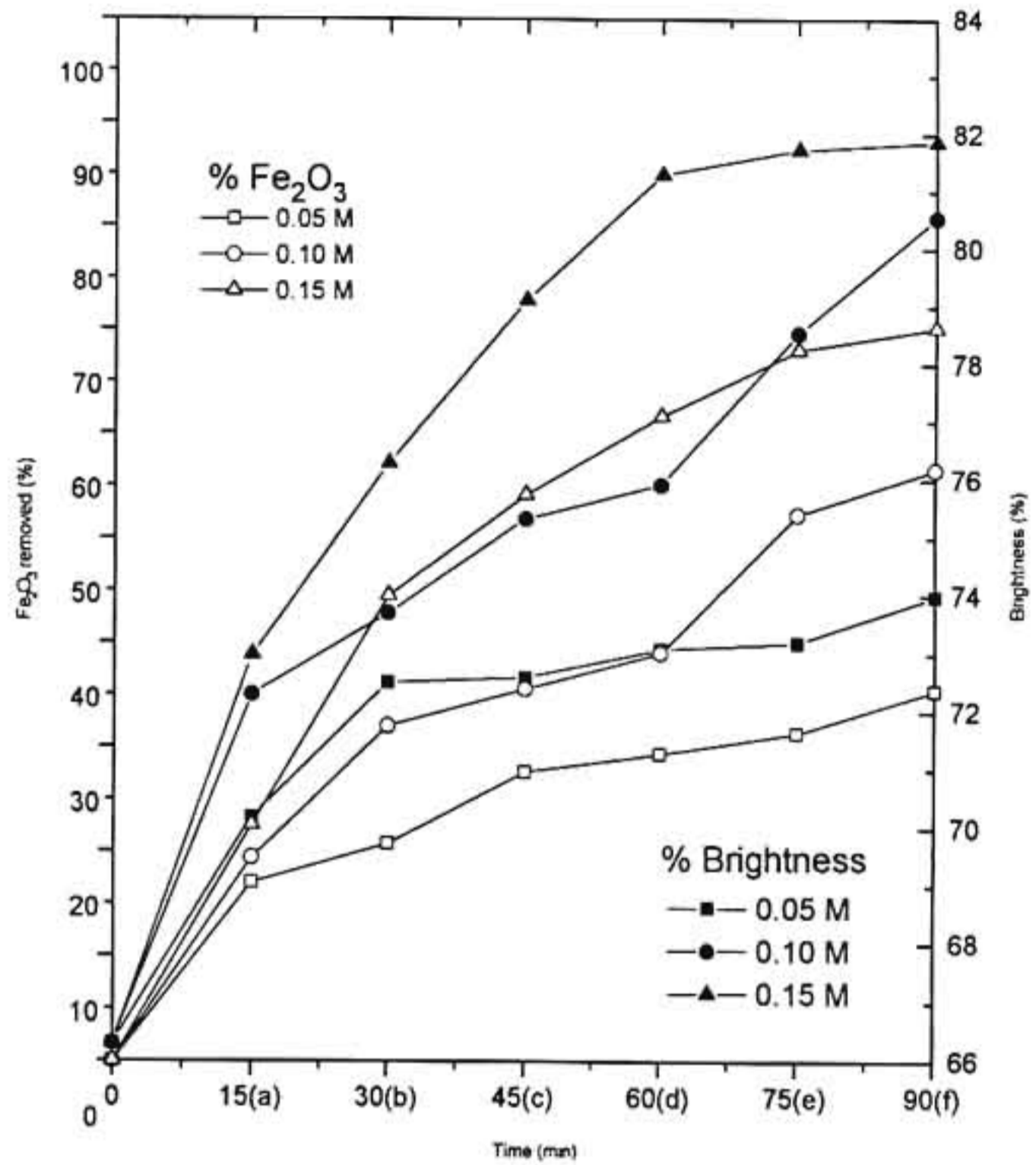
Fig.4.7. Effect of 0.05, 0.1 and 0.15 M oxalic acid on iron removal and brightness

and the results were monitored at 15 minutes interval (Fig.4.7). The experiments were denoted as $A_{a...f}$, $B_{a...f}$ and $C_{a...f}$ respectively. The experimental conditions sufficient enough to produce a desired minimum value (80%) of brightness were met at an acid concentration of 0.10 M and a reaction period of 90 minutes (expt. B_f). In experiment C_d, the same result was achieved at 60 minutes. In experiment A, brightness values were always < 80%.

4B.3.3. Combined effect of magnetic separation and oxalic acid bleaching

Aiming at better deferration and improved reflectance values, leaching studies were carried out using the nonmagnetic fraction of the samples beneficiated by WHIMS, WHGMS and SC-HGMS processes (Table 4.11). 2.70-5.28% of the crystalline iron oxides were removed during the magnetic separation process, but only a slight improvement in brightness (1.5%) could be observed. Hence it can be assumed that brightness is much dependent on the surface coated iron oxides than the descrete fines. However the magnetic separation followed by chemical leaching enhanced the brightness to 82.36, 82.56 and 83.36% by WHIMS, WHGMS and SC-HGMS respectively. These values were slightly higher than those obtained for the raw clay which was not subjected to magnetic separation.

Table 4.10. Effect of time and temperature on iron removal by 0.15 M oxalic acid

Temperature (°C)	Time (min)	Fe_2O_3 (%)	Brightness (B) (%)	ΔB
60	90	23.58	72.01	5.68
80	90	39.12	73.59	7.26
80	180	58.68	79.20	12.87
100	90	70.21	81.85	15.52

Table 4.11. Effect of leaching on the Fe_2O_3 content and brightness of the nonmagnetic fraction

| Process | Fe_2O_3 removed (%) | | | Brightness (%) | | |
	Magnetic separation	Magnetic separation + chemical leaching	Magnetic separation (B)	Magnetic separation + chemical leaching (B_1)	ΔB	ΔB_1
WHIMS	2.70	70.01	66.79	82.36	0.46	16.03
WHGMS	3.01	69.82	67.23	82.56	0.90	16.23
SC-HGMS	5.28	69.72	67.85	83.36	1.52	17.03

4B.3.4. Effect of oxalic acid in sulphuric acid medium

Since it is known that the presence of protons promote the iron dissolution at comparatively faster rate[9] experiments were also conducted on raw clays in presence of sulphuric acid (0.1 M and 0.5 M H_2SO_4). Results of the experiments are presented in Table 4.12. The combination 0.5 M H_2SO_4 and 0.15 M oxalic acid (experiment D) produced an enhancement in brightness and iron removal (Fig.4.8). It should be noted that the addition of protons generate more surface active centres which enhance a faster iron oxide dissolution rate. In this case, the brightness was found to increase to 83.01% with a corresponding iron removal of 72.89%.

Table 4.12. Effect of sulphuric acid on iron removal and brightness at 100°C for 90 min

Acid	Fe_2O_3 (%)	Brightness (%)
0.1 M H_2SO_4	6.34	68.40
0.1 M H_2SO_4 + 0.15 M oxalic acid	70.28	81.87
0.5 M H_2SO_4	52.32	78.90
0.5 M H_2SO_4 + 0.15 M oxalic acid	72.89	83.01
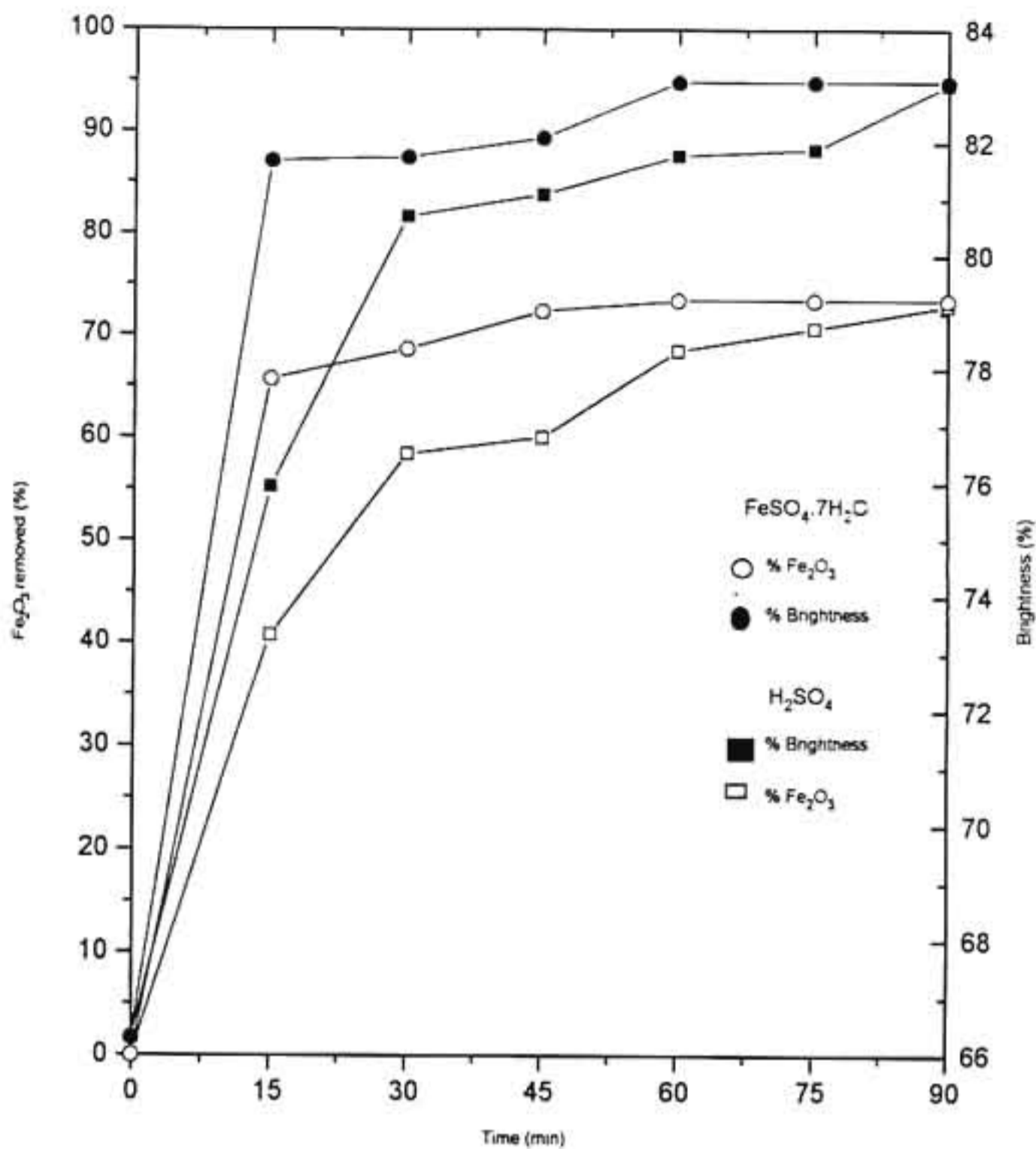
Fig.4.8. Effect of H_2SO_4 (0.5 M) + oxalic acid (0.15 M) and $FeSO_4.7H_2O$ (0.08 g/l) + oxalic acid (0.15 M) on iron removal and brightness

4B.3.5. Effect of ferrous ion addition in oxalic acid solution

It has been reported by several researchers that the external addition of ferrous iron into the oxalate solution[6,9,48] accelerates the Fe^{2+} generation which comparatively reduces the longer induction period of autocatalytic Fe^{2+} generation[9,6]. In order to study the effect of added Fe^{2+}, $FeSO_4.7H_2O$ (0.08 g/l)was added in combination with oxalic acid The results are given in Fig.4.8. It has been observed that the reaction was completed in

143

60 minutes with the iron oxide removal (73.43%) corresponding to a brightness value of 83.06%.

4B.3.6. Physical property variation on deferration

The changes in physical properties such as viscosity, plasticity, surface area and pore volume after clay deferration are investigated. Crystalline and noncrystalline materials associated with kaolinitic clay can strongly influence these properties. For example, iron oxides as fine crystalline forms increase the specific surface area of the matrix owing to their smaller particle size[49,50]. The Kalliyur clay shows surface coating of amorphous iron oxides. In addition to this, non-crystalline alumina and silica also have been identified. In the clay the sample concentration of amorphous iron oxide, alumina and silica amount to 0.31, 0.34 and 0.95% respectively. At lower pH conditions, these materials show tendency to aggregate or cementate on clay particles and the coating thus formed can be continuous or intermittent[51].

(a) Viscosity studies

The comparison of viscosity of the raw and the processed samples showed that the dispersant required for achieving a viscosity of 500 cps was maximum for the untreated clay and minimum for the oxalic-sulphuric acid treated sample (Table 4.13). It is known that 1 to 5% of amorphous iron oxides, alumina and silica are capable of altering the entire clay properties[52]. In acidic pH, kaolinite coated by these materials show a net positive surface charge[53] which get reduced during the addition of deflocculants such as sodium polyphosphate. The surface shows a negative net charge above pH 7 and deflocculation takes place. Since the coatings have been removed during the acid treatment, the deflocculant demand for the processed samples is very low compared to that of the untreated clay.

144

Table 4.13. Variations in physical properties on acid treatment

Property	Untreated clay	Oxalic acid	Oxalic + sulphuric acid
Water of plasticity (%)	41.9	39.5	38.9
Dispersant requirement (gl^{-1}) at 500 cps viscosity	0.77	0.17	0.01
Surface area (m^2g^{-1})	13.55	16.00	18.74
Pore volume (cm^3g^{-1})	0.006	0.007	0.008

(b) Plasticity Index

The difference in the water content between the lower limit of fluidity (liquid limit) and the rolling limit (plastic limit) is termed as the Atterberg number which describes the range of water content of a clay for which it is plastic[53]. Table 4.14 shows the Atterberg limits of Kalliyur clay before and after the leaching process. Acid treatments do not change the plastic limits but reduce the liquid limits considerably. The reason for this observation could be that under wet conditions, the amorphous materials such as alumina, silica and iron oxides show high hydration capacity forming highly porous three dimensional net works which can hold large amounts of water[52]. One could also consider the possibility of a better orientation of clay particles in the absence of these amorphous coatings.

Table 4.14. Atterberg limits of treated and untreated samples

	Liquid limit	Plastic limit	Plasticity Index
Raw	70.50	31.40	39.10
Oxalic acid	60.00	31.40	28.60
Oxalic +sulphuric acid	52.7	31.40	21.30

(c) Specific surface area and pore volume

Table 4.13 indicates that the specific surface area and the pore volume of the untreated clay slightly increase after the acid leaching which could undoubtedly be due to the removal of the amorphous cements from the clay matrix. The analysis of the leachates indicated that 0.4% alumina and 1.5% silica were exsolved from the surface of the clay during the 0.5 M sulphuric acid plus 0.15 M oxalic acid treatment (Table 4.15). Moreover the acid treatment may cause the delamination of the clay to a certain extent enhancing the surface area.

Table 4.15. Effect of acid leaching on Al_2O_3 and SiO_2

Treatment	% Removal	With time (min)					
		15	30	45	60	75	90
0.15 M oxalic acid	Al_2O_3	0.009	0.01	0.15	0.20	0.24	0.31
	SiO_2	0.370	0.51	0.65	0.69	0.72	0.75
0.15 M oxalic +	Al_2O_3	0.130	0.17	0.19	0.31	0.37	0.44
0.5 M sulphuric acid	SiO_2	0.930	0.95	1.0	1.08	1.12	1.57

4B.3.7. Structural changes

The crystallinity indices of the raw as well as the acid treated samples were calculated by comparing the (110) and (111) reflections[37]. Amorphous iron oxides and other non-crystalline materials tend to inhibit the dispersion of the clay thereby preventing the proper orientation and increasing the background count. Removal of these materials increased the crystallinity index from 0.7 to 0.9 for the Kalliyur clay.

4B.4. CONCLUSIONS

Among the organic acids tested such as formic, acetic, succinic, tartaric, citric, L-ascorbic and oxalic acid, the last one shows remarkable ability to leach out ferric oxides associated with a kaolinitic clay. The optimum conditions for improving the brightness up to 80% are found to be 100°C, 0.15 M oxalic acid and 90 minutes reaction time. Addition of protons and ferrous irons positively contribute to the brightness as well as the percentage iron removal at comparatively lower reaction periods. Leaching studies on samples beneficiated by WHIMS, WHGMS and SC-HGMS have also given better results. The brightness increased by 15-17 units ISO after the deferration processes after 30 days ageing. The acid leaching process removed the amorphous alumina, silica and iron oxides associated with the clay. It also reduced the viscosity and liquid limits but increase the specific surface area, pore volume and crystallinity index.

The improvement in brightness and rheological properties clearly indicate that the iron-stained kaolinite from Kalliyur can be a value-added material for paper filling and coating applications.

PART-C
METAL POWDER CATALYSED IRON REMOVAL
4C.1. INTRODUCTION

Kaolin with brightness >80% goes into paper filling applications, whereas for paper coating, the desired brightness is of the order of >85%. But kaolin having brightness >87% finds use in very special applications such as super quality ceramics, glazes, filler in white paints etc. In this part, a new process has been introduced to bring the brightness of kaolin in the range 85-91%. The technique is quite attractive as it is a low energy process. In addition to this, unit operations involved in this are minimal.

Detailed studies on the effect of organic acids, especially oxalic acid on the deferration of iron-stained kaolinite has been reported in Part B-2. Oxalic acid proved to be an excellent reagent for removing iron oxides from Kalliyur kaolin[54]. A comparative study on the effect of protons (H^+ ions from H_2SO_4) and Fe^{2+} ions (from $FeSO_4.7H_2O$) with that of oxalic acid has also been discussed. It has been found that protonation and Fe^{2+} addition minimize the time consuming induction period, thereby facilitating the iron oxide dissolution at a faster rate.

The present study envisages the catalytic effect of metal powders like, Al, Fe and Zn in oxalic acid medium in a wide range of temperature (27-100°C).

4C.2. MATERIALS AND METHODS

The iron-stained clay samples JK and KK were selected for the deferration studies. Sample KK was from the same mine but from a different seam. Minus 45 μm fractions were obtained as described in section 2.2.2.
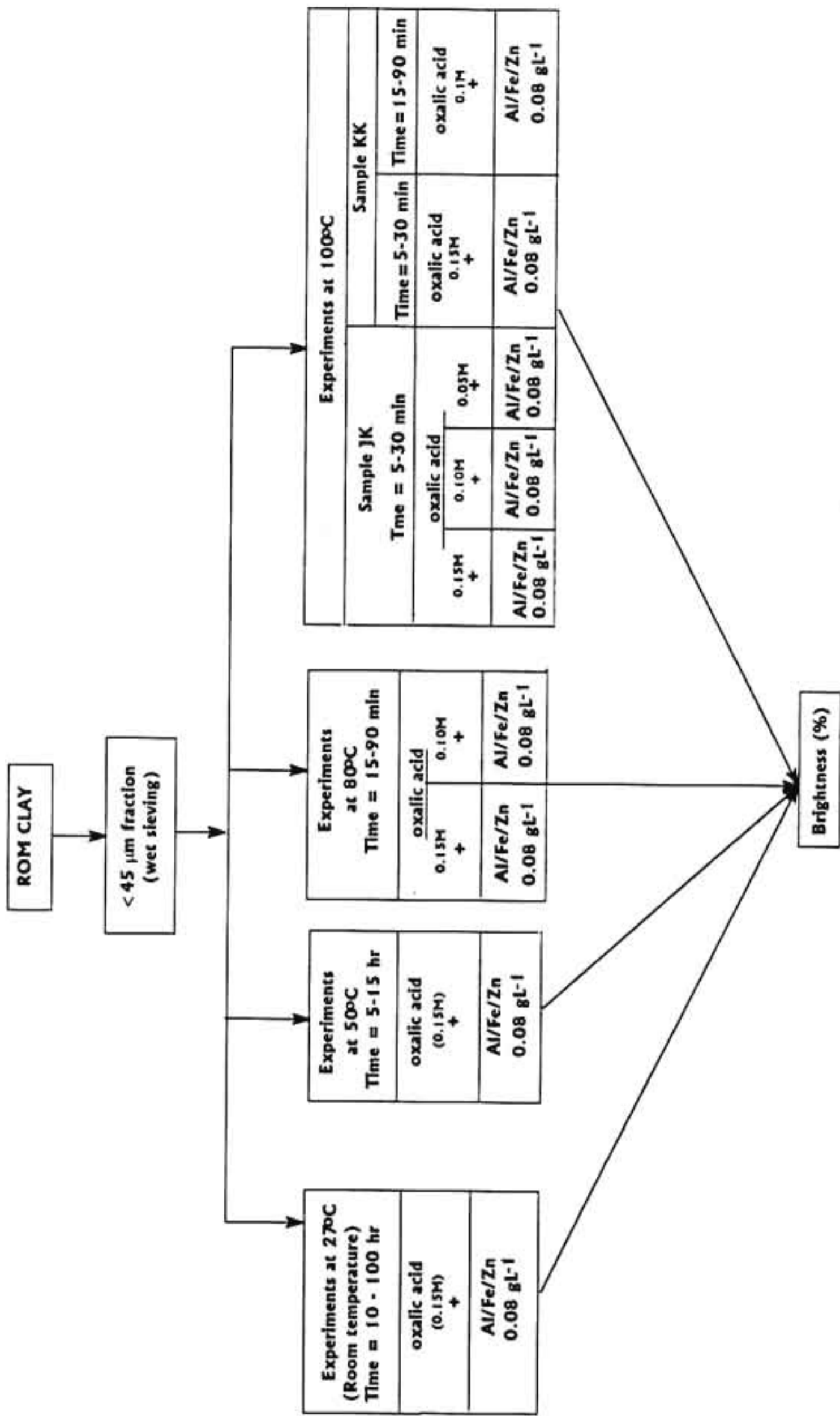
148

Fig.4.9. Schematic representation of the entire process

Experimental

The Fe_2O_3 contents of the samples were 1.02 and 1.69% w/w for JK and KK respectively. The experimental runs were performed in a two necked round bottomed flask kept inside a thermostatically controlled mantle. The slurry was given a mild stirring throughout the experiment.

In each experiment, a 20% clay slurry was prepared in 0.05-0.15 M of oxalic acid and 0.08 g/L metal (Al/Fe/Zn) powder was added as catalyst. Experiments were carried out at 4 different temperatures (27°C, 50°C, 80°C and 100°C) for a wide range of time (5 min to 100 hours). The whole process is schematically represented in Fig.4.9.

Three sets of experiments were carried out at 27°C (room temperature). The clay suspension (20%) was mixed with 0.08 g/L metal powder and 0.15 M oxalic acid and kept stirring over a period of 100 hr. The progress of the reaction was monitored by measuring the change in brightness of the samples at intervals of 10 hr.

For the experiments carried out at 50°C, the clay-oxalic acid-metal-powder mix was the same as above, but the time of treatment was 5-15 hr at 5 hr time interval monitoring.

In the case of experiments conducted at 80°C, the clay slurry (20%) was mixed with two oxalic acid concentrations (0.10 & 0.15 M), the time of treatment being further reduced to 15-90 minutes with an interval of 15 minutes for monitoring.

For the experiments conducted at 100°C clay was treated with acids of three concentrations 0.15, 0.10 & 0.05 M, and catalyst conc. 0.08 g/L, time of treatment : 5-30 min. For sample KK, the slurry was treated with (0.15 and 0.1 M acids only). The time of contact was 5-30 minutes for 0.15 M and 90 min. for 0.1M of acid.

After each experiment, the clay slurry was filtered and washed thoroughly with deionized water to free the dissolved products. The filter cakes were dried at 80°C for 2 hr and the brightness values measured (Ref.4A-2).

150

4C.3. RESULTS AND DISCUSSION

4C.3.1. Brightness studies

The brightness values of the whole experiments are presented in Table 4. Figure 4.10a represents the brightness measurements of sample JK for the experiments conducted at room temperature (27°C). For all these three sets of experiments, the brightness got

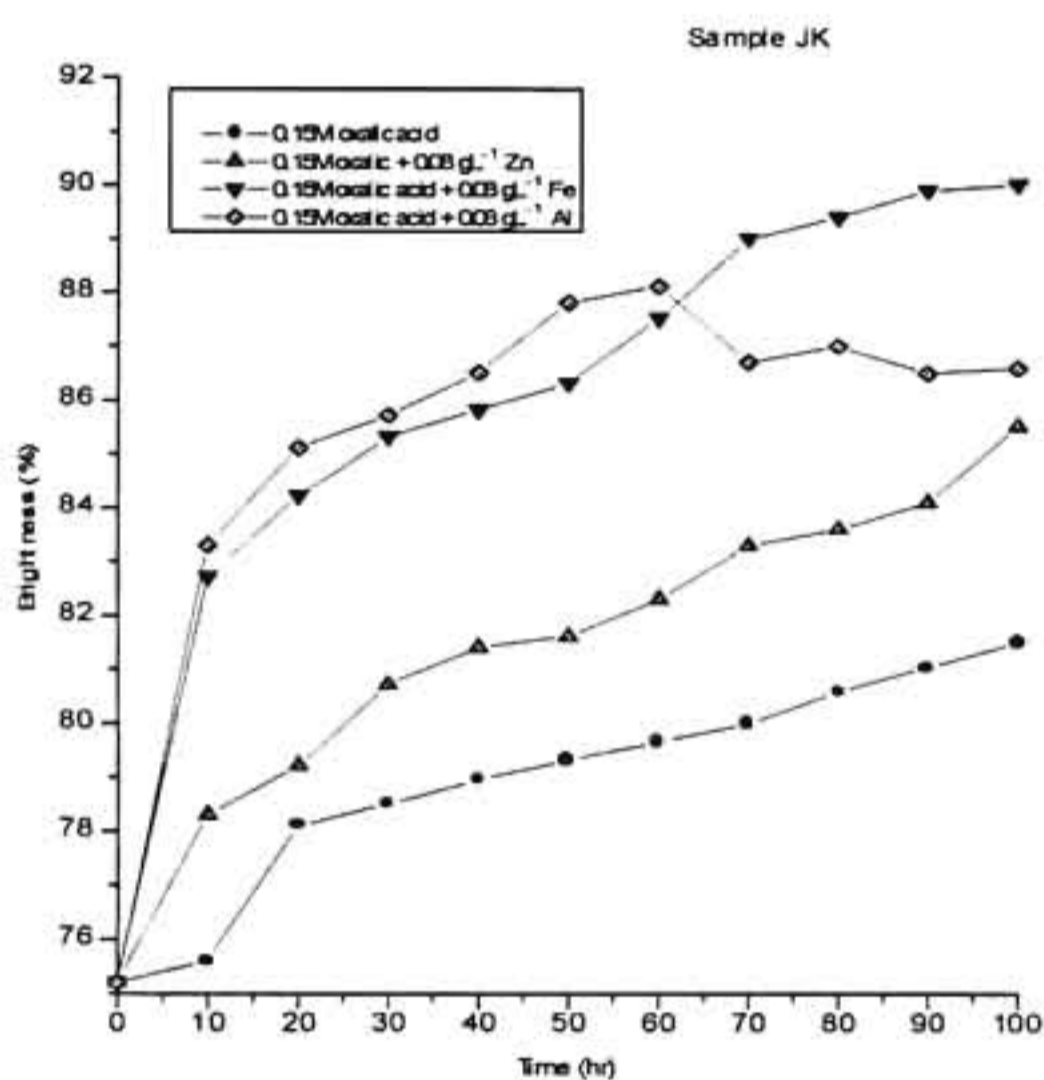Fig.4.10a.Brightness results of the experiments at 27°C room temperature in 0.15M oxalic acid alone and in presence of metal powders

increased above 80%. The maximum improvement in brightness, i.e. 90% was obtained when Fe was used the catalyst. However, the Al-catalysed reactions were comparatively faster than that of reactions with Fe and Zn catalysts. From the brightness values it is also

151

found that the reactions with Al showed a different trend from the other two catalysts (ie. Fe &Zn). The Al-catalysed reactions showed an increase in brightness upto 60 hr experimental time. Brightness at 60 hr being 88%. After 60 hr, the brightness value decreased to 86.7 and then stabilized. Meanwhile, the experiments with Fe and Zn showed an increase in brightness with increase in time upto 100 hr. The maximum brightness vlaues corresponding to Fe and Zn catalysed reactions were 90 and 86.6% respectively. The very same experiments conducted in the absence of the catalysts showed only 6 units improvement in brightness (ie.75 to 81% ISO). Use of metal powder catalysts, Zn, Al and Fe improved the brightness by 10, 13 and 15 units respectively.

The brightness results of sample KK for the experiments carried out at room temperature (27°C) are shown in Figure 4.10b. The experiments conducted using Al-catalyst howed a different pathway as observed in the case of sample JK. The maximum
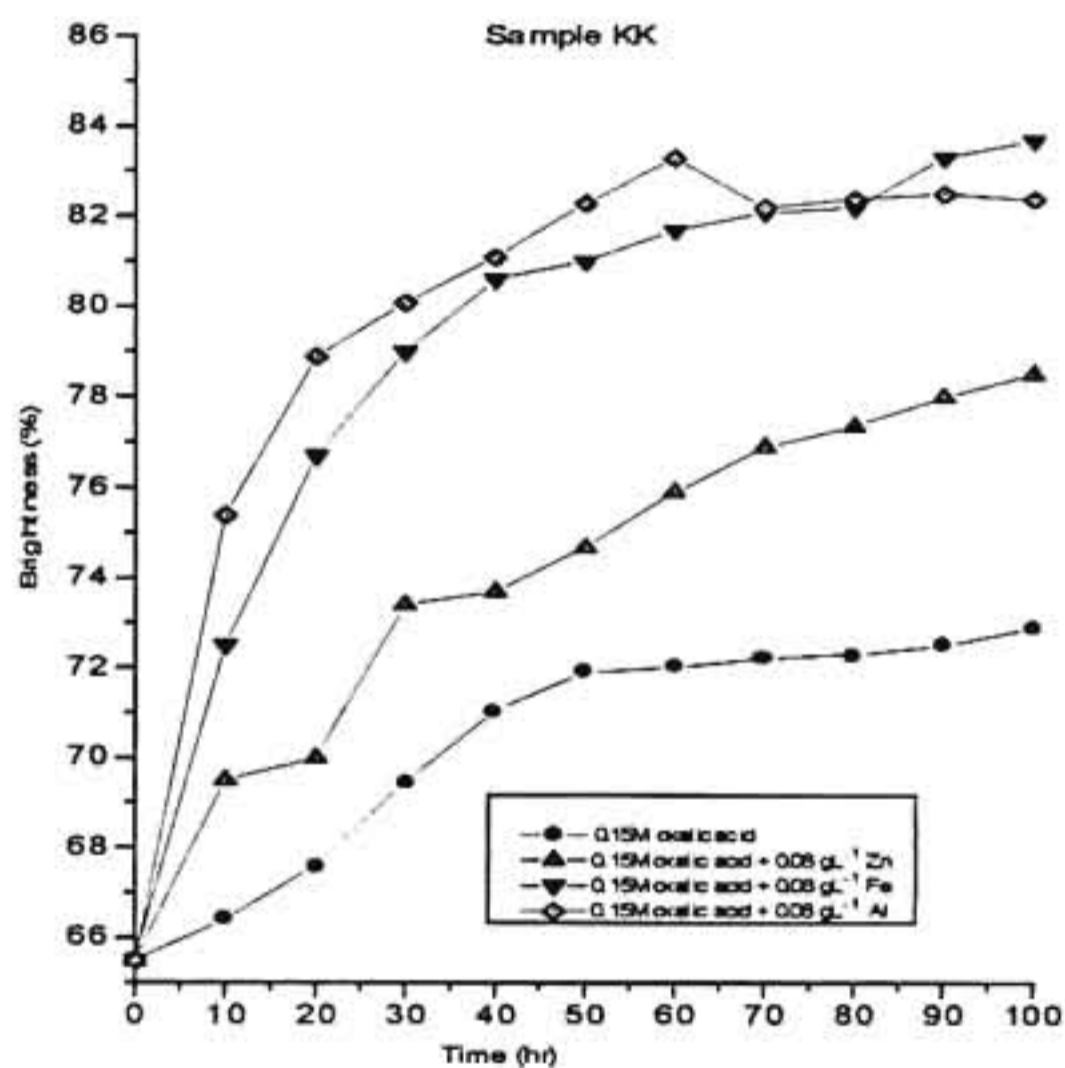

Fig.4.10b. Brightness results of the experiments at 27°C (room temperature) in 0.15 M oxalic acid alone and in presence of metal powders

value encountered in this set of experiments was 83.7% which was obtained for the Fe-catalysed experiment at a period of 100 hr. The corresponding brightness improvement obtained for Al and Zn catalysed experiments were 83.3 and 78.5% respectively.

Table 4.16 Brightness Values obtained after metal catalysed iron oxide dissolution

Experiment 1: Temp. – 27°C; Oxalic acid – 0.15M; Al/Fe/Zn – 0.08 gL^{-1}

Time (hr)	Sample JK				Sample KK			
	Without metal	Zn	Fe	Al	Without metal	Zn	Fe	Al
10	75.60	78.30	82.70	83.30	66.40	69.50	72.50	75.40
20	78.10	79.20	84.20	85.10	67.60	70.00	76.70	78.90
30	78.50	80.70	85.30	85.70	69.45	73.40	79.00	80.10
40	78.94	81.40	85.80	86.50	71.04	73.70	80.60	81.10
50	79.30	81.60	86.30	87.80	71.90	74.67	81.00	82.50
60	79.65	82.30	87.50	88.10	72.02	75.90	81.70	83.30
70	79.98	83.30	89.00	86.70	72.21	76.90	82.10	82.22
80	80.58	83.60	89.40	86.60	72.31	77.35	82.20	82.40
90	81.03	84.10	89.90	86.56	72.50	78.00	83.32	82.34
100	81.50	85.50	90.01	86.60	72.89	78.50	83.70	82.39

Experiment 2: Temp. – 50°C; Oxalic acid – 0.15M; Al/Fe/Zn – 0.08 gL^{-1}

Time (hr)	Zn	Fe	Al		Zn	Fe	Al
5	82.50	83.43	88.50		72.70	77.90	83.60
10	82.90	86.10	86.40		73.30	80.30	82.60
15	83.40	88.70	86.43		73.90	83.70	82.61

Experiment 3: Temp. – 80°C; Oxalic acid – 0.15M; Al/Fe/Zn – 0.08 g/L^{-1}

Time (min)	Zn	Fe	Al		Zn	Fe	Al
15	81.10	82.50	85.00		70.98	75.70	79.90
30	81.90	83.10	86.00		72.60	78.50	82.70
45	83.25	88.40	89.60		73.81	81.60	83.20
60	84.39	90.10	88.10		76.59	82.90	83.56
75	85.04	90.20	88.24		78.77	83.70	83.98
90	86.70	90.40	88.32		80.08	84.10	83.60

Experiments without catalysts were tested only at the highest and lowest temperatures

Experiment 4: Temp. – 80°C; Oxalic acid – 0.1M; Al/Fe/Zn – 0.08 gL⁻¹

Time (min)	Zn	Fe	Al	Zn	Fe	Al
15	76.05	77.60	83.40	70.01	74.70	78.55
30	79.08	82.60	85.30	71.89	76.90	80.70
45	81.00	85.00	86.40	73.00	78.70	81.10
60	81.83	84.50	87.10	75.48	80.08	81.48
75	82.93	86.50	88.50	76.89	80.90	81.50
90	83.21	88.10	87.60	78.30	81.70	81.29

Experiment 5: Temp. 100°C; Oxalic acid – 0.15M; Al/Fe/Zn – 0.08 gL⁻¹

Time (min)	Without metal	Zn	Fe	Al	Without metal	Zn	Fe	Al
5	78.00	80.40	83.50	86.30	69.90	71.00	75.50	79.90
10	78.30	86.70	88.10	90.29	71.30	75.80	79.50	82.80
15	79.48	87.10	89.10	90.40	72.80	79.90	83.30	83.60
20	80.15	88.60	89.50	91.40	73.50	82.00	84.90	84.10
25	81.72	89.30	90.40	91.90	74.02	83.28	85.00	84.21
30	82.60	90.01	90.90	90.40	74.70	83.50	85.10	84.16

Experiment 6: Temp. –100°C; Oxalic acid – 0.1M; Al/Fe/Zn – 0.08 gL⁻¹

Time (min)	Zn	Fe	Al	Time (min)	Zn	Fe	Al
5	80.00	82.70	85.90	15	76.80	81.10	82.50
10	82.20	85.20	90.20	30	80.21	83.50	83.40
15	86.60	88.90	90.40	45	81.36	83.70	83.21
20	86.92	89.10	90.70	60	81.60	83.72	83.18
25	87.02	89.40	91.00	75	81.90	83.74	83.20
30	87.60	90.20	90.40	90	82.05	83.75	83.21

Experiment 7 : Temp. – 100°C; Oxalic acid – 0.05M; Al/Fe/Zn – 0.08 gL⁻¹

		Time (min)	Zn	Fe	Al	
		5	76.42	77.24	77.70	
		10	77.02	78.30	81.70	
		15	79.23	80.30	87.90	
		20	82.70	86.00	87.99	
		25	83.14	86.89	88.10	
		30	84.90	87.40	87.92	

Figure 4.11a&b represent the results of experiments carried out at 50°C. It is observed that the increase in temperature, from 27-50°C, reduces the time of treatment from 100-5 hr. In the case of sample JK, the experiment conducted with Al as catalyst
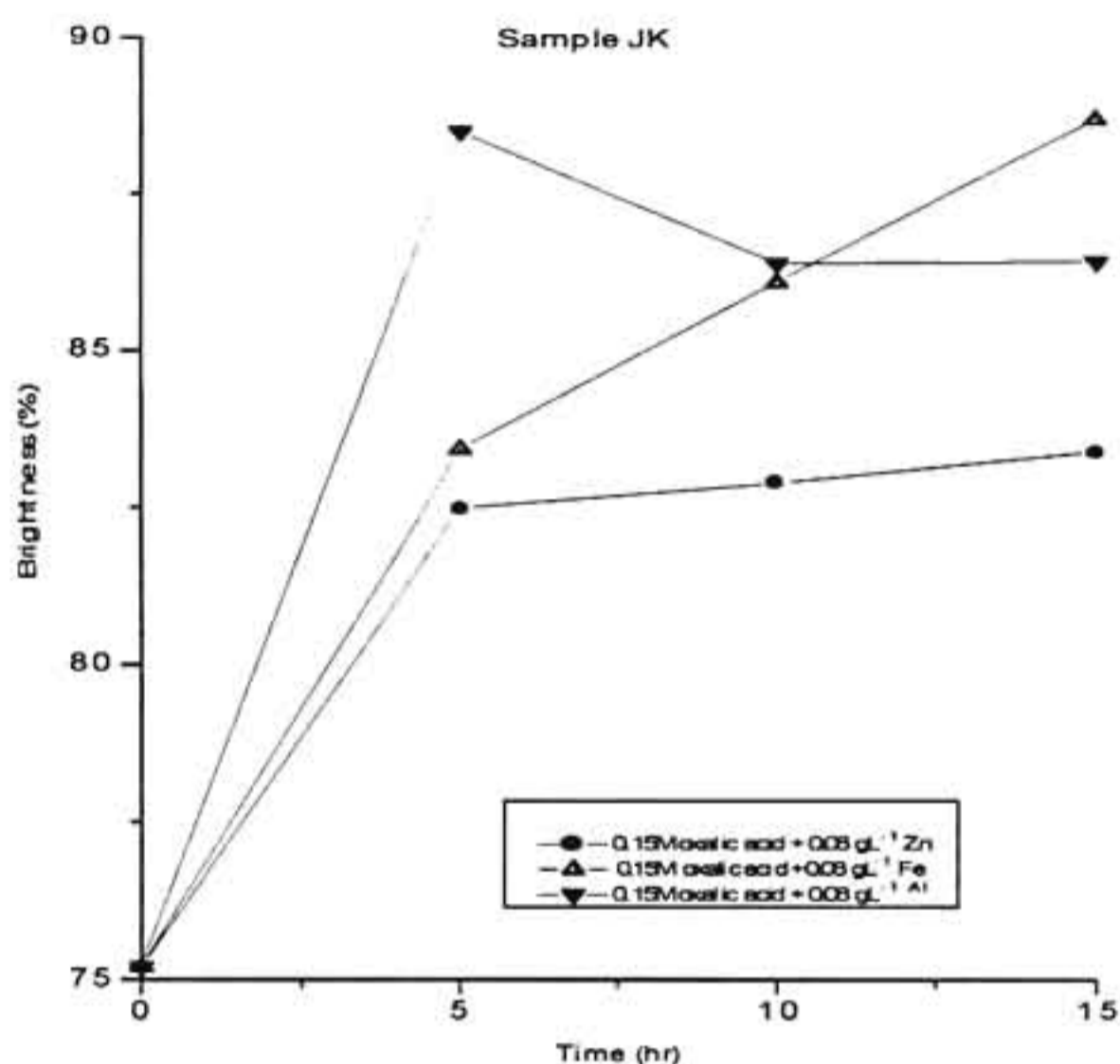

Fig.4.11a. Brightness results of the experiments at 50°C in 0.15 M oxalic acid in presence of metal powder

showed a maximum brightness improvement, 88.5% within a 5 hr treatment (Fig.4.11a). It is also found that increase in time of contact decreased the brightness values to 86%.But, Fe and Zn catalysts showed a gradual increase in brightness with time (upto 15 hr). The maximum values of brightness obtained at 15 hr with Zn and Fe poweders were
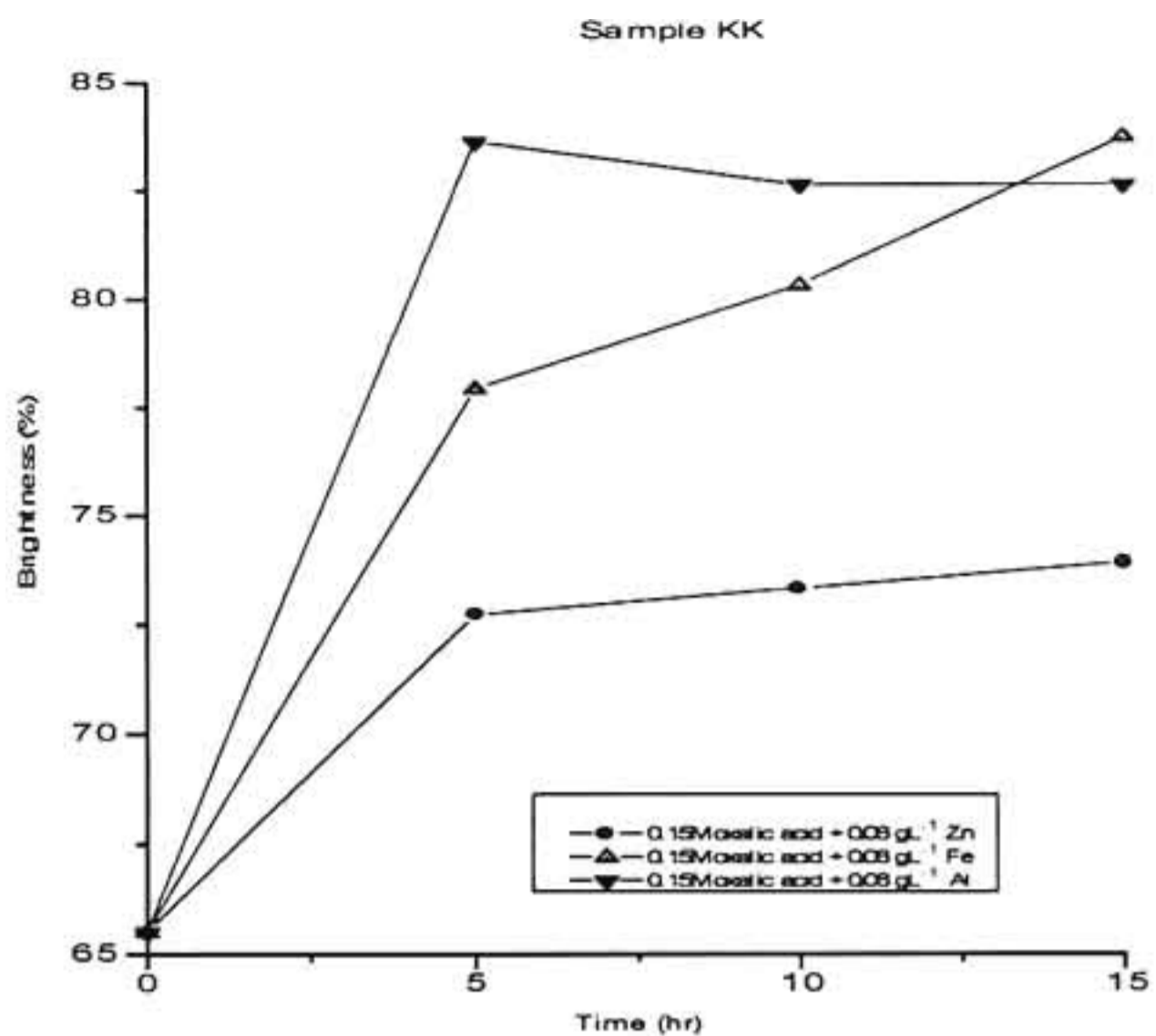
Fig.4.11b. Brightness results of the experiments at 50°C in
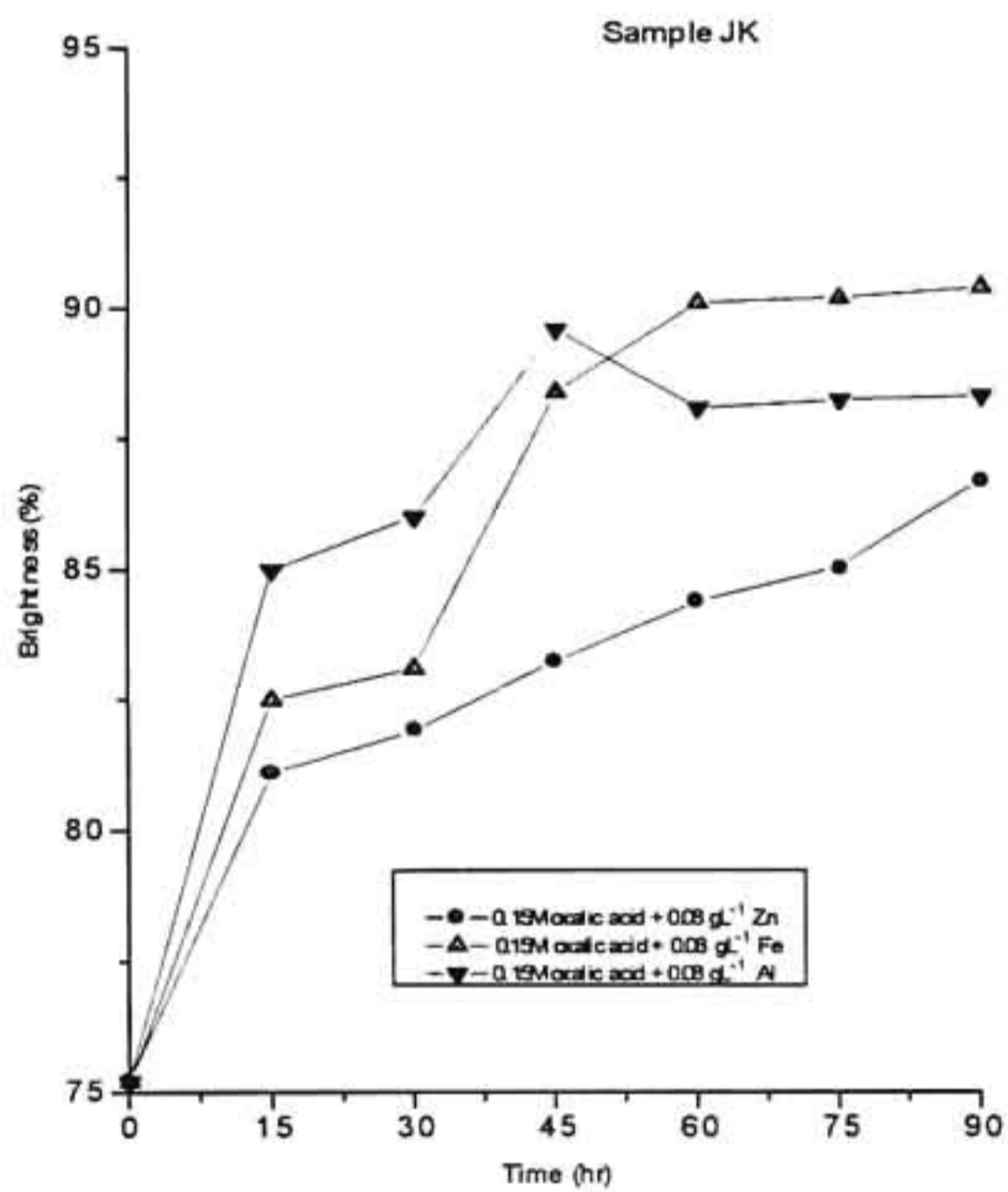0.15M oxalic acid in presence of metal powders

Fig.4.12a. Brightness results of the experiments at 80°C in
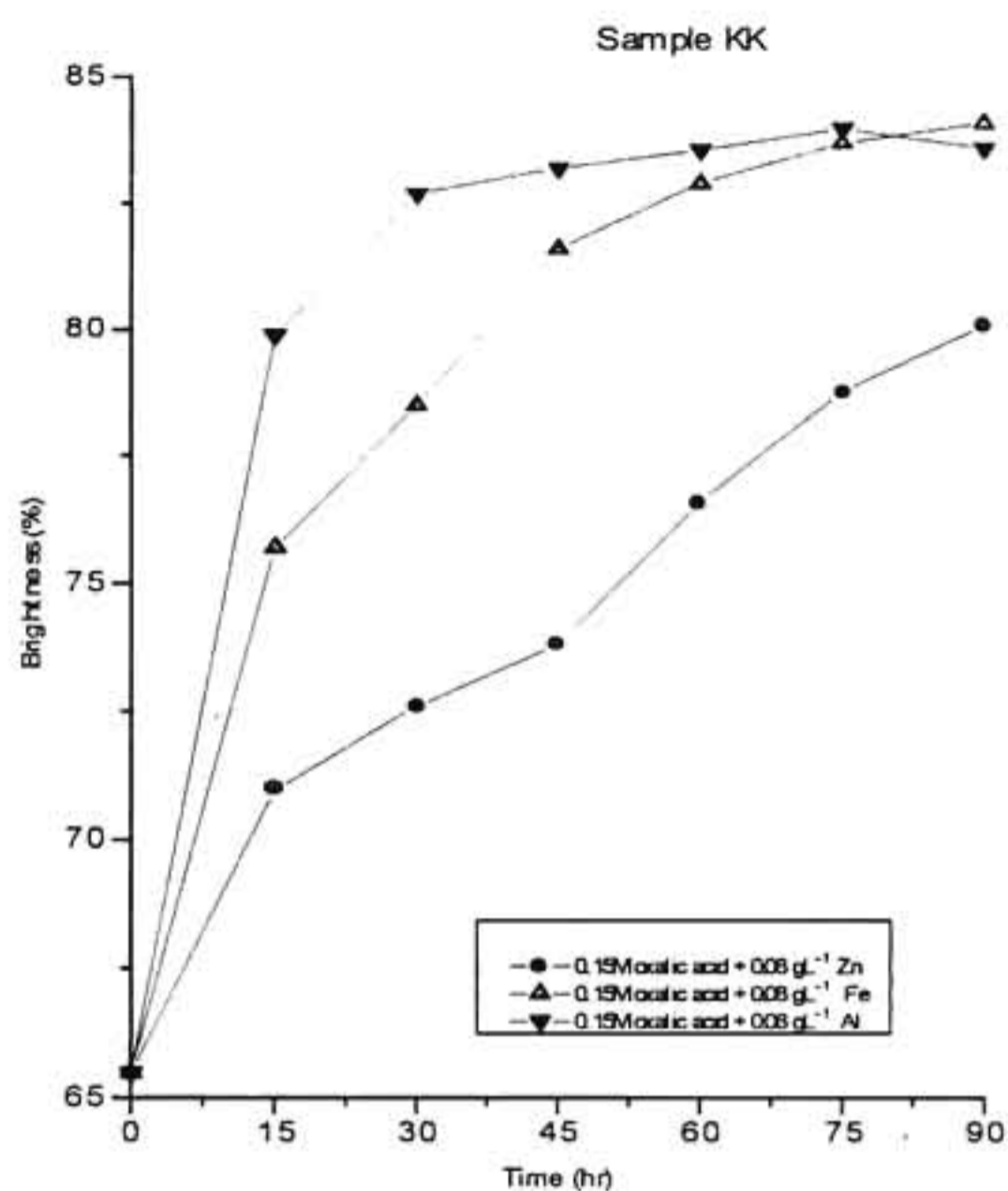0.15M oxalic acid in presence of metal powders

156

Fig.4.12b. Brightness results of the experiment at 80°C in
0.15M oxalic acid in presence of metal powders

83.4 and 88.70%. It is noticed that higher value of brightness was obtained for the experiment with Fe catalyst for a reaction time of 15 hr. Similar reaction trends were noticed for KK as well. The corresponding improvement in brightners brought out by Zn,Al and Fe were 73.9, 83.7 and 83.6% respectively (Fig.4.11b). A similar trend was observed at 80°C also.

The catalytic effect of Al, Fe and Zn was at the highest level at 100°C. Three acid concentrations (0.05, 0.1 and 0.15M) were tried for sample JK, but for sample KK, 0.15M treatment was less efficient when compared to the other two, ie., 0.10 and 0.15 M. Excellent improvement in brightness values were also obtained for both the clay samples at this temperature.

The brightness values of sample JK at 100°C with 0.15M oxalic acid shown in figure 4.14a. The highest value for brightness, 91.9% was otbained when Al was used as the catalyst where the time of treatment was 25 min. In presence of Al, the initial 10 min reaction time increased the brightness above 90%. The brightness value increased with time
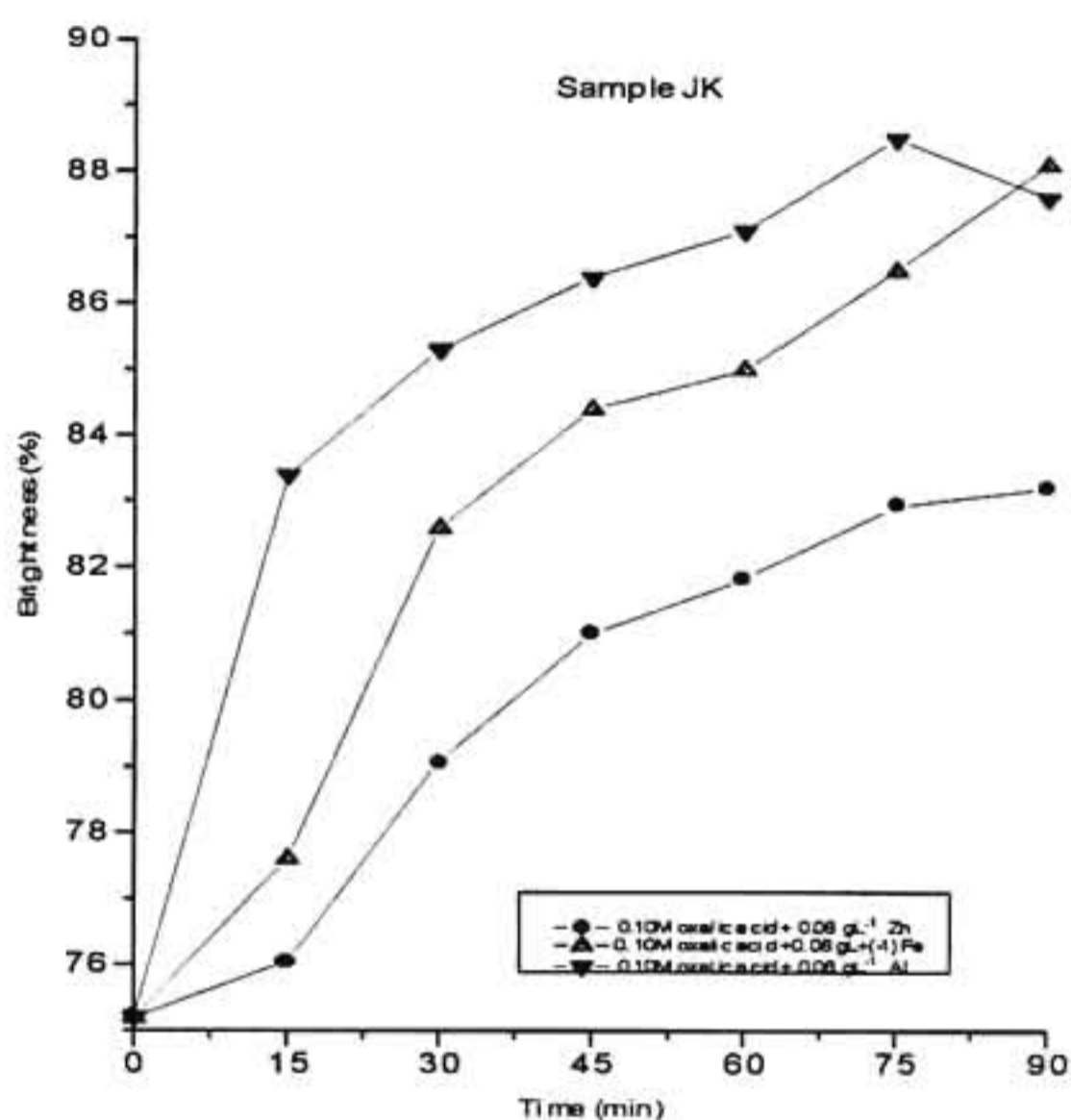

Fig.4.13a. Brightness results of the experiments at 80° C in
0.1 M oxalic acid in presence of metal powders

Upto 25 min and then decreased to 90% at 30 min. But, in the case of Fe and Zn, the brightness values were increasing with increasing time (the maximum time investigated was 30 min). At the end of 30min, the values of brightness corresponding to Zn and Fe catalysed experiments were 90.0 and 90.9% respectively.
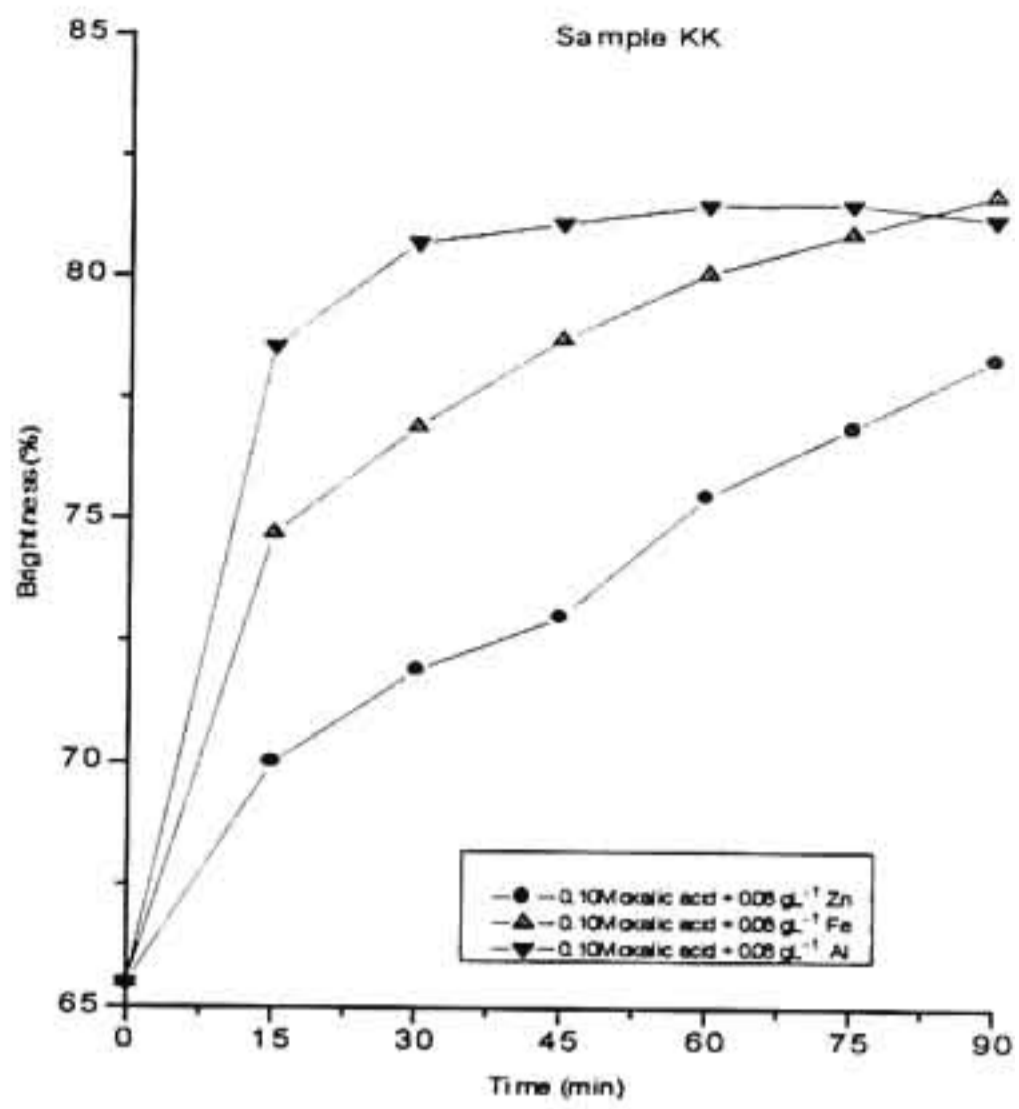
Sample KK

Fig.4.13b. Brightness results of experiments at 80°C in
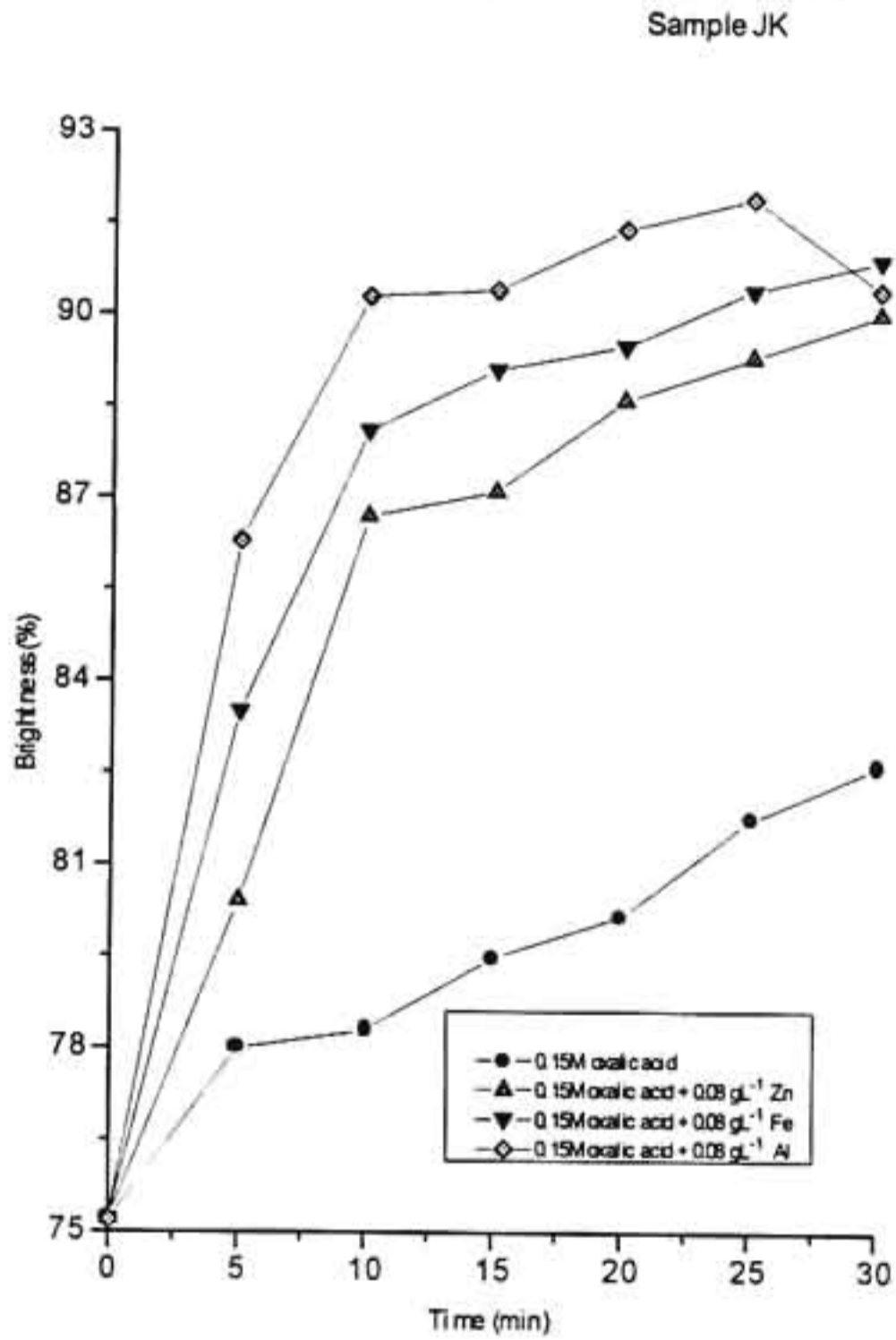0.1 M oxalic acid in presence of metal powders

Sample JK

Fig.4.14a. Brightness results of the experiments at 100°C in
0.15M oxalic acid in presence of metal powders

159

Figure 4.15a&b show the results of experiments conducted at 100°C and 0.1M oxalic acid. The lowering in acid concentration produced only a slight decrease in the brightness values for JK, whereas for KK, the time of experiments were extended to 90 min to achieve the desired brightness.
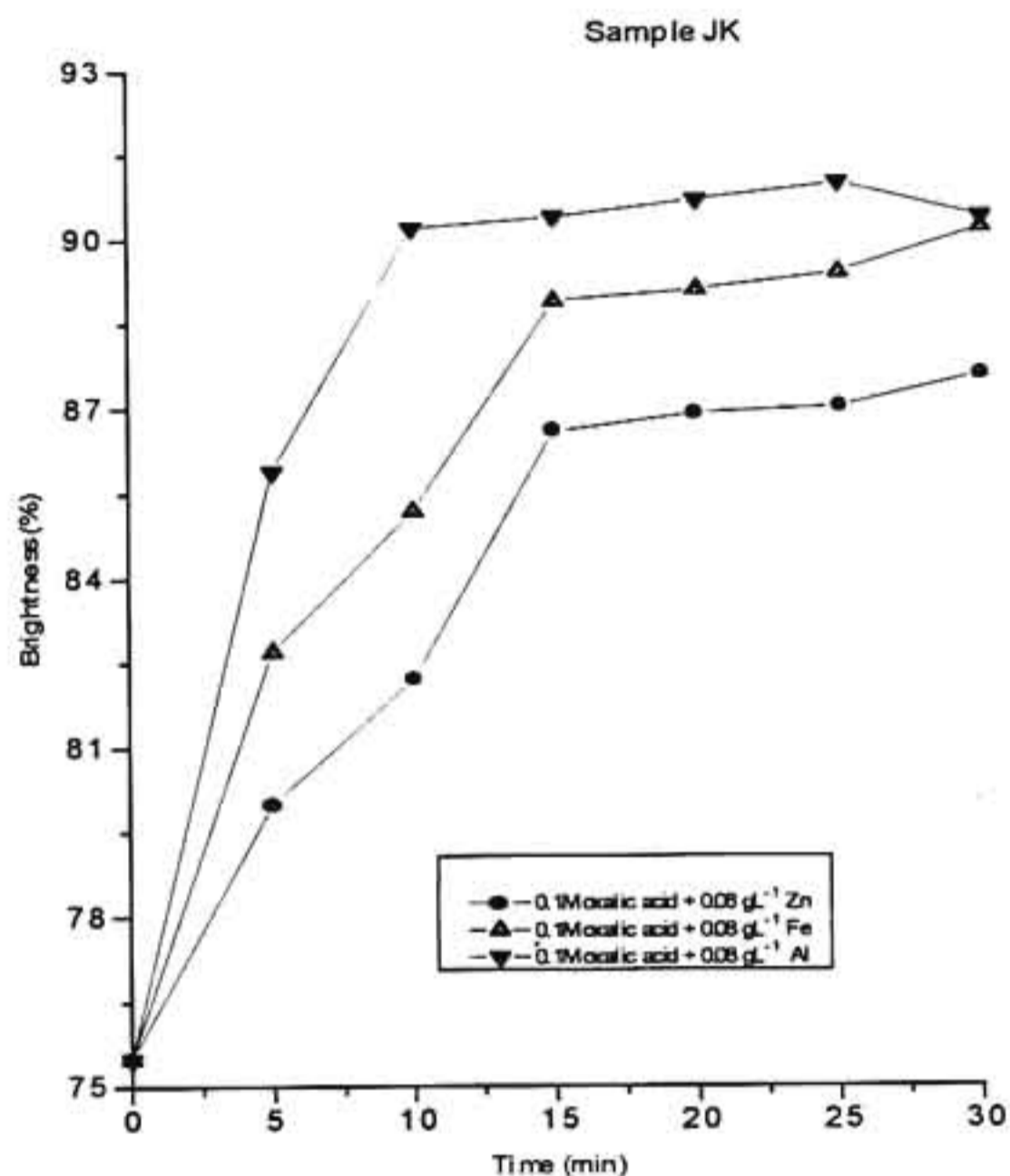
Fig.4.15a. Brightness results of the experiments at 100°C
in 0.10M oxalic acid in presence of metal powders

The effect of lowest concentration of acid tested,ie. 0.05M on the brightness improvement was very low in the case of sample KK, whereas this concentration produced significant improvement for sample JK. The results of the experiments are shown in
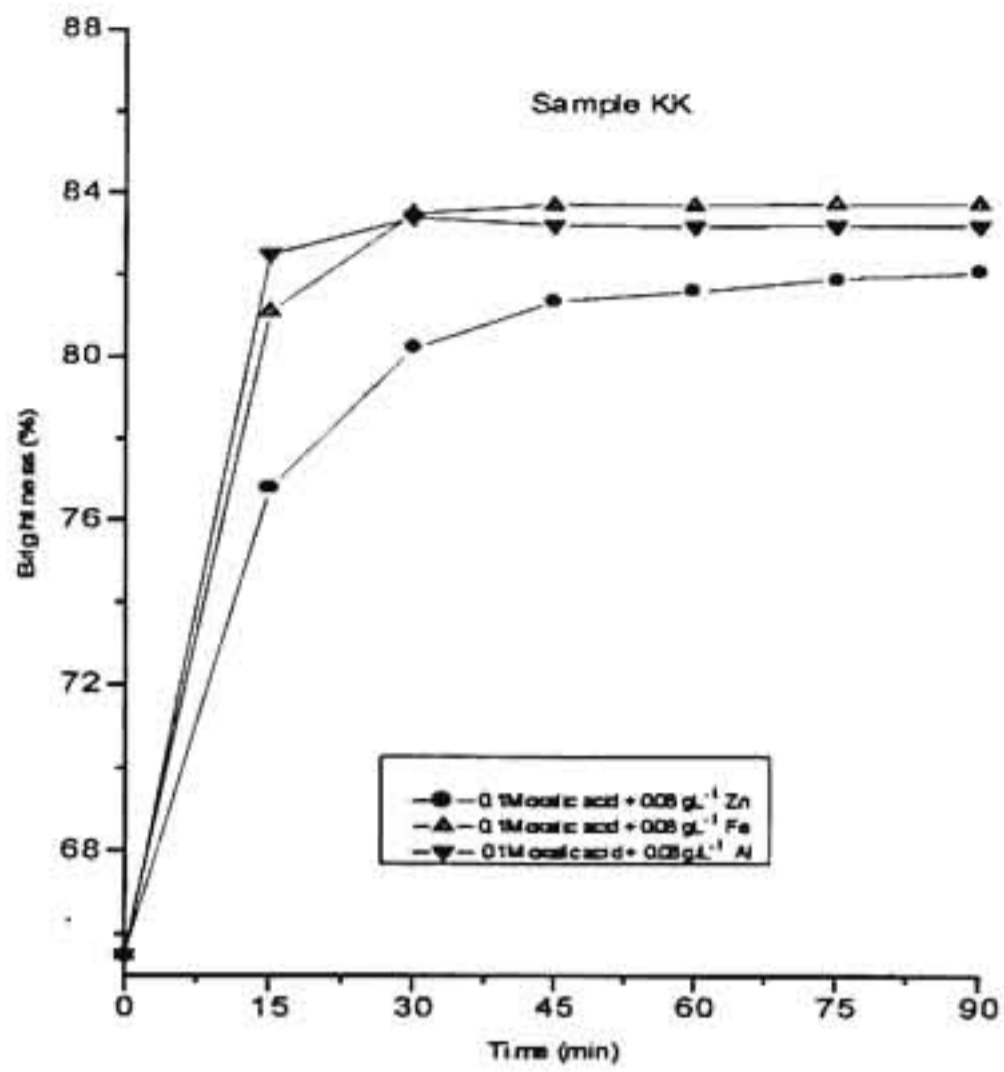
Fig.4.15b. Brightness results of the experiments at 100°C
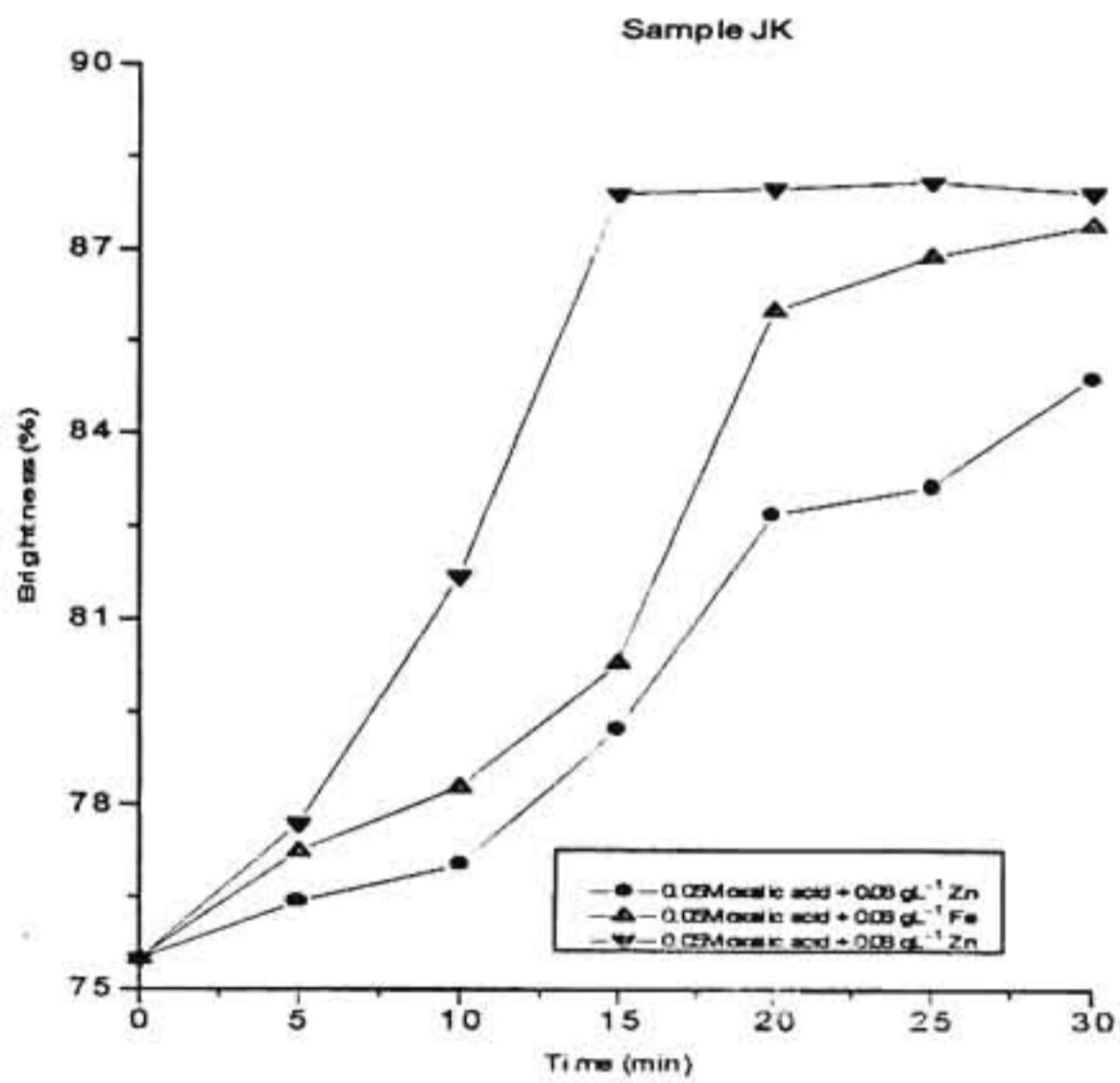in 0.1M oxalic acid in presence of metal powders

Fig.4.16. Brightness results of the experiments at 100°C
in 0.05M oxalic acid in presence of metal powders

figure 4.16. The rate of reaction and the corresponding brightness were fairly good. The maximum values of brightness were 88, 87 and 85%, respectivley for the experiments using Al, Fe and Zn as catalysts.

4C.3.2. Mechanism of dissolution of iron oxides in oxalic acids in presence of metal powders

The dissolution mechanism involves different simultaneous processes: (a) Proton generation by the reaction of metal powder in the acid medium. (b) Fe^{II} ions generation from the liberated ferric oxide. (c) Generation of ferrous oxalate. (d) Adsorption of this on the system interface and (e) Atuocatalytic reaction (formation of a ferric oxalate-ferrous oxalate labile complex followed by electron transfer and dissolution).

$$Fe^{3+} - O + H^+ \rightarrow Fe^{3+}O \ldots. H^+$$
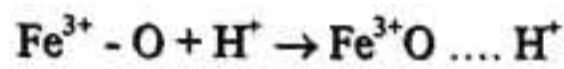
(Protonation)
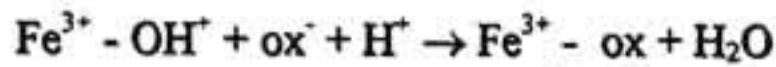
$$Fe^{3+} - OH^+ + ox^- + H^+ \rightarrow Fe^{3+} - ox + H_2O$$
Surface complexation

When sufficient amount of ferrous oxalate have been formed, the secondary reductive step becomes operative and the whole process get accelerated.

$$Fe^{3+} - ox + [Fe^{2+} - ox]_{aq} \rightarrow Fe^{3+} -ox \ldots. Fe^{2+} - ox$$
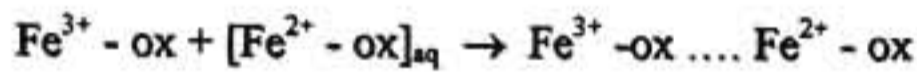
Adsorption at the interface to form a labile complex

$$Fe^{3+} - ox \ldots. Fe^{2+} - ox \rightarrow Fe^{2+} -ox \ldots Fe^{3+} -ox$$

Electron transfer

$$Fe^{2+} -ox . Fe^{3+} - ox \rightarrow [Fe^{2+} - ox]_{aq} + [Fe^{3+} -ox]_{aq}$$
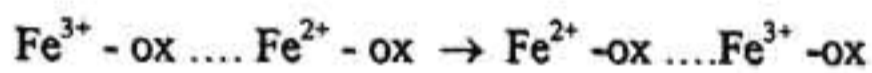
Dissolution

The anomolous behaviour of Al on Fe extraction can be explained as follows. It has been reported that the reductive dissolution of iron oxides in oxalic acid solution gets accelerated by the generation of Fe^{2+} ions in the medium (induction period). But the Fe^{2+} generation is a time consuming process. Therefore, on external supply of Fe^{2+} ions or H^- ions (which in turn generate Fe^{2+} from the liberated iron oxides present in the clay) considerably fasten the induction period. Addition of Al and Zn generates H^+ ions in the medium. The higher reactivity of Al quickly releases H^+ into the medium.

It is quite likely that the insoluble aluminium oxalate may be getting adsorbed on the surface of the remaining aluminium particles slowing down the proton liberation which in turn slackens the extraction of Fe from the surface of clay particles. In the case of iron, the problem of surface coating does not arise as the product (ferric/ferrous oxalate) remains soluble. In the case of zinc, the proton generation is very slow consequently the possibility of Zn-oxalate getting adsorbed on its surface also is a very slow process. Since proton generation continues even after 100 hr although in a very slow rate, the timeiron dissolution curves show a linear behaviour. Increase in temperature and acid concentration increase the reaction rate in all the cases.

4C.4. CONCLUSIONS

Iron-stained kaolinitic clays were subjected to oxalic acid treatment catalysed by metals (Al, Fe and Zn in powdered form) in order to improve the brightness so as to obtain a high value-added product.

From the experimental results achieved by the combinations of various experimental parameters viz. time of treatment, temperature and oxalic acid concentration, the best conditions for obtaining highest brightness values are listed below.

Sample	Time (hr)	Temp. (°C)	Acid conc. (M)	Catalyst used (0.08 gL⁻¹)	Brrightness (%)
JK	60	27	0-15	Al	88.10
KK	60	27	0.15	Al	83.30
JK	5	50	0.15	Al	88.50
KK	5	50	0.15	Al	83.60
JK	45	80	0.15	Al	83.60
KK	45	80	0.15	Al	83.20
JK	75	80	0.10	Al	88.50
KK	75	80	0.10	Al	81.50
JK	25	100	0.15	Al	91.90
KK	25	100	0.15	Fe	85.00
JK	25	100	0.10	Al	9.100
KK	15	100	0.10	Fe	83.70
JK	25	100	0.05	Al	88.10

The metal catalysed oxalic acid bleaching has several advantages such as:

1. Low energy technique when compared to the existing techniques.

1. Brightness of 85-91% ISO could be achieved within 10 to 60 min.

2. A technically feasible method

3. Reagents are easily available

4. The process is eco-friendly

Future experimentation is planned on:

(a) The recycling of oxalic acid, and

(b) Converting the extracted Fe to pure Fe-oxide

REFERENCES

1. Jepson,W.B. Structural iron in kaolinites and in associated ancillary minerals. In: Stucki, J.W., Goodman, B.A. and Schuwertmann, U.(Eds), 1988. Iron in Soils and Clay Minerals. D. Reidel, 468-536.

2. Cecil, T.A. and Jacobs, D.A. , 1971. Method for bleaching gray kaolin clay, US Patents No.3,616,900.

3. Brin, V.G. and Eremin, N.I., 1969. Removal of iron and titanium from kaolins by chlorination. Zh. Prikl. Khim. 42, 1889-1991.

4. Chiarizia, R., Horwitz, E.P., 1991. New formulations for iron oxides dissolution. Hydrometallurgy, 27, 339-360.

5. Blesa, M.A. and Maroto, A.J.G., 1986. Dissolution of metal oxides. J. Chim. Phys., 83, 757-764.

6. Blesa, M.A., Marinovich, H.A., Baumgartner, E.C., Maroto, A.J.G., 1987. Mechanism of dissolution of magnetite by oxalic acid-ferrous ion solutions. Inorg. Chem., 26, 3713-3717.

7. Panias, D., Taxiarchou, M., Paspaliaris,I., Kontopoulos, A., 1996. Mechanism of dissolution of iron oxides in aqueous oxalic acid solutions.Hydrometallurgy,42, 257-265.

8. Cornell, R.M., Schindler, P.W., 1987. Photochemical dissolution of goethite in acid/oxalate solution. Clays Clay Miner., 35, 347-352.

9. Panias, D., Taxiarchou, M., Douni, I., Paspaliaris, I. and Kontopoulos, A., 1996. Dissolution of hematite in acidic oxalate solutions. The effect of ferrous ions addition. Hydrometallurgy, 43, 219-230.

10. Torres, R., Blesa, M.A. and Matijevic, E., 1989. Interactions of metal hydrous oxides with chelating agents: Dissolution of hematite. J. Colloid Interface Sci., 131, 567-579.

11. Blesa, M.A., Borghi, E.B., Maroto,A.J.G. and Regazzoni, A.E., 1984. Adsorption of EDTA and iron-EDTA complexes on magnetite and mechanism of dissolution of magnetite by EDTA. J. Colloid Interface Sci., 98, 295-305.

12. Borggaard, O.K., 1981. Selective extraction of amorphous iron oxides by EDTA from soils from Denmark and Tanzania. J. Soil. Sci., 32, 427-432.

13. McBride, M.B., Goodman, B.A., Russel, J.D. and Fraser, A.R., 1983. Characterization of iron in alkaline EDTA and NH_4OH extracts of podzols. J. Soil Sci., 34, 825-840.

14. Borggaard, O.K., 1982. Selective extraction of amorphous iron oxides by EDTA from selected silicates and mixtures of amorphous and crystalline iron oxides. Clay Miner., 17, 365-368.

15. Borggaard, O.K., 1979. Selective extraction of amorphous iron oxides by EDTA from a Danish sandy loam. J. Soil Sci., 30, 727-734.

16. Litter, M.I. and Blesa, M.A., 1988. Photodissolution of iron oxides: magnetite in EDTA solutions. J. Colloid Interface Sci., 125, 679-687.

17. Borggaard, O.K., 1976. Selective extraction of amorphous iron oxide by EDTA from a mixture of amorphous iron oxide, goethite and hematite.

18. Rubio, J. and Matijevic, E., 1979. Interactions of metal hydrous oxides with chelating agents: β-FeOOH-EDTA. J. Colloid Interface Sci., 68, 409-421.

19. Dos Santos Alfonso, M., Morando, P.J., Belsa, M.A., Banwart, S. and Stumm,W., 1990. The reductive dissolution of iron oxides by ascorbate: the role of carboxylate anions in accelerating reductive dissolution. J. Colloid Interface Sci., 138, 74-82.

20. Baumgartner,E., Blesa, M.A. and Maroto, A.J.G., 1982. Kinetics of the dissolution of magnetite in thioglycolic acid solutions. J. Chem. Soc. Dalton Trans. 1, 1649-1654.

21. Waite, T.D. and Morel, M.M., 1984. Photoreductive dissolution and colloidal iron oxide: Effect of the citrate. J. Colloid Interface Sci., 102, 121-137.

22. Torres, R., Blesa, M.A. and Matijevic, E., 1990. Interactions of hydrous oxides and magnetite by aminocarboxylic acids. J. Colloid Interface Sci., 134, 475-485.

23. Gill, J.B., Goodall, D.C. and Jeffereys, B., 1984. New leaching agents for oxides. The reaction of metal oxides with the mixed non-aqueous system: dimethyl sulphoxide-sulphur dioxide, dimethyl formamide-sulphur dioxide acetonitrile-sulphur dioxide. Hydrometallurgy, 13, 221-226.

24. de Mesquita, L.M.S., Rodrigues, T., Gomes, S.S., 1996. Bleaching of Brazilian kaolins using organic acids and fermented medium. Miner. Eng. 9, 965-971.

25. Groudev, S.N., 1987. Use of heterotrophic microorganisms in mineral biotechnology. Acta Biotechnol. 7, 299-306.

26. Toro, L., Paponetti, B., Veglio, F. and Marabini, A., 1992. Removal of iron from kaolin ores using different microorganisms. The role of the organic acids and ferric iron reductase. Partic. Sci. Technol., 10, 201-208.

27. Veglio, F., Pagliarini, A. and Toro, L., 1993. Factorial experiments for the development of a kaolin bleaching process. Int. J. Miner. Process, 39, 87-99.

28. Veglio, F., Toro, C., 1994. Process development of kaolin pressure bleaching using carbohydrates in acid media. Int. J. Miner. Process. 41, 239-255.

29. Conley, R.F., Lloyd, M.K., 1970. Improvement of iron leaching in clays - optimizing processing parameters in sodium dithionite reduction. Ind. Eng. Chem. Process. Des. Develop. 9, 595-601.

30. Jefferson, D.A., Tricker, M.J. and Winterbottom, A.P., 1975. Electron Microscopic and Mössbauer spectroscopic studies of iron-stained kaolinite minerals. Clays Clay Miner., 23, 355-360.

31. Smith, B.F.L., Mitchell, B.D., 1984. Characterization of X-ray amorphous material in a Scottish soil by selective chemical techniques. Clay Miner., 19, 737-744.

32. Torrent, J., Schwertmann, U. and Barron, V., 1987. The reductive dissolution of synthetic goethite and hematite in dithionite. Clay Miner., 22, 329-337.

33. Toro, L., Marabini, A.M., Paponetti, B. and Passariello, B., 1990. Processo per La rimozione del ferro da concentrati di Caolino, quartzo ed altri minerali di interesse industriale. Italian Patent No.21707 A/90. In: Veglio, F. and Toro, L.1994. Process development of kaolin pressure bleaching using carbohydrates in acid media. Int. J. Miner. Process, 41, 239-255.

34. Grimshaw, R.W., 1958. Chemistry and Physics of Clays, 3rd edn., Western Printer., Great Britain, 942p.

35. Ryan, W., 1978. Properties of Ceramic Materials, Pergamon, Oxford, In: Oaikhinan, E.P., 1991. Rheological properties of certain Nigerian Clays. Interceram., 40, 9-11.

36. Oaikhinan,E.P.,1991. Rheological properties of certain Nigerian clays. Interceram., 40, 9-11.

37. Hinckley, D.N., 1963. Variability in "Crystallinity" values among the kaolin deposits of the coastal plain of Georgia and South Carolina. Clays Clay Miner., 11,229-235.

38. Moore, D.M. and Reynolds, R.C., 1998. X-ray diffraction and the identification and analysis of clay minerals. Oxfrod Univ. Press, New York, 332p.

39. Tzeferis, P.G., Leonardou, S.A., 1994. Leaching of nickel and iron from Greek non-sulphide nickeliferous ores by organic acids. Hydrometallurgy, 36, 345-360.

40. Ubaldini, S., Piga, L., Fornari, P., Massidda, R., 1996. Removal of iron from quartz sands. A study by column leaching using a complete factorial design. Hydrometallurgy, 40, 369-379.

41. Veglio, F., Passariello, B., Toro and Marabini, A.M., 1996. Development of a bleaching process for a kaolin of industrial interest by oxalic, ascorbic and sulphuric acids: Preliminary study using statistical methods of experimental design. Ind. Eng. Chem. Res., 35, 1680-1687.

42. Marabini, A.M., Falbo,A., Passariello, B., Esposito, M.A. and Barbaro, M., 1993. Chemical leaching of iron from industrial minerals. Publ. Australas. Inst. Min. Metall., 3/93, 1253-9.

43. Bonney, C.F., 1994. Removal of iron from kaolin and quartz: dissolution with organic acids. Proc. Int. Symp. Hydrometallurgy, London, 313-323.

44. Tsimas, S.G., Komiotou, M.A., Moutsatsou, A.K. and Parissakis, G.K., 1995. Reducing the iron content of kaolin from Milos, Greece, by a hydrometallurgical process. Trans. Inst. Min. Metall., Sec.C, 104, 110-114.

45. Ambikadevi, V.R., Gopalakrishna, S.J., 1997. Iron stain removal by bleaching and leaching techniques. Proc. 10th Kerala Science Congress, 445-448.

46. Ambikadevi, V.R., Rao,R.B., Lalithambika, M., 1999. Physico-chemical techniques for brightness improvement of kaolin. Int.Symp. on Beneficiation, Agglomeration and Environment (ISBAN-99), Bhubaneswar, 231-238.

47. Bureau of Indian Standards (BIS):: 4589-1968.

48. Baumgarther, E., Blesa, M.A., Marinovich, H.A. and Maroto, A.J.G., 1983. Heterogeneous electron transfer as a pathway in the dissolution of magnetite in oxalic acid solutions. Inorg. Chem., 22, 2224-2226.

49. Arias, M., Barral, M.T. and Diaz-Fierros, F., 1995; Effects of iron and aluminium oxides on the colloidal and surface properties of kaolin.Clays Clay Miner.,43,406-416.

50. Ma, K., Pierre, A.C., 1997. Effect of interaction between clay particles and Fe^{3+} ions on colloidal properties of kaolinite suspensions. Clay and Clay Miner. 45, 733-744.

51. Schwertmann, U., Some properties of soil and synthetic iron oxides. In: Stucki, J.W., Goodman, B.A. and Schwertmann, U. (Eds.), Iron in soils and clay minerals, D.Reidel, Holland, 893p.

52. Robert, M., Berrier, J., Veneau, G. and Vicente, M.A., 1981. Action of amorphous compounds on clay particle associations. In: van Olphen, H., Veniale, F. (Eds.), 1982. Developments in Sedimentology-35, Int. Clay Conf., 35, 411-422.

53. Lagaly, G., 1989. Principles of flow of kaolin and bentonite dispersions. Appl. Clay Sci., 4, 105-123.

54. Ambikadevi, V.R. and Lalithambika, M., 1999. Effect of organic acids on ferric iron removal from iron-stained kaolinite. Appl. Clay Sci., (in Press)..

CHAPTER 5

EFFECT OF NATURAL AND SYNTHETIC GOETHITES ON THE DISCOLORATION ON KAOLIN

5.1. INTRODUCTION

Goethite is a common constituent of many soils and clays. Usually soils and clays owe their yellow pigmentation mainly to the presence of goethite. When it occurs in finely dispersed form, it can be recognized by its characteristic Munsell hue in the range of 10YR – 7YR[1]. Variations in this colour may attribute to a number of parameters like, the variations in crystal size, cation substitution, presence of humic materials, Mn-oxides, and various depositional environments[1,2]. Many attempts were reported to correlate the colour notations (hue, value and chroma) with different controlling factors like soil organic matter, crystallinity, etc[3-6]. Techniques based on spectral reflectancy has been used with success by many workers to interpret the masking effect of organic matter, water content etc. on the yellow pigmentation[3,5,7]. Apart from this, other iron oxides with distinct colours also attribute colour in reasonable amounts. For example, presence of iron oxide mineral, ferrihydrite which is yellowish brown in colour does contribute to the yellow pigmentation. Moreover, it may persist for long periods in soils[2,8].

In the present work, a comparative study has been made to correlate the yellow pigmentation on kaolinitic clays imparted by natural and synthetic goethites.

5.2. MATERIALS AND METHODS

Three naturally occurring kaolinite with goethite as the dominant iron oxide mineral were selected from Akulam (AK), Mulavana (MK) and Thonnakkal (TK). For

this, goethite with two distinct morphologies were synthesized at laboratory conditions. The possibility of Al-substitution in the natural goethites were also envisaged. The sample preparation was done as described in section 2.2.2.1.

5.2.1. Removal of organic matter

10 g of the sample in 25 ml, 6% solution of H_2O_2 was allowed to boil on a water bath for 30min. After 30 min, the contents were washed free of dissolved salts, filtered, dried at 60°C and gently crushed.

5.2.2. Removal of amorphous iron oxides

The amorphous iron oxides like ferrihydrite and poorly crystalline lepedocrocite were freed from the samples by ammonium oxalate treatment (Ref.2.2.2.5).

5.2.3. Removal of total free iron oxide

The organic matter and amorphous iron oxide freed samples were subjected to CDB treatment (Ref. 2.2.2.5) in order to find out the remaining free iron oxide in the samples. The leached liquiors were subjected to iron content analysis. The filter cakes were dried at 60°C for 2 hr.

5.2.4. Synthetic goethite preparation

(a) *Star-shaped goethite crystals*: The star-shaped goethite crystals were synthesized by the method of Bibak[9]. In this procedure, 50 ml of 1M $Fe(NO_3)_3$ solution was rapidly mixed with 650 ml of 0.7 M NaOH solution previously heated to 70°C and aged at this temperature for seven days.

(b) *Lath-shaped goethite crystals[9]*: Within a period of 30 min, 50 ml of 1M $Fe(NO_3)_3$ solution was titrated to pH 4.5 with ~ 150 ml 1M NaOH under vigorous stirring. After stirring the suspension for additional 30 min, 500 ml of 1M NaOH was added.

Then kept the suspension for 24 hr at 21°C followed by 7 days at 70°C in a waterbath. The precipitate was collected by centrifugation and extracted several times in acid ammonium oxalate to remove the amorphous Fe if present. After repeated washing, the residue was dried at 60°C and gently crushed.

5.2.5. Concentration of goethite from the yellow-stained natural kaolinites:
Superconducting high gradient magnetic separation was employed to separate the iron oxides from the yellow-stained clay samples (Ref.3.2). Concentration of these iron oxides from the magnetic fraction was done by dissolving the adhered clay particles in 5M boiling NaOH solution (Ref.2.2.2.5).

5.2.6. Identification and morphology of goethites

The identification of goethite was made using CoKα X-ray diffraction analysis (Ref.2.2.2.5). Scanning electron microscopy was used for the morphological studies (Ref.2.2.2.5).

5.2.7. Kaolinite-synthetic goethite mix preparation

Synthetic goethite corresponding to the total free crystalline iron was added to a 10g of iron oxide-removed clay sample. An aqueous slurry of the above mix was thoroughly dispersed by 1 hr sonication (Julabo USR-3). The contents were centrifuted, dried at 60°C and gently crushed.

5.2.8.Yellowness measurement

The yellowness of the natural yellow-stained kaolinites and the kaolinite-synthetic goethite mix were carried out by making pressed powder discs (Ref.3.2), the reflectance at 457 and 570 nm were measured. The difference between these two values gave the yellowness of the material which is an index of the colouring impurities[10].

173

5. 3. RESULTS AND DISCUSSION

From the CoKα X-ray diffraction (Fig.2.14) studies on the 5M NaOH concentrated iron oxide fractions, it was evident that goethite is the dominant iron oxide mineral in all the three clays viz. AK, MK and TK.

The hydrogen peroxide treatment was done in order to remove the discoloration due to the organic matter. The oxalate pretreatment enabled the removal of amorphous iron oxides such as, ferrihydrite and poorly ordered lepidocrocite if present[11,12]. The remaining iron oxide was considered to be the "total free crystalline iron content" which was removed by the CDB treatment. Now the samples were free of free iron oxides, into which the synthetic goethite was dispersed.

5.3.1. Scanning Electron Microscopic studies

An almost uniform mixing of goethite on the clay samples were obtained after 1 hr sonication (Fig.5.1). It has been observed that the CDB treatment and sonication did not affect the crystal morphology. The clay stacks were retained intact (Fig.5.2). The synthetic goethite obtained were larger in crystal size. Figure 5.3 shows the star-shaped crystals of goethite. The crystal size varied from 10-5 μm. The synthetic lath-shaped crystals were shown in figure 5.4. The size of the goethite crystals vary from 1–5 μm. In the case of the naturally occurring kaolinite (Fig.5.5) the morphology is different. The crystals are extremely small (<1 μm). Moreover they are shorter and thicker than the synthetic ones[13,14]. Such morphological variations are mainly attributed to Al-substitution in the goethite structure[14,15]. It has been reported that the presence of specially adsorbing/replacing ions like, Al, Co, Mn, etc can significantly alter the morphology of goethites during their formation[9]. Studies by Robert et al.[16] reported that a considerable
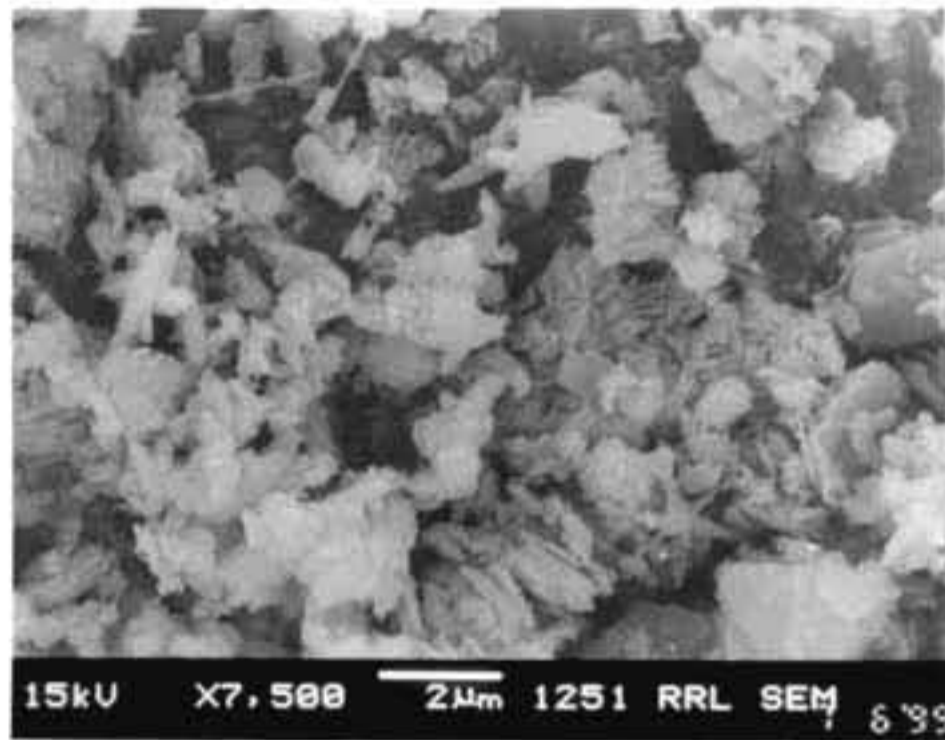
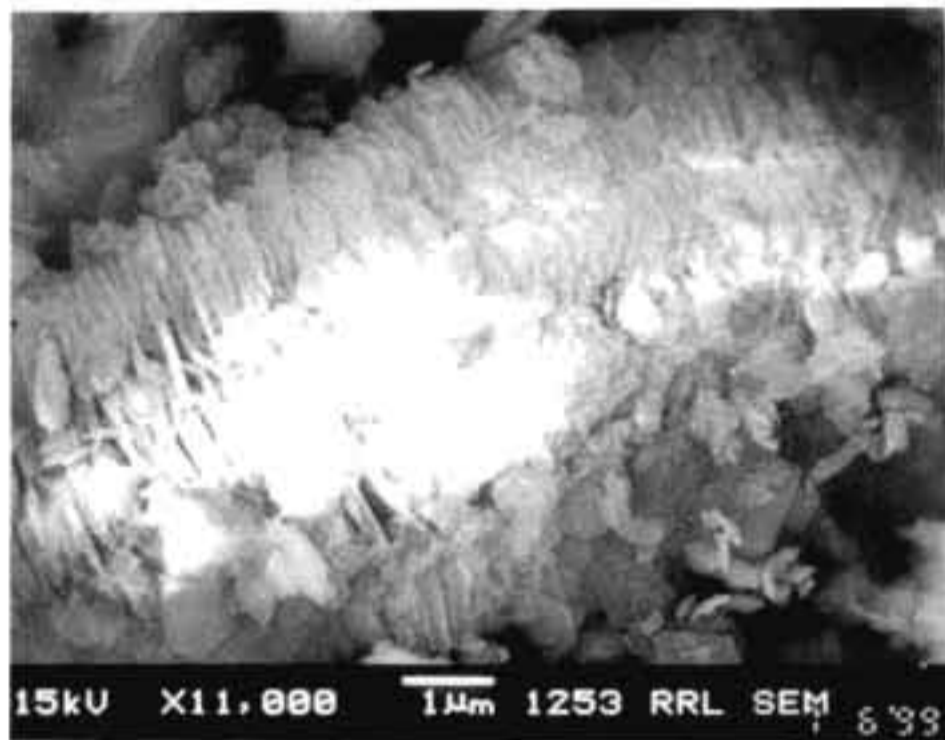Fig.5.1. Uniform distribution of synthetic goethie on kaolinite

Fig.5.2. A composite book of kaolin retained intact after CDB treatment
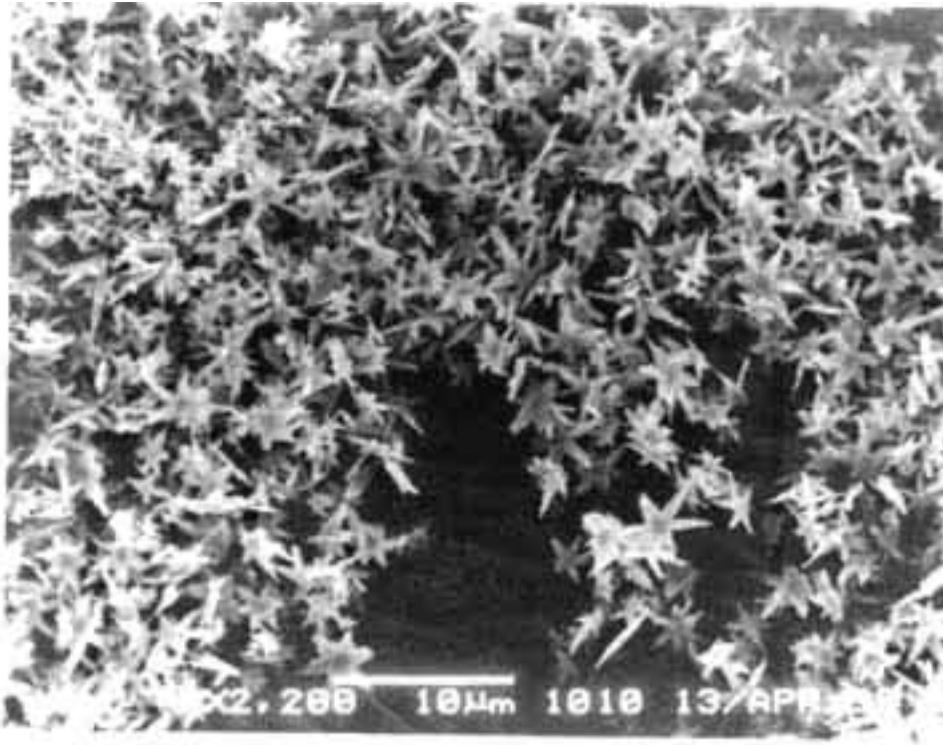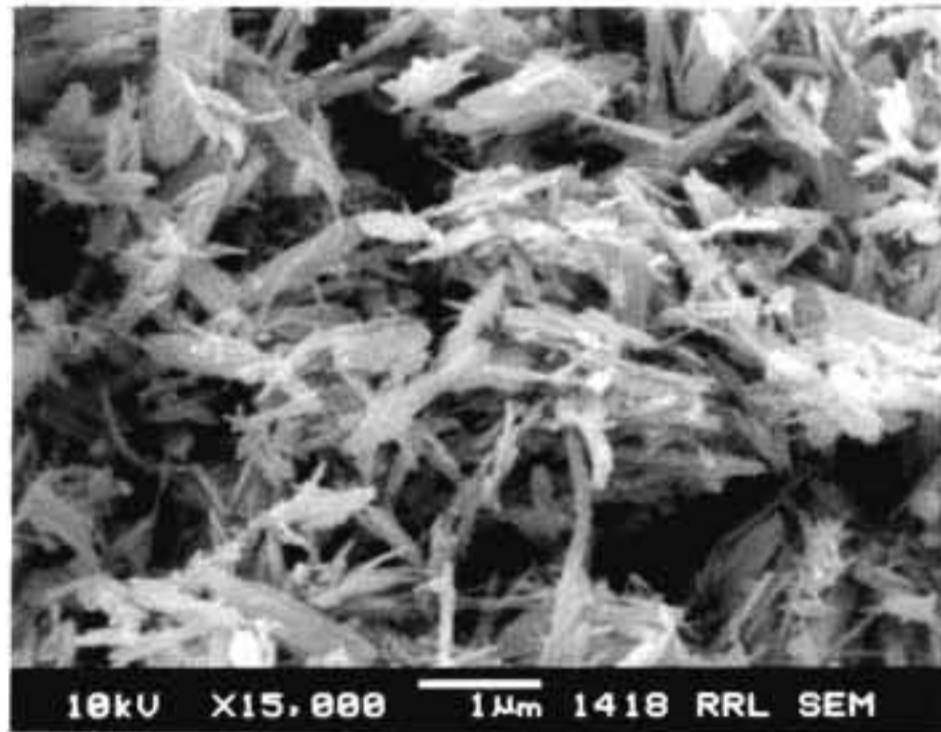
175

Fig.5.3. Star-shaped goethite crystals

Fig.5.4. Lath-shaped goethite crystals

Fig.5.5. Natural goethite in sample TK after removing the clay fraction in 5M NaOH solution

176

change in goethite morphology occurred when it precipitated in presence of Al. However, in nature, goethite may be associated with foreign elements like Al, Co, Cu, Cd, etc. because of sorption, substitution and occlusion[9]. In the case of Al substitution, the b and c dimension, decrease with increasing substitution[17]. That is, the substitution of Fe by the smaller Al ions leads to an overall reduction of the unit-cell parameters, but the structural defects cause changes in a dimension. It can be the reason for the smaller size and shape observed in natural goethites. Apart from this, it has been found that the stability of substituted goethites are higher than those of non-substituted[14,18-20] ones because Al modifies the crystallization conditions, and hence the crystal growth rate, crystal size, morphology and degree of order. Natural goethite may exhibit upto 33 mole% Al substitution and the amount is dependent of conditions of formations[21].

In the present study, the morphology exhibited by goethites in the naturally occurring kaolinites are suggestive of a certain degree of substitution of Fe by Al. The possibility of trace element (Co, Cu etc.) binding can also be considered because the trace element analysis indicated that all the three samples AK, MK and TK contained a good proportion of Co and Cu in them.

5.3.2. Correlation of pigmentation imparted by natural and synthetic goethites

Since the star-shaped crystals exhibit a distinct pinkish red colouration, their colour could not be correlated with that of the naturally occurring yellowish goethites. The naturally occurring kaolinite samples AK, MK and TK are deep yellow in appearance. Since lath-shaped goethite crystals are deep yellow in colour, this material was considered for comparing the yellowness.

177

Table 5.1. Results of yellowness measurement

Sample	Yellowness (%)	
	Naturally occurring goethite in kaolinite	Synthetic goethite in kaolinite
AK	46.14	38.98
MK	32.50	28.32
TK	51.03	41.52

The results of yellowness measurement are given in Table 5.1. It was observed that the yellowness of the naturally occurring samples have shown higher values than that of kaolinite with synthetic goethite. As mentioned earlier, it has been observed that colour of goethite is governed by a number of parameters like, crystal shape, size, substitution by Al, Co, Cu, etc. In addition to this, organic matter also affects the colour[2,9]. But the organic material interference was eliminated by the hydrogen peroxide treatment. Moreover, scanning electron microscopy revealed that the morphology of goethite in the natural samples were idicative of a certain degree of substitution of Fe by Al, Co, Cu, etc. It has been reported that Al substitution in goethites turned the hue from 10YR to 7.5 YR and their Munsell value decreased slightly as structural Al increased[1]. That is, goethite samples became darker with increasing Al substitution[1,3]. Color variations also have been found with crystal size. For goethites, the decrease in crystal size decreases their values and chroma[1], meaning thereby that as the crystal size decreases the material becomes more yellowish.

5.4. CONCLUSION

From the scanning electron microscopy and yellowness values, it is evident that the goethite in the iron stained clays from Akulam (AK), Mulavana (MK), and Thonnakkal (MK) show a certain degree of Al substitution. The higher yellowness values of the naturally occurring clays can thus be attributed to the cation substituion as well as the extremely fine crystalline size of goethite particles.

REFERENCES

1. Schwertmann, U., 1993. Relations between iron oxides, soil colour, and soil formation. Soil Sci. Soc. America, SSSA Special Publication No.31, Madison, WI, 51-69.

2. Taylor, R.M., 1981. Colour in soils and sediments – a review. In: van Olphen, H. and Veniale, F. (Eds.), 1982. Developments in Sedimentology-35, Elsevier, Amsterdam, 749-761.

3. Kosmas, C.S., Franzmeier, D.P. and Schulze, D.G., 1986. Relationship among derivative spectroscopy, colour, crystallite dimensions, and Al substitution of synthetic goethites and hematites. Clays Clay Miner., 34, 625-634.

4. Ebinger, M.H. and Schulze, D.G., 1989. Mn-substituted goethite and Fe-substituted groutite synthesized at acid pH. Clay Clay Miner., 37, 151-156.

5. Fernandez, R.N. and Schulze, D.G., 1987. Calculation of soil colour from reflectance spectra. Soil Sci. Soc. Am. J., 51, 1277-1282.

6. Barron, V. and Torrent, J., 1984. Influence of aluminium substitution on the colour of synthetic hematites. Clay Clay Miner., 32, 157-158.

7. Kosmas, C.S., Curi, N., Bryant, R.B. and Franzmeier, D.P., 1984. Characterization of iron oxide minerals by second derivative visible spectrosc   . Soil Sci. Soc. Am. J., 48, 401-405.

8. Lambor, L.J. and Dutrizac, J.E., 1998. Occurrence and constitution of natural and synthetic ferrihydrite, a widespread iron oxhydroxide. Chem. Rev., 98, 2549-2585.

9. Bibak, A., Gerth, J. and Borggaard, O.K., 1995. Retention of cobalt by pure and foreign – element associated goethites. Clay Clay Miner., 43, 141-149.

10. Jepson, W.B. Structural iron in kaolinites and in associated ancillary minerals. In: Stucki, J.W., Goodman, B.A. and Schwertmann, U. (Eds.), 1988. Iron in Soils and Clay Minerals. D. Reidel, Holland, 893p.

11. Angel, B.R. and Vincent, W.E.J., 1978. Electron spin resonance studies of iron oxides associated with the surface of kaolins. Clays Clay Miner., 26, 263-272.

12. Schwertmann, U., Schulze, D.G. and Murad, E., 1982. Identification of ferrihydrite in soils by dissolution kinoties, Differential X-ray diffraction and Mössbauer Spectroscopy. Soil Sci Soc. Am. J., 46, 869-875.

13. Cornell, R.M., Posner, A.M. and Quirk, J.P., 1974. Crystal morphology and the dissolution of goethite. J. Inorg. Nucl. Chem., 36, 1937-1946.

14. Schwertmann, U., 1984. The influence of aluminium on iron oxides:IX. Dissolution of Al-goethites in 6M HCl. Clay Miner., 19, 9-19.

15. Ford, R.G., Bertsch, P.M. and Seaman, J.C., 1997. Geothite morphologies investigated via. X-ray diffraction of oriented samples. Clays Clay Miner., 45, 769-772.

16. Robert, M., Veneau, G. and Hervio, M., 1983. Influence des polycations du fer et de l' aluminium sur les proprietés des argiles. Science du Sol., 3, 235-251.

17. Schulze, D.G., 1984. The influence on iron oxides. VIII. Unit-cell dimensions of Al-substituted goethites and estimation of Al from them. Clays Clay Miner., 32, 36-44.

18. Schwertmann, U., Some properties of soil and synthetic iron oxides. In: Stucki, J.W., Goodman, B.A. and Schwertmann, U., 1988. Iron in Soils and Clay Minerals, D. Reidel, Holland, 203-250.

19. Torrent, J., Schwertmann, U. and Barron, V., 1987. The reductive dissolution of synthetic goethite and hematite in dithionite. Clay Miner., 22, 329-337.

20. Cornell, R.M., Posner, A.M. and Quirk, J.P., 1976. Kinetics and mechanisms of the acid dissolution of goethite (α - FeOOH). J. Inorg. Nucl. Chem., 38, 563-567.

21. Fitzpatrick, R.W. and Schwertmann, U., 1982. Al-substituted goethite – an indicator of pedogenic and other weathering environments in South Africa. Geoderma, 27, 335-347.

PUBLICATIONS/PRESENTATIONS

- Ambikadevi, V.R. and Gopalakrishna, S.J., 1997. Iron stain removal by bleaching and leaching techniques. Proc. 10th Kerala Science Congress, 445-448.

- Ambikadevi, V.R., Rao, R.B. and Lalithambika, M., 1999. Physico-Chemical techniques for brightness improvement of kaolin. Int. Symp. Beneficiation, Agglomeration and Environment. India, 231-238.

- Ambikadevi, V.R. and Lalithambika, M., 1998. Brightness improvement of china clays using organic acids. Natn. Symp. recent Trends in Clay Research (Abstracts).

- Ambikadevi, V.R. and Lalithambika, M., 1999. Effect of organic acids on ferric iron removal from iron-stained kaolinite. Applied Clay Science (in Press).

- Ambikadevi, V.R. and Lalithambika, M. Discolouration of natural and synthetic goethite on kaolin (to be communicated)..

- Ambikadevi, V.R. and Lalithambika, M. A novel technique for beneficiating iron-stained china clays (to be communicated).

- Ambikadevi, V.R. and Lalithambika, M. Geology and Geochemistry of iron-stained clays from India (to be communicated).

PATENT

- Ambikadevi, V.R., Rugmini Sukumar and Lalithambika, M., 1999. Deferration of silica and aluminosilicate minerals using organic acids in presence of metal ions. The Indian Patents Act 1970.